Chapter 1

Preview

As an academic discipline, robotics is a relatively young field with highly ambitious goals, the ultimate one being the creation of machines that behave and think like humans. This attempt to create intelligent machines naturally leads us to first examine ourselves—to ask, for example, why our bodies are designed the way they are, how our limbs are coordinated, and how we learn and refine complex motions. The sense that the fundamental questions in robotics are ultimately questions about ourselves is part of what makes robotics such a fascinating and engaging endeavor.

In contrast to the lofty goals set by robotics researchers, the aims of this textbook are more modest. Our focus will be on the mechanics, planning and control of **robot mechanisms**. Robot arms are one familiar example. So are wheeled platforms, as are robot arms mounted on wheeled platforms. Basically, a mechanism is constructed by connecting rigid bodies, called **links**, together with **joints**, so that relative motion between adjacent links becomes possible. **Actuation** of the joints, typically by electric motors, then causes the robot to move and exert forces in desired ways.

The links of a robot mechanism can be arranged in serial fashion, like the familiar serial-chain arm shown in Figure 1.1(a). Robot mechanisms can also have closed loops, such as the Stewart-Gough platform shown in Figure 1.1(b). In the case of a serial chain, all of its joints are actuated, while in the case of mechanisms with closed loops only a subset of its joints may be actuated.

Let us examine more closely the current technology behind robot mechanisms. The links are moved by actuators, which are typically electrically driven (e.g., DC or AC servo motors, stepper motors, even shape memory alloys), or sometimes by pneumatic or hydraulic cylinders, or internal combustion engines. In the case of rotating electric motors, they should ideally be lightweight, operate at relatively low rotational speeds (e.g., in the range of hundreds of RPM) and be able to generate large forces and torques. Since most currently available motors operate in the range of thousands of RPM, speed reduction devices with low slippage and backlash are often required. Belts, sprockets, and spur gears are usually not well-suited for this purpose; instead, specially designed

low backlash gears, harmonic drives, and ball screws are used to simultaneously reduce speed and amplify the delivered torque. Brakes may also be attached to quickly stop the robot or to maintain a stationary posture.

Robots are also equipped with sensors to measure the position and velocity at the joints. For both revolute and prismatic joints, optical encoders measure the displacement, while tachometers measure their velocity. Forces at the links or at the tip can be measured using various types of force-torque sensors. Additional sensors may be used depending on the nature of the task, e.g., cameras, sonar and laser range finders to locate and measure the position and orientation of objects.

This textbook is about the mechanics, motion planning, and control of such robots. We now provide a preview of the later chapters.

Chapter 2: Configuration Space

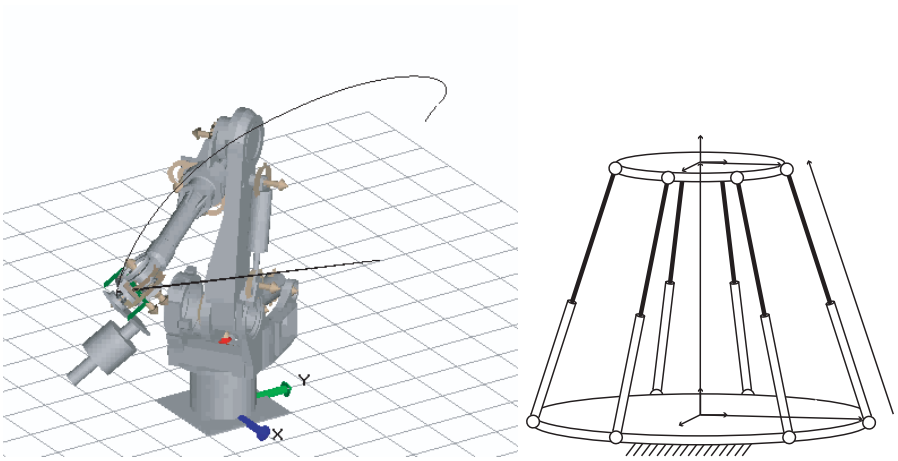

(a) An open chain industrial manipulator. (b) Stewart-Gough platform.

Figure 1.1: Open chain and closed chain robot mechanisms.

At its most basic level, a robot consists of rigid bodies connected by joints, with the joints driven by actuators. In practice the links may not be completely rigid, and the joints may be affected by factors such as elasticity, backlash, friction, and hysteresis. In this book we shall ignore these effects for the most part and assume all links are rigid. The most commonly found joints are revolute joints (allowing for rotation about the joint axis) and prismatic joints (allowing for linear translation along the joint axis). Revolute and prismatic joints have one degree of freedom (either rotation or translation); other joints, such as the spherical joint (also called the ball-in-socket joint), have higher degrees of freedom.

In the case of a serial chain robot such as the industrial manipulator of Figure 1.1(a), all of its joints are independently actuated. This is the essential idea behind the **degrees of freedom** of a robot: it is the sum of all the independently actuated degrees of freedom of the joints. For serial chains the degrees of freedom is obtained simply by adding up all the degrees of freedom associated with the joints.

For closed chains like the Stewart-Gough platform shown in Figure 1.1(b), the situation is somewhat more complicated. First, joints with multiple degrees of freedom like the spherical joint are quite common. Second, it is usually not possible to independently actuate all of the joints—fixing a certain set of joints to prescribed values automatically determines the values of the remaining joints. For even more complicated closed chains with multiple loops and different joint types, determining the degrees of freedom may not be straightforward or intuitive.

A more abstract but equivalent definition of the degrees of freedom of a robot begins with the notion of its **configuration space**: a robot's **configuration** is a complete specification of the positions and orientations of each link of a robot, and its configuration space is the set of all possible configurations of the robot. The degrees of freedom, then, is the minimum number of independent parameters required to specify the position and orientation of each of the links. Based on this definition we obtain a formula—Grübler's formula—that relates the number of links and joints (including the degrees of freedom of each joint) comprising a robot with its degrees of freedom.

Robot motion planning and control both begin by choosing coordinates that parametrize the robot's configuration space. Often the coordinates of choice are the joint variables, and the configuration space can be parametrized either explicitly or implicitly in terms of these joint variables. Also, to grasp and manipulate objects, a robot is typically equipped with an **end-effector**, e.g., a mechanical hand or gripper. The **task space**, also called the workspace, is the configuration space of the end-effector. In this chapter we study the various ways in which the configuration and task spaces of a robot can be parametrized.

Chapter 3: Grasp Statics

For a multifingered robot hand grasping an object (Figure 1.2), one way to formulate the grasping problem is to determine the fingertip contact points such that the object to be grasped is completely immobilized. This chapter considers the problem of how to restrain a rigid body using a fixed number of point contacts. The problem of fixturing a workpiece with a set of point contact restraints can also be formulated in the same way. Everyday experience tells us that friction at the contacts obviously helps matters, and throughout we consider point contacts both with and without friction. If the object is completely immobilized by the fixed point contacts, the object is said to be in **form closure**. Even if the object is not in form closure, if forces can be applied at the point contacts to cancel any external forces and moments applied to the object—imagine holding a cup sufficiently tightly so as to resist gravity—then

Figure 1.2: A multi-fingered robot hand grasping an object.

the object is said to be in **force closure**. In this chapter we develop both form and force closure tests for planar and spatial grasps.

Chapter 4: Rigid-Body Motions

This chapter addresses the problem of how to mathematically describe the motion of a rigid body moving in three-dimensional physical space. One convenient way is to attach a reference frame to the rigid body, and to develop a way to quantitatively describe the frame's position and orientation as it moves. As a first step, we cover some preliminaries on the analysis of velocities and accelerations of particles with respect to moving frames. We then introduce the 3×3 matrix representation for describing a frame's orientation; such a matrix is referred to as a **rotation matrix**. Two well-known three-parameter representations for rotation matrices, the Euler angles and roll-pitch-yaw angles, are described.

We then introduce the exponential representation for rotations. This representation, which can also be identified with the familiar angle-axis representation for rotations, is derived in a somewhat roundabout way as the solution to a certain linear vector differential equation. Doing so allows us to, among other things, proceed directly to the exponential description of general rigid body motions, which forms the cornerstone for our later kinematic analysis of serial chains.

The exponential description of rigid body motions can also be identified with classical screw theory. In addition to the basic rules for the matrix representation and manipulation of rigid body motions, we also cover in detail the linear algebraic constructs of screw theory, including the unified description of linear and angular velocities as six-dimensional **spatial velocities**. Analogously, it is also natural to combine three-dimensional forces and moments into a six-

dimensional **spatial force**.

Chapter 5: Forward Kinematics

For an open chain, the position and orientation of the end-effector are uniquely determined from the joint positions. This is precisely the **forward kinematics** problem for a robot: given a set of input joint values, find the output position and orientation of the reference frame attached to the end-effector. In this chapter we study two methods for describing the forward kinematics of open chains: the Denavit-Hartenberg (D-H) representation, and the product-of-exponentials (PoE) formula. The D-H representation uses a fewer number of parameters, but requires that reference frames be attached to each link. The PoE formula requires more parameters, but there is no need to attach reference frames to each link. Instead it relies solely on information about the location of each joint axis—essentially, a line in space—making this the preferred forward kinematic representation for our subsequent analysis in the later chapters.

Chapter 6: Velocity Kinematics and Statics

Velocity kinematics refers to the relationship between joint rates and the linear and angular velocities of the end-effector frame. Central to velocity kinematics is the **Jacobian** of the forward kinematics. By multiplying the vector of joint rates by this matrix, the linear and angular velocities of the end-effector frame can be obtained for any given robot configuration. **Kinematic singularities**, which are configurations in which the end-effector frame loses the ability to move or rotate in one or more directions—imagine, for example, a two-link planar chain with its two links folded over each other—correspond to those configurations at which the Jacobian matrix fails to have maximal rank. The closely related and more general notion of the **manipulability ellipsoid**, whose shape indicates the ease with which the robot can move in various directions, is also derived from the Jacobian.

Finally, the Jacobian is also central to static force analysis. In static equilibrium settings, the Jacobian is used to determine what forces and torques need to be exerted at the input joints in order for the end-effector to apply a certain force or moment in a particular direction. In this chapter we show how to obtain the Jacobian for general serial chains, and its many practical uses in the above and other settings.

Chapter 7: Inverse Kinematics

In the **inverse kinematics** problem, given a desired position and orientation of the end-effector frame, the objective is to determine the set of joint positions that achieves this desired end-effector configuration. For serial chain robots, the inverse kinematics is in general more involved than the forward kinematics: for a given set of joint values there usually exist a unique end-effector position

and orientation, but for a particular end-effector position and orientation, there may exist multiple solutions, or even none at all.

In this chapter we first examine a special class of six-dof serial chain structures whose inverse kinematics admits a closed-form analytic solution. Iterative numerical algorithms are then derived for solving the inverse kinematics of general six-dof serial chains. We also examine the inverse kinematics of redundant serial chains (that is, those with more than seven degrees of freedom) in the context of tracking a desired end-effector trajectory. For this problem, we present a solution for obtaining the corresponding input joint rates that relies on the generalized inverse of the forward kinematics Jacobian.

Chapter 8: Kinematics of Closed Chains

While serial chains have unique forward kinematics solutions, closed chains will often have multiple forward kinematics solutions, and sometimes even multiple solutions for the inverse kinematics as well. Also, because closed chains possess both actuated and passive joints, the kinematic singularity analysis of closed chains presents unusual subtleties not encountered in serial chains. In this chapter we study the basic concepts and tools for the kinematic analysis of closed chains. We begin with a detailed case study of mechanisms like the planar five-bar linkage and the Stewart-Gough Platform. These results are then generalized into a systematic methodology for the kinematic analysis of more general closed chains.

Chapter 9: Dynamics of Open Chains

This chapter derives the dynamic equations for serial chains. As a first step, the dynamic equations for a single rigid body are derived in terms of spatial velocities, accelerations, and forces. The dynamics for a serial chain robot are then derived by applying the single body equation to each link of the robot. Analogous to the notions of forward and inverse kinematics, the **forward dynamics** problem involves determining the resulting joint trajectory for a given input joint torque profile. Similarly, the **inverse dynamics** problem is concerned with determining the input joint torque profile for a desired joint trajectory. The main result of this chapter is a set of recursive algorithms for the forward and inverse dynamics problem. Unlike traditional methods that rely on a separate analysis of the linear and angular components of the dynamic equations, our algorithms are formulated entirely in terms of six-dimensional spatial quantities, and rely upon the product-of-exponentials formula to model the kinematics.

Chapter 10: Trajectory Generation

What sets a robot apart from an automated machine is that it should be easily reprogrammable for different tasks. Different tasks require different motions, and it would be unreasonable to expect the user to specify the entire time-history

of each joint for every task; clearly it would be desirable for the computer to "fill in the details" from a small set of task input data.

This chapter is concerned with the automatic generation of joint trajectories from this set of task input data. Often this input data is given in the form of an ordered set of joint values, called control points, together with a corresponding set of control times. Based on this data the trajectory generation algorithm produces a smooth trajectory for each joint that satisfies various user-supplied conditions.

We will study some popular algorithms for trajectory generation that were originally developed for computer-aided curve design applications. Algorithms that are of particular interest are cubic splines and Bézier curves. Versions of these algorithms are offered for the generation of trajectories in both joint space and end-effector space. In the latter case, algorithms are presented for interpolating through an ordered set of end-effector reference frames.

Chapter 11: Motion Planning with Obstacles

This chapter addresses the problem of finding a collision-free path for a robot through a cluttered workspace. The most intuitive approach is to work in configuration space, which because of the workspace obstacles will now have forbidden regions. We begin with the most basic of planning algorithms involving grid search. A convenient way to navigate through such cluttered regions is through the use of **artificial potential fields**. Briefly, in these methods the obstacles generate artificial forces that repel the robot should it venture too near. When they work, these methods have the advantage of being able to generate collision-free trajectories in real-time. There are a number of subtleties associated with these methods, however, e.g., the possibility of getting "stuck" in local equilibria without reaching the goal configuration, and we discuss some methods to overcome these difficulties. We also cover a basic randomized algorithm for planning collision-free paths, based on **rapidly-exploring random trees**.

Chapter 12: Robot Control

A robot arm can exhibit a number of different behaviors depending on the task and its environment. It can act as a source of programmed motions for tasks such as moving an object from one place to another, or tracing a trajectory for manufacturing applications. It can act as a source of forces, for example when grinding or polishing a workpiece. In tasks such as writing on a chalkboard, it must control forces in some directions (the force pressing the chalk against the board) and motions in others (motion in the plane of the board). In certain applications, e.g., haptic displays, we may want the robot to act like a spring, damper, or mass, controlling its position, velocity, or acceleration in response to forces applied to it.

In each of these cases, it is the job of the robot controller to convert the task specification to forces and torques at the actuators. Control strategies

to achieve the behaviors described above are known as **motion (or position) control**, **force control**, **hybrid motion-force control**, and **impedance control**. Which of these behaviors is appropriate depends on both the task and the environment. For example, a force control goal makes sense when the end-effector is in contact with something, but not when it is moving in free space. We also have a fundamental constraint imposed by mechanics, irrespective of the environment: the robot cannot independently control both motions and forces in the same direction. If the robot imposes a motion, then the environment determines the force, and vice versa.

Most robots are driven by actuators that apply a force or torque to each joint. Hence, to precisely control a robot would require an understanding of the relationship between joint forces and torques and the motion of the robot; this is the domain of dynamics. Even for simple robots, however, the dynamic equations are usually very complex, Also, to accurately derive the dynamics requires, among other things, precise knowledge of the mass and inertia of each link, which may not be readily available. Even if they were, the dynamic equations would still not reflect physical phenomena like friction, elasticity, backlash, and hysteresis.

Most practical control schemes compensate for these errors by using **feedback**. One effective method of industrial robot control is to neglect the robot's dynamics, and instead model each actuator as a scalar second-order linear system. As such we first introduce basic concepts from linear control, and show how they can be used to effectively control complex multi-dof robots.

This chapter also introduces some basic robot control techniques that assume a dynamic model of the robot is available; such **feedforward control** techniques use the dynamic model of the robot and its environment to determine actuator control inputs that achieve the desired task. Because of modeling and other errors, feedforward control is rarely used by itself, but is often used in conjunction with feedback control. After considering feedback and forward strategies for model-based motion control, we then examine force control, hybrid motion-force control, and impedance control.

Chapter 13: Wheeled Robots

This chapter addresses the kinematics, motion planning, and control of wheeled robots that are subject to no-slip rolling constraints. Such constraints are fundamentally different from the loop closure constraints found in closed chains—the former are **holonomic**, the latter **nonholonomic**—and as such we begin with a discussion of nonholonomic constraints. We then examine the kinematics of some popular wheeled robots: car-like, differential drive, Dubins, and omnidirectional robots. The **controllability** problem of determining whether a wheeled robot is able to move from a given initial configuration to an arbitrary final configuration is then examined. The chapter concludes with a discussion of motion planning and control algorithms for wheeled robots, including the problem of characterizing and finding optimal paths, and feedback control of wheeled robots.

Chapter 2

Configuration Space

A typical robot is mechanically constructed from several bodies, or **links**, that are connected by various types of **joints**. The robot moves when certain joints are driven by **actuators** (such as electric motors) that deliver forces or torques to the joints. Usually an **end-effector**, such as a gripper or hand for grasping and manipulating objects, is attached to some link of the robot. All of the robots considered in this book will have links that can be modeled as rigid bodies.

Given a particular robot, perhaps the most fundamental question one can ask is "where is the robot?"[1] The answer to this question is the robot's **configuration**—a specification of the positions of all points of the robot. Since the robot's links are rigid and of known shape, only a few numbers are needed to represent the configuration.[2] For example, to represent the configuration of a door, we need only one number, the angle θ that the door rotates about its hinge. The configuration of a point on a plane can be described by two coordinates, (x, y). To represent the configuration of a coin lying on a flat table, we need three coordinates: two specifying the location (x, y) on the table of a particular point on the coin, and one specifying the coin's orientation, θ. (See Figure 2.1.)

The minimum number of real-valued coordinates needed to represent the configuration is the **degrees of freedom** (**dof**) of the robot. Thus a coin (viewed as a robot) lying on a table has three degrees of freedom. If the coin could lie heads up or tails up, the configuration space still has only three degrees of freedom, since the fourth variable, representing which side of the coin is up, can only take values in the discrete set $\{\text{heads}, \text{tails}\}$; it does not take a continuous range of real values as required by our definition.

Definition 2.1. The **configuration** of a robot is a complete specification of the positions of every point of the robot. The minimum number n of real-valued coordinates needed to represent the configuration is the **degrees of freedom** (dof) of the robot. The n-dimensional space containing all possible

[1] In the sense of "where are the links of the robot situated?"

[2] Compare with trying to represent the configuration of a pillow.

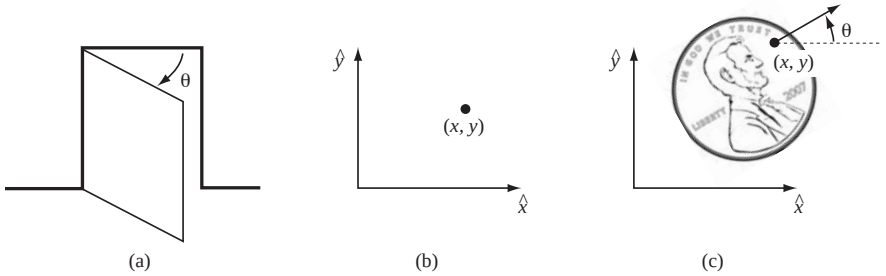

Figure 2.1: (a) The configuration of a door is described by its angle θ. (b) The configuration of a point in a plane is described by coordinates (x, y). (c) The configuration of a penny on a table is described by (x, y, θ).

configurations of the robot is called the **configuration space**.

In this chapter we study the configuration space and degrees of freedom of general robots. Since our robots are constructed of rigid bodies, we first examine the configuration space and degrees of freedom of rigid bodies. We then examine these concepts for general robots. The chapter concludes with a discussion of the configuration space of a robot's end-effector, or its **task space**. In the next chapter we study in more detail the various mathematical representations for the configuration space of rigid bodies.

2.1 Configuration Space of a Rigid Body

Continuing with the example of the coin lying on the table, choose three points A, B, and C fixed to the coin (Figure 2.2(a)). The positions of these points in the plane are written (x_A, y_A), (x_B, y_B), and (x_C, y_C). If these points could be placed independently anywhere in the plane, we would have six degrees of freedom—two for each of the three points. However, a rigid body is defined as one where all points on the body maintain constant distances from each other, i.e.,

$$d(A, B) = \sqrt{(x_A - x_B)^2 + (y_A - y_B)^2}$$
$$d(B, C) = \sqrt{(x_B - x_C)^2 + (y_B - y_C)^2}$$
$$d(A, C) = \sqrt{(x_A - x_C)^2 + (y_A - y_C)^2}$$

cannot change no matter how the coin moves. Let's call these constant distances d_{AB}, d_{BC}, and d_{AC}.

To determine the degrees of freedom of the coin, we first choose the position of point A in the plane (Figure 2.2(b)). We may choose it to be anything we want, so we have two degrees of freedom to specify, (x_A, y_A). Once this is specified, however, the constraint $d(A, B) = d_{AB}$ restricts the choice of (x_B, y_B) to those points on the circle of radius d_{AB} centered at A. Thus the two apparent

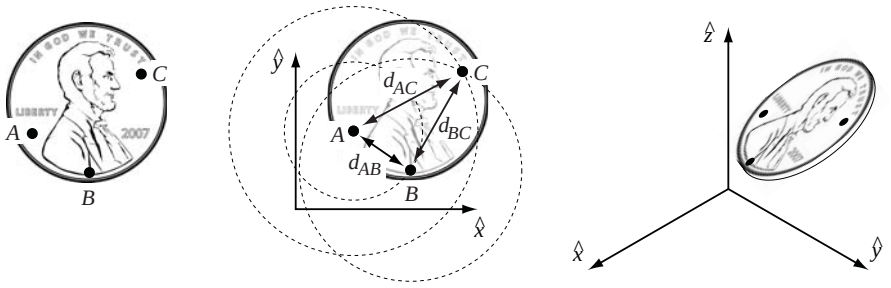

Figure 2.2: (a) Choosing three points fixed to the penny. (b) Once the location of A is chosen, B must lie on a circle of radius d_{AB} centered at A. Once the location of B is chosen, C must lie at the intersection of circles centered at A and B. Only one of these two intersections corresponds to the "heads up" configuration. (c) The configuration of a penny in three-dimensional space is given by the three coordinates of A, two angles to the point B on the sphere of radius d_{AB} centered at A, and one angle to the point C on the circle defined by the intersection of the a sphere centered at A and a sphere centered at B.

freedoms (x_B and y_B) are reduced by one constraint, for a total of one actual freedom in choosing the location of B. This freedom is the angle specifying the location of B on the circle centered at A; let's call this angle ϕ_{AB}, and define it to be the angle that the vector $\overrightarrow{AB}$ makes with the $\hat{x}$-axis.

Finally, once we have chosen the location of point B, the two apparent freedoms to place C (x_C and y_C) are eliminated by the two constraints $d(A,C) = d_{AC}$ and $d(B,C) = d_{BC}$. In other words, once we have placed A and B, the location of C is fixed. The coin has exactly three degrees of freedom in the plane, which can be specified by (x_A, y_A, ϕ_{AB}).

Suppose we were to choose an additional point on the coin, D, thus introducing three additional constraints: $d(A,D) = d_{AD}$, $d(B,D) = d_{BD}$, and $d(C,D) = d_{CD}$. Although these constraints may appear to be independent, they are in fact *redundant*—only two of the three constraints are independent. To see why, the constraint $d(A,D) = d_{AD}$ restricts D to lie on a circle of radius d_{AD} centered at A. Similarly, the constraint $d(B,D) = d_{BD}$ restricts D to lie on a circle of radius d_{BD} centered at B. These two constraints together thus uniquely specify D to be the point of intersection of these two circles. The third constraint $d_{CD} = d_{CD}$ is therefore not needed; points C, D, and in fact all other points on the coin, do not add any more freedoms or constraints to the coin's configuration space.

We have been applying the following general rule for determining the number of degrees of freedom of a system:

$$\begin{aligned}\text{Degrees of freedom} = {} & (\text{Sum of freedoms of the points}) - \\ & (\text{Number of independent constraints}). \end{aligned} \tag{2.1}$$

This rule can also be expressed in terms of the number of variables and independent equations that describe the system:

$$\begin{aligned}\text{Degrees of freedom} = &\ (\text{Number of variables}) - \\ &\ (\text{Number of independent equations}).\end{aligned} \tag{2.2}$$

We can use this general rule to determine the number of freedoms of a rigid body in three dimensions as well. For example, assume our coin is no longer confined to the table (Figure 2.2(c)). The three points A, B, and C are now defined by (x_A, y_A, z_A), (x_B, y_B, z_B), and (x_C, y_C, z_C). Point A can be placed freely (three degrees of freedom). The location of point B is subject to the constraint $d(A, B) = d_{AB}$, meaning it must lie on the sphere of radius d_{AB} centered at A. Thus we have $3 - 1 = 2$ freedoms to specify, which can be expressed as a latitude and longitude for a point on the sphere. Finally, the location of point C must lie at the intersection of spheres centered at A and B of radius d_{AC} and d_{BC}, respectively. The intersection of two spheres is a circle, and thus the location of point C can be described by an angle that parametrizes this circle. Point C therefore adds $3-2 = 1$ freedom. Once the position of point C is chosen, the coin is fixed in space.

In summary, a rigid body in three-dimensional space has six freedoms, which can be described by the three coordinates parametrizing point A, the two angles parametrizing point B, and one angle parametrizing point C. Other six-parameter representations for the six freedoms of a rigid body are discussed in Chapter 3.

We have just estabilshed that a rigid body moving in three-dimensional space, which we henceforth call a **spatial rigid body**, has six degrees of freedom, three of which are linear and three angular. Similarly, a rigid body moving in a two-dimensional plane, which we henceforth call a **planar rigid body**, has two linear freedoms and one angular freedom. This latter result can also be obtained by considering the planar rigid body to be a spatial rigid body with six degrees of freedom, but with the three independent constraints $z_A = z_B = z_C = 0$ imposed.

Since our robots will be constructed of rigid bodies, we express Equation (2.1) as follows:

$$\begin{aligned}\text{Degrees of freedom} = &\ (\text{Sum of freedoms of the bodies}) - \\ &\ (\text{Number of independent constraints}).\end{aligned} \tag{2.3}$$

Equation (2.3) forms the basis for determining the degrees of freedom of general robots, which is the topic of the next section.

2.2 Configuration Space of a Robot

Consider once again the door example of Figure 2.1(a), consisting of a single rigid body connected to the wall by a hinge joint. From the previous section we know that the door has only one degree of freedom, conveniently parametrized

by the hinge joint angle θ. The reasoning goes as follows. Without the hinge joint, the door is free to move in three-dimensional space and has six degrees of freedom. By connecting the door to the wall via the hinge joint, five independent constraints are imposed on the motion of the door; from Equation (2.3) we conclude that the door has one degree of freedom. Alternatively, we can view the door from above and regard it as a planar body, which has three degrees of freedom. The hinge joint then imposes two independent constraints, and again from Equation (2.3) we conclude that the door has one degree of freedom. Its configuration space is parametrized by some range in the interval $[0, 2\pi]$ over which θ is allowed to vary.

In both cases we see that joints have the effect of constraining the motion of the rigid body, and thus reducing the overall degrees of freedom. It seems plausible that a formula can be obtained for determining the degrees of freedom of a robot, simply by counting the number of rigid bodies and joints. This is in fact the case, and in this section we derive Grübler's formula for determining the degrees of freedom of planar and spatial robots. We then examine mathematical representations of a robot's configuration space.

2.2.1 Degrees of Freedom of a Robot

Robot Joints

Figure 2.3 illustrates the basic joints found in typical robots. Every joint connects exactly two links; we do not allow joints that simultaneously connect three or more links. The **revolute joint** (R), also called a hinge joint, allows for rotational motion about the joint axis. The **prismatic joint** (P), also called a sliding or linear joint, allows for translational (or rectilinear) motion along the direction of the joint axis. Both revolute and prismatic joints are one-dof joints; for the revolute joint, its degree of freedom is parameterized by the angle of rotation about the joint axis, while the prismatic joint's degree of freedom is parameterized by the translation distance along the joint axis. The **screw joint** (H), also called a helical joint, is another one-dof joint whose motion consists of simultaneous rotation and translation.

Joints can also have multiple degrees of freedom. The **cylindrical joint** (C) is a two-dof joint that allows for independent translations and rotations about a single fixed joint axis. The **universal joint** (U) is another two-dof joint constructed by serially connecting a pair of revolute joints so that their joint axes are orthogonal. The **spherical joint** (S), also called a ball-and-socket joint, has three degrees of freedom and functions much like our shoulder joint.

Grübler's Formula for Planar Robots

Grübler's formula allows one to calculate the mobility of a robot based on the number of links, and the number and type of joints. The formula is in fact a more formal expression of Equation **??**, and in this section we state this formula for planar robots, i.e., robots whose links all move in a single fixed plane. First,

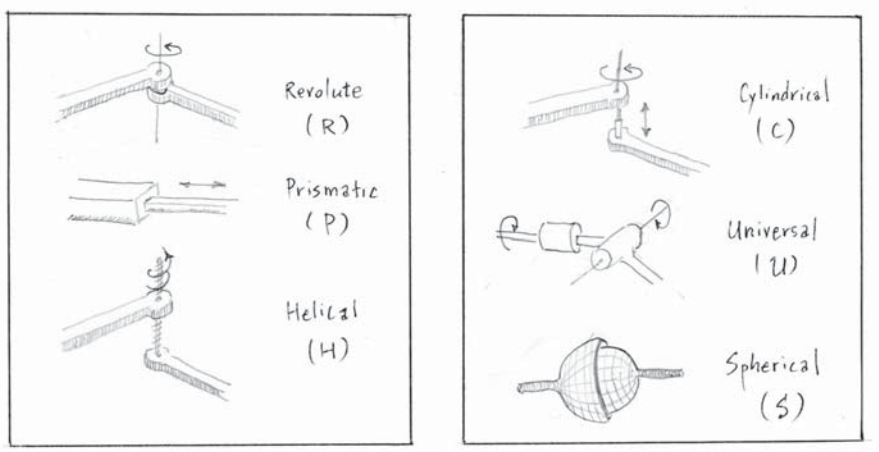

Figure 2.3: Typical robot joints.

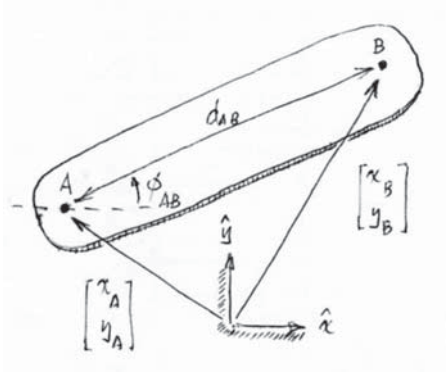

Figure 2.4: Coordinates for a planar rigid body.

consider a single rigid body in the plane (Figure 2.4). Choose two points A and B whose (x, y) coordinates with respect to some fixed reference frame are (x_A, y_A) and (x_B, y_B), respectively. Of the four coordinates, we know that only three of these coordinates can be chosen independently, because of the rigid body constraint that the distance between A and B is a fixed constant, i.e.,

$$d_{AB} = \sqrt{(x_A - x_B)^2 + (y_A - y_B)^2} \tag{2.4}$$

is constant. Define ϕ_{AB} to be the angle between the x-axis of the fixed frame and the vector $\overrightarrow{AB}$. Then (x_A, y_A, ϕ_{AB}) serve as a set of three independent coordinates that parametrizes the configuration of the planar rigid body. In

fact, (x_B, y_B) can be determined to be

$$\begin{aligned} x_B &= x_A + d_{AB}\cos\phi_{AB} \\ y_B &= y_A + d_{AB}\sin\phi_{AB}. \end{aligned}$$

Now consider another planar rigid body with two points C and D chosen. Let their coordinates with respect to the same fixed frame be (x_C, y_C) and (x_D, y_D), respectively, subject to the distance constraint

$$d_{CD} = \sqrt{(x_C - x_D)^2 + (y_C - y_D)^2} \tag{2.5}$$

is constant. Defining angle ϕ_{CD} in a similar fashion, it then follows that

$$\begin{aligned} x_D &= x_C + d_{CD}\cos\phi_{CD} \\ y_D &= y_C + d_{CD}\sin\phi_{CD}. \end{aligned}$$

Suppose point B of the first body and point C of the second body are connected by a revolute joint. Then in addition to the distance constraints (2.4) and (2.5), the revolute joint connecting the two bodies imposes an additional two independent constraints:

$$x_B = x_C \tag{2.6}$$
$$y_B = y_C \tag{2.7}$$

Thus, we have eight coordinates $(x_A, y_A, \ldots, x_D, y_D)$ and four constraint equations, leading to $8 - 4 = 4$ degrees of freedom for this system. If we define the revolute joint angle θ by $\theta = \phi_{CD} - \phi_{AB}$, then $(x_A, y_A, \phi_{AB}, \theta)$ serve as a convenient set of four independent coordinates that parametrize the configuration space of this system.

If points B and C are instead connected by a prismatic joint, allowing for translation in some fixed direction (t_x, t_y) (assume this direction vector is a unit vector, i.e., $\sqrt{t_x^2 + t_y^2} = 1$), then the two constraints (2.6) and (2.7) are now replaced by

$$x_C = x_B + d\,t_x \tag{2.8}$$
$$y_C = y_B + d\,t_y, \tag{2.9}$$

where the scalar d now represents the translation distance in the direction (t_x, t_y). Again we have four constraints imposed on eight variables, leading to $8 - 4 = 4$ degrees of freedom for this system. The coordinates (x_A, y_A, ϕ_{AB}, d) serve as a set of four independent coordinates that parametrize the configuration space of this system.

Now suppose the two bodies are instead connected by a two-dof joint, obtained as the serial connection of the above R and P joints. In this case deriving the additional constraints on the eight point coordinates $\{(x_A, y_A), \ldots, (x_D, y_D)\}$ is not as straightforward as in the two previous cases. It would seem, for example, that the constraints will depend on the sequence in which the R and P

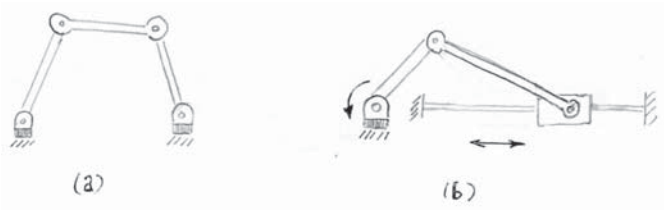

Figure 2.5: (a) Four-bar linkage (b) slider-crank mechanism.

joints are connected, e.g., whether it is an RP joint or a PR joint. What is clear, however, is that knowledge of the two joint values θ and d completely specifies coordinates (x_C, y_C) and (x_D, y_D) on the second body. Equivalently, the eight coordinates for points $\{A, B, C, D\}$ can be uniquely determined from knowledge of the five variables $(x_A, y_A, \phi_{AB}, \theta, d)$. The two-dof joint thus imposes a single constraint on the six independent variables $(x_A, y_A, \phi_{AB}, x_C, y_C, \phi_{CD})$, leading to five degrees of freedom.

In summary, a one-dof joint reduces the degrees of freedom of the system by two, while a two-dof joint reduces the degrees of freedom by one. This observation is in fact exactly what is expressed by (2.3). We now state Grübler's formula for planar robots:

Proposition 2.1. *Consider a planar robot consisting of N links, where the ground is also regarded as a link. Let J denote the total number of joints, and let f_i be the degrees of freedom of the i-th joint. The degrees of freedom (dof) of the robotic mechanism can then be evaluated from the formula*

$$\begin{aligned} dof &= 3(N-1) - \sum_{i=1}^{J}(3 - f_i) \\ &= 3(N-1-J) + \sum_{i=1}^{J} f_i \end{aligned} \tag{2.10}$$

Example 2.1. Four-bar linkage and slider-crank mechanism
Consider the four-bar linkage shown in Figure 2.5(a). This planar mechanism consists of four links (one of them ground) connected in a single closed loop by four revolute joints. Subsituting $N = 4$, $J = 4$, and $f_i = 1, i = 1, \ldots, 4$ into the planar version of Grübler's formula, we determine that the four-bar linkage has one degree of freedom.

The slider-crank mechanism of Figure 2.5(b) can be analyzed in two ways: (i) the mechanism consists of three revolute joints and one prismatic joint ($J = 4$, and each $f_i = 1$), and four links ($N = 4$, including the ground link), or (ii) the mechanism consists of two revolute joints ($f_i = 1$) and one RP joint ($f_i = 2$; the RP joint is a concatenation of a revolute and prismatic joint), and three links ($N = 3$; remember that each joint connects precisely two bodies). In both cases the the mechanism has one degree of freedom.

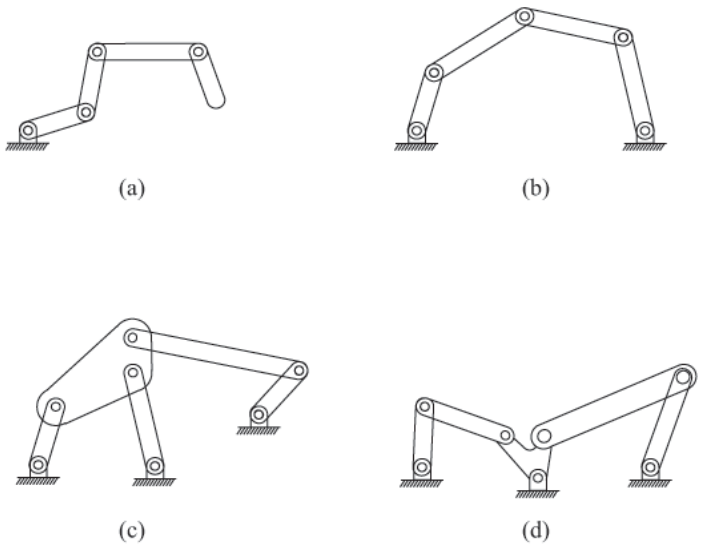

Figure 2.6: (a) k-link planar serial chain. (b) Five-bar planar linkage. (c) Stephenson six-bar linkage. (d) Watt six-bar linkage.

Example 2.2. Some classical planar mechanisms
Let us now apply Grübler's formula to several classical planar mechanisms as shown in Figure 2.6. For the k-link planar serial chain in (a), $N = k + 1$ (k links plus ground), $J = k$, and since all the joints are revolute, each $f_i = 1$. Therefore,

$$\text{dof} = 3((k + 1) - 1 - k) + k = k$$

as expected. For the five-bar linkage of (b), $N = 5$ (4 links plus ground), $J = 5$, and since all joints are revolute, each $f_i = 1$. Therefore,

$$\text{dof} = 3(5 - 1 - 5) + 5 = 2.$$

For the Stephenson six-bar linkage in (c), we have $N = 6$, $J = 7$, and $f_i = 1$ for all i, so that

$$\text{dof} = (3(6 - 1 - 7) + 7 = 1.$$

Finally, for the Watt six-bar linkage in (d), we have $N = 6$, $J = 7$, and $f_i = 1$ for all i, so that like the Stephenson six-bar linkage,

$$\text{dof} = (3(6 - 1 - 7) + 7 = 1.$$

Example 2.3. A planar mechanism with overlapping joints
Consider the planar mechanism illustrated in Figure 2.7. Again, there are a

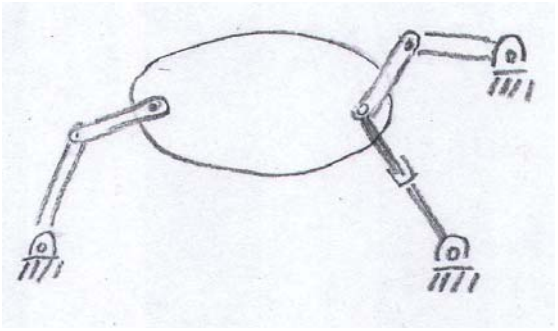

Figure 2.7: A planar mechanism with two overlapping joints.

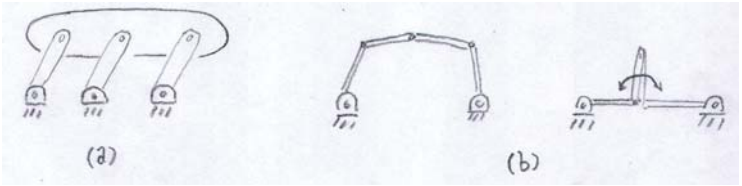

Figure 2.8: (a) A parallelogram linkage; (b) The five-bar linkage in a regular and singular configuration.

number of ways to derive its mobility using Grübler's formula. If all the joints are regarded as either revolute or prismatic, then the mechanism consists of seven links ($N = 7$), eight revolute joints, and one prismatic joint. Note that three bodies meet at a single point on the right. Recalling that a joint connects exactly two links, the joint at this intersection point is not a single revolute joint, but in fact two revolute joints overlapping each other. Substituting into Grübler's formula,

$$\text{dof} = 3(8 - 1 - 9) + 9(1) = 3.$$

Alternatively, the revolute-prismatic pair connected to this intersection point can be regarded as a single two-dof joint. In this case the number of links is $N = 7$, with six revolute joints and a single two-dof revolute-prismatic pair. Grübler's formula identically yields

$$\text{dof} = 3(7 - 1 - 9) + 6(1) + 1(2) = 3.$$

Example 2.4. Grübler's formula and singularities
Consider the parallelogram linkage of Figure 2.8(a). Here $N = 5$, $J = 6$, and $f_i = 1$ for each link; from Grübler's formula, the degrees of freedom is given by $3(5-1-6)+6 = 0$. A mechanism with zero degrees of freedom is by definition a rigid structure. However, if the three parallel links are of the same length and the two horizontal rows of joints are collinear as implied by the figure, the mechanism can in fact move, with one degree of freedom.

A similar situation occurs for the five-bar linkage of Figure 2.8(b). If the two joints connected to ground are fixed, then the five-bar linkage should, given that it has two degrees of freedom, become a rigid structure. Note however that if the two middle links overlap each other as shown in the figure, then these links are able to rotate freely about the two overlapping joints. Of course, the link lengths need to be chosen in such a way that this configuration is feasible. If a different pair of joints is fixed, then the mechanism does become a rigid structure as expected.

Grübler's formula is unable to distinguish singular cases like those just described. These phenomena are examples of configuration space singularities arising in closed chains, which is discussed in detail in Chapter 7.

Grübler's Formula for Spatial Robots

Having established that a minimum of six independent parameters is required to describe the position and orientation of a spatial rigid body, we now proceed as we did in the derivation of the planar version of Grübler's formula. If two spatial rigid bodies are connected by a k-dof joint, then only $12-(6-k) = 6+k$ independent parameters are required. Based on this observation, **Grübler's formula for spatial robots** can be stated as follows:

Proposition 2.2. *Consider a spatial robot consisting of N links (including ground), J joints (labelled from from 1 to J), and denote by f_i the degrees of freedom of joint i. The degrees of freedom (dof) of the robot can then be evaluated from the formula*

$$\begin{aligned} dof &= 6(N-1) - \sum_{i=1}^{J}(6-f_i) \\ &= 6(N-1-J) + \sum_{i=1}^{J} f_i. \end{aligned} \tag{2.11}$$

We remind the reader that the spatial version of this formula should **not** be applied to planar mechanisms, and vice versa. We now consider some well-known examples of spatial robots.

Example 2.5. Stewart-Gough Platform
The Stewart-Gough platform shown in Figure 2.9 consists of two platforms—the lower one stationary, the upper one mobile—connected by six serial chain structures, or legs. Each leg consists of a universal-prismatic-spherical (*UPS*) joint arrangement. The total number of links (including the fixed lower platform, which is regarded as the ground link) is $N = 14$. There are six universal joints (each with two degrees of freedom, $f_i = 2$), six prismatic joints (each with a single degree of freedom, $f_i = 1$), and six spherical joints (each with three degrees of freedom, $f_i = 3$). The total number of joints is 18. Substituting these values into the spatial version of Grübler's formula,

$$\text{dof} = 6(14-1-18) + 6(1) + 6(2) + 6(3) = 6.$$

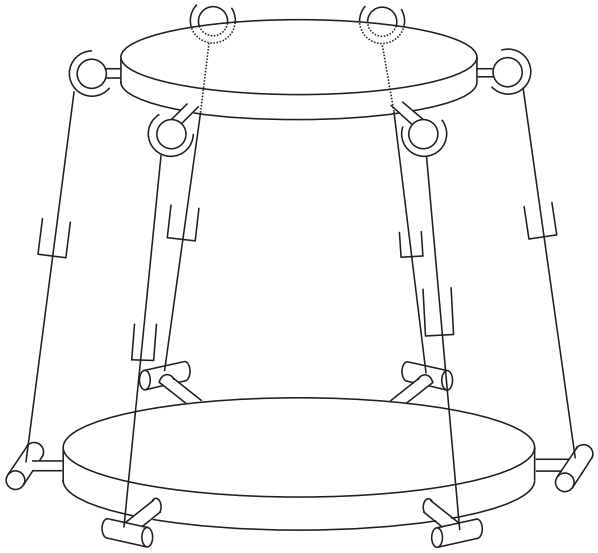

Figure 2.9: The Stewart-Gough Platform.

In some versions of the Stewart-Gough platform the six universal joints are replaced by spherical joints. Grübler's formula then indicates that this mechanism has twelve degrees of freedom. This result may seem surprising but is correct; replacing each universal joint by a spherical joint introduces an extra degree of mobility in each leg, by allowing torsional rotations about the axis leg. Note however that this torsional rotation has no effect on the motion of the mobile platform.

Example 2.6. $3 \times UPU$ platform
The next example, shown in Figure 2.10 is also a platform structure, in which the two platforms are connected by three UPU serial chain structures. The total number of links is $N = 8$. There are six universal joints, and three prismatic joints, making for a total of $J = 9$ joints. Substituting these values into Grübler's formula leads to

$$\text{dof} = 6(8 - 1 - 9) + 3(1) + 6(2) = 3.$$

The $3 \times UPU$ mechanism has three degrees of freedom according to Grübler's formula, but constructed prototypes of this mechanism reveal extra degrees of freedom not predicted by Grübler's formula. These and other subtle aspects of the $3 \times UPU$ platform are further discussed in Chapter 7.

2.2.2 Parametrizing the Configuration Space

Recall that by definition a robot's configuration is a complete specification of the positions of every point on the robot, and that the set of all configurations constitutes the robot's configuration space. For a single planar rigid body,

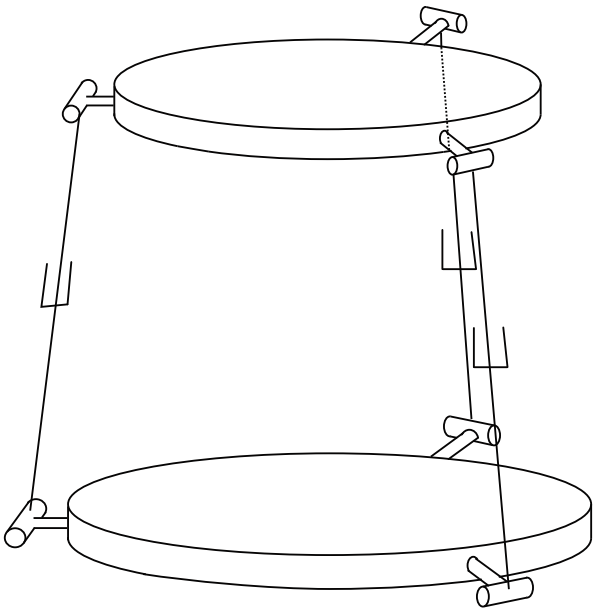

Figure 2.10: The $3 \times UPU$ platform.

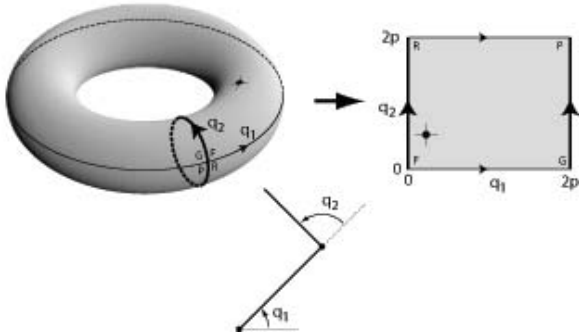

Figure 2.11: The configuration space of the 2R planar serial chain.

its configuration can be completely characterized by specifying three independent coordinates: (x, y, θ), where $(x, y) \in \mathbb{R}$ and $\theta \in [0, 2\pi]$. The configuration space is thus three-dimensional, and the coordinates (x, y, θ) are an **explicit parametrization**. Alternatively, we could choose to parametrize its configuration by the coordinates of two points A and B on the body, denoted (x_A, y_A) and (x_B, y_B), respectively. Of course, the rigid body constraint

$$\sqrt{(x_A - y_A)^2 + (x_B - y_B)^2} = d_{AB} \tag{2.12}$$

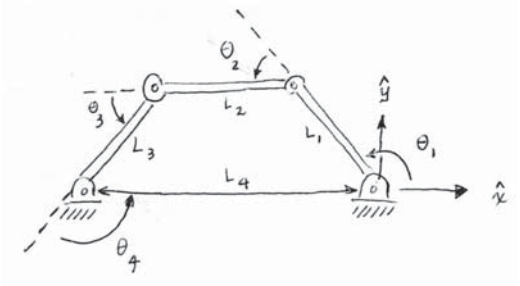

Figure 2.12: The four-bar linkage.

where d_{AB} is constant, means these four coordinates are not independent. Thus the equality (2.12) is an **implicit parametrization** of the configuration space.

The configuration spaces of general robots usually admit both explicit and implicit parametrizations. In the case of open chains, an explicit parametrization for the configuration space is offered by the joint variables. For the planar $2R$ open chain of Figure 2.11, specifying values for the two revolute joints (q_1, q_2) completely specifies the position and orientation of the two links. The configuration space in this case is $[0, 2\pi] \times [0, 2\pi]$, which can be visualized as the two-dimensional torus (the doughnut-like surface) shown in Figure 2.11. Note that by cutting the torus along the two solid lines indicated in the figure, the torus can be "flattened" into the rectangle on the right (called the "flat torus").

For closed chains (that is, robots containing one or more closed loops), usually an implicit parametrization is more easily obtained; obtaining an explicit parametrization will typically involve solving a set of nonlinear equations. As an example, consider the planar four-bar linkage of Figure 2.12, which has one degree of freedom. The fact that the four links always form a closed loop can be expressed in the form of the following three equations:

$$\begin{aligned} L_1 \cos\theta_1 + L_2 \cos(\theta_1 + \theta_2) + \ldots + L_4 \cos(\theta_1 + \ldots + \theta_4) &= 0 \\ L_1 \sin\theta_1 + L_2 \sin(\theta_1 + \theta_2) + \ldots + L_4 \sin(\theta_1 + \ldots + \theta_4) &= 0 \\ \theta_1 + \theta_2 + \theta_3 + \theta_4 + \pi &= 0. \end{aligned}$$

These equations are obtained by viewing the four-bar linkage as a serial chain with four revolute joints, in which (i) the tip of link L_4 always coincides with the origin, and (ii) the orientation of link L_4 is always horizontal.

These equations are sometimes referred to as the loop closure equations. For the four four-bar linkage they are given by a set of three equations in four unknowns. The set of all solutions forms a curve in the four-dimensional joint space parametrized by the coordinates $(\theta_1, \ldots, \theta_4)$, and constitutes the configuration space.

For general robots containing one or more closed loops, the configuration

space can be implicitly parametrized by loop closure equations of the form

$$g(\theta) = \begin{bmatrix} g_1(\theta_1, \ldots, \theta_n) \\ \vdots \\ g_k(\theta_1, \ldots, \theta_n) \end{bmatrix} = 0, \tag{2.13}$$

where $\theta \in \mathbb{R}^n$ denotes the vector of joint variables, and $g : \mathbb{R}^n \to \mathbb{R}^k$ is a set of k independent equations, with $k \leq n$. Such constraints are known as **holonomic constraints**. The configuration space can thus be viewed as a multidimensional surface of dimension $n - k$ embedded in $\mathbb{R}^n$.

2.2.3 Pfaffian Constraints

Suppose a closed chain robot with loop closure equations $g(\theta) = 0$, $g : \mathbb{R}^n \to \mathbb{R}^k$, is in motion, following the time trajectory $\theta(t)$. Then differentiating both sides of $g(\theta(t)) = 0$ with respect to t, we obtain

$$\begin{aligned} \frac{d}{dt} g(\theta(t)) &= \begin{bmatrix} \frac{\partial g_1}{\partial \theta_1}(\theta)\dot{\theta}_1 + \ldots + \frac{\partial g_1}{\partial \theta_n}(\theta)\dot{\theta}_n \\ \vdots \\ \frac{\partial g_k}{\partial \theta_1}(\theta)\dot{\theta}_1 + \ldots + \frac{\partial g_k}{\partial \theta_n}(\theta)\dot{\theta}_n \end{bmatrix} \\ &= \begin{bmatrix} \frac{\partial g_1}{\partial \theta_1}(\theta) & \cdots & \frac{\partial g_1}{\partial \theta_n}(\theta) \\ \vdots & \ddots & \vdots \\ \frac{\partial g_k}{\partial \theta_1}(\theta) & \cdots & \frac{\partial g_k}{\partial \theta_n}(\theta) \end{bmatrix} \begin{bmatrix} \dot{\theta}_1 \\ \vdots \\ \dot{\theta}_n \end{bmatrix} \\ &= \frac{\partial g}{\partial \theta}(\theta)\dot{\theta} \\ &= 0. \end{aligned} \tag{2.14}$$

Here $\dot{\theta}_i$ denotes the time derivative of θ_i with respect to time t, $\frac{\partial g}{\partial \theta}(\theta) \in \mathbb{R}^{k \times n}$, and $\theta, \dot{\theta} \in \mathbb{R}^n$. From the above we see that the joint velocity vector $\dot{\theta} \in \mathbb{R}^n$ cannot be arbitrary, but must always satisfy

$$\frac{\partial g}{\partial \theta}(\theta)\dot{\theta} = 0. \tag{2.15}$$

Constraints on $\dot{\theta}$ of the form

$$A(\theta)\dot{\theta} = 0, \tag{2.16}$$

where $A(\theta) \in \mathbb{R}^{k \times n}$, are called **Pfaffian constraints**. We saw earlier that differentiating the loop closure equation $g(\theta(t)) = 0$ with respect to t leads to such a constraint. Conversely, one could regard $g(\theta)$ as being the "integral" of $\frac{\partial g}{\partial \theta}(\theta)$; for this reason constraints of the form $g(\theta) = 0$ are also called **integrable constraints**, or **holonomic constraints**.

We now consider another class of Pfaffian constraint that is fundamentally different from the holonomic type. To illustrate with a concrete example, consider the coin of radius r rolling on the plane as shown in Figure 2.13. A

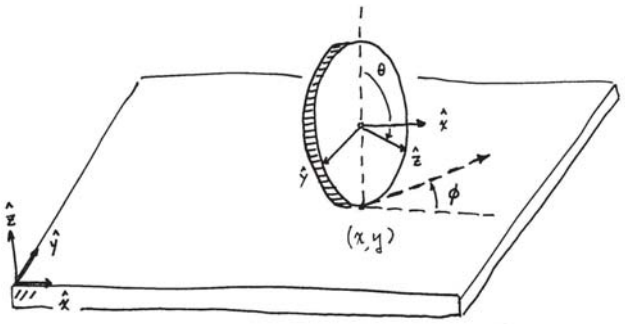

Figure 2.13: A coin rolling on a plane without slipping.

body-fixed frame is attached to the center of the coin, in such a way that the axis of rotation is always directed along the $\hat{x}$-axis. Since this frame is attached to the coin, the $\hat{y}$- and $\hat{z}$-axes rotate about the $\hat{x}$-axis at the same rate as the disk. The coin is assumed to always remain normal to the plane (that is, the $\hat{x}$-axis of the coin reference frame always remains parallel to the plane).

Under these assumptions, a minimum of four parameters are needed to completely describe the configuration of the coin. A convenient set is given by the contact point coordinates (x, y), the steering angle ϕ, and the angle of rotation θ (see Figure 2.13). The configuration space of the coin is therefore $\mathbb{R}^2 \times T^2$, where T^2 is the two-dimensional torus parametrized by the angles ϕ and θ. This configuration space is four-dimensional.

Let us now express, in mathematical form, the fact that the coin rolls without slipping. The coin must always roll in the direction indicated by $(\cos\phi, \sin\phi)$, with forward speed $r\dot{\theta}$:

$$\begin{bmatrix} \dot{x} \\ \dot{y} \end{bmatrix} = r\dot{\theta} \begin{bmatrix} \cos\phi \\ \sin\phi \end{bmatrix}. \tag{2.17}$$

Collecting the four configuration space coordinates into a single vector $q = (x, y, \phi, \theta) \in \mathbb{R}^2 \times T^2$, the above no-slip rolling constraint can then be expressed in the form

$$\begin{bmatrix} 1 & 0 & 0 & -r\cos q_3 \\ 0 & 1 & 0 & -r\sin q_3 \end{bmatrix} \dot{q} = 0. \tag{2.18}$$

This is also a differential constraint of the form $A(q)\dot{q} = 0$, $A(q) \in \mathbb{R}^{2\times 4}$.

This constraint is not integrable; that is, That is, for the $A(q)$ given in (2.18), there does not exist any differentiable $g : \mathbb{R}^4 \to \mathbb{R}^2$ such that $\frac{\partial g}{\partial q} = A(q)$. To see why, there would have to exist a differentiable $g_1(q)$ that satisfied the following

four equalities:

$$\begin{aligned}
\frac{\partial g_1}{\partial q_1} &= 1 \rightarrow g_1(q) = q_1 + h_1(q_2, q_3, q_4) \\
\frac{\partial g_1}{\partial q_2} &= 0 \rightarrow g_1(q) = h_2(q_1, q_3, q_4) \\
\frac{\partial g_1}{\partial q_3} &= 0 \rightarrow g_1(q) = h_3(q_1, q_2, q_4) \\
\frac{\partial g_1}{\partial q_4} &= -r\cos q_3 \rightarrow g_1(q) = -rq_4 \cos q_3 + h_4(q_1, q_2, q_3),
\end{aligned}$$

for some h_i, $i = 1, \ldots, 4$ differentiable in each of its variables, and by inspection it should be clear that no such $g_1(q)$ exists. It can be similarly be shown that $g_2(q)$ also does not exist, so that the constraint (2.18) is nonintegrable. A Pfaffian constraint that is nonintegrable is also called a **nonholonomic constraint.** Such constraints arise in a number of robotics contexts that involve rolling with slipping, e.g., wheeled vehicle kinematics, grasp contact kinematics. We examine nonholonomic constraints in greater detail later in the chapter on wheeled vehicles.

2.2.4 Task Space

We introduce one more piece of terminology via an example involving the planar $2R$ open chain (see Figure 2.14(a)). Suppose we take the Cartesian tip (a point) to be the end-effector. The region in the plane that the tip can reach is then called the **task space**, or the **workspace**, of the chain. The task space can be regarded as the configuration space of the end-effector. It is distinct from the configuration space of the robot in that any point in task space is not required to specify the full configuration of the robot; there may be a multitude or even infinity of robot configurations that map to the same task space point.

Two mechanisms with different configuration spaces may also have the same task space. For example, considering the Cartesian tip of the robot to be the end-effector and ignoring orientations, the planar $2R$ open chain with links of equal length three, and the planar $3R$ open chain with links of equal length two (see Figure 2.14(b)), will have the same task space despite having different configuration spaces.

Two mechanisms with the same configuration space may also have different task spaces. For example, taking the Cartesian tip to be the end-effector and ignoring orientations, the $2R$ open chain of Figure 2.14(a) has a planar disk as its task space, while the $2R$ open chain of Figure 2.14(c) has a sphere as its task space. Similarly, the $3R$ open chain of Figure 2.14(b) has a planar disk as its task space, while the $3R$ open chain of Figure 2.14(d) has the space of all possible orientations as its task space (this can be seen by noting that the three joint axes always intersect at the tip, so that the tip remains fixed—if a gripper were attached at the tip, then this gripper would be able to change orientations only).

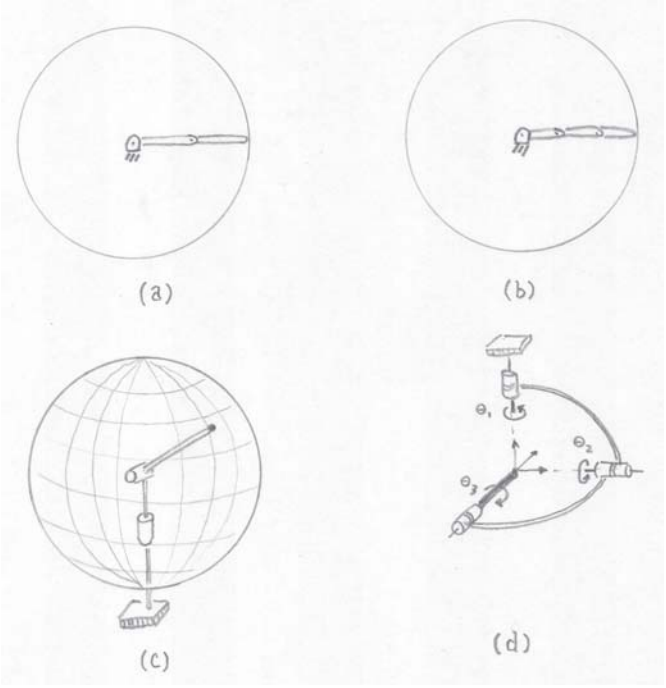

Figure 2.14: Examples of task spaces for various robots: (a) a planar $2R$ open chain; (b) a planar $3R$ open chain; (c) a spherical $2R$ open chain; (d) a $3R$ orienting mechanism.

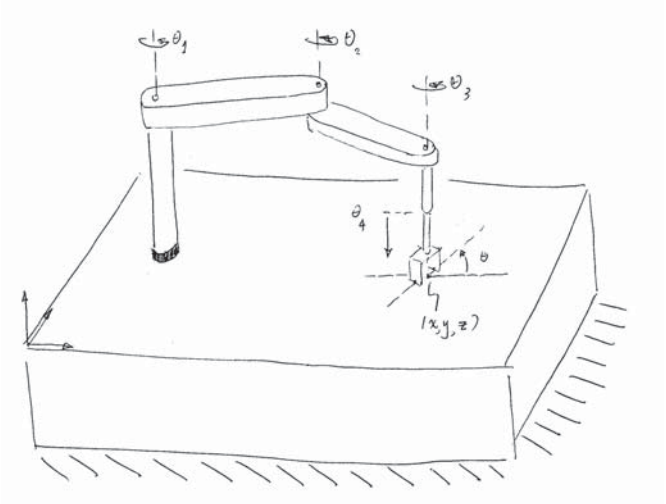

Figure 2.15: SCARA robot.

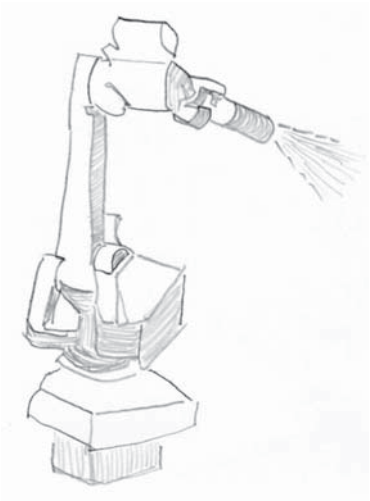

Figure 2.16: A spray painting robot.

Example 2.7. The SCARA robot of Figure 2.15 is an $RRRP$ open chain that is widely used for tabletop pick-and-place tasks. The end-effector configuration is completely described by the four parameters (x, y, z, ϕ), where (x, y, z) denotes the Cartesian position of the end-effector center point, and ϕ denotes the orientation of the end-effector in the x-y plane. Its task space is therefore $\mathbb{R}^3 \times [0, 2\pi]$.

Example 2.8. A standard $6R$ industrial manipulator can be adapted to spray painting applications as shown in Figure 2.16. The paint spray nozzle attached to the tip can be regarded as the end-effector. What is important is the Cartesian position of the spray nozzle, together with the direction in which the spray nozzle is pointing; rotations about the nozzle axis (which points in the direction in which paint is being sprayed) do not matter. The nozzle configuration can therefore be described by five coordinates: (x, y, z) for the Cartesian position of the nozzle, and spherical coordinates (θ, ϕ) to describe the direction in which the nozzle is pointing. Since (θ, ϕ) also parametrizes the unit sphere in $\mathbb{R}^3$, the task space as described is given by $\mathbb{R}^3 \times S^2$, where S^2 denotes the two-dimensional unit sphere in $\mathbb{R}^3$.

2.3 Summary

- A robot is mechanically constructed from **links** that are connected by various types of **joints**. The links are usually modelled as rigid bodies. An **end-effector** such as a gripper or gripper is attached to some link of the robot. **Actuators** deliver forces and torques to the joints, thereby causing motion of the robot.

- The most widely used one-dof joints are the **revolute joint**, which allows for rotation about the joint axis, and the **prismatic joint**, which allows for translation in the direction of the joint axis. Some common two-dof joints include the **cylindrical joint**, which is constructed by serially connecting a revolute and prismatic joint, and the **universal joint**, which is constructed by orthogonally connecting two revolute joints. The **spherical joint**, also known as **ball-in-socket joint**, is a three-dof joint whose function is similar to the human shoulder joint.

- The **configuration** of a rigid body is a specification of all of its points. For a rigid body moving in the plane, three independent parameters taking on a continuous range of values are needed to specify its configuration . For a rigid body moving in three-dimensional sapce, six independent parameters taking on a continuous range of values are needed to specify its configuration.

- The configuration of a robot is a specification of the configuration of all of its links. The robot's **configuration space** is the set of all possible robot configurations. The **degrees of freedom** of a robot is to the number of continuous parameters required to specify a robot's configuration.

- A robot's degrees of freedom can be calculated using **Grübler's formula**. For planar robots, i.e., robots whose links all move in a single fixed plane, the planar version of Grübler's formula is given by

$$\text{dof} = 3(N - 1 - J) + \sum_{i=1}^{J} f_i,$$

  where N is the number of links (including the ground link), J is the number of joints (the joints are labelled from 1 to J), and f_i is the degrees of freedom of joint i. For general spatial robots, i.e., robots whose links move in three-dimensional space, the spatial version of Grübler's Formula is given by

$$M = 6(N - 1 - J) + \sum_{i=1}^{J} f_i.$$

- A robot's configuration space can be parametrized explicitly or implicitly. For a robot with n degrees of freedom, an **explicit parametrization** requires n coordinates—usually taken to be the joint variables—with each coordinate taking on values in a continuous range. An **implicit parametrization** involves m coordinates with $m \geq n$, with the m coordinates subject to $m - n$ constraint equations. With the implicit parametrization, a robot's configuration space can be viewed as a multidimensional surface of dimension n embedded in a space of higher dimension m.

- The configuration space of an n-dof robot whose structure contains one or more closed loops can be implicitly parametrized by **loop closure equations** of the form $g(\theta) = 0$, where $\theta \in \mathbb{R}^m$ and $g : \mathbb{R}^m \to \mathbb{R}^{m-n}$, $m \geq n$. Such a constraint equation is called a **holonomic constraint**. Assuming $\theta(t)$ varies with time t, the holonomic constraint $g(\theta(t)) = 0$ can be differentiated with respect to t to yield

$$\frac{\partial g}{\partial \theta}(\theta)\dot{\theta} = 0,$$

  where $\frac{\partial g}{\partial \theta}(\theta)$ is a $(m-n) \times m$ matrix.

- A robot's motion can also be subject to velocity constraints of the form

$$A(\theta)\dot{\theta} = 0,$$

  where $A(\theta)$ is a $k \times m$ that cannot be expressed as the differential of some function $g(\theta)$, i.e., there does not exist any $g(\theta), g : \mathbb{R}^m \to \mathbb{R}^k$ such that

$$A(\theta) = \frac{\partial g}{\partial \theta}(\theta).$$

  Such constraints are said to be **nonholonomic constraints**, or **nonintegrable constraints**. Wheeled vehicles, and other applications in which robots are subject to rolling contact without slip, are subject to nonholonomic constraints.

- A robot's **task space** is the configuration space of its end-effector.

Notes and References

In the classical kinematics literature, structures that consist of links connected by joints are called **mechanisms** or **linkages**. The of the degrees of freedom of mechanisms is treated in most texts on mechanism analysis and design, e.g., [9]. In general, a robot's kinematic configuration space has the mathematical structure of a differentiable manifold. Some accessible introductions to differential geometry are [22], [8]. Configuration spaces are further examined in a motion planning context in [14], [5].

Chapter 3

Grasp Statics

Figure 3.1 shows a planar rigid body constrained by a set of four point contacts. Imagining the four point contacts to be the fingertips of a hand grasping an object, we will also refer to such an arrangement as a **grasp**. Let us now pose the following question: of the two contact arrangements shown, which is more stable, in the sense of being better able to withstand arbitrary external forces and moments applied to the grasped object?

Clearly whether there is friction at the contacts is relevant—that friction can only help matters should be fairly obvious. Our intuition, however, tells us that it should be possible to immobilize the object using only frictionless point contacts, provided we have a sufficient number of them and they are arranged properly. Let us examine this frictionless case more carefully. In grasp (a), any pure moment applied about the object center is likely to cause infinitesimal rotations in the plane. Grasp (b), on the other hand, seems better able to withstand arbitrary external forces and moments. If we imagine that the contacts were positioned somewhat loosely against the object, allowing the object some slight wiggle room, then grasp (a) would be more sensitive to external moments and forces, and thus more susceptible to unwanted displacements of the object, than grasp (b).

Now imagining the contacts to be the fingertips of a hand grasping an object,

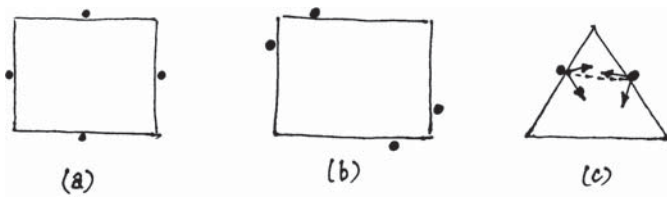

Figure 3.1: (a), (b) A planar rigid body constrained by four frictionless point contacts. (c) A rigid body constrained by two point contacts with friction. Gravity acts downward.

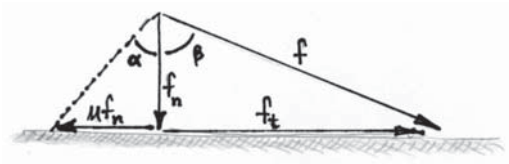

Figure 3.2: Tangential and normal components of the applied force. To avoid slipping, the angle β must not exceed α.

if there is no friction at each of the contacts, then the fingertips can only apply pushing forces that are normal to the object surface at the point of contact. If there is friction, then the fingertips can now apply forces in non-normal directions, up to a certain angle as measured from the surface normal (the extent of this angle depends on the amount of friction present; the greater the friction, the larger this angle). If the fingertips are able to generate forces at the contacts so as to resist any external force or moment applied to the object, then the object is said to be in **force closure**, and the grasp is a **force closure grasp**. If the contacts are placed so as to make any motion of the object impossible, the object is then said to be in **form closure**.

All form closure grasps are also force closure, but the reverse is not always true. For example, in Figure 3.1, two fingers with frictional point contacts are grasping a triangle in the presence of gravity (acting downward); if, e.g., the motors powering the fingers cannot provide sufficient forces, the triangle may fall despite the grasp being force closure.

In this chapter we shall develop methods for determining whether or not a grasp is force closure. The objects to be grasped are all assumed to be rigid bodies, and only grasps that can be modelled as a collection of point contacts will be considered. This is not as restrictive as it may first seem; other types of contacts (e.g., line and surface contacts) are, for practical purposes, often approximated as a collection of point contacts. Also, in the case of grasps that consist only of frictionless point contacts, it turns out that all force closure grasps are simultaneously form closure.

The conditions for force closure follow directly from the equations for static force-moment equilibrium. The analysis of force closure in the end reduces to a question about the existence of solutions to a linear equation of the form $Ax = b$, with a small but important twist. The main results of this chapter are a set of computational and graphical procedures for determining whether a grasp is force closure. We begin this chapter by first examining contact models, followed by an analysis of frictionless grasps, then grasps with friction.

3.1 Contact Models

We shall assume all objects are rigid bodies, and use Coulomb's law to model contact friction. Suppose a force f is applied at some point as shown in Fig-

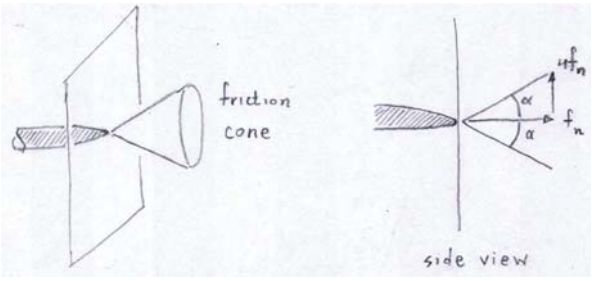

Figure 3.3: The friction cone in the case of point contact with a spatial rigid body.

ure 3.2. If there is no sliding at the contact point, Coulomb's law states that the tangential component of the force, denoted f_t, is related to the normal component, denoted f_n, by

$$|f_t| \leq \mu |f_n|, \tag{3.1}$$

where μ is called the **coefficient of friction**. μ is a dimensionless parameter that depends on the two materials in contact. $\mu = 0$ indicates no friction, while larger values of μ indicate increasing friction. Values of μ for typical materials generally range between 0.1 and 1. Sliding occurs when $|f_t| > \mu |f_n|$, with the friction friction force mu_n directed opposite to the direction of motion.

Another phenomenon that should be familiar from experience is that once sliding begins, the resisting frictional force tends to decrease—frictional resistance is usually greatest before the occurrence of sliding. To account for this difference, two friction coefficients are sometimes used: a static friction coefficient μ_s when the object is stationary, and a kinetic friction coefficient μ_k when the object is sliding, with $\mu_k \leq \mu_s$.

The underlying mechanisms of friction, which are microscopic in nature, are highly complex and difficult to model. Sophisticated friction models have been developed that take into account factors such as the speed of sliding, or the duration of static contact before sliding occurs. In this chapter we shall not use these advanced models, but instead work with a single static friction coefficient μ, which works reasonably well for the hard, dry materials that typical rigid bodies are made of.

The no-slip condition $|f_t| \leq \mu |f_n|$ can also be visualized geometrically. Referring again to Figure 3.2, to prevent the magnitude of the tangential force f_t from exceeding that of the frictional force μf_n, the angle β must not exceed α. In other words, the applied force must lie inside a cone of angle 2α, where α is

given by

$$\alpha = \tan^{-1} \mu. \tag{3.2}$$

Rather than characterize friction by its friction coefficient μ, in this chapter we shall for the most part use this friction cone characterization. The friction cone for a spatial rigid body is illustrated in Figure 3.3.

With this background, we now describe the three main contact models:

- A **frictionless point contact** occurs when there is no friction between the fingertip and the object. In this case $\mu = 0$, and forces can only be applied in the direction of the surface normal.

- In the case of a **point contact with friction**, any contact forces that lie within the friction cone will not cause any slipping at the contact point. Defining the $\hat{z}$-axis of the reference frame to be in the direction normal to the contact surface (see Figure 3.3), and expressing the contact force in terms of this frame by $f = (f_x, f_y, f_z)$, the friction cone is then characterized by
$$\left\{ f \in \mathbb{R}^3 \mid \sqrt{f_x^2 + f_y^2} < |\mu f_z| \right\}. \tag{3.3}$$

- In the **soft-finger contact** model, not only can forces be applied within the friction cone, but torques can also be applied about the contact normal. This is similar to the situation for human fingers, in which a finite patch of area on our fingertips is in contact with the object, allowing us to apply a torque τ about the contact normal. Similar to the Coulomb friction model, a simple model for the frictional moment is given by the torsional friction coefficient γ. In this case the friction cone is given by
$$\left\{ f \in \mathbb{R}^3 \text{ and } \tau \in \mathbb{R} \mid \sqrt{f_x^2 + f_y^2} < \mu |f_z| \text{ and } |\tau| \leq \gamma |f_z| \right\}, \tag{3.4}$$
where $f = (f_x, f_y, f_z)$ is defined in terms of the same reference frame used earlier. Although we shall not have occasion to use soft finger contact models in this chapter, we include its characterization here for completeness.

3.2 Frictionless Grasps

3.2.1 Static Equilibrium and Force Closure

Consider a rigid object that is in contact with a set of n stationary and frictionless point contacts. If an arbitrary external force is applied to the object, each of the point contacts may exert some reaction force on the body. Because the point contacts are frictionless, any reaction forces will only be exerted in the direction of the object surface normal (it goes without saying that only pushing forces are generated—no pulling is allowed).

To make things more precise, choose a body-fixed reference frame, and denote by $f_{ext} \in \mathbb{R}^3$ and $m_{ext} \in \mathbb{R}^3$ the resultant external force and moment

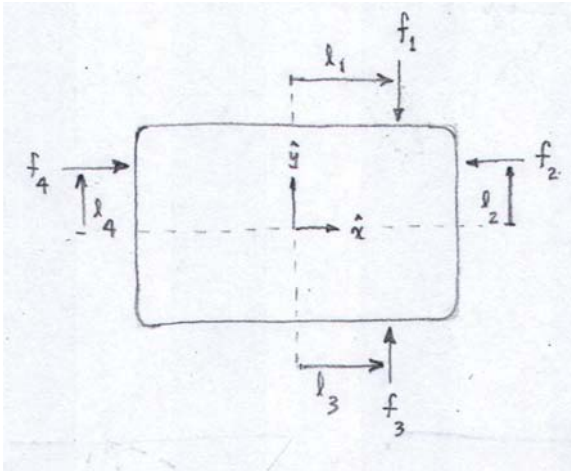

Figure 3.4: A rectangular rigid body constrained by four frictionless point contacts.

applied to the object, respectively. Let $r_i \in \mathbb{R}^3$ denote the vector from the reference frame origin to contact i. Further denote by $\hat{n}_i \in \mathbb{R}^3$ the unit normal vector indicating the direction in which forces can be applied at contact i, $i = 1, \ldots, n$; each force f_i can then be expressed in the form $f_i = x_i \hat{n}_i$, where x_i is a nonnegative scalar indicating the magnitude of the applied force at contact i. The rigid body is in **force closure** if there exists a set of normal contact forces that satisfy static equilibrium. Specifically, there must exist n nonnegative scalars $x_1, \ldots, x_n$ such that the following static equilibrum equations are satisfied:

$$f_{ext} + \sum_{i=1}^{n} x_i \hat{n}_i = 0 \tag{3.5}$$

$$m_{ext} + \sum_{i=1}^{n} x_i (r_i \times \hat{n}_i) = 0, \tag{3.6}$$

for any arbitrary f_{ext} and m_{ext}. If such a set of contact forces exists, then the object can withstand any external force and moment, and is in static equilibrium.

If the object is completely restrained by the point contacts so as to prevent any motions, independent of the contact forces, then the object is said to be in **form closure**. Any grasp that is form closure is also force closure, but a force closure grasp may not necessarily be form closure. We show later that that for force closure grasps in which all the point contacts are frictionless, such grasps are also form closure.

3.2.2 A Motivating Planar Example

So far we have managed a mathematical characterization for frictionless force closure based on the static force-moment equilibrium equations, but as of yet we do not have a computational procedure for determining whether a particular frictionless grasp is force closure. As an intermediate step to developing such a general procedure, let us attempt to determine if the rectangle in the planar example of Figure 3.4, which is subject to four frictionless point contacts, is a force closure grasp. Choosing a fixed reference frame as indicated, the components of each contact reaction force $f_i \in \mathbb{R}^2$, $i = 1, \ldots, 4$, can be written as follows:

$$f_1 = \begin{bmatrix} 0 \\ -1 \end{bmatrix} x_1, \quad f_2 = \begin{bmatrix} -1 \\ 0 \end{bmatrix} x_2, \quad f_3 = \begin{bmatrix} 0 \\ 1 \end{bmatrix} x_3, \quad f_4 = \begin{bmatrix} 1 \\ 0 \end{bmatrix} x_4, \tag{3.7}$$

where each $x_i \geq 0$, $i = 1, 2, 3, 4$ are nonnegative to reflect the fact that only pushing forces are exerted. The resultant force exerted on the object is then

$$\sum_{i=1}^{4} f_i = \begin{bmatrix} x_4 - x_2 \\ x_3 - x_1 \end{bmatrix}, \tag{3.8}$$

while the resultant moment exerted on the object is

$$\sum_{i=1}^{4} r_i \times f_i = \begin{bmatrix} 0 \\ 0 \\ -x_1 l_1 \end{bmatrix} + \begin{bmatrix} 0 \\ 0 \\ x_2 l_2 \end{bmatrix} + \begin{bmatrix} 0 \\ 0 \\ x_3 l_3 \end{bmatrix} + \begin{bmatrix} 0 \\ 0 \\ -x_4 l_4 \end{bmatrix}. \tag{3.9}$$

Since only the z-component of the resultant moment vector is nonzero, from now on we will write the moment equations for planar grasps as a scalar equation.

Now, in order for the object to be in force closure, the resultant force and moment should be able to resist any applied external force and moment. That is, there should exist nonnegative scalars $x_1, \ldots, x_4 \geq 0$ such that the resultant force (3.8) can cancel any arbitrary external force $f_e \in \mathbb{R}^2$, and the resultant moment (3.9) can also cancel any arbitrary external moment $m_e \in \mathbb{R}$. Defining $b = (-f_e, -m_e) \in \mathbb{R}^3$, the conditions for force closure can now be arranged into a linear equation of the form $Ax = b$:

$$\begin{bmatrix} 0 & -1 & 0 & 1 \\ -1 & 0 & 1 & 0 \\ -l_1 & l_2 & l_3 & -l_4 \end{bmatrix} \begin{bmatrix} x_1 \\ x_2 \\ x_3 \\ x_4 \end{bmatrix} = \begin{bmatrix} b_1 \\ b_2 \\ b_3 \end{bmatrix}. \tag{3.10}$$

If a nonnegative solution $x \in \mathbb{R}^4$ exists for all $b \in \mathbb{R}^3$, we can then assert that the grasp is force closure.

Without the requirement that $x \geq 0$, it is a simple matter to determine whether a solution to $Ax = b$ exists for all arbitrary b: it is enough to verify that the columns of A span $\mathbb{R}^3$, or equivalently, that A is of maximal rank (three in this case). However, the question of existence of solutions becomes less straightforward when the nonnegativity constraint $x \geq 0$ is imposed.

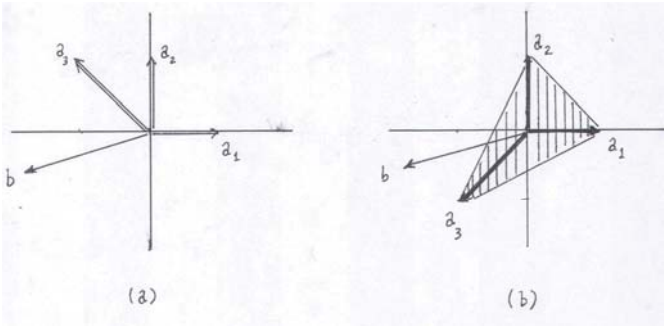

Figure 3.5: A simplified example: (a) For the given b, no nonnegative solution $x \in \mathbb{R}^3$ exists. (b) A nonnegative $x \in \mathbb{R}^3$ exists for any arbitrary $b \in \mathbb{R}^2$.

To gain insight into this question of existence of solutions, consider the following lower-dimensional version of the same problem:

$$\begin{bmatrix} 1 & 0 & -1 \\ 0 & 1 & 1 \end{bmatrix} \begin{bmatrix} x_1 \\ x_2 \\ x_3 \end{bmatrix} = \begin{bmatrix} b_1 \\ b_2 \end{bmatrix}, \tag{3.11}$$

where here $A \in \mathbb{R}^{2\times 3}$, $x \in \mathbb{R}^3$, and $b \in \mathbb{R}^2$. Denoting the three columns of A by $a_1, a_2, a_3 \in \mathbb{R}^2$, Equation (3.11) can be rewritten in the form

$$a_1x_1 + a_2x_2 + a_3x_3 = b. \tag{3.12}$$

If we take b as shown in Figure 3.5(a), it is clear that no nonnegative solution $x \in \mathbb{R}^3$ exists; b falls outside the space spanned by all nonnegative linear combinations of the columns $\{a_1, a_2, a_3\}$ (by nonnegative linear combination we mean that all the weights x_i in Equation (3.12) are nonnegative). If on the other hand the third column a_3 were replaced by $(-1, -1)$ (see Figure 3.5(b)), then clearly the set of all nonnegative linear combinations of $\{a_1, a_2, a_3\}$ does span all of $\mathbb{R}^2$. In this case it is always possible to find, for all $b \in \mathbb{R}^2$, a nonnegative solution $x \geq 0$ to $Ax = b$.

A more geometric way to characterize this condition is in terms of the triangle whose vertices are given by the columns $\{a_1, a_2, a_3\}$ (see Figure 3.5). It is not difficult to see that a nonnegative solution $x \in \mathbb{R}^2$ exists if and only if the origin lies in the interior of the triangle (note that it must lie in the interior, and not on the boundary).

Returning now to our original example involving the rectangular object, from the previous low-dimensional analogy we can now reasonably conjecture

that in order for the grasp of Figure 3.4 to be force closure, nonnegative linear combinations of the columns of $A \in \mathbb{R}^{3\times 4}$ in Equation (3.10) must span $\mathbb{R}^3$. Equivalently, the tetrahedron in $\mathbb{R}^3$ whose vertices are given by the four columns of A must completely enclose the origin; that is, the origin must lie in the interior of the tetrahedron. One immediate and important consequence of this characterization is that a minimum of four frictionless contact points are required for planar force closure.

Continuing with the rectangular example, if the offsets $l_1, \ldots, l_4$ are all positive, then with some effort one can draw and visualize the tetrahedron formed by the columns of A, and verify that the origin does indeed lie in its interior. If on the other hand $l_1 = l_2 = l_3 = l_4 = 0$, then the A matrix in this case becomes

$$A = \begin{bmatrix} 0 & -1 & 0 & 1 \\ -1 & 0 & 1 & 0 \\ 0 & 0 & 0 & 0 \end{bmatrix}. \tag{3.13}$$

In this case the associated tetrahedron collapses to a planar polygon with vertices at $\{(1,0),(0,1),(-1,0),(0,-1)\}$. Because the tetrahedron is no longer three-dimensional, the origin cannot be regarded as lying in its interior. Physically, the contacts are unable to resist pure moments applied to the object.

3.2.3 A Convex Hull Test for Force Closure

We saw in the previous section that in the case of planar rigid bodies, a minimum of four frictionless point contacts is needed to have any hope of force closure. Let us now formulate the force closure conditions for general spatial rigid bodies, involving an arbitrary number of frictionless point contacts. Answering the question of whether a grasp is force closure ultimately reduces, in the end, to a question of existence of nonnegative solutions $x \geq 0$ to a linear equation $Ax = b$, for arbitrary b. We therefore begin with some general results relating to this question. Specifically, let us consider the equation $Ax = b$, where $x \in \mathbb{R}^n$, $A \in \mathbb{R}^{m\times n}$, $m < n$, and $b \in \mathbb{R}^m$. The precise question we wish to answer is, under what conditions on A does a nonnegative solution x exist for any arbitrary b?

The answer is that nonnegative linear combinations of the columns of A must span $\mathbb{R}^m$. That is, for any arbitrary $b \in \mathbb{R}^m$, there must exist nonnegative scalar weights $x_1, x_2, \ldots, x_n \geq 0$ such that

$$a_1 x_1 + a_2 x_2 + \ldots + a_n x_n = b, \tag{3.14}$$

where each $a_i \in \mathbb{R}^m$, $i = 1, \ldots, n$, denotes the i-th column of A. We shall not offer a rigorous mathematical proof of this this result here, but intuitively it can be seen that the results of our earlier planar motivating example generalize directly to this result. Also, like the planar example, the answer to this existence question can be characterized geometrically in terms of whether the origin lies in the interior of some polyhedron in $\mathbb{R}^n$.

Figure 3.6: The convex hull of various sets of points in $\mathbb{R}^2$.

To state this equivalent geometric condition more precisely, we will first need to define the notion of **convex hull**. Given a set $\mathcal{S}$ of n vectors in $\mathbb{R}^m$, i.e.,

$$\mathcal{S} = \{a_1, \ldots, a_n\}, \quad a_i \in \mathbb{R}^m, \; i = 1, \ldots, n, \tag{3.15}$$

the convex hull of $\mathcal{S}$ is the set of convex combinations of $\{a_1, \ldots, a_n\}$, i.e.,

$$\text{Convex hull of } S \; = \left\{ \sum_{i=1}^{n} w_i a_i \;\middle|\; \sum_{i=1}^{n} w_i = 1, \; w_i \geq 0 \text{ for all } i \right\}. \tag{3.16}$$

Figure 3.6 illustrates the convex hull of various sets of points in $\mathbb{R}^2$. The requirement that the nonnegative linear combinations of the columns of A span $\mathbb{R}^m$ can now be equivalently stated as follows: *there must exist some m-dimensional open ball in $\mathbb{R}^m$, centered at the origin, that lies in the interior of the convex hull of the columns of A.*

Let us now return to the question originally posed at the beginning of this section. Consider a rigid body in $\mathbb{R}^3$ constrained by n frictionless point contacts. Let $r_i \in \mathbb{R}^3$ denote the vector from the reference frame frame origin to contact point i, expressed in fixed frame coordinates, and let $\hat{n}_i \in \mathbb{R}^3$ denote a vector normal to the body at contact point i, directed toward the interior of the body. Assuming the body is in static equilibrium, an arbitrary external force $f_{ext} \in \mathbb{R}^3$ and external moment $m_{ext} \in \mathbb{R}^3$ applied to the body generates a set of contact forces at each contact point. Let $f_i \in \mathbb{R}^3$ denote the contact force at contact i; because the contact can only generate forces directed toward the interior of the body, each f_i is of the form

$$f_i = \hat{n}_i x_i, \tag{3.17}$$

where each $x_i \geq 0$ is a nonnegative scalar. The equations for static equilibrium (3.5)-(3.6) can then be written in the form

$$\begin{bmatrix} n_1 & \cdots & n_n \\ r_1 \times n_1 & \cdots & r_n \times n_n \end{bmatrix} \begin{bmatrix} x_1 \\ \vdots \\ x_n \end{bmatrix} = \begin{bmatrix} -f_e \\ -m_e \end{bmatrix}. \tag{3.18}$$

The above equations are of the form $Ax = b$, with $A \in \mathbb{R}^{6 \times n}$, $x \in \mathbb{R}^n$, and $b \in \mathbb{R}^6$. The grasp is force closure if there exists, for all arbitrary b, a

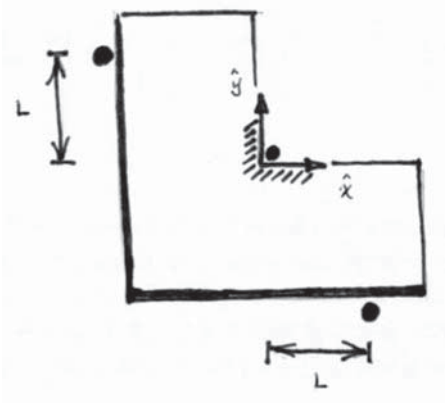

Figure 3.7: A planar object restrained by three frictionless point contacts.

nonnegative $x \in \mathbb{R}^n$ satisfying $Ax = b$. Geometrically, the grasp is force closure if and only if there exists a six-dimensional open ball centered at the origin that lies in the interior of the convex hull formed by the columns of A. This is both a necessary and sufficient condition for force closure, as first shown by Mishra, Schwartz, and Sharir [23]. An immediate consequence of this geometric characterization is that, for spatial rigid bodies, a minimum of seven frictionless contact points (that is, $n = 7$) are required to have any hope of force closure.

Clearly it is not an easy matter to visually determine whether an open ball lies in the interior of some convex hull for even $n = 3$, let alone $n = 6$. In the next section we shall develop a numerical procedure for doing so.

3.2.4 A Computational Test for Force Closure

As noted earlier, the test for force closure ultimately reduces to a linear algebraic question of whether there exists, for every arbitrary $b \in \mathbb{R}^m$, a nonnegative solution $x \geq 0$, $x \in \mathbb{R}^n$, to the linear equation $Ax = b$, where $A \in \mathbb{R}^{m \times n}$, $m \leq n$. In the case where $n = m + 1$—for example, in the planar rectangle example considered earlier, $n = 3$ while the number of contacts $m = 4$—Gauss-Jordan elimination, a widely used method for finding solutions to the linear equation $Ax = b$ with no constraints imposed on x, is helpful.

We first review Gauss-Jordan elimination by means of an example. Consider the planar grasp of Figure 3.7, in which an L-shaped object is restrained by three frictionless point contacts. Fix a reference frame as shown at the interior corner. Note that the contact placed at the interior corner can exert reaction forces in both the $-\hat{x}$ and $-\hat{y}$ directions; denote these reaction forces respectively by f_1 and f_2, and the reaction forces at the remaining two contacts by f_3 and f_4. In terms of the chosen reference frame coordinates,

$$f_1 = \begin{bmatrix} -1 \\ 0 \end{bmatrix} x_1, \quad f_2 = \begin{bmatrix} 0 \\ -1 \end{bmatrix} x_2, \quad f_3 = \begin{bmatrix} 1 \\ 0 \end{bmatrix} x_3, \quad f_4 = \begin{bmatrix} 0 \\ 1 \end{bmatrix} x_4, \quad (3.19)$$

where each $x_i \geq 0$, $i = 1, \ldots, 4$. Let $f_{ext} \in \mathbb{R}^2$ denote an arbitrary external force, and $m_{ext,z} \in \mathbb{R}$ an arbitrary external moment. Force closure can then be determined by examining if there exist nonnegative solutions $x \in \mathbb{R}^4$ to the linear equation

$$\begin{bmatrix} -1 & 0 & 1 & 0 \\ 0 & -1 & 0 & 1 \\ 0 & 0 & -L & L \end{bmatrix} \begin{bmatrix} x_1 \\ x_2 \\ x_3 \\ x_4 \end{bmatrix} = \begin{bmatrix} -f_{ext,x} \\ -f_{ext,y} \\ -m_{ext,z} \end{bmatrix} \tag{3.20}$$

for arbitrary $(f_{ext,x}, f_{ext,y}, m_{ext,z})$. By using elementary row operations, the above equation can be reduced into the following row echelon form:

$$\begin{bmatrix} 1 & 0 & -1 & 0 \\ 0 & 1 & 0 & -1 \\ 0 & 0 & 1 & -1 \end{bmatrix} \begin{bmatrix} x_1 \\ x_2 \\ x_3 \\ x_4 \end{bmatrix} = \begin{bmatrix} f_{ext,x} \\ f_{ext,y} \\ m_{ext,z}/L \end{bmatrix} \tag{3.21}$$

$$\begin{bmatrix} 1 & 0 & 0 & -1 \\ 0 & 1 & 0 & -1 \\ 0 & 0 & 1 & -1 \end{bmatrix} \begin{bmatrix} x_1 \\ x_2 \\ x_3 \\ x_4 \end{bmatrix} = \begin{bmatrix} f_{ext,x} + m_{ext,z}/L \\ f_{ext,y} \\ m_{ext,z}/L \end{bmatrix}. \tag{3.22}$$

Recall that in Gauss-Jordan elimination, zeros are placed both above and below each pivot in the matrix, whereas Gaussian elimination only places zeros below each pivot, and not above (consult any linear algebra reference for details of these two algorithms). The matrix A has been transformed to reduced row echelon form while still preserving the solution. That is, any solution to (3.20) is also a solution to (3.22), and vice versa. The fourth column of the reduced row echelon form matrix has all elements negative, which ensures that a nonnegative solution $x \geq 0$ will exist for any given set of external forces and moments. Stated another way, nonnegative linear combinations of the four columns of the reduced row echelon matrix span $\mathbb{R}^3$, and thus the grasp is a force closure grasp.

In the previous example, the matrix $A \in \mathbb{R}^{m \times n}$ was of dimension $m = 3$ and $n = 4$. If $n > m + 1$, things get slightly more complicated. Suppose $A \in \mathbb{R}^{m \times n}$, $n > m + 1$, is of full rank m, and can be reduced to the following row echelon form via Gauss-Jordan elimination:

$$\begin{bmatrix} I & S \end{bmatrix}, \tag{3.23}$$

where $I \in \mathbb{R}^{m \times m}$ is the $m \times m$ identity matrix, and $S \in \mathbb{R}^{m \times (n-m)}$. In this case, force closure holds if there exists a positive linear combination of the columns of S such that all its entries are negative. That is, if there exists some $\omega \in \mathbb{R}^{n-m}$, $\omega \geq 0$, such that $v = S\omega$ has all entries negative, then force closure holds.

Based on the above, one way to determine force closure is to formulate it as the optimization problem:

$$\min_{\omega, \mu} \mu \tag{3.24}$$

subject to the linear inequality constraints $\omega \geq 0$ and $S\omega < \mu \cdot \mathbf{1}$, where $\mathbf{1}$ is an m-dimensional vector all of whose entries are 1. Because both the objective function (i.e., the function being minimized, in our case μ) and the constraints are linear in the optimization variables (ω, μ), this type of optimization problem is called a linear programming problem. The details of the optimization are beyond the scope of this book, but numerical solvers are readily available. For the problem at hand, given an initial guess for ω and μ, the optimizer then proceeds to minimize μ. If the final value of μ is greater than or equal to zero, then there is no feasible ω that satisfies $S\omega < 0$ and $\omega \geq 0$, and the grasp is not force closure. It is common practice to add a negative lower bound on the set of feasible values of μ is so as to terminate the optimization within a reasonable time (the closer to zero this lower bound for μ, the faster the algorithm will terminate).

We now have a computational procedure for determining whether a frictionless grasp is force closure:

Computational Algorithm for Spatial Force Closure

- **Preliminaries**: Given a spatial rigid body constrained by a set of n frictionless point contacts, where $n \geq 7$, choose a fixed reference frame, and let $r_i \in \mathbb{R}^3$ be the vector from the fixed frame origin to contact point i, $i = 1, \ldots, n$.

- **Initialization**: Let $\hat{n}_i \in \mathbb{R}^3$ be the vector normal to the rigid body at contact i that is directed toward the interior of the body. Construct the following matrix $A \in \mathbb{R}^{6 \times n}$:

$$A = \begin{bmatrix} \hat{n}_1 & \cdots & \hat{n}_n \\ r_1 \times \hat{n}_1 & \cdots & r_n \times \hat{n}_n \end{bmatrix}. \tag{3.25}$$

- **Force Closure Test**: If $\text{rank}(A)$ is less than six, then the grasp is not force closure. Otherwise, transform A to the following reduced row-echelon form:

$$A \to \begin{bmatrix} I & S \end{bmatrix}, \tag{3.26}$$

  where I is the 6×6 identity matrix, and $S \in \mathbb{R}^{6 \times (n-6)}$.

- Solve the following linear programming problem:

$$\min_{\omega, \mu} \mu \tag{3.27}$$

  subject to $\mu \geq \mu_{min}$, $\omega > 0$ and $S\omega < \mu \cdot \mathbf{1}$, where μ_{min} is a user-supplied negative lower bound on μ close to zero, and $\mathbf{1}$ is a vector all of whose entries are 1. If the optimal value of μ is strictly less than zero, then the grasp is force closure. If the optimal value of μ is greater than or equal to zero, then the grasp is not force closure.

3.2.5 Form Closure for Frictionless Grasps

In this section we show that a frictionless point grasp that is force closure is also form closure. Recall that a grasp is form closure if the location of the contacts makes any motion of the objects impossible. Since each point contact restricts possible motions of the object, one way to establish form closure is to determine the set of all possible linear and angular velocities of the object that do not violate the velocity constraints imposed by the contacts. If the set of possible linear and angular velocities is zero, then the object is stationary and therefore in form closure.

We first work out the details for planar grasps. Given a planar object in the x-y plane subject to a set of n frictionless point contacts, first choose a body-fixed reference frame, and let $r_i = (x_i, y_i, 0)$ denote the coordinates of point contact i. Denote by $\hat{n}_i = (n_{i,x}, n_{i,y}, 0)$ the inward-pointing unit vector that is normal to the object surface at contact i. Suppose the body-fixed frame undergoes a linear velocity $v = (v_x, v_y, 0)$ and angular velocity $\omega = (0, 0, \omega_z)$. Then the velocity of the object at contact i, denoted v_i, is given by $v_i = v + \omega \times r_i$, or

$$\begin{bmatrix} v_{i,x} \\ v_{i,y} \end{bmatrix} = \begin{bmatrix} v_x - r_{i,y}\omega_z \\ v_y + r_{i,x}\omega_z \end{bmatrix} \tag{3.28}$$

$$= \begin{bmatrix} 1 & 0 & -r_{i,y} \\ 0 & 1 & r_{i,x} \end{bmatrix} \begin{bmatrix} v_x \\ v_y \\ \omega_z \end{bmatrix}. \tag{3.29}$$

The constraint on the object's linear and angular velocity imposed by point contact i is then given by

$$v_i^T \hat{n}_i \geq 0, \tag{3.30}$$

which works out to

$$\begin{bmatrix} n_{i,x} & n_{i,y} & r_{i,x}n_{i,y} - r_{i,y}n_{i,x} \end{bmatrix} \begin{bmatrix} v_x \\ v_y \\ \omega_z \end{bmatrix} \geq 0. \tag{3.31}$$

We thus have n constraints of the form $a_i^T x \geq 0$, where $a_i \in \mathbb{R}^3$ is given, and $x \in \mathbb{R}^3$ is to be determined. Note that such a constraint defines a half-space in $\mathbb{R}^3$, bounded by the plane $a_i^T x = 0$. In order for the object to be in form closure, the set of solutions x to the n inequalities must be uniquely $x = 0$. For this to be true, (i) n must be at least 4 or greater, and (ii) the vectors $a_i \in \mathbb{R}^3$ must positively span all of $\mathbb{R}^3$ (try to convince yourself geometrically of this fact, by imagining what would happen if the a_i failed to positively span $\mathbb{R}^3$).

Let's compare this result with the static equilibrium equations corresponding to force closure. The contact force f_i can be expressed as $f_i = x_i \hat{n}_i$, and the force closure equations for the planar case become

$$\begin{bmatrix} n_{1,x} & \cdots & n_{n,x} \\ n_{1,y} & \cdots & n_{n,y} \\ r_{1,x}n_{1,y} - r_{1,y}n_{1,x} & \cdots & r_{n,x}n_{n,y} - r_{n,y}n_{n,x} \end{bmatrix} \begin{bmatrix} x_1 \\ \vdots \\ x_n \end{bmatrix} = \begin{bmatrix} b_1 \\ b_2 \\ b_3 \end{bmatrix}. \tag{3.32}$$

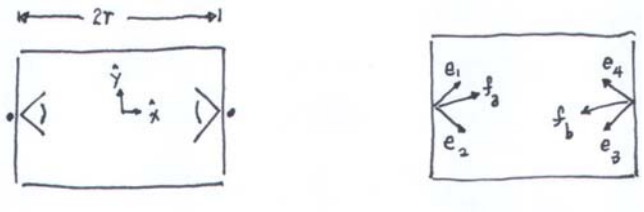

Figure 3.8: (a) A planar rigid body constrained by two point contacts with friction. (b) Force decomposition diagram.

A nonnegative solution $x \in \mathbb{R}^n$ to the above equation must exist for any given arbitrary $b \in \mathbb{R}^3$. Note that the columns of the matrix are identical to the row vectors in (3.31). Recall also that the force closure condition—that the columns of A must positively span $\mathbb{R}^3$—is identical to the form closure condition derived earlier.

The details for form closure of spatial grasps can also be worked out by generalizing the above planar derivation to the spatial case. Here it will be seen that the form closure equations exactly match those for force closure, and that a minimum of seven frictionless point contacts are needed for form (or force) closure of spatial objects.

3.3 Grasps with Friction

3.3.1 A Motivating Planar Example

We now consider grasps involving point contacts with friction. To develop intuition, first consider the rectangular planar object of Figure 3.8(a), which is constrained at each of the two vertical sides by a single point contact with friction. Recall from our earlier discussion of contact models that the friction coefficient at the point of contact can be characterized geometrically by its friction cone: the interior angle of the friction cone, denoted 2α, is related to the friction coefficient μ by $\mu = \tan\alpha$. Let $e_1, e_2 \in \mathbb{R}^2$ be vectors whose directions are aligned along the respective two edges of the left friction cone; define $e_3, e_4 \in \mathbb{R}^2$ in a similar way for the right friction cone. Attaching a reference frame at the center as shown in the figure, the directions for the e_i can be written as

$$e_1 = \begin{bmatrix} 1 \\ \mu \end{bmatrix}, \quad e_2 = \begin{bmatrix} 1 \\ -\mu \end{bmatrix}, \quad e_3 = \begin{bmatrix} -1 \\ -\mu \end{bmatrix}, \quad e_4 = \begin{bmatrix} -1 \\ \mu \end{bmatrix}. \tag{3.33}$$

Assuming the contact forces at the two contacts, denoted f_a and f_b, respectively, both lie inside their respective friction cones, f_a and f_b can then be written

$$f_a = e_1 x_1 + e_2 x_2 \tag{3.34}$$
$$f_b = e_3 x_3 + e_4 x_4, \tag{3.35}$$

for $x_1, \ldots, x_4 \geq 0$. The force closure condition now follows from the equations for static equilibrium: for any arbitrary external force $f_e \in \mathbb{R}^2$ and external moment $m_e \in \mathbb{R}$, there must exist contact forces f_a and f_b such that

$$\begin{aligned} f_a + f_b &= -f_e \\ m_a + m_b &= -m_e. \end{aligned}$$

These equations can also be written explicitly in the form $Ax = b$:

$$\begin{bmatrix} 1 & 1 & -1 & -1 \\ \mu & -\mu & -\mu & \mu \\ -\mu r & \mu r & -\mu r & \mu r \end{bmatrix} \begin{bmatrix} x_1 \\ x_2 \\ x_3 \\ x_4 \end{bmatrix} = \begin{bmatrix} -f_e \\ -m_e \end{bmatrix}. \tag{3.36}$$

Force closure requires that, for any arbitrary $b \in \mathbb{R}^3$ as given above, there exist some nonnegative $x \in \mathbb{R}^4$ that satisfies $Ax = b$.

3.3.2 A Convex Hull Test for Planar Force Closure

By now the reader should have observed that the previously derived convex hull test derived for force closure can also be applied here. More generally, determining whether a grasp is force closure ultimately reduces, in the end, to the same question of existence of nonegative solutions $x \geq 0$ to $Ax = b$, for any arbitrary b.

Without further ado, we present the convex hull test for determining force closure of planar frictional grasps.

Convex Hull Algorithm for Evaluating Planar Force Closure

- **Preliminaries**: Given a planar rigid body restrained by n point contacts with friction, fix a reference frame, and let $r_i = (r_{ix}, r_{iy} \in \mathbb{R}^2$ be the vector directed from the origin of the fixed frame to contact point i, $i = 1, \ldots, n$. Let $e_{2i-1} = (e_{(2i-1)x}, e_{(2i-1)y}) \in \mathbb{R}^2$, $e_{2i} = (e_{2ix}, e_{2iy}) \in \mathbb{R}^2$ respectively be vectors directed along the the two edges of the friction cone at contact i, $i = 1, \ldots, n$.
- **Constructing the A Matrix**: Define the $3 \times 2n$ matrix A as follows:

$$A = \begin{bmatrix} e_{1x} & e_{2x} & \cdots & \cdots & e_{(n-1)x} & e_{nx} \\ e_{1y} & e_{2y} & \cdots & \cdots & e_{(n-1)y} & e_{ny} \\ r_{1x}e_{1y} - r_{1y}e_{1x} & r_{1x}e_{2y} - r_{1y}e_{2x} & \cdots & \cdots & r_{nx}e_{(n-1)y} - r_{ny}e_{(n-1)x} & r_{nx}e_{ny} - r_{ny}e_{nx} \end{bmatrix}. \tag{3.37}$$

- **Convex Hull Test**: Determine if the origin lies in the interior of the convex hull of the columns of A.

For the convex hull test, one can use, *e.g.*, the computational procedure described earlier.

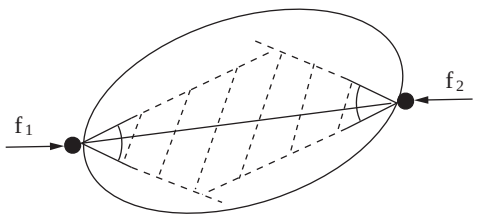

Figure 3.9: Nguyen's Theorem for point contacts with friction.

3.3.3 Nguyen's Theorem for Planar Force Closure

In the case of planar grasps involving two point contacts with friction, Nguyen's Theorem [26] provides a particularly simple and appealing test for determining force closure (see Figure 3.9):

Theorem 3.1. *(V. Nguyen) A planar rigid body constrained by two point contacts with friction is in force closure if and only if the line connecting the contact points lies inside both friction cones.*

Let us now show why Nguyen's Theorem is true. Referring to Figure 3.10, without loss of generality a reference frame can be chosen such that its origin is the midpoint of the line between the contact points, with the y-axis overlapping the line. Again without loss of generality, let the distance between the contact points be 2. We now consider the four possible cases shown in Figure 3.10: (i) when the line of contact lies inside both friction cones; (ii) when it lies inside only one friction cone; (iii) when it lies outside both friction cones, and the friction cones are on opposite sides of the line of contact; (iv) when it lies outside both friction cones, and both friction cones lie on the same side of the line of contact.

For each of these four cases we apply the planar version of the convex hull test. In the first case when the line of contact lies inside both friction cones, the static equilibrium equations are of the form

$$\begin{bmatrix} -\sin\theta_1 & \sin\theta_2 & -\sin\theta_3 & \sin\theta_4 \\ \cos\theta_1 & \cos\theta_2 & -\cos\theta_3 & -\cos\theta_4 \\ -\sin\theta_1 & \sin\theta_2 & \sin\theta_3 & -\sin\theta_4 \end{bmatrix} \begin{bmatrix} x_1 \\ x_2 \\ x_3 \\ x_4 \end{bmatrix} = \begin{bmatrix} b_1 \\ b_2 \\ b_3 \end{bmatrix}$$

where θ_i denotes the angle from the line of contact to the friction cone (see Figure 3.10). The object is in force closure if, for every $b \in \mathbb{R}^3$, there exists

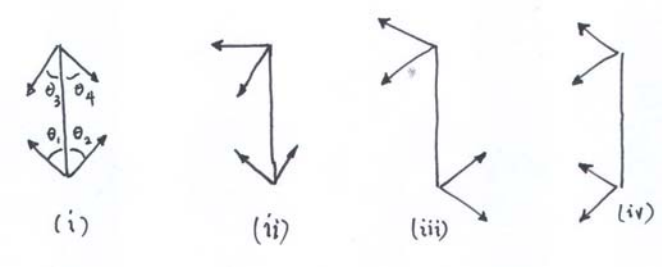

Figure 3.10: An illustration of the proof of Nguyen's Theorem.

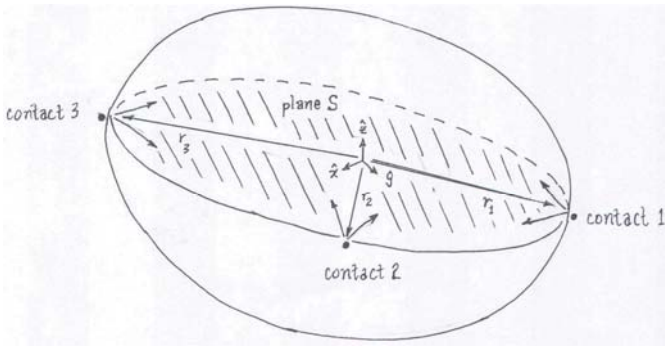

Figure 3.11: A spatial rigid body restrained by three point contacts with friction.

$x \geq 0$ that satisfies (3.3.3). Applying the convex hull test, it can be verified that this case satisfies the force closure conditions. In a similar fashion, it can be verified that the remaining three cases are not force closure.

3.3.4 Spatial Force Closure for Rigid Bodies Subject to Three Point Contacts with Friction

We now consider force closure for spatial rigid bodies. The first question to ask is how many point contacts with friction are required to achieve force closure. We saw that for planar bodies, Nguyen's Theorem asserts that two are enough, as long as the line between the two contact points lies inside both friction cones. For spatial bodies two is clearly not enough—even if the line between the contacts lies inside both friction cones (note that these are now cones in $\mathbb{R}^3$), it is not possible to resist any external moment applied about this line. The next question, then, is whether three point contacts with friction are enough to con-

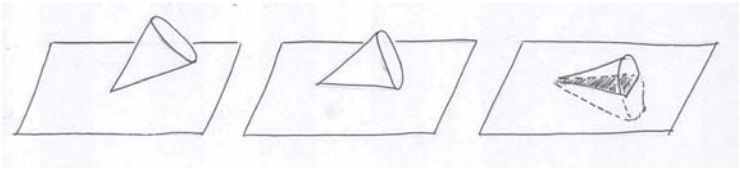

Figure 3.12: Three possibilities for the intersection between a friction cone and a plane.

struct a force closure grasp.

The answer is yes; in fact, there is a particularly simple and appealing result due to Li *et al* [16] that reduces the force closure analysis of spatial frictional grasps into a planar force closure problem. Referring to Figure 3.11, suppose a rigid body is constrained by three point contacts with friction. If the three contact points happened to be collinear, then obviously any moment applied about this line cannot be resisted by the three contacts. We can therefore exclude this case, and assume that the three contact points are not collinear. The three contacts then define a unique plane S, and at each contact point, three possibilities arise (see Figure 3.12):

- The friction cone intersects S in a planar cone;
- The friction cone intersects S in a line;
- The friction cone intersects S in a point.

Li *et al* [16] show that the object is in force closure if and only if each of the friction cones intersects S in a planar cone, and S is also in planar force closure:

Theorem 3.2. *Given a spatial rigid body restrained by three point contacts with friction, assume that the three contact points lie on a unique plane S, and the friction cone at each of the contacts intersects S in a cone. The body is in force closure if and only if the the plane S is in a planar force closure grasp.*

We now prove this result. First, the necessity condition—if the spatial rigid body is in force closure, then each of the friction cones intersects S in a planar

cone and S is also in planar force closure—is easily verified: if the body is in spatial force closure, then S (which is a part of the body) must also be in planar force closure. Moreover, if even one friction cone intersects S in a line or point, then there will be external moments (*e.g.*, about the line between the remaining two contact points) that cannot be resisted by the grasp.

To prove the sufficiency condition—if each of the friction cones intersects S in a planar cone and S is also in planar force closure, then the spatial rigid body is in force closure—choose a fixed reference frame such that S lies in the x-y plane, and let $r_i \in \mathbb{R}^3$ denote the vector from the fixed frame origin to contact point i (see Figure 3.11). Denoting the contact force at i by $f_i \in \mathbb{R}^3$, the contact spatial force $F_i \in \mathbb{R}^6$ is then of the form

$$\mathcal{F}_i = \begin{bmatrix} f_i \\ m_i \end{bmatrix}, \tag{3.38}$$

where each $m_i = r_i \times f_i$, $i = 1, 2, 3$. Denote the arbitrary external spatial force $\mathcal{F}_{ext} \in \mathbb{R}^6$ by

$$\mathcal{F}_{ext} = \begin{bmatrix} f_{ext} \\ m_{ext} \end{bmatrix} \in \mathbb{R}^6. \tag{3.39}$$

Force closure then requires that there exist contact spatial forces $\mathcal{F}_i$, $i = 1, 2, 3$, each lying inside its respective friction cone, such that for any external spatial disturbance force F_{ext}, the following equality is satisfied:

$$\mathcal{F}_1 + \mathcal{F}_2 + \mathcal{F}_3 + \mathcal{F}_{ext} = 0, \tag{3.40}$$

or equivalently,

$$f_1 + f_2 + f_3 + f_{ext} = 0 \tag{3.41}$$

$$(r_1 \times f_1) + (r_2 \times f_2) + (r_3 \times f_3) + m_{ext} = 0, \tag{3.42}$$

If each of the contact forces and moments, as well as the external force and moment, is orthogonally decomposed into components lying on the plane spanned by S (corresponding to the x-y plane in our chosen reference frame) and its normal subspace N (corresponding to the z-axis in our chosen reference frame), then the previous force closure equality relations can be written

$$f_{1S} + f_{2S} + f_{3S} = -f_{ext,S} \tag{3.43}$$

$$(r_1 \times f_{1S}) + (r_2 \times f_{2S}) + (r_3 \times f_{3S}) = -m_{ext,S} \tag{3.44}$$

$$f_{1N} + f_{2N} + f_{3N} = -f_{ext,N} \tag{3.45}$$

$$(r_1 \times f_{1N}) + (r_2 \times f_{2N}) + (r_3 \times f_{3N}) = -m_{ext,N}. \tag{3.46}$$

In what follows we shall use S to refer both to the slice of the rigid body corresponding to the x-y plane, as well as the x-y plane itself. N will always be identified with the z-axis.

Proceeding with the proof of sufficiency, we now show that if S is in planar force closure, then the body is in spatial force closure. In terms of Equations (3.45)-(3.46) we wish to show that, for any arbitrary forces $f_{ext,S} \in S$,

$f_{ext,N} \in N$ and arbitrary moments $m_{ext,S} \in S$, $m_{ext,N} \in N$, there exist contact forces $f_{iS} \in S$, $f_{iN} \in N$, $i = 1, 2, 3$, that satisfy (3.45)-(3.46), and such that for each $i = 1, 2, 3$, the contact force $f_i = f_{iS} + f_{iN}$ lies in friction cone i.

First consider the force closure equations (3.45)-(3.46) in the normal direction N. Given an arbitrary external force $f_{ext,N} \in N$ and external moment $m_{ext,S} \in S$, Equations (3.45)-(3.46) constitute a set of three linear equations in three unknowns. From our hypothesis that the three contact points are never collinear, these equations will always have a unique solution set $\{f_{1N}^*, f_{2N}^*, f_{3N}^*\}$ in N.

Since S is assumed to be in planar force closure, for any arbitrary $f_{ext,S} \in S$ and $m_{ext,N} \in N$, there will exist planar contact forces $f_{iS} \in S$, $i = 1, 2, 3$, that lie inside their respective planar friction cones and also satisfy Equations (3.43)-(3.44). This solution set is not unique: one can always find a set of internal forces $\eta_i \in S$, $i = 1, 2, 3$, each lying inside its respective friction cone, satisfying

$$\eta_1 + \eta_2 + \eta_3 = 0 \tag{3.47}$$

$$(r_1 \times \eta_1) + (r_2 \times \eta_2) + (r_3 \times \eta_3) = 0. \tag{3.48}$$

(To see why such η_i exist, recall that since S is assumed to be in planar force closure, solutions to (3.43)-(3.44) must exist for $f_{ext,S} = \mu_{ext,N} = 0$; these solutions are precisely the internal forces η_i). Note that these two equations constitute three linear equality constraints involving six variables, so that there exists a three-dimensional linear subspace of solutions for $\{\eta_1, \eta_2, \eta_3\}$.

Now if $\{f_{1S}, f_{2S}, f_{3S}\}$ satisfy (3.43)-(3.44), then so will $\{f_{1S} + \eta_1, f_{2S} + \eta_2, f_{3S} + \eta_3\}$. The internal forces $\{\eta_1, \eta_2, \eta_3\}$ can in turn be chosen to have sufficiently large magnitude so that the contact forces

$$f_1 = f_{1N}^* + f_{1S} + \eta_1 \tag{3.49}$$

$$f_2 = f_{2N}^* + f_{2S} + \eta_2 \tag{3.50}$$

$$f_3 = f_{3N}^* + f_{3S} + \eta_3 \tag{3.51}$$

all lie inside their respective friction cone. This completes the proof of the sufficiency condition.

3.4 Summary

- A rigid body subject to a set of fixed point contacts is called a **grasp**. A grasp is said to be **form closure** if arbitrary external forces and moments applied to the body do not cause any motion of the body. A grasp is said to be **force closure** if forces can be generated at the contacts such that the resultant force can cancel any arbitrary external forces or moments applied to the object.
- If the point contact is **frictionless**, contact forces can only be generated in the direction normal to the object surface, and only directed toward the interior of the object (contact forces can only push the object; they cannot pull).

- A **point contact with friction** is characterized by the Coulomb friction coefficient μ; $\mu = 0$ indicates no friction, with increasing values of μ corresponding to greater friction. The **friction cone** at a given point contact indicates the set of all directions in which a force can be applied at the contact such that there is no slipping. The cone's central axis is directed along the surface normal, and the width of the cone is 2α radians, with $\alpha \in [0, \pi/2]$ determined from $\mu = \tan\alpha$.

- The **convex hull** of a set of m points $\{p_1, \ldots, p_m\}$ in $\mathbb{R}^n$ is defined to be

$$\{\sum_{i=1}^{m} w_i p_i \,\Big|\, \sum_{i=1}^{m} w_i = 1, \text{ each } w_i \geq 0\}.$$

- Given a spatial rigid body constrained by a set of n frictionless point contacts, determining force closure reduces to a question about the existence of nonnegative solutions $x \in \mathbb{R}^n$ to the linear equation $Ax = b$, for arbitrary $b \in \mathbb{R}^6$, where $A \in \mathbb{R}^{6\times n}$ is specified by the grasp parameters. A solution always exists if the convex hull formed by the columns of A contains some six-dimensional open ball centered at the origin in $\mathbb{R}^6$ (or more intuitively, the origin lies in the interior of this convex hull). For planar rigid bodies, $A \in \mathbb{R}^{3\times n}$, and planar force closure requires that the convex hull formed by the columns of A contains some three-dimensional open ball centered at the origin in $\mathbb{R}^3$ (or more intuitively, the origin lies in the interior of this convex hull).

- For a planar rigid body, a minimum of four frictionless point contacts are required to achieve planar force closure. For a spatial rigid body, a minimum of seven frictionless point contacts are required to achieve spatial force closure. Force closure for frictionless grasps can also be determined from a computational procedure: in the spatial case, reducing the matrix $A \in \mathbb{R}^{6\times n}$ to the following row echelon form

$$\begin{bmatrix} I & S \end{bmatrix},$$

  where I is the 6×6 identity matrix and $S \in \mathbb{R}^{6\times(n-6)}$, if there exists some $\omega \geq 0$ that satisfies $S\omega < 0$, then the grasp is force closure. In the planar case, $A \in \mathbb{R}^{3\times n}$, and S in the reduced row echelon form is $3 \times (n-3)$; the same condition on S still applies for planar force closure. Determining the existence of such a ω can be formulated as an optimization problem of the linear programming type.

- For grasps with only frictionless point contacts, a force closure grasp is also form closure, and vice versa.

- For planar grasps involving n point contacts with friction, determining force closure again leads, in the end, to the question of existence of nonnegative solutions $x \in \mathbb{R}^{2n}$ to the linear equation $Ax = b$ for arbitrary

$b \in \mathbb{R}^3$, where $A \in \mathbb{R}^{3\times 2n}$. The same methods involving, *e.g.*, convex hulls and computational procedures for determining frictionless planar grasps, can also be used for planar grasps with friction.

- In the case of two-finger planar grasps with friction, Nguyen's Theorem states that force closure is achieved if and only if the line connecting the two contact points lies inside both friction cones.
- In the case of three-finger spatial grasps with friction, a theorem by Li *et al* [16] provides a set of three necessary and sufficient conditions for spatial force closure: (i) the three contact points define a unique plane S (in other words, they cannot be collinear), and (ii) the friction cone at each of the three contact points intersects S in a planar cone, and (iii) the plane S (more specifically, the intersection between S and the rigid body) must be in planar force closure.

Notes and References

The existence of form and force closure grasps, and the minimum number of fingers necessary to achieve these grasps, have been studied in [23], [12], [19], among others. Proofs of Nguyen's Theorem for both planar and spatial grasps, as well as algorithms for computing two-finger planar force closure grasps, are provided in his original paper [26]. [16] offers a more detailed statement and proof of the force closure result for spatial three-finger grasps with friction, as well as constructive algorithms for both planar and spatial force closure grasps. [36] contains a more detailed survey of the grasping literature, including more advanced notions of form and force closure (i.e., second-order form and force closure [34]).

Exercises

Chapter 4

Rigid-Body Motions

In the previous chapter, we saw that a minimum of six numbers are needed to specify the position and orientation of a rigid body in three-dimensional physical space. We established this by selecting three points on a rigid body, and arguing that the distances between any pair of these three points must always be preserved regardless of where the rigid body is located. This led to three constraints, which when imposed on the nine Cartesian coordinates—(x, y, z) coordinates for each of the three points—led us to conclude that only six of these nine coordinates could be independently chosen.

In this chapter we will develop a more systematic way to describe the position and orientation of a rigid body. Rather than choosing three points on a body, we instead attach a reference frame to the body, and develop ways to describe this reference frame with respect to some fixed reference frame in space (we know of course that this can be done using as few as six coordinates). This is the **descriptive** aspect of the rigid body motions.

There is also a **prescriptive** aspect to the rigid body motions. Suppose a rigid body is moved from one configuration in physical space to another. Once a reference frame and length scale for physical space have been chosen, the displacement of this rigid body can then described by a transformation from $\mathbb{R}^3$ to $\mathbb{R}^3$. It turns out that the same set of mathematical representations can be used for both the descriptive and prescriptive interpretations of rigid body motions.

To illustrate the simultaneous descriptive-prescriptive features of rigid body motions, and also to provide a synopsis of the main concepts and tools that we will learn in this chapter, we begin with a motivating planar example. Before doing so, we make some remarks about vector notation.

A Word about Vector Notation

Recall that a vector is a geometric quantity with a length and direction. A vector will be denoted by a regular text symbol, e.g., v. If a reference frame and length scale have been chosen for the underlying space in which the vector

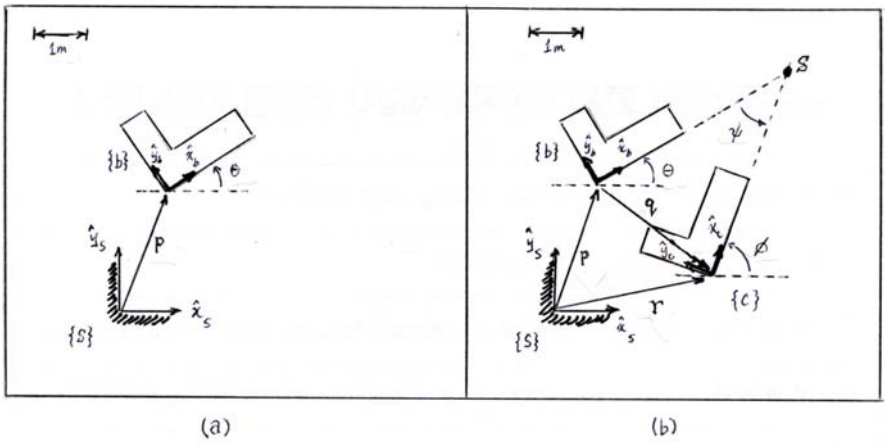

Figure 4.1: Rigid body motion in the plane.

v lies, then this vector can be represented as a column vector with respect to this reference frame (imagine moving the base of v to the reference frame origin while maintaining its direction; such a notion of vector is sometimes referred to as a **free vector**). The column vector representation of v will be denoted in italics by $v \in \mathbb{R}^n$. Note that if a different reference frame and length scale are chosen, then the column vector representation v will change.

A point p in physical space can also be represented as a vector. Given a choice of reference frame and length scale for physical space, the point p can be represented as a vector from the reference frame origin to p; its column vector representation will be denoted in italics by $p \in \mathbb{R}^n$. Here as before, a different choice of reference frame and length scale for physical space will lead to a different column vector representation $p \in \mathbb{R}^n$ for the same point p in physical space.

4.1 A Motivating Example

Consider the planar body of Figure 4.1(a), whose motion is confined to the plane. Suppose a length scale and a fixed reference frame have been chosen as shown. We will call the fixed reference frame the **fixed frame**, or the **space frame**, denoted {s}, and label its unit axes $\hat{x}_s$ and $\hat{y}_s$. Similarly, we attach a reference frame with unit axes $\hat{x}_b$ and $\hat{y}_b$ to the planar body. Because this frame moves with the body, it will be called the **moving frame**, or **body frame**, and denoted {b}.

To describe the configuration of the planar body, only the position and orientation of the body frame with respect to the fixed frame needs to be specified. The vector from the fixed frame origin to the body frame origin, denoted p, can

be expressed in terms of the fixed frame unit axes as

$$\mathrm{p} = p_x \hat{\mathrm{x}}_\mathrm{s} + p_y \hat{\mathrm{y}}_\mathrm{s}. \tag{4.1}$$

You are probably more accustomed to writing this vector as simply (p_x, p_y); this is fine when there is no possibility of ambiguity about reference frames, but when expressing the same vector in terms of multiple reference frames, writing p as in Equation (4.1) clearly indicates the reference frame with respect to which (p_x, p_y) is defined.

The simplest way to describe the orientation of the body frame {b} relative to the fixed frame {s} is by specifying the angle θ as shown in the figure. Another (admittedly less simple) way is to specify the directions of the unit axes $\hat{\mathrm{x}}_\mathrm{b}$ and $\hat{\mathrm{y}}_\mathrm{b}$ of the body frame, in the form

$$\hat{\mathrm{x}}_\mathrm{b} = \cos\theta\, \hat{\mathrm{x}}_\mathrm{s} + \sin\theta\, \hat{\mathrm{y}}_\mathrm{s}, \tag{4.2}$$

$$\hat{\mathrm{y}}_\mathrm{b} = -\sin\theta\, \hat{\mathrm{x}}_\mathrm{s} + \cos\theta\, \hat{\mathrm{y}}_\mathrm{s}. \tag{4.3}$$

At first sight this seems a rather inefficient way to represent the body frame orientation. However, imagine if now the body were to move arbitrarily in three-dimensional space; a single angle θ alone clearly would not suffice to describe the orientation of the displaced reference frame. We would in fact need three angles, but as yet it is not clear how to define an appropriate set of three angles. On the other hand, expressing the displaced body frame's unit axes in terms of the fixed frame, as we have done above for the planar case, is straightforward.

Assuming we agree to express everything in terms of the fixed frame coordinates, then just as the vector p of Equation (4.1) can be represented as a column vector $p \in \mathbb{R}^2$ of the form

$$p = \begin{bmatrix} p_x \\ p_y \end{bmatrix}, \tag{4.4}$$

Equations (4.2)-(4.3) can also be packaged into the following 2×2 matrix P:

$$P = \begin{bmatrix} \cos\theta & -\sin\theta \\ \sin\theta & \cos\theta \end{bmatrix}, \tag{4.5}$$

Observe that the first column of P corresponds to $\hat{\mathrm{x}}_\mathrm{b}$, and the second column to $\hat{\mathrm{y}}_\mathrm{b}$. It can be easily verified that that $P^T P = I$, and that $P^{-1} = P^T$. The matrix P as constructed here is an example of a **rotation matrix**, and the pair (P, p) provides a description of the orientation and position of the body frame relative to the fixed frame. Of the six entries involved—two for p and four for P—only three are independent. In fact, the condition $P^T P = I$ implies three equality constraints, so that of the four entries that make up P, only one can be chosen independently. The three coordinates (θ, p_x, p_y) would seem to offer an intuitive minimal representation for the configuration of a planar rigid body. In any event, the rotation matrix-vector pair (P, p) serves as a description of the configuration of the rigid body as seen from the fixed frame.

Now referring to Figure 4.1(b), suppose the body at {b} is displaced to the configuration at {c}. Repeating the above analysis for the position vector r and

the unit axes of frame {c}, we can write

$$\begin{aligned} \mathrm{r} &= r_x \hat{\mathrm{x}}_\mathrm{s} + r_y \hat{\mathrm{y}}_\mathrm{s} && (4.6)\\ \hat{\mathrm{x}}_\mathrm{c} &= \cos\phi\, \hat{\mathrm{x}}_\mathrm{s} + \sin\phi\, \hat{\mathrm{y}}_\mathrm{s}, && (4.7)\\ \hat{\mathrm{y}}_\mathrm{c} &= -\sin\phi\, \hat{\mathrm{x}}_\mathrm{s} + \cos\phi\, \hat{\mathrm{y}}_\mathrm{s}. && (4.8) \end{aligned}$$

The above can be arranged into the following column vector $r \in \mathbb{R}^2$ and rotation matrix $R \in \mathbb{R}^{2\times 2}$:

$$r = \begin{bmatrix} r_x \\ r_y \end{bmatrix}, \quad R = \begin{bmatrix} \cos\phi & -\sin\phi \\ \sin\phi & \cos\phi \end{bmatrix}. \tag{4.9}$$

We could also repeat the above to describe frame {c} as seen from frame {b} (that is, pretend {b} is now the fixed frame, and repeat the previous analysis for {c}). Letting q denote the vector from the {b}-frame origin to the {c}-frame origin, we get

$$\begin{aligned} \mathrm{q} &= q_x \hat{\mathrm{x}}_\mathrm{b} + q_y \hat{\mathrm{y}}_\mathrm{b}, && (4.10)\\ \hat{\mathrm{x}}_\mathrm{c} &= \cos\psi\, \hat{\mathrm{x}}_\mathrm{b} + \sin\psi\, \hat{\mathrm{y}}_\mathrm{b}, && (4.11)\\ \hat{\mathrm{y}}_\mathrm{c} &= -\sin\psi\, \hat{\mathrm{x}}_\mathrm{b} + \cos\psi\, \hat{\mathrm{y}}_\mathrm{b}, && (4.12) \end{aligned}$$

where $\psi = \phi - \theta$. As before, the vector $q \in \mathbb{R}^2$ and rotation matrix $Q \in \mathbb{R}^{2\times 2}$ can be defined as follows:

$$q = \begin{bmatrix} q_x \\ q_y \end{bmatrix}, \quad Q = \begin{bmatrix} \cos\psi & -\sin\psi \\ \sin\psi & \cos\psi \end{bmatrix}. \tag{4.13}$$

Here q is the representation of q in frame {b} coordinates. Similarly, the rotation matrix Q describes the orientation of frame {c} relative to frame {b}.

Now, if we imagine the body is displaced from frame {b} to frame {c}, then clearly the point on the rigid body corresponding to p is displaced to r. We can then ask, how is the column vector representation p transformed into r? The answer is given by

$$r = p + Pq. \tag{4.14}$$

To see why, from Figure 4.1(b) it can be seen that r is the vector sum of p and q. Since p and r are respectively the column vector representations of p and r in frame $\{s\}$ coordinates, to obtain r as a function of p and q we first need to represent q in frame $\{s\}$ coordinates before adding this to p. This is precisely Pq (verify this for yourself), and Equation (4.14) now follows accordingly. Since $\theta + \psi = \phi$, it can also be verified that

$$R = PQ. \tag{4.15}$$

The pair (Q, q) thus describes how the rigid body is displaced from {b} to {c}: given any point p on the rigid body at configuration {b}, represented by the vector $p \in \mathbb{R}^3$, it is then transformed to the point in physical space corresponding to the vector $r = p + Pq \in \mathbb{R}^3$. Also, the rotation matrix P

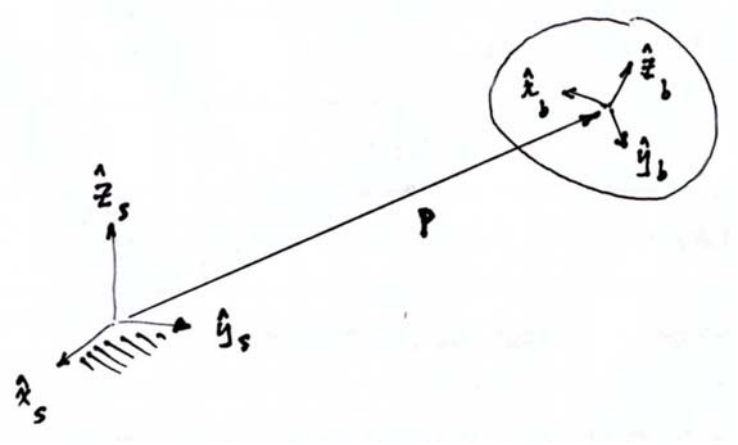

Figure 4.2: Mathematical description of position and orientation.

at configuration {b} is now transformed to $R = PQ$ at configuration {c} as a result of this displacement. For this reason we call the rotation matrix-vector pair (Q, q) a **rigid body displacement**, or more commonly a **rigid body motion**.

We thus see that a rotation matrix-vector pair can serve as a description of a rigid body's configuration (the descriptive interpretation as illustrated by (P, p)), or as a prescription of a rigid body's displacement in physical space (the prescriptive interpretation as illustrated by (Q, q)).

We make one final observation. Once again referring to Figure 4.1(b), note that the displacement from configuration {b} to {c} can be obtained by rotating the planar body at {b} about the point s by an angle ψ. The displacement can therefore be parametrized by the three coordinates (ψ, s_x, s_y), where (s_x, s_y) denote the coordinates for point s in fixed frame coordinates. This alternative three-parameter representation of a rigid body motion is a (planar) example of a **screw motion**. If the displacement is a pure translation—that is, the orientation does not change, so that $\theta = \phi$—then s is assumed to lie at infinity.

In the remainder of this chapter we will generalize the above concepts to three-dimensional rigid body motions. For this purpose consider a rigid body occupying three-dimensional physical space as shown in Figure 4.2. Assume that a length scale for physical space has been chosen, and that both the fixed frame {s} and body frame {b} have been chosen as shown. Throughout this book all reference frames will be right-handed, i.e., the unit axes $\{\hat{\mathrm{x}}, \hat{\mathrm{y}}, \hat{\mathrm{z}}\}$ always satisfy $\hat{\mathrm{x}} \times \hat{\mathrm{y}} = \hat{\mathrm{z}}$. Denote the unit axes of the fixed frame by $\{\hat{\mathrm{x}}_\mathrm{s}, \hat{\mathrm{y}}_\mathrm{s}, \hat{\mathrm{z}}_\mathrm{s}\}$, and the unit axes of the body frame by $\{\hat{\mathrm{x}}_\mathrm{b}, \hat{\mathrm{y}}_\mathrm{b}, \hat{\mathrm{z}}_\mathrm{b}\}$. Let p denote the vector from the fixed frame origin to the body frame origin. In terms of the fixed frame coordinates, p can be expressed as

$$\mathrm{p} = p_1 \hat{\mathrm{x}}_\mathrm{s} + p_2 \hat{\mathrm{y}}_\mathrm{s} + p_3 \hat{\mathrm{z}}_\mathrm{s} \tag{4.16}$$

The axes of the body frame can also be expressed as

$$\hat{\mathrm{x}}_{\mathrm{b}} = r_{11}\hat{\mathrm{x}}_{\mathrm{s}} + r_{21}\hat{\mathrm{y}}_{\mathrm{s}} + r_{31}\hat{\mathrm{z}}_{\mathrm{s}} \tag{4.17}$$

$$\hat{\mathrm{y}}_{\mathrm{b}} = r_{12}\hat{\mathrm{x}}_{\mathrm{s}} + r_{22}\hat{\mathrm{y}}_{\mathrm{s}} + r_{32}\hat{\mathrm{z}}_{\mathrm{s}} \tag{4.18}$$

$$\hat{\mathrm{z}}_{\mathrm{b}} = r_{13}\hat{\mathrm{x}}_{\mathrm{s}} + r_{23}\hat{\mathrm{y}}_{\mathrm{s}} + r_{33}\hat{\mathrm{z}}_{\mathrm{s}}. \tag{4.19}$$

Defining $p \in \mathbb{R}^3$ and $R \in \mathbb{R}^{3\times 3}$ by

$$p = \begin{bmatrix} p_1 \\ p_2 \\ p_3 \end{bmatrix}, \quad R = \begin{bmatrix} r_{11} & r_{12} & r_{13} \\ r_{21} & r_{22} & r_{23} \\ r_{31} & r_{32} & r_{33} \end{bmatrix}, \tag{4.20}$$

the twelve parameters given by (R, p) then provide a description of the position and orientation of the rigid body relative to the fixed frame.

Since a minimum of six parameters are required to describe the configuration of a rigid body, if we agree to keep the three parameters in p as they are, then of the nine parameters in R, only three can be chosen independently. We begin by examining some basic three-parameter representations for rotation matrices: the **Euler angles** and the related **roll-pitch-yaw angles**, the **exponential coordinates**, and the **unit quaternions**. We then examine six-parameter representations for the combined position and orientation of a rigid body. Augmenting the three-parameter representation for R with $p \in \mathbb{R}^3$ is one obvious and natural way to do this. Another relies on the Chasles-Mozzi Theorem, which states that every rigid body displacement can be described as a screw motion about some fixed axis in space.

We conclude with a discussion of linear and angular velocities, and also of forces and moments. Rather than treat these quantities as separate three-dimensional quantities, we shall merge the linear and angular velocity vectors into a single six-dimensional **spatial velocity**, and also the moment and force vectors into a six-dimensional **spatial force**. These six-dimensional quantities, and the rules for manipulating them, will form the basis for the kinematic and dynamic analyses in the subsequent chapters.

4.2 Rotations

4.2.1 Definition

We argued earlier that of the nine entries in the rotation matrix R, only three can be chosen independently. We begin by deriving a set of six explicit constraints on the entries of R. Note that the three columns of R correspond to the body frame's unit axes $\{\hat{\mathrm{x}}, \hat{\mathrm{y}}, \hat{\mathrm{z}}\}$. The following conditions must therefore be satisfied:

(i) Unit norm condition: $\hat{\mathrm{x}}$, $\hat{\mathrm{y}}$, and $\hat{\mathrm{z}}$ are all of unit norm, or

$$\begin{aligned} r_{11}^2 + r_{21}^2 + r_{31}^2 &= 1 \\ r_{12}^2 + r_{22}^2 + r_{32}^2 &= 1 \\ r_{13}^2 + r_{23}^2 + r_{33}^2 &= 1. \end{aligned} \tag{4.21}$$

(ii) Orthogonality condition: $\hat{\mathrm{x}} \cdot \hat{\mathrm{y}} = \hat{\mathrm{x}} \cdot \hat{\mathrm{z}} = \hat{\mathrm{y}} \cdot \hat{\mathrm{z}} = 0$ (here $\cdot$ denotes the inner product), or

$$\begin{aligned} r_{11}r_{12} + r_{21}r_{22} + r_{31}r_{32} &= 0 \\ r_{12}r_{13} + r_{22}r_{23} + r_{32}r_{33} &= 0 \\ r_{11}r_{13} + r_{21}r_{23} + r_{31}r_{33} &= 0. \end{aligned} \tag{4.22}$$

These six constraints can be expressed more compactly as a single constraint on the matrix R:

$$R^T R = I, \tag{4.23}$$

where R^T denotes the transpose of R, and I denotes the 3×3 identity.

There is still the small matter of accounting for the fact that the frame is right-handed (i.e., $\hat{\mathbf{x}} \times \hat{\mathbf{y}} = \hat{\mathbf{z}}$, where $\times$ denotes the cross-product) rather than left-handed (i.e., $\hat{\mathbf{x}} \times \hat{\mathbf{y}} = -\hat{\mathbf{z}}$); our six equality constraints above do not distinguish between right- and left-handed frames. We recall the following formula for evaluating the determinant of a 3×3 matrix M: denoting its three columns by a, b, c, respectively, its determinant is given by

$$\det M = a^T(b \times c) = c^T(a \times b) = b^T(c \times a). \tag{4.24}$$

Substituting the columns for R into this formula then leads to the constraint

$$\det R = 1. \tag{4.25}$$

Note that if the frame had been left-handed, we would have $\det R = -1$. In summary, the six equality constraints represented by (4.23) imply that $\det R = \pm 1$; imposing the additional constraint $\det R = 1$ means that only right-handed frames are allowed. Thus, the constraint $\det R = 1$ does not change the number of independent continuous variables needed to parametrize R.

The set of 3×3 rotation matrices forms the **Special Orthogonal Group** $SO(3)$, which we now formally define:

Definition 4.1. The **Special Orthogonal Group** $SO(3)$, also known as the group[1] of rotation matrices, is the set of all 3×3 real matrices R that satisfy (i) $R^T R = I$, and (ii) $\det R = 1$.

The set of 2×2 rotation matrices is a subgroup of $SO(3)$, and denoted $SO(2)$.

Definition 4.2. The **Special Orthogonal Group** $SO(2)$ is the set of all 2×2 real matrices R that satisfy (i) $R^T R = I$, and (ii) $\det R = 1$.

From the definition it follows that every $R \in SO(2)$ is of the form

$$R = \begin{bmatrix} \cos\theta & -\sin\theta \\ \sin\theta & \cos\theta \end{bmatrix},$$

where $\theta \in [0, 2\pi]$. In what follows, all properties derived for $SO(3)$ also apply to $SO(2)$.

[1] The formal algebraic notion of a group is discussed in the exercises.

4.2.2 Properties

We now list some basic properties of rotation matrices. First, the identity I is a trivial example of a rotation matrix. The inverse of a rotation matrix is also a rotation matrix:

Proposition 4.1. *The inverse of a rotation matrix $R \in SO(3)$ always exists and is given by its transpose, R^T. R^T is also a rotation matrix.*

Proof. The condition $R^T R = I$ implies that $R^{-1} = R^T$, which clearly exists for every R. Since $\det R^T = \det R = 1$, R^T is also a rotation matrix. Another consequence of the equality $R^T = R^{-1}$ is that $RR^T = I$. □

Proposition 4.2. *The product of two rotation matrices is a rotation matrix.*

Proof. Given $R_1, R_2 \in SO(3)$, it readily follows that their product $R_1 R_2$ satisfies $(R_1 R_2)^T (R_1 R_2) = I$ and $\det R_1 R_2 = \det R_1 \cdot \det R_2 = 1$. □

Proposition 4.3. *For any vector $x \in \mathbb{R}^3$ and $R \in SO(3)$, the vector $y = Rx$ is of the same length as x.*

Proof. This follows from $\|y\|^2 = y^T y = x^T R^T R x = x^T x = \|x\|^2$. □

The next property provides a descriptive interpretation for the product of two rotation matrices. We first introduce some notation. Given two reference frames {a} and {b}, the orientation of frame {b} as seen from frame {a} will be represented by the rotation matrix R_{ab}; that is, the three columns of R_{ab} are just vector representations of the $\hat{\mathrm{x}}$-, $\hat{\mathrm{y}}$-, and $\hat{\mathrm{z}}$-axes of frame {b} expressed in terms of coordinates for frame {a}. From this definition it follows readily that $R_{aa} = I$.

Proposition 4.4. $R_{ab} R_{bc} = R_{ac}$.

Proof. To prove this result, introduce a third reference frame {c}, and define the unit axes of frames {a}, {b}, and {c} by the triplet of orthogonal unit vectors $\{\hat{\mathrm{x}}_\mathrm{a}, \hat{\mathrm{y}}_\mathrm{a}, \hat{\mathrm{z}}_\mathrm{a}\}$, $\{\hat{\mathrm{x}}_\mathrm{b}, \hat{\mathrm{y}}_\mathrm{b}, \hat{\mathrm{z}}_\mathrm{b}\}$, and $\{\hat{\mathrm{x}}_\mathrm{c}, \hat{\mathrm{y}}_\mathrm{c}, \hat{\mathrm{z}}_\mathrm{c}\}$, respectively. Suppose that the unit axes of frame {b} can be expressed in terms of the unit axes of frame {a} by

$$\begin{aligned} \hat{\mathrm{x}}_\mathrm{b} &= r_{11}\hat{\mathrm{x}}_\mathrm{a} + r_{21}\hat{\mathrm{y}}_\mathrm{a} + r_{31}\hat{\mathrm{z}}_\mathrm{a} \\ \hat{\mathrm{y}}_\mathrm{b} &= r_{12}\hat{\mathrm{x}}_\mathrm{a} + r_{22}\hat{\mathrm{y}}_\mathrm{a} + r_{32}\hat{\mathrm{z}}_\mathrm{a} \\ \hat{\mathrm{z}}_\mathrm{b} &= r_{13}\hat{\mathrm{x}}_\mathrm{a} + r_{23}\hat{\mathrm{y}}_\mathrm{a} + r_{33}\hat{\mathrm{z}}_\mathrm{a}. \end{aligned}$$

Similarly, suppose the unit axes of frame $\{c\}$ can be expressed in terms of the unit axes of frame $\{b\}$ by

$$\begin{aligned} \hat{\mathrm{x}}_\mathrm{c} &= s_{11}\hat{\mathrm{x}}_\mathrm{b} + s_{21}\hat{\mathrm{y}}_\mathrm{b} + s_{31}\hat{\mathrm{z}}_\mathrm{b} \\ \hat{\mathrm{y}}_\mathrm{c} &= s_{12}\hat{\mathrm{x}}_\mathrm{b} + s_{22}\hat{\mathrm{y}}_\mathrm{b} + s_{32}\hat{\mathrm{z}}_\mathrm{b} \\ \hat{\mathrm{z}}_\mathrm{c} &= s_{13}\hat{\mathrm{x}}_\mathrm{b} + s_{23}\hat{\mathrm{y}}_\mathrm{b} + s_{33}\hat{\mathrm{z}}_\mathrm{b}. \end{aligned}$$

The above equations can also be expressed more compactly as

$$\begin{bmatrix} \hat{\mathrm{x}}_\mathrm{b} & \hat{\mathrm{y}}_\mathrm{b} & \hat{\mathrm{z}}_\mathrm{b} \end{bmatrix} = \begin{bmatrix} \hat{\mathrm{x}}_\mathrm{a} & \hat{\mathrm{y}}_\mathrm{a} & \hat{\mathrm{z}}_\mathrm{a} \end{bmatrix} \begin{bmatrix} r_{11} & r_{12} & r_{13} \\ r_{21} & r_{22} & r_{23} \\ r_{31} & r_{32} & r_{33} \end{bmatrix} \tag{4.26}$$

$$\begin{bmatrix} \hat{\mathrm{x}}_\mathrm{c} & \hat{\mathrm{y}}_\mathrm{c} & \hat{\mathrm{z}}_\mathrm{c} \end{bmatrix} = \begin{bmatrix} \hat{\mathrm{x}}_\mathrm{b} & \hat{\mathrm{y}}_\mathrm{b} & \hat{\mathrm{z}}_\mathrm{b} \end{bmatrix} \begin{bmatrix} s_{11} & s_{12} & s_{13} \\ s_{21} & s_{22} & s_{23} \\ s_{31} & s_{32} & s_{33} \end{bmatrix}. \tag{4.27}$$

Note that the 3×3 matrix of Equation (4.26) is R_{ab}, while that of Equation (4.27) is R_{bc}. Substituting (4.26) into (4.27),

$$\begin{bmatrix} \hat{\mathrm{x}}_\mathrm{c} & \hat{\mathrm{y}}_\mathrm{c} & \hat{\mathrm{z}}_\mathrm{c} \end{bmatrix} = \begin{bmatrix} \hat{\mathrm{x}}_\mathrm{a} & \hat{\mathrm{y}}_\mathrm{a} & \hat{\mathrm{z}}_\mathrm{a} \end{bmatrix} \begin{bmatrix} r_{11} & r_{12} & r_{13} \\ r_{21} & r_{22} & r_{23} \\ r_{31} & r_{32} & r_{33} \end{bmatrix} \begin{bmatrix} s_{11} & s_{12} & s_{13} \\ s_{21} & s_{22} & s_{23} \\ s_{31} & s_{32} & s_{33} \end{bmatrix}.$$

From the above it follows that $R_{ab}R_{bc} = R_{ac}$. □

Proposition 4.5.

$$R_{ab}^{-1} = R_{ba}. \tag{4.28}$$

Proof. This result follows immediately by choosing {c} to be the same as {a} in the previous proposition $R_{ab}R_{bc} = R_{ac}$, and recalling that $R_{aa} = I$. □

For the next property, consider a free vector v in physical space with a defined direction and magnitude. Given two reference frames {a} and {b} in physical space, let $v_a, v_b \in \mathbb{R}^3$ denote representations of v with respect to these two frames; that is, v_a and v_b are obtained by placing the base of v at the origin of frames {a} and {b}, respectively, and expressing v in terms of the given reference frame.

Proposition 4.6.

$$R_{ba}v_a = v_b \tag{4.29}$$

$$R_{ab}v_b = v_a. \tag{4.30}$$

Proof. In terms of the unit axes of {a} and {b}, v can be written as follows:

$$\mathrm{v} = v_{a_1}\hat{\mathrm{x}}_\mathrm{a} + v_{a_2}\hat{\mathrm{y}}_\mathrm{a} + v_{a_3}\hat{\mathrm{z}}_\mathrm{a} \tag{4.31}$$

$$= v_{b_1}\hat{\mathrm{x}}_\mathrm{b} + v_{b_2}\hat{\mathrm{y}}_\mathrm{b} + v_{b_3}\hat{\mathrm{z}}_\mathrm{b}, \tag{4.32}$$

or, letting $v_a = (v_{a_1}, v_{a_2}, v_{a_3})^T$, $v_b = (v_{b_1}, v_{b_2}, v_{b_3})^T$,

$$\mathbf{v} = \begin{bmatrix} \hat{\mathrm{x}}_\mathrm{a} & \hat{\mathrm{y}}_\mathrm{a} & \hat{\mathrm{z}}_\mathrm{a} \end{bmatrix} v_a \tag{4.33}$$

$$= \begin{bmatrix} \hat{\mathrm{x}}_\mathrm{b} & \hat{\mathrm{y}}_\mathrm{b} & \hat{\mathrm{z}}_\mathrm{b} \end{bmatrix} v_b. \tag{4.34}$$

From the previous proposition the unit axes of {a} and {b} are related by

$$\begin{bmatrix} \hat{\mathrm{x}}_\mathrm{a} & \hat{\mathrm{y}}_\mathrm{a} & \hat{\mathrm{z}}_\mathrm{a} \end{bmatrix} = \begin{bmatrix} \hat{\mathrm{x}}_\mathrm{b} & \hat{\mathrm{y}}_\mathrm{b} & \hat{\mathrm{z}}_\mathrm{b} \end{bmatrix} R_{ba}, \tag{4.35}$$

from which it follows that $R_{ba}v_a = v_b$. □

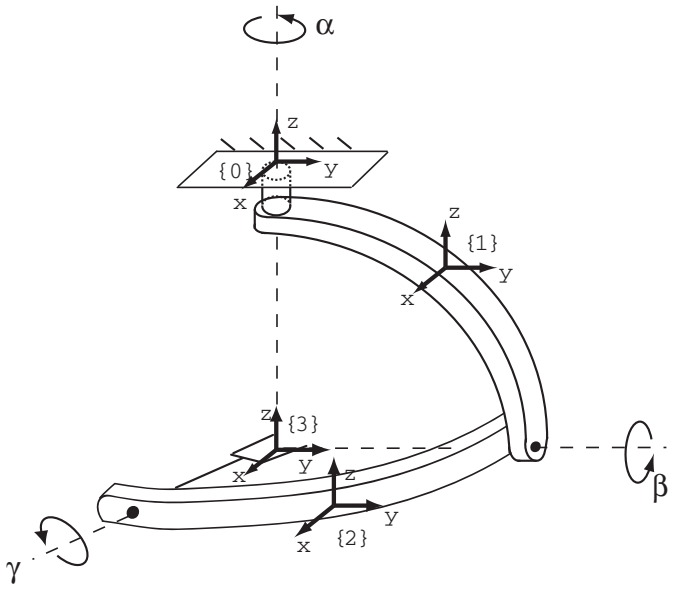

Figure 4.3: Wrist mechanism illustrating the ZYX Euler angles.

4.2.3 Euler Angles

As we established above, a rotation matrix can be parametrized by three independent coordinates. Here we introduce one popular three-parameter representation of rotations, the **ZYX Euler angles**. One way to visualize these angles is through the wrist mechanism shown in Figure 4.3. The ZYX Euler angles (α, β, γ) refer to the angle of rotation about the three joint axes of this mechanism. In the figure the wrist mechanism is shown in its zero position, i.e., when all three joints are set to zero.

Four reference frames are defined as follows: frame $\{0\}$ is the fixed frame, while frames $\{1\}$, $\{2\}$, and $\{3\}$ are attached to the three links of the wrist mechanism as shown. When the wrist is in the zero position, all four reference frames have the same orientation. We now consider the relative frame orientations R_{01}, R_{12}, and R_{23}. First, it can be seen that R_{01} depends only on the angle α: rotating about the $\hat{z}$-axis of frame $\{0\}$ by an angle α (a positive rotation about an axis is taken by aligning the thumb of the right hand along the axis, and rotating in the direction of the fingers curling about the axis), it can be seen that

$$R_{01} = \begin{bmatrix} \cos\alpha & -\sin\alpha & 0 \\ \sin\alpha & \cos\alpha & 0 \\ 0 & 0 & 1 \end{bmatrix} = \mathrm{Rot}(\hat{z}, \alpha). \tag{4.36}$$

The notation $\mathrm{Rot}(\hat{z}, \alpha)$ describes a rotation about the $\hat{z}$-axis by angle α. Simi-

larly, R_{12} depends only on β, and is given by

$$R_{12} = \begin{bmatrix} \cos\beta & 0 & \sin\beta \\ 0 & 1 & 0 \\ -\sin\beta & 0 & \cos\beta \end{bmatrix} = \text{Rot}(\hat{y}, \beta), \tag{4.37}$$

where the notation $\text{Rot}(\hat{y}, \beta)$ describes a rotation about the $\hat{y}$-axis by angle β. Finally, R_{23} depends only on γ, and is given by

$$R_{23} = \begin{bmatrix} 1 & 0 & 0 \\ 0 & \cos\gamma & -\sin\gamma \\ 0 & \sin\gamma & \cos\gamma \end{bmatrix} = \text{Rot}(\hat{x}, \gamma), \tag{4.38}$$

where the notation $\text{Rot}(\hat{x}, \gamma)$ describes a rotation about the $\hat{x}$-axis by angle γ. $R_{03} = R_{01}R_{12}R_{23}$ is therefore given by

$$R_{03} = \begin{bmatrix} c_\alpha c_\beta & c_\alpha s_\beta s_\gamma - s_\alpha c_\gamma & c_\alpha s_\beta c_\gamma + s_\alpha s_\gamma \\ s_\alpha c_\beta & s_\alpha s_\beta s_\gamma + c_\alpha c_\gamma & s_\alpha s_\beta c_\gamma - c_\alpha s_\gamma \\ -s_\beta & c_\beta s_\gamma & c_\beta c_\gamma \end{bmatrix}, \tag{4.39}$$

where s_α is shorthand for $\sin\alpha$, c_α for $\cos\alpha$, etc.

We now ask the following question: given an arbitrary rotation matrix R, does there exist (α, β, γ) such that Equation (4.39) is satisfied? If the answer is yes, then the wrist mechanism of Figure 4.3 can reach any orientation. This is indeed the case, and we prove this fact constructively as follows. Let r_{ij} be the ij-th element of R. Then from Equation (4.39) we know that $r_{11}^2 + r_{21}^2 = \cos^2\beta$; as long as $\cos\beta \neq 0$, or equivalently $\beta \neq \pm 90°$, we have

$$\beta = \tan^{-1}\left(\frac{\sin\beta}{\cos\beta}\right) = \tan^{-1}\left(\frac{-r_{31}}{\pm\sqrt{r_{11}^2 + r_{21}^2}}\right).$$

We now define the atan2 function, which is a two-argument function implemented in a variety of computer languages for computing the arctangent. Specifically, the function $\text{atan2}(y, x)$ evaluates $\tan^{-1}(y/x)$ by taking into account the signs of x and y. For example, $\text{atan2}(1, 1) = \pi/4$, while $\text{atan2}(-1, -1) = -3\pi/4$. Using atan2, the possible values for β can be expressed as

$$\beta = \text{atan2}\left(-r_{31}, \sqrt{r_{11}^2 + r_{21}^2}\right)$$

and

$$\beta = \text{atan2}\left(-r_{31}, -\sqrt{r_{11}^2 + r_{21}^2}\right).$$

In the first case β will lie in the range $[-90°, 90°]$, while in the second case β lies in the range $[90°, 270°]$. Assuming the β obtained above is not $\pm 90°$, α and γ can then be determined from the following relations:

$$\begin{aligned} \alpha &= \text{atan2}(r_{21}, r_{11}) \\ \gamma &= \text{atan2}(r_{32}, r_{33}) \end{aligned}$$

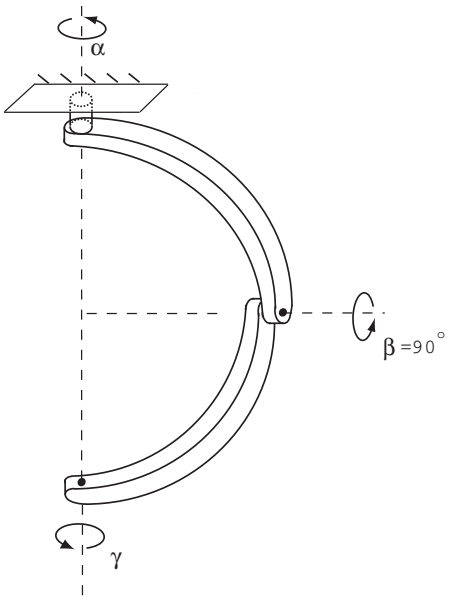

Figure 4.4: Configuration corresponding to $\beta = 90°$ for ZYX Euler angles.

In the event that $\beta = \pm 90°$, there exists a one-parameter family of solutions for α and γ. This is most easily seen from Figure 4.4. If $\beta = 90°$, then α and γ represent rotations (in the opposite direction) about the same vertical axis. Hence, if $(\alpha, \beta, \gamma) = (\bar{\alpha}, 90°, \bar{\gamma})$ is a solution for a given rotation R, then any triple $(\bar{\alpha}', 90°, \bar{\gamma}')$ where $\bar{\alpha}' - \bar{\gamma}' = \bar{\alpha} - \bar{\gamma}$ is also a solution.

Algorithm for Computing the ZYX Euler Angles

Given $R \in SO(3)$, we wish to find angles $\alpha, \gamma \in [0, 2\pi)$ and $\beta \in [-\pi/2, \pi/2)$ that satisfy

$$R = \begin{bmatrix} \mathrm{c}_\alpha \mathrm{c}_\beta & \mathrm{c}_\alpha \mathrm{s}_\beta \mathrm{s}_\gamma - \mathrm{s}_\alpha \mathrm{c}_\gamma & \mathrm{c}_\alpha \mathrm{s}_\beta \mathrm{c}_\gamma + \mathrm{s}_\alpha \mathrm{s}_\gamma \\ \mathrm{s}_\alpha \mathrm{c}_\beta & \mathrm{s}_\alpha \mathrm{s}_\beta \mathrm{s}_\gamma + \mathrm{c}_\alpha \mathrm{c}_\gamma & \mathrm{s}_\alpha \mathrm{s}_\beta \mathrm{c}_\gamma - \mathrm{c}_\alpha \mathrm{s}_\gamma \\ -\mathrm{s}_\beta & \mathrm{c}_\beta \mathrm{s}_\gamma & \mathrm{c}_\beta \mathrm{c}_\gamma \end{bmatrix}, \tag{4.40}$$

where s_α is shorthand for $\sin\alpha$, c_α for $\cos\alpha$, etc. Denote by r_{ij} the ij-th entry of R.

(i) If $r_{31} \neq \pm 1$, set

$$\beta = \mathrm{atan2}\left(-r_{31}, \sqrt{r_{11}^2 + r_{21}^2}\right) \tag{4.41}$$

$$\alpha = \mathrm{atan2}(r_{21}, r_{11}) \tag{4.42}$$

$$\gamma = \mathrm{atan2}(r_{32}, r_{33}), \tag{4.43}$$

where the square root is taken to be positive.

(ii) If $r_{31} = 1$, then $\beta = \pi/2$, and a one-parameter family of solutions for α and γ exists. One possible solution is $\alpha = 0$ and $\gamma = \text{atan2}(r_{12}, r_{22})$.

(iii) If $r_{31} = -1$, then $\beta = -\pi/2$, and a one-parameter family of solutions for α and γ exists. One possible solution is $\alpha = 0$ and $\gamma = -\text{atan2}(r_{12}, r_{22})$.

From the earlier wrist mechanism illustration of the ZYX Euler angles it should be evident that the choice of zero position for β is, in some sense, arbitrary. That is, we could just as easily have defined the home position of the wrist mechanism to be as in Figure 4.4; this would then lead to another three-parameter representation (α, β, γ) for $SO(3)$. Figure 4.4 is precisely the definition of the **ZYZ Euler angles**. The resulting rotation matrix can be obtained via the following sequence of rotations:

$$\begin{aligned} R(\alpha,\beta,\gamma) &= \text{Rot}(\hat{z},\alpha)\cdot\text{Rot}(\hat{y},\beta)\cdot\text{Rot}(\hat{z},\gamma) \\ &= \begin{bmatrix} c_\alpha & -s_\alpha & 0 \\ s_\alpha & c_\alpha & 0 \\ 0 & 0 & 1 \end{bmatrix} \begin{bmatrix} c_\beta & 0 & s_\beta \\ 0 & 1 & 0 \\ -s_\beta & 0 & c_\beta \end{bmatrix} \begin{bmatrix} c_\gamma & -s_\gamma & 0 \\ s_\gamma & c_\gamma & 0 \\ 0 & 0 & 1 \end{bmatrix} \\ &= \begin{bmatrix} c_\alpha c_\beta c_\gamma - s_\alpha s_\gamma & -c_\alpha c_\beta s_\gamma - s_\alpha c_\gamma & c_\alpha s_\beta \\ s_\alpha c_\beta c_\gamma + c_\alpha s_\gamma & -s_\alpha c_\beta s_\gamma + c_\alpha c_\gamma & s_\alpha s_\beta \\ -s_\beta c_\gamma & s_\beta s_\gamma & c_\beta \end{bmatrix}. \end{aligned} \tag{4.44}$$

Just as before, we can show that for every rotation $R \in SO(3)$, there exists a triple (α, β, γ) that satisfies $R = R(\alpha, \beta, \gamma)$ for $R(\alpha, \beta, \gamma)$ as given in Equation (4.44). (Of course, the resulting formulas will differ from those for the ZYX Euler angles.)

From the wrist mechanism interpretation of the ZYX and ZYZ Euler angles, it should be evident that for Euler angle parametrizations of $SO(3)$, what really matters is that rotation axis 1 is orthogonal to rotation axis 2, and that rotation axis 2 is orthogonal to rotation axis 3 (axis 1 and axis 3 need not necessarily be orthogonal to each other). Specifically, any sequence of rotations of the form

$$\text{Rot}(\text{axis1},\alpha)\cdot\text{Rot}(\text{axis2},\beta)\cdot\text{Rot}(\text{axis3},\gamma), \tag{4.45}$$

where axis1 is orthogonal to axis2, and axis2 is orthogonal to axis3, can serve as a valid three-parameter representation for $SO(3)$. Later in this chapter we shall see how to express a rotation about an arbitrary axis that is not a unit axis of the reference frame.

4.2.4 Roll-Pitch-Yaw Angles

Earlier in the chapter we asserted that a rotation matrix can also be used to describe a transformation of a rigid body from one orientation to another. Here we will use this prescriptive viewpoint to derive another three-parameter representation for rotation matrices, the **roll-pitch-yaw angles**. Referring to Figure 4.5, given a frame in the identity configuration (that is, $R = I$), we first rotate this frame by an angle γ about the $\hat{x}$-axis of the fixed frame, followed by

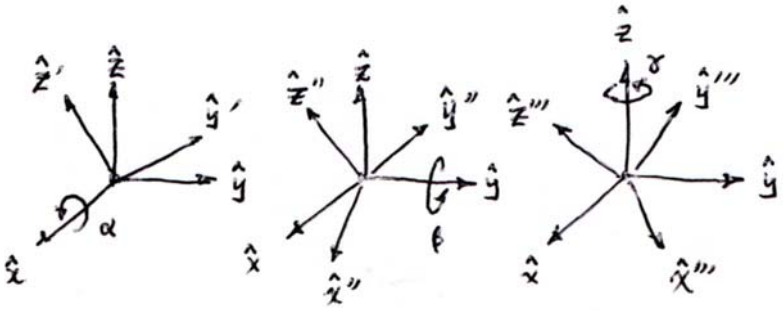

Figure 4.5: Illustration of XYZ roll-pitch-yaw angles.

an angle β about the ŷ-axis of the fixed frame, and finally by an angle α about the ẑ-axis of the fixed frame.

Let us derive the explicit form of a vector $v \in \mathbb{R}^3$ (expressed as a column vector using fixed frame coordinates) that is rotated about the fixed frame x̂-axis by an angle γ. The rotated vector, denoted v', will be

$$v' = \begin{bmatrix} 1 & 0 & 0 \\ 0 & \cos\gamma & -\sin\gamma \\ 0 & \sin\gamma & \cos\gamma \end{bmatrix} v. \tag{4.46}$$

If v' is now rotated about the fixed frame ŷ-axis by an angle β, then the rotated vector v'' can be expressed in fixed frame coordinates as

$$v'' = \begin{bmatrix} \cos\beta & 0 & \sin\beta \\ 0 & 1 & 0 \\ -\sin\beta & 0 & \cos\beta \end{bmatrix} v'. \tag{4.47}$$

Finally, rotating v'' about the fixed frame ẑ-axis by an angle α yields the vector

$$v''' = \begin{bmatrix} \cos\alpha & -\sin\alpha & 0 \\ \sin\alpha & \cos\alpha & 0 \\ 0 & 0 & 1 \end{bmatrix} v''. \tag{4.48}$$

If we now take v to successively be the three unit axes of the reference frame in the identity orientation $R = I$, then after applying the above sequence of rotations to the three axes of the reference frame, its final orientation will be

$$\begin{aligned} R(\alpha,\beta,\gamma) &= \mathrm{Rot}(\hat{\mathrm{x}},\alpha)\cdot\mathrm{Rot}(\hat{\mathrm{y}},\beta)\cdot\mathrm{Rot}(\hat{\mathrm{z}},\gamma)\cdot I \\ &= \begin{bmatrix} \mathrm{c}_\alpha & -\mathrm{s}_\alpha & 0 \\ \mathrm{s}_\alpha & \mathrm{c}_\alpha & 0 \\ 0 & 0 & 1 \end{bmatrix} \begin{bmatrix} \mathrm{c}_\beta & 0 & \mathrm{s}_\beta \\ 0 & 1 & 0 \\ -\mathrm{s}_\beta & 0 & \mathrm{c}_\beta \end{bmatrix} \begin{bmatrix} 1 & 0 & 0 \\ 0 & \mathrm{c}_\gamma & -\mathrm{s}_\gamma \\ 0 & \mathrm{s}_\gamma & \mathrm{c}_\gamma \end{bmatrix} \cdot I \\ &= \begin{bmatrix} \mathrm{c}_\alpha\mathrm{c}_\beta & \mathrm{c}_\alpha\mathrm{s}_\beta\mathrm{s}_\gamma - \mathrm{s}_\alpha\mathrm{c}_\gamma & \mathrm{c}_\alpha\mathrm{s}_\beta\mathrm{c}_\gamma + \mathrm{s}_\alpha\mathrm{s}_\gamma \\ \mathrm{s}_\alpha\mathrm{c}_\beta & \mathrm{s}_\alpha\mathrm{s}_\beta\mathrm{s}_\gamma + \mathrm{c}_\alpha\mathrm{c}_\gamma & \mathrm{s}_\alpha\mathrm{s}_\beta\mathrm{c}_\gamma - \mathrm{c}_\alpha\mathrm{s}_\gamma \\ -\mathrm{s}_\beta & \mathrm{c}_\beta\mathrm{s}_\gamma & \mathrm{c}_\beta\mathrm{c}_\gamma \end{bmatrix}. \end{aligned} \tag{4.49}$$

This product of three rotations is exactly the same as that for the ZYX Euler angles given in (4.40). We see that the same product of three rotations admits two different physical interpretations: as a sequence of rotations with respect to the body frame (ZYX Euler angles), or, reversing the order of rotations, as a sequence of rotations with respect to the fixed frame (the XYZ roll-pitch-yaw angles).

The terms roll, pitch, and yaw are often used to describe the rotational motion of a ship or aircraft. In the case of a typical fixed-wing aircraft, for example, suppose a body frame is attached such that the $\hat{x}$-axis is in the direction of forward motion, the $\hat{z}$-axis is the vertical axis pointing downward toward ground (assuming the aircraft is flying level with respect to ground), and the $\hat{y}$-axis extends in the direction of the wing. The roll, pitch, and yaw motions are then defined according to the XYZ roll-pitch-yaw angles (α, β, γ) of Equation (4.49).

In fact, for any sequence of rotations of the form (4.45) in which consecutive axes are orthogonal, a similar descriptive-prescriptive interpretation exists for the corresponding Euler angle formula. Euler angle formulas can be defined in a number of ways depending on the choice and order of the rotation axes, but their common features are:

- The angles represent three successive rotations taken about the axes of either the body frame or the fixed frame.
- The first axis must be orthogonal to the second axis, and the second axis must be orthogonal to the third axis.
- The angle of rotation for the first and third rotations ranges in value over a 2π interval, while that of the second rotation ranges in value over an interval of length π.

4.2.5 Exponential Coordinates

We now introduce another three-parameter representation for rotations, the **exponential coordinates**. In the Euler angle representation, a rotation matrix is expressed as a product of three rotations, each depending on a single parameter. The exponential coordinates parametrize a rotation matrix in terms of a single rotation axis (represented by a vector ω of unit length), together with an angle of rotation θ about that axis; The vector $r = \omega\theta \in \mathbb{R}^3$ then serves as a three-parameter representation of the rotation. This representation is most naturally introduced in the setting of linear differential equations, whose main results we now review.

4.2.5.1 Some Basic Results from Linear Differential Equations

Let us begin with the simplest scalar linear differential equation

$$\dot{x}(t) = ax(t), \tag{4.50}$$

where $x(t) \in \mathbb{R}$, $a \in \mathbb{R}$ is constant, and initial condition $x(0) = x_0$ is assumed given ($\dot{x}(t)$ denotes the derivative of $x(t)$ with respect to t). Equation (4.50) has solution

$$x(t) = e^{at}x_0.$$

It is also useful to remember the series expansion of the exponential function:

$$e^{at} = 1 + at + \frac{(at)^2}{2!} + \frac{(at)^3}{3!} + \dots$$

Now consider the vector linear differential equation

$$\dot{x}(t) = Ax(t) \tag{4.51}$$

where $x(t) \in \mathbb{R}^n$, $A \in \mathbb{R}^{n\times n}$ is constant, and initial condition $x(0) = x_0$ is given. From the earlier scalar result, one can conjecture a solution of the form

$$x(t) = e^{At}x_0 \tag{4.52}$$

where the matrix exponential e^{At} now needs to be defined in a meaningful way. Again mimicking the scalar case, we define the matrix exponential to be

$$e^{At} = I + At + \frac{(At)^2}{2!} + \frac{(At)^3}{3!} + \dots \tag{4.53}$$

The first question to be addressed is under what conditions this series converges, so that the matrix exponential is well-defined. It can be shown that if A is constant and finite, this series is always guaranteed to converge to a finite limit; the proof can be found in most texts on ordinary linear differential equations and will not be covered here.

The second question is whether (4.52) is indeed a solution to (4.51). Taking the time derivative of $x(t) = e^{At}x_0$,

$$\begin{aligned}
\dot{x}(t) &= \left(\frac{d}{dt}e^{At}\right)x_0 \\
&= \frac{d}{dt}\left(I + At + \frac{A^2t^2}{2!} + \frac{A^3t^3}{3!} + \dots\right)x_0 \\
&= \left(A + A^2t + \frac{A^3t^2}{2!} + \dots\right)x_0 \\
&= Ae^{At}x_0 \\
&= Ax(t),
\end{aligned} \tag{4.54}$$

which proves that $x(t) = e^{At}x_0$ is indeed a solution. That this is a unique solution follows from the basic existence and uniqueness result for linear ordinary differential equations, which we will just invoke here without proof.

Note that in the fourth line of (4.54), A could also have been factored to the right, i.e.,

$$\dot{x}(t) = e^{At}Ax_0.$$

While for arbitrary square matrices A and B we have in general that $AB \neq BA$, it is always true that

$$Ae^{At} = e^{At}A \tag{4.55}$$

for any square A and scalar t (you can verify this directly using the series expansion for the matrix exponential).

While the matrix exponential e^{At} is defined as an infinite series, closed-form expressions are often available. For example, if A can be expressed as $A = PDP^{-1}$ for some $D \in \mathbb{R}^{n\times n}$ and invertible $P \in \mathbb{R}^{n\times n}$, then

$$\begin{aligned} e^{At} &= I + At + \frac{(At)^2}{2!} + \dots \\ &= I + (PDP^{-1})t + (PDP^{-1})(PDP^{-1})\frac{t^2}{2!} + \dots \\ &= P(I + Dt + \frac{(Dt)^2}{2!} + \dots)P^{-1} \\ &= Pe^{Dt}P^{-1}. \end{aligned} \tag{4.56}$$

If moreover D is diagonal, i.e., $D = \text{diag}\{d_1, d_2, \dots, d_n\}$, then its matrix exponential is particularly simple to evaluate:

$$e^{Dt} = \begin{bmatrix} e^{d_1 t} & 0 & \cdots & 0 \\ 0 & e^{d_2 t} & \cdots & 0 \\ \vdots & \vdots & \ddots & \vdots \\ 0 & 0 & \cdots & e^{d_n t} \end{bmatrix}. \tag{4.57}$$

We summarize the above results in the following proposition:

Proposition 4.7. *The linear differential equation $\dot{x}(t) = Ax(t)$ with initial condition $x(0) = x_0$, where $A \in \mathbb{R}^{n\times n}$ is constant and $x(t) \in \mathbb{R}^n$, has solution*

$$x(t) = e^{At}x_0 \tag{4.58}$$

where

$$e^{At} = I + tA + \frac{t^2}{2!}A^2 + \frac{t^3}{3!}A^3 + \dots. \tag{4.59}$$

The matrix exponential e^{At} further satisifies the following properties:

(i) $\frac{d}{dt}e^{At} = Ae^{At} = e^{At}A$.

(ii) *If $A = PDP^{-1}$ for some $D \in \mathbb{R}^{n\times n}$ and invertible $P \in \mathbb{R}^{n\times n}$, then $e^{At} = Pe^{Dt}P^{-1}$.*

(iii) *If $AB = BA$, then $e^Ae^B = e^{A+B}$.*

(iv) $(e^A)^{-1} = e^{-A}$.

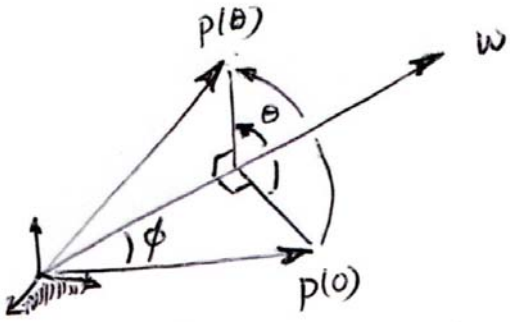

Figure 4.6: The vector $p(0)$ is rotated by an angle θ about the axis ω, to $p(\theta)$.

The third property can be established by expanding the exponentials and comparing terms. The fourth property follows by setting $B = -A$ in the third property.

A final linear algebraic result useful in finding closed-form expressions for e^{At} is the Cayley-Hamilton Theorem, which we state here without proof:

Proposition 4.8. *Let $A \in \mathbb{R}^{n\times n}$ be constant, with characteristic polynomial*

$$p(s) = \det(Is - A) = s^n + c_{n-1}s^{n-1} + \ldots + c_1 s + c_0.$$

Then

$$p(A) = A^n + c_{n-1}A^{n-1} + \ldots + c_1 A + c_0 I = 0.$$

4.2.5.2 Exponential Coordinates for Rotations

In the exponential coordinate representation for rotations, a rotation is represented by a single axis of rotation together with a rotation angle about the axis. Referring to Figure 4.6, suppose a three-dimensional vector $p(0)$ is rotated by an angle θ about the fixed rotation axis ω to $p(\theta)$; here we assume all quantities are expressed in fixed frame coordinates and $\|\omega\| = 1$. This rotation can be achieved by imagining that $p(0)$ is subject to a rotation about ω at a constant rate of 1 rad/sec, from time $t = 0$ to $t = \theta$. Let $p(t)$ denote this path. The velocity of $p(t)$, denoted $\dot{p}$, is then given by

$$\dot{p} = \omega \times p. \tag{4.60}$$

To see why this is true, let ϕ be the angle between $p(t)$ and ω. Observe that p traces a circle of radius $\|p\| \sin\phi$ about the ω-axis. Then $\dot{p} = \omega \times p$ is tangent to the path with magnitude $\|p\| \sin\phi$, which is exactly (4.60).

We now propose an alternative way of expressing the cross-product between two vectors. To do this we introduce the following notation:

Definition 4.3. Given a vector $\omega \in \mathbb{R}^3$, define

$$[\omega] = \begin{bmatrix} 0 & -\omega_3 & \omega_2 \\ \omega_3 & 0 & -\omega_1 \\ -\omega_2 & \omega_1 & 0 \end{bmatrix}. \tag{4.61}$$

The matrix $[\omega]$ as defined above is **skew-symmetric**; that is,

$$[\omega] = -[\omega]^T.$$

With this representation it is a simple calculation to verify the following property:

Proposition 4.9. *Given two vectors $x, y \in \mathbb{R}^3$, their cross product $x \times y$ can be obtained as*

$$x \times y = [x]y, \tag{4.62}$$

where $[x]$ is the skew-symmetric matrix representation of x. Also,

$$[x \times y] = [x][y] - [y][x]. \tag{4.63}$$

Another useful property involving rotations and skew-symmetric matrices is the following:

Proposition 4.10. *Given any $\omega \in \mathbb{R}^3$ and $R \in SO(3)$, the following always holds:*

$$R[\omega]R^T = [R\omega]. \tag{4.64}$$

Proof. Letting r_i^T be the ith row of R,

$$\begin{aligned} R[\omega]R^T &= \begin{bmatrix} r_1^T(\omega \times r_1) & r_1^T(\omega \times r_2) & r_1^T(\omega \times r_3) \\ r_2^T(\omega \times r_1) & r_2^T(\omega \times r_2) & r_2^T(\omega \times r_3) \\ r_3^T(\omega \times r_1) & r_3^T(\omega \times r_2) & r_3^T(\omega \times r_3) \end{bmatrix} \\ &= \begin{bmatrix} 0 & -r_3^T\omega & r_2^T\omega \\ r_3^T\omega & 0 & -r_1^T\omega \\ -r_2^T\omega & r_1^T\omega & 0 \end{bmatrix} \\ &= [R\omega], \end{aligned} \tag{4.65}$$

where the second line makes use of the determinant formula for 3×3 matrices, i.e., if M is a 3×3 matrix with columns $\{a, b, c\}$, then $\det M = a^T(b \times c) = c^T(a \times b) = b^T(c \times a)$. □

With the above results, the differential equation (4.60) can be expressed as

$$\dot{p} = [\omega]p, \tag{4.66}$$

with initial condition $p(0) = 0$. This is a linear differential equation of the form $\dot{x} = Ax$ that we have studied earlier; its solution is given by

$$p(t) = e^{[\omega]t}p(0).$$

Since t and θ are interchangeable as a result of assuming that $p(t)$ rotates at a constant rate of 1 rad/sec (after t seconds, $p(t)$ will have rotated t radians), the above can also be written

$$p(\theta) = e^{[\omega]\theta} p(0).$$

We now derive a closed-form expression for $e^{[\omega]\theta}$. Here we make use of the Cayley-Hamilton Theorem for $[\omega]$. First, the characteristic polynomial associated with the 3×3 matrix $[\omega]$ is given by

$$p(s) = \det(Is - [\omega]) = s^3 + s.$$

The Cayley-Hamilton Theorem then implies $[\omega]^3 + [\omega] = 0$, or

$$[\omega]^3 = -[\omega].$$

Let us now expand the matrix exponential $e^{[\omega]\theta}$ in series form. Replacing $[\omega]^3$ by $-[\omega]$, $[\omega]^4$ by $-[\omega]^2$, $[\omega]^5$ by $-[\omega]^3 = [\omega]$, and so on, we obtain

$$\begin{aligned} e^{[\omega]\theta} &= I + [\omega]\theta + [\omega]^2 \frac{\theta^2}{2!} + [\omega]^3 \frac{\theta^3}{3!} + \dots \\ &= I + \left(\theta - \frac{\theta^3}{3!} + \frac{\theta^5}{5!} - \cdots\right)[\omega] + \left(\frac{\theta^2}{2!} - \frac{\theta^4}{4!} + \frac{\theta^6}{6!} - \cdots\right)[\omega]^2. \end{aligned}$$

Now recall the series expansions for $\sin\theta$ and $\cos\theta$:

$$\begin{aligned} \sin\theta &= \theta - \frac{\theta^3}{3!} + \frac{\theta^5}{5!} - \dots \\ \cos\theta &= 1 - \frac{\theta^2}{2!} + \frac{\theta^4}{4!} - \dots \end{aligned}$$

The exponential $e^{[\omega]\theta}$ therefore simplifies to the following:

Proposition 4.11. *Given a vector $\omega \in \mathbb{R}^3$ such that $\|\omega\| = 1$, and any scalar $\theta \in \mathbb{R}$,*

$$e^{[\omega]\theta} = I + \sin\theta\,[\omega] + (1 - \cos\theta)[\omega]^2. \tag{4.67}$$

This formula is also known as the **Rodrigues formula** for rotations.

4.2.5.3 Matrix Logarithm of a Rotation Matrix

So far we have shown that multiplying a vector $v \in \mathbb{R}^3$ by the exponential matrix $e^{[\omega]\theta}$ above amounts to rotating v about the axis ω by an angle θ. Our next task is to show that for any given rotation matrix $R \in SO(3)$, one can always find a unit vector ω and scalar θ such that $R = e^{[\omega]\theta}$. Defining $r = \omega\theta \in \mathbb{R}^3$, we shall call the skew-symmetric matrix $[r]$ the **matrix logarithm** of R. In this way we can assert that r provides another three-parameter representation for rotations. Expanding each of the entries for $e^{[\omega]\theta}$ in (4.67) leads to the following expression:

$$\begin{bmatrix} \mathrm{c}_\theta + \omega_1^2(1-\mathrm{c}_\theta) & \omega_1\omega_2(1-\mathrm{c}_\theta) - \omega_3\mathrm{s}_\theta & \omega_1\omega_3(1-\mathrm{c}_\theta) + \omega_2\mathrm{s}_\theta \\ \omega_1\omega_2(1-\mathrm{c}_\theta) + \omega_3\mathrm{s}_\theta & \mathrm{c}_\theta + \omega_2^2(1-\mathrm{c}_\theta) & \omega_2\omega_3(1-\mathrm{c}_\theta) - \omega_1\mathrm{s}_\theta \\ \omega_1\omega_3(1-\mathrm{c}_\theta) - \omega_2\mathrm{s}_\theta & \omega_2\omega_3(1-\mathrm{c}_\theta) + \omega_1\mathrm{s}_\theta & \mathrm{c}_\theta + \omega_3^2(1-\mathrm{c}_\theta) \end{bmatrix}, \tag{4.68}$$

where $(\omega_1, \omega_2, \omega_3)$ are the elements of ω, and we use the shorthand notation $\mathrm{s}_\theta = \sin\theta$, $\mathrm{c}_\theta = \cos\theta$. Setting the above equal to the given $R \in SO(3)$ and subtracting the transpose from both sides leads to the following:

$$\begin{aligned} r_{32} - r_{23} &= 2\omega_1 \sin\theta \\ r_{13} - r_{31} &= 2\omega_2 \sin\theta \\ r_{21} - r_{12} &= 2\omega_3 \sin\theta. \end{aligned}$$

Therefore as long as $\sin\theta \neq 0$ (or equivalently, θ is not an integer multiple of π), we can write

$$\begin{aligned} \omega_1 &= \frac{1}{2\sin\theta}(r_{32} - r_{23}) \\ \omega_2 &= \frac{1}{2\sin\theta}(r_{13} - r_{31}) \\ \omega_3 &= \frac{1}{2\sin\theta}(r_{21} - r_{12}). \end{aligned}$$

The above equations can also be expressed in skew-symmetric matrix form as

$$[\omega] = \begin{bmatrix} 0 & -\omega_3 & \omega_2 \\ \omega_3 & 0 & -\omega_1 \\ -\omega_2 & \omega_1 & 0 \end{bmatrix} = \frac{1}{2\sin\theta}\left(R - R^T\right). \tag{4.69}$$

Recall that ω represents the axis of rotation for the given R. Because of the $\sin\theta$ term in the denominator, $[\omega]$ is not well-defined if θ is an integer multiple of π. We address this situation next, but for now let us assume this is not the case and find an expression for θ. Setting R equal to (4.68) and taking the trace of both sides (recall that the trace of a matrix is the sum of its diagonals),

$$\operatorname{tr} R = r_{11} + r_{22} + r_{33} = 1 + 2\cos\theta. \tag{4.70}$$

The above follows since $\omega_1^2 + \omega_2^2 + \omega_3^2 = 1$. For any θ satisfying $1 + 2\cos\theta = \operatorname{tr} R$ such that θ is not an integer multiple of π, R can be expressed as the exponential $e^{[\omega]\theta}$ with $[\omega]$ as given in (4.69).

Let us now return to the case $\theta = k\pi$, where k is some integer. When k is an even integer (corresponding to $\theta = 0, \pm 2\pi, \pm 4\pi, \ldots$) we have $\operatorname{tr} R = 3$, or equivalently $R = I$, and it follows straightforwardly that $\theta = 0$ is the only possible solution. When k is an odd integer (corresponding to $\theta = \pm\pi, \pm 3\pi, \ldots$, which in turn implies $\operatorname{tr} R = -1$), the exponential formula (4.67) simplifies to

$$R = e^{[\omega]\pi} = I + 2[\omega]^2. \tag{4.71}$$

The three diagonal terms of (4.71) can be manipulated to

$$\omega_i = \pm\sqrt{\frac{r_{ii} + 1}{2}}, \quad i = 1, 2, 3. \tag{4.72}$$

These may not always lead to a feasible unit-norm solution ω. The off-diagonal terms lead to the following three equations:

$$\begin{aligned} 2\omega_1\omega_2 &= r_{12} \\ 2\omega_2\omega_3 &= r_{23} \\ 2\omega_1\omega_3 &= r_{13}, \end{aligned} \tag{4.73}$$

From (4.71) we also know that R must be symmetric: $r_{12} = r_{21}$, $r_{23} = r_{32}$, $r_{13} = r_{31}$. Both (4.72) and (4.73) may be necessary to obtain a feasible solution. Once a solution ω has been found, then $R = e^{[\omega]k\pi}$, $k = \pm\pi, \pm 3\pi, \ldots$.

From the above it can be seen that solutions for θ exist at 2π intervals. If we restrict θ to the interval $[0, \pi]$, then the following algorithm can be used to compute the **matrix logarithm** of the rotation matrix $R \in SO(3)$:

Algorithm: Given $R \in SO(3)$, find $r = \omega\theta \in \mathbb{R}^3$, where $\theta \in [0, \pi]$ and $\omega \in \mathbb{R}^3$, $\|\omega\| = 1$, such that

$$R = e^{[r]} = e^{[\omega]\theta} = I + \sin\theta\,[\omega] + (1 - \cos\theta)[\omega]^2. \tag{4.74}$$

The skew-symmetric matrix $[r] \in \mathbb{R}^{3\times 3}$ is then said to be a **matrix logarithm** of R.

(i) If $R = I$, then $\theta = 0$ and $[r] = 0$.

(ii) If $\operatorname{tr} R = -1$, then $\theta = \pi$, and set ω to any of the three following vectors that is a feasible solution:

$$\omega = \frac{1}{\sqrt{2(1 + r_{33})}} \begin{bmatrix} r_{13} \\ r_{23} \\ 1 + r_{33} \end{bmatrix} \tag{4.75}$$

or

$$\omega = \frac{1}{\sqrt{2(1 + r_{22})}} \begin{bmatrix} r_{12} \\ 1 + r_{22} \\ r_{32} \end{bmatrix} \tag{4.76}$$

or

$$\omega = \frac{1}{\sqrt{2(1 + r_{11})}} \begin{bmatrix} 1 + r_{11} \\ r_{21} \\ r_{31} \end{bmatrix}. \tag{4.77}$$

(iii) Otherwise $\theta = \cos^{-1}\left(\frac{\operatorname{tr} R - 1}{2}\right) \in [0, \pi)$ and

$$[\omega] = \frac{1}{2\sin\theta}(R - R^T). \tag{4.78}$$

The formula for the logarithm suggests a picture of the rotation group $SO(3)$ as a solid ball of radius π (see Figure 4.7): given a point $r \in \mathbb{R}^3$ in this solid ball, let $\omega = r/\|r\|$ and $\theta = \|r\|$, so that $r = \omega\theta$. The rotation matrix corresponding

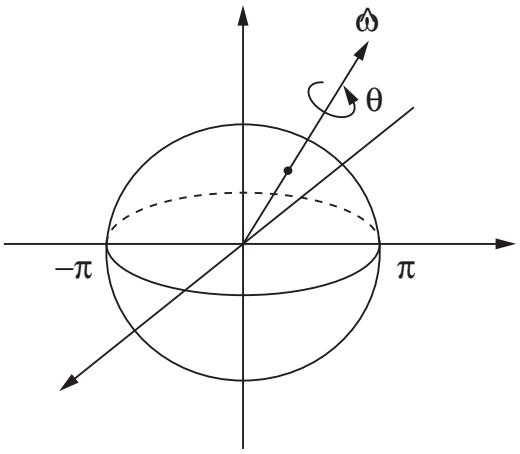

Figure 4.7: *SO(3)* as a solid ball of radius π.

to r can then be regarded as a rotation about the axis ω by an angle θ. For any $R \in SO(3)$ such that $\operatorname{tr} R \neq -1$, there exists a unique r in the interior of the solid ball such that $e^{[r]} = R$. In the event that $\operatorname{tr} R = -1$, $\log R$ is given by two antipodal points on the surface of this solid ball. That is, if if there exists some r such that $R = e^{[r]}$, then $\|r\| = \pi$, and $R = e^{[-r]}$ also holds; both r and $-r$ correspond to the same rotation R.

4.2.6 Unit Quaternions

One disadvantage with the exponential coordinates on $SO(3)$ is that because of the division by $\sin\theta$ in the logarithm formula, the logarithm can be numerically sensitive to small rotation angles θ. The **unit quaternions** are an alternative representation of rotations that alleviates some of these numerical difficulties, but at the cost of introducing an additional fourth parameter. We now illustrate the definition and use of these coordinates.

Let $R \in SO(3)$ have exponential coordinate representation $R = e^{[\omega]\theta}$, where as usual $\|\omega\| = 1$ and $\theta \in [0, \pi]$. The unit quaternion representation of R is constructed as follows. Define $q \in \mathbb{R}^4$ according to

$$q = \begin{bmatrix} q_0 \\ q_1 \\ q_2 \\ q_3 \end{bmatrix} = \begin{bmatrix} \cos\frac{\theta}{2} \\ \omega \sin\frac{\theta}{2} \end{bmatrix} \in \mathbb{R}^4. \tag{4.79}$$

q as defined clearly satifies $\|q\| = 1$. Geometrically, q is a point lying on the three-dimensional unit sphere in $\mathbb{R}^4$, and for this reason the unit quaternions are also identified with the three-sphere, denoted S^3. Naturally among the

four coordinates of q, only three can be chosen independently. Recalling that $1 + 2\cos\theta = \text{tr}\, R$, and using the cosine double angle formula, i.e., $\cos 2\phi = 2\cos^2\phi - 1$, the elements of q can be obtained directly from the entries of R as follows:

$$q_0 = \frac{1}{2}\sqrt{1 + r_{11} + r_{22} + r_{33}} \tag{4.80}$$

$$\begin{bmatrix} q_1 \\ q_2 \\ q_3 \end{bmatrix} = \frac{1}{4q_0}\begin{bmatrix} r_{32} - r_{23} \\ r_{13} - r_{31} \\ r_{21} - 2_{12} \end{bmatrix}. \tag{4.81}$$

Going the other way, given a unit quaternion (q_0, q_1, q_2, q_3), the corresponding rotation matrix R is obtained as a rotation about the unit axis in the direction of (q_1, q_2, q_3), by an angle $2\cos^{-1} q_0$. Explicitly,

$$R = \begin{bmatrix} q_0^2 + q_1^2 - q_2^2 - q_3^2 & 2(q_1q_2 - q_0q_3) & 2(q_0q_2 + q_1q_3) \\ 2(q_0q_3 + q_1q_2) & q_0^2 - q_1^2 + q_2^2 - q_3^2 & 2(q_2q_3 - q_0q_1) \\ 2(q_1q_3 - q_0q_2) & 2(q_0q_1 + q_2q_3) & q_0^2 - q_1^2 - q_2^2 + q_3^2 \end{bmatrix}. \tag{4.82}$$

From the above explicit formula it should be apparent that both $q \in S^3$ and its antipodal point $-q \in S^3$ produce the same rotation matrix R. For every rotation matrix there exists two unit quaternion representations that are antipodal to each other.

The final property of the unit quaternions concerns the product of two rotations. Let $R_q, R_p \in SO(3)$ denote two rotation matrices, with unit quaternion representations $\pm q, \pm p \in S^3$, respectively. The unit quaternion representation for the product R_qR_p can then be obtained by first arranging the elements of q and p in the form of the following 2×2 complex matrices:

$$Q = \begin{bmatrix} q_0 + iq_1 & q_2 + ip_3 \\ -q_2 + iq_3 & q_0 - iq_1 \end{bmatrix}, \quad P = \begin{bmatrix} p_0 + ip_1 & p_2 + ip_3 \\ -p_2 + ip_3 & p_0 - ip_1 \end{bmatrix}, \tag{4.83}$$

where i denotes the imaginary unit. Now take the product $N = QP$, where the entries of N are written

$$N = \begin{bmatrix} n_0 + in_1 & n_2 + in_3 \\ -n_2 + in_3 & n_0 - in_1 \end{bmatrix}. \tag{4.84}$$

The unit quaternion for the product R_qR_p is then given by $\pm(n_0, n_1, n_2, n_3)$ obtained from the entries of N:

$$\begin{bmatrix} n_0 \\ n_1 \\ n_2 \\ n_3 \end{bmatrix} = \begin{bmatrix} q_0p_0 - q_1p_1 - q_2p_2 - q_3p_3 \\ q_0p_1 + p_0q_1 + q_2p_3 - q_3p_2 \\ q_0p_2 + p_0q_2 - q_1p_3 + q_3p_1 \\ q_0p_3 + p_0q_3 + q_1p_2 - q_2p_1 \end{bmatrix}. \tag{4.85}$$

Verification of this formula is left as an exercise at the end of this chapter.

4.3 Rigid-Body Motions

4.3.1 Definition

We now consider representations for the combined orientation and position of a rigid body. This would seem to be fairly straightforward: once fixed and moving frames are defined, the orientation can be described by a rotation matrix $R \in SO(3)$, and the position by a vector $p \in \mathbb{R}^3$. Rather than identifying R and p separately, we shall combine them into a single matrix as follows.

Definition 4.4. The **Special Euclidean Group** $SE(3)$, also known as the group of **rigid body motions** or **homogeneous transformations** in $\mathbb{R}^3$, is the set of all 4×4 real matrices T of the form

$$T = \begin{bmatrix} R & p \\ 0 & 1 \end{bmatrix}, \tag{4.86}$$

where $R \in SO(3)$, $p \in \mathbb{R}^3$, and 0 denotes the three-dimensional row vector of zeros.

An element $T \in SE(3)$ will also sometimes be denoted more compactly as $T = (R, p)$. We begin this section by establishing some basic properties of $SE(3)$, and explaining why we package R and p into this somewhat unusual matrix form.

From the definition it should be apparent that six coordinates are needed to parametrize $SE(3)$. The most obvious choice of coordinates would be to use any of the earlier three-parameter representations for $SO(3)$ (e.g., Euler angles, exponential coordinates) to parametrize the orientation R, and the usual three Cartesian coordinates in $\mathbb{R}^3$ to parametrize the position p. Instead, we shall derive a six-dimensional version of exponential coordinates on $SE(3)$ that turns out to have several advantages over these other parametrizations.

Many of the robotic mechanisms we have encountered thus far are planar. With planar rigid-body motions in mind, we make the following definition:

Definition 4.5. The **Special Euclidean Group** $SE(2)$ is the set of all 3×3 real matrices T of the form

$$T = \begin{bmatrix} R & p \\ 0 & 1 \end{bmatrix}, \tag{4.87}$$

where $R \in SO(2)$, $p \in \mathbb{R}^2$, and 0 denotes the two-dimensional row vector of zeros.

A matrix $T \in SE(2)$ will always be of the form

$$T = \begin{bmatrix} \cos\theta & -\sin\theta & p_x \\ \sin\theta & \cos\theta & p_y \\ 0 & 0 & 1 \end{bmatrix},$$

where $\theta \in [0, 2\pi]$ and $(p_x, p_y) \in \mathbb{R}^2$.

4.3.2 Properties

The following two properties of $SE(3)$ can be verified by direct calculation.

Proposition 4.12. *The product of two $SE(3)$ matrices is also an $SE(3)$ matrix.*

Proposition 4.13. *The inverse of an $SE(3)$ matrix always exists, and has the following explicit form:*

$$\begin{bmatrix} R & p \\ 0 & 1 \end{bmatrix}^{-1} = \begin{bmatrix} R^T & -R^T p \\ 0 & 1 \end{bmatrix}. \tag{4.88}$$

Before stating the next proposition, we introduce the following notation:

Definition 4.6. Given $T = (R, p) \in SE(3)$ and $x \in \mathbb{R}^3$, the product $Tx \in \mathbb{R}^3$ is then defined to be

$$Tx = Rx + p. \tag{4.89}$$

The above is a slight abuse of notation, but is motivated by the fact that if $x \in \mathbb{R}^3$ is turned into a four-dimensional vector by appending a '1', then

$$\begin{bmatrix} R & p \\ 0 & 1 \end{bmatrix} \begin{bmatrix} x \\ 1 \end{bmatrix} = \begin{bmatrix} Rx + p \\ 1 \end{bmatrix}. \tag{4.90}$$

The four-dimensional vector obtained by appending a '1' to x is an example of **homogeneous coordinates**; the transformation $T \in SE(3)$ is also accordingly called a homogeneous transformation.

With the above definition of Tx, the next proposition can also be verified by direct calculation:

Proposition 4.14. *Given $T = (R, p) \in SE(3)$ and $x, y \in \mathbb{R}^3$, the following hold:*

(i) $\|Tx - Ty\| = \|x - y\|$, *where $\|\cdot\|$ denotes the standard Euclidean norm in $\mathbb{R}^3$, i.e., $\|x\| = \sqrt{x^T x}$.*

(ii) $\langle Tx - Tz, Ty - Tz \rangle = \langle x - z, y - z \rangle$ *for all $z \in \mathbb{R}^3$, where $\langle \cdot, \cdot \rangle$ denotes the standard Euclidean inner product in $\mathbb{R}^3$, i.e., $\langle x, y \rangle = x^T y$.*

In the above proposition, T is regarded as a transformation on points in $\mathbb{R}^3$, i.e., T transforms a point x to Tx. The first property then asserts that T preserves distances, while the second asserts that T preserves angles. Specifically, if $x, y, z \in \mathbb{R}^3$ represent the three vertices of a triangle, then the triangle formed by the transformed vertices $\{Tx, Ty, Tz\}$ has the same set of lengths and angles as those of the triangle $\{x, y, z\}$ (or, the two triangles are said to be isometric). One can easily imagine taking x to be the points on a rigid body, in which case Tx results in a displaced version of the rigid body. It is in this sense that $SE(3)$ can be identified with the rigid body motions.

The remaining properties describe the different physical contexts in which rigid-body motions are used. Like rotations, both descriptive and prescriptive

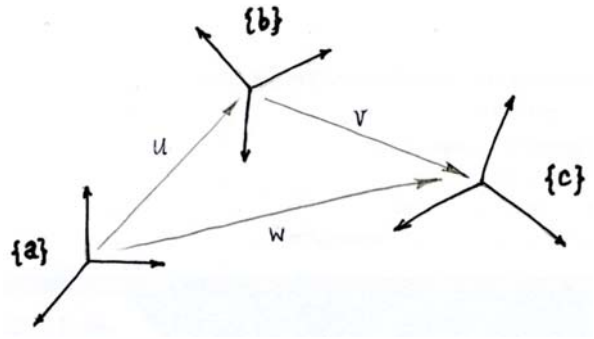

Figure 4.8: Three reference frames in space.

interpretations for rigid body motions are possible, and we begin with the former. Referring to Figure 4.8, consider three reference frames {a}, {b}, and {c} in physical space. Define u to be the vector from the origin of frame {a} to the origin of frame {b}; v and w are also defined as indicated in the figure. Denote by $T_{ab} \in SE(3)$ the position and orientation of frame {b} as seen from frame {a}; that is, R_{ab} denotes the orientation of frame {b} expressed in frame {a} coordinates, and $p_{ab} \in \mathbb{R}^3$ is the vector representation of u in $\{a\}$ frame coordinates. T_{bc} and T_{ac} are defined in a similar fashion, with $p_{ac} \in \mathbb{R}^3$ the vector representation of w in $\{a\}$ frame coordinates, and $p_{bc} \in \mathbb{R}^3$ the vector representation of **v** in $\{b\}$ frame coordinates.

Proposition 4.15. *Given three reference frames $\{a\}$, $\{b\}$, $\{c\}$ in physical space, let $T_{ab}, T_{bc}, T_{ac} \in SE(3)$ denote the relative displacements between these frames. Then $T_{ab}T_{bc} = T_{ac}$.*

Proof. Let $T_{ab}, T_{bc}, T_{ac} \in SE(3)$ be given by

$$T_{ab} = \begin{bmatrix} R_{ab} & p_{ab} \\ 0 & 1 \end{bmatrix}, \; T_{bc} = \begin{bmatrix} R_{bc} & p_{bc} \\ 0 & 1 \end{bmatrix}, \; T_{ac} = \begin{bmatrix} R_{ac} & p_{ac} \\ 0 & 1 \end{bmatrix}.$$

From a previously derived property of rotation matrices we know that $R_{ab}R_{bc} = R_{ac}$. Referring to Figure 4.8, to express the vector relation u+v = w in {a} frame coordinates, we first need to find an expression for v in {a} frame coordinates. From Proposition 4.6, this is simply $R_{ab}p_{bc}$. It now follows that

$$p_{ac} = R_{ab}p_{bc} + p_{ab}. \tag{4.91}$$

The above can be combined into the following matrix equation:

$$\begin{bmatrix} R_{ab} & p_{ab} \\ 0 & 1 \end{bmatrix} \begin{bmatrix} R_{bc} & p_{bc} \\ 0 & 1 \end{bmatrix} = \begin{bmatrix} R_{ac} & p_{ac} \\ 0 & 1 \end{bmatrix}, \tag{4.92}$$

or equivalently, $T_{ab}T_{bc} = T_{ac}$. □

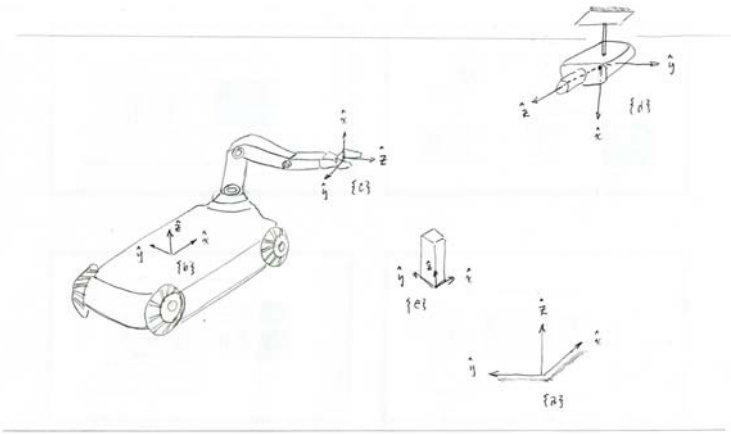

Figure 4.9: Assignment of reference frames.

The T_{ab} notation is a very convenient way of keeping track of the relationships between multiple reference frames. The following is a direct consequence of the previously established property:

Proposition 4.16. *$T_{aa} = I$, and $T_{ab}^{-1} = T_{ba}$.*

Referring again to Figure 4.8, we now change our perspective slightly, and let q denote the point in physical space corresponding to the $\{c\}$ frame origin. Let $q_b \in \mathbb{R}^3$ be the vector representation of the point q in $\{b\}$ frame coordinates; that is, $q_b = p_{bc}$. Similarly, let $q_a \in \mathbb{R}^3$ be the vector representation of the same point q in $\{a\}$ frame coordinates; that is, $q_a = p_{ac}$. Since p_{ac} and p_{bc} are related by Equation 4.91, it follows that the same relationship also exists between q_a and q_b:

$$\begin{bmatrix} q_a \\ 1 \end{bmatrix} = \begin{bmatrix} R_{ab} & p_{ab} \\ 0 & 1 \end{bmatrix} \begin{bmatrix} q_b \\ 1 \end{bmatrix}, \tag{4.93}$$

or in homogeneous coordinate notation,

$$q_a = T_{ab} q_b. \tag{4.94}$$

We have in fact just proven the following:

Proposition 4.17. *Given a point q in physical space, let $q_a \in \mathbb{R}^3$ and $q_b \in \mathbb{R}^3$ denote its coordinates in terms of reference frames $\{a\}$ and $\{b\}$, respectively. Then*

$$q_a = T_{ab} q_b, \tag{4.95}$$

with the product $T_{ab}q_b$ interpreted in the sense of the right-hand side of Equation (4.93).

Example

Figure 4.9 shows a robot arm mounted on a wheeled mobile platform, and a camera fixed to the ceiling. Frames {b} and {c} are respectively attached to the wheeled platform and the end-effector of the robot arm, and frame {d} is attached to the camera. A fixed frame {a} has been established, and the robot must pick up the object with body frame {e}. Suppose that the transformations T_{db} and T_{de} can be calculated from measurements obtained with the camera. The transformation T_{bc} can be determined by evaluating the forward kinematics for the current joint measurements. The transformation T_{ad} is assumed to be known in advance. Suppose these known transformations are given as follows:

$$
\begin{aligned}
T_{db} &= \begin{bmatrix} 0 & 0 & -1 & 250 \\ 0 & -1 & 0 & -150 \\ -1 & 0 & 0 & 200 \\ 0 & 0 & 0 & 1 \end{bmatrix} \\
T_{de} &= \begin{bmatrix} 0 & 0 & -1 & 300 \\ 0 & -1 & 0 & 100 \\ -1 & 0 & 0 & 120 \\ 0 & 0 & 0 & 1 \end{bmatrix} \\
T_{ad} &= \begin{bmatrix} 0 & 0 & -1 & 400 \\ 0 & -1 & 0 & 50 \\ -1 & 0 & 0 & 300 \\ 0 & 0 & 0 & 1 \end{bmatrix} \\
T_{bc} &= \begin{bmatrix} 0 & -1/\sqrt{2} & -1/\sqrt{2} & 30 \\ 0 & 1/\sqrt{2} & -1/\sqrt{2} & -40 \\ 1 & 0 & 0 & 25 \\ 0 & 0 & 0 & 1 \end{bmatrix}.
\end{aligned}
$$

In order for the robot arm to pick up the object, T_{ce} must be determined. We know that

$$T_{ab}T_{bc}T_{ce} = T_{ad}T_{de},$$

where the only quantity besides T_{ce} not given to us directly is T_{ab}. However, since $T_{ab} = T_{ad}T_{de}$, we can determine T_{ce} as follows:

$$T_{ce} = (T_{ad}T_{db}T_{bc})^{-1}\, T_{ad}T_{de}.$$

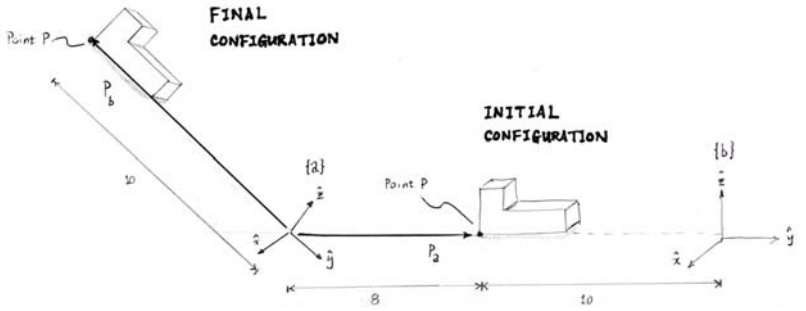

Figure 4.10: Displacement of a rigid body from an initial to final configuration.

From the given transformations,

$$T_{ad}T_{de} = \begin{bmatrix} 1 & 0 & 0 & 280 \\ 0 & 1 & 0 & -50 \\ 0 & 0 & 1 & 0 \\ 0 & 0 & 0 & 1 \end{bmatrix}$$

$$T_{ad}T_{db}T_{bc} = \begin{bmatrix} 0 & -1/\sqrt{2} & -1/\sqrt{2} & 230 \\ 0 & 1/\sqrt{2} & -1/\sqrt{2} & 160 \\ 1 & 0 & 0 & 75 \\ 0 & 0 & 0 & 1 \end{bmatrix}$$

$$(T_{ad}T_{db}T_{bc})^{-1} = \begin{bmatrix} 0 & 0 & 1 & -75 \\ -1/\sqrt{2} & 1/\sqrt{2} & 0 & 70/\sqrt{2} \\ -1/\sqrt{2} & -1/\sqrt{2} & 0 & 390/\sqrt{2} \\ 0 & 0 & 0 & 1 \end{bmatrix}$$

from which T_{ce} is evaluated to be

$$T_{ce} = \begin{bmatrix} 0 & 0 & 1 & -75 \\ -1/\sqrt{2} & 1/\sqrt{2} & 0 & -260/\sqrt{2} \\ -1/\sqrt{2} & -1/\sqrt{2} & 0 & 130/\sqrt{2} \\ 0 & 0 & 0 & 1 \end{bmatrix}.$$

We conclude this section with an examination of the prescriptive interpretation of a rigid body motion. Figure 4.10 shows a rigid body that has been displaced from some initial configuration to a new configuration. {a} is the fixed frame, and the rigid body motion is represented by the $SE(3)$ matrix T_{ba} (we shall specify in a moment how to locate the $\{b\}$ frame from the two given configurations of the rigid body). Let p denote a point on the rigid body; $p_a \in \mathbb{R}^3$ is then the coordinates for p in the initial configuration, and $p_b \in \mathbb{R}^3$ is the coordinates for p in the displaced configuration. In terms of T_{ba} we then have the relation

$$p_b = T_{ba}p_a. \tag{4.96}$$

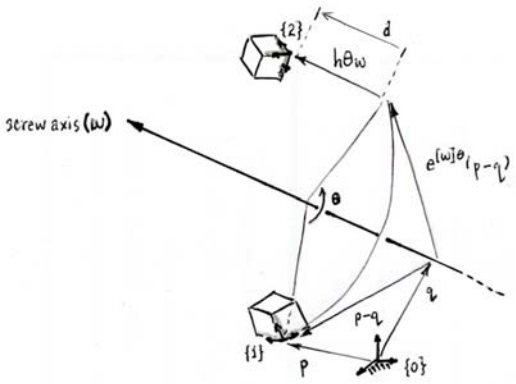

Figure 4.11: A rigid body displacement expressed as a screw motion.

The frame {b} is now drawn such that its location relative to the initial rigid body configuration is the same as the location of frame {a} relative to the displaced rigid body configuration (see Figure 4.10). For the given example, T_{ba} is given by

$$T_{ba} = \begin{bmatrix} 1 & 0 & 0 & 0 \\ 0 & 1/\sqrt{2} & 1/\sqrt{2} & -18 \\ 0 & -1/\sqrt{2} & 1/\sqrt{2} & 0 \\ 0 & 0 & 0 & 1 \end{bmatrix}. \tag{4.97}$$

4.3.3 Screw Motions

4.3.3.1 Mathematical Representation

In the planar example given at the beginning of this chapter, we saw that any planar rigid body displacement can be achieved by rotating the rigid body about some fixed point in the plane (for a pure translation, this point lies at infinity). A similar result also exists for spatial rigid body displacements: called the **Chasles-Mozzi Theorem**, it states that every rigid body displacement can be expressed as a rotation about some fixed axis in space, followed by a pure translation parallel to that axis. In fact, switching the order of the rotation and translation will still result in the same displacement. One can therefore imagine the rotation and translation occuring simultaneously, resulting in the familiar motion of a screw.

In this section we shall develop a mathematical representation for screw motions. Figure 4.11 shows a rigid body undergoing a displacement in three-dimensional space; all vectors in the figure are expressed in terms of the fixed {0} frame coordinates. The initial and final configurations of the rigid body are labelled by frames {1} and {2}, respectively. According to the Chasles-Mozzi Theorem, there exists a screw axis—represented by the line passing through the point q and in the direction of the unit vector ω—such that the displacement can be characterized as a screw motion about this axis. The screw motion consists of

a rotation about the screw axis by some angle θ, and a translation parallel to the screw axis by a distance d. As mentioned earlier, the order of the rotation and translation are interchangeable. We now derive the homogeneous transformation corresponding to this screw motion. Suppose the relative displacements T_{01} and T_{02} are given by

$$T_{01} = \begin{bmatrix} R & p \\ 0 & 1 \end{bmatrix} \tag{4.98}$$

$$T_{02} = \begin{bmatrix} R' & p' \\ 0 & 1 \end{bmatrix}. \tag{4.99}$$

The **screw pitch**, denoted h, is a scalar quantity defined as

$$h = \frac{d}{\theta}. \tag{4.100}$$

From the figure we can express R' and p' as

$$R' = e^{[\omega]\theta} R \tag{4.101}$$

$$p' = q + e^{[\omega]\theta}(p - q) + h\theta\omega. \tag{4.102}$$

The first equation is a consequence of the fact that the orientation of frame $\{2\}$ is obtained by rotating frame $\{1\}$ about the ω axis by an angle θ. The second equation follows by verifying that p' is the vectorial sum of the three vectors q, $e^{[\omega]\theta}(p - q)$, and $h\theta\omega$ as indicated in the figure. The above two equations can be combined into the following matrix equation:

$$\begin{bmatrix} R' & p' \\ 0 & 1 \end{bmatrix} = \begin{bmatrix} e^{[\omega]\theta} & \left(I - e^{[\omega]\theta}\right) q + h\theta\omega \\ 0 & 1 \end{bmatrix} \begin{bmatrix} R & p \\ 0 & 1 \end{bmatrix}. \tag{4.103}$$

The $SE(3)$ matrix

$$\begin{bmatrix} e^{[\omega]\theta} & \left(I - e^{[\omega]\theta}\right) q + h\theta\omega \\ 0 & 1 \end{bmatrix} \tag{4.104}$$

is the homogeneous transformation representation of the screw motion. In the remainder of this chapter and also the next chapter on kinematics, we shall be making the case that it is better to express this matrix as a pure matrix exponential, in the same way that a rotation matrix can be expressed as the exponential of a skew-symmetric matrix.

In the meantime we first introduce some notation.

Definition 4.7. Given $\omega, v \in \mathbb{R}^3$, let

$$\mathcal{S} = \begin{bmatrix} \omega \\ v \end{bmatrix} \in \mathbb{R}^6, \tag{4.105}$$

which we also write more compactly as $\mathcal{S} = (\omega, v) \in \mathbb{R}^6$. The six-dimensional vector $\mathcal{S} = (\omega, v)$ is called a **twist**. Define $[S] \in \mathbb{R}^{4\times 4}$ to be the following 4×4 matrix:

$$[\mathcal{S}] = \begin{bmatrix} [\omega] & v \\ 0 & 0 \end{bmatrix}, \quad [\omega] = \begin{bmatrix} 0 & -\omega_3 & \omega_2 \\ \omega_3 & 0 & -\omega_1 \\ -\omega_2 & \omega_1 & 0 \end{bmatrix}, \tag{4.106}$$

where the bottom row of $[\mathcal{S}]$ consists of all zeros.

With the above notation, let us now derive a closed-form expression for the matrix exponential $e^{[\mathcal{S}]\theta}$, where $\mathcal{S} = (\omega, v)$ with $\omega \in \mathbb{R}^3$ satisfying $\|\omega\| = 1$. By an appropriate choice of v, the exponential $e^{[\mathcal{S}]\theta}$ can be made equal to the matrix of Equation (4.104); our immediate task is to find this v. Expanding the matrix exponential in series form leads to

$$\begin{aligned} e^{[\mathcal{S}]\theta} &= I + [\mathcal{S}]\theta + [\mathcal{S}]^2\frac{\theta^2}{2!} + [\mathcal{S}]^3\frac{\theta^3}{3!} + \dots \\ &= \begin{bmatrix} e^{[\omega]\theta} & G(\theta)v \\ 0 & 1 \end{bmatrix}, \quad G(\theta) = I\theta + [\omega]\frac{\theta^2}{2!} + [\omega]^2\frac{\theta^3}{3!} + \dots \end{aligned} \tag{4.107}$$

Noting the similarity between $G(\theta)$ and the series definition for $e^{[\omega]\theta}$, it is tempting to write $I + G(\theta)[\omega] = e^{[\omega]\theta}$, and to conclude that $G(\theta) = (e^{[\omega]\theta} - I)[\omega]^{-1}$. This is wrong: $[\omega]^{-1}$ does not exist (try computing $\det[\omega]$).

Instead we make use of the result $[\omega]^3 = -[\omega]$ that was obtained from the Cayley-Hamilton Theorem. In this case $G(\theta)$ can be simplified to

$$\begin{aligned} G(\theta) &= I\theta + [\omega]\frac{\theta^2}{2!} + [\omega]^2\frac{\theta^3}{3!} + \dots \\ &= I\theta + \left(\frac{\theta^2}{2!} - \frac{\theta^4}{4!} + \frac{\theta^6}{6!} - \dots\right)[\omega] + \left(\frac{\theta^3}{3!} - \frac{\theta^5}{5!} + \frac{\theta^7}{7!} - \dots\right)[\omega]^2 \\ &= I\theta + (1 - \cos\theta)[\omega] + (\theta - \sin\theta)[\omega]^2. \end{aligned} \tag{4.108}$$

Putting everything together,

Proposition 4.18. *Let $\omega, v \in \mathbb{R}^3$ and define $\mathcal{S} = (\omega, v)$. If ω satisfies $\|\omega\| = 1$, then for any $\theta \in \mathbb{R}$,*

$$e^{[\mathcal{S}]\theta} = \begin{bmatrix} e^{[\omega]\theta} & \left(I\theta + (1 - \cos\theta)[\omega] + (\theta - \sin\theta)[\omega]^2\right) v \\ 0 & 1 \end{bmatrix}. \tag{4.109}$$

If $\omega = 0$ so that $\mathcal{S} = (0, v)$, then

$$e^{[\mathcal{S}]\theta} = \begin{bmatrix} I & v\theta \\ 0 & 1 \end{bmatrix}. \tag{4.110}$$

The latter result of the propostion can be verified directly from the series expansion of $e^{[\mathcal{S}]\theta}$ with ω set to zero.

We now answer the question of what choice of v results in (4.109) equaling (4.104). The answer is

$$v = -[\omega]q + h\omega. \tag{4.111}$$

This can be verified by substituting this v into Equation (4.109) and making use of the identities $[\omega]\omega = 0$ and $[\omega]^3 = -[\omega]$. With this choice of v, the pitch h of the screw motion can then be expressed as

$$h = \omega^T v. \tag{4.112}$$

4.3.3.2 Matrix Logarithm of a Homogeneous Transformation

The above derivation essentially provides a constructive proof of the Chasles-Mozzi Theorem. That is, given an arbitrary $(R, p) \in SE(3)$, one can always find some $\mathcal{S} = (\omega, v)$ and a scalar θ such that

$$e^{[\mathcal{S}]\theta} = \begin{bmatrix} R & p \\ 0 & 1 \end{bmatrix}. \tag{4.113}$$

In the simplest case, if $R = I$, then $\omega = 0$, and the preferred choice for v is $v = p/\|p\|$ (this would make $\theta = \|p\|$ the translation distance). If R is not the identity matrix and $\operatorname{tr} R \neq -1$, the solution is given by

$$[\omega] = \frac{1}{2\sin\theta}(R - R^T) \tag{4.114}$$

$$v = G^{-1}(\theta)p, \tag{4.115}$$

where θ satisfies $1 + 2\cos\theta = \operatorname{tr} R$. We leave as an exercise the verification of the following formula for $G^{-1}(\theta)$:

$$G^{-1}(\theta) = \frac{1}{\theta}I + \frac{1}{2}[\omega] + (\frac{1}{\theta} - \frac{1}{2}\cot\frac{\theta}{2})[\omega]^2. \tag{4.116}$$

Finally, if $\operatorname{tr} R = -1$, we choose $\theta = \pi$, and $[\omega]$ can be obtained via the matrix logarithm formula on $SO(3)$. Once $[\omega]$ and θ have been determined, v can then be obtained as $v = G^{-1}(\theta)p$.

Algorithm: Given $(R, p) \in SE(3)$, we seek $\mathcal{S} = (\omega, v) \in \mathbb{R}^6$ and $\theta \in [0, \pi]$ such that $e^{[\omega]\theta} = R$.

(i) If $R = I$, then set $\omega = 0$, $v = p/\|p\|$, and $\theta = \|p\|$.

(ii) If $\operatorname{tr} R = -1$, then set $\theta = \pi$, and $[\omega] = \log R$ as determined by the matrix logarithm formula on $SO(3)$ for the case $\operatorname{tr} R = -1$.

(iii) Otherwise set $\theta = \cos^{-1}\left(\frac{\operatorname{tr} R - 1}{2}\right) \in [0, \pi)$ and

$$[\omega] = \frac{1}{2\sin\theta}(R - R^T) \tag{4.117}$$

$$v = G^{-1}(\theta)p, \tag{4.118}$$

where $G^{-1}(\theta)$ is given by Equation (4.116).

Example

As an example, we consider the special case of planar rigid body motions and examine the matrix logarithm formula on $SE(2)$. Referring once again to Fig-

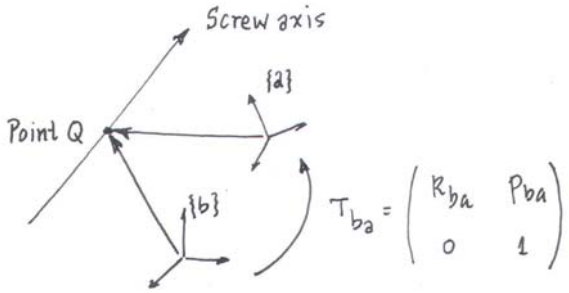

Figure 4.12: Transformation of the twist vector for a screw motion under a change of reference frames.

ure 4.1(b), suppose the initial and final configurations of the body are respectively represented by the $SE(2)$ matrices

$$T_{sb} = \begin{bmatrix} \cos 30^\circ & -\sin 30^\circ & 1 \\ \sin 30^\circ & \cos 30^\circ & 2 \\ 0 & 0 & 1 \end{bmatrix}$$
$$T_{sb} = \begin{bmatrix} \cos 60^\circ & -\sin 60^\circ & 2 \\ \sin 60^\circ & \cos 60^\circ & 1 \\ 0 & 0 & 1 \end{bmatrix}.$$

For this example, the rigid body displacement occurs in the x-y plane. The corresponding screw motion will therefore have its screw axis in the direction of the z-axis, and be of zero pitch. The twist vector (ω, v) representing the screw motion will be of the form

$$\omega = (0, 0, \omega_3)$$
$$v = (v_1, v_2, 0).$$

Using this reduced form, we seek the screw motion that displaces the frame at T_{sb} to T_{sc}, i.e., $T_{sc} = e^{[\mathcal{S}]\theta} T_{sb}$, or

$$T_{sc} T_{sb}^{-1} = e^{[\mathcal{S}]\theta},$$

where

$$[\mathcal{S}] = \begin{bmatrix} 0 & -\omega_3 & v_1 \\ \omega_3 & 0 & v_2 \\ 0 & 0 & 0 \end{bmatrix}.$$

We can apply the matrix logarithm algorithm directly to $T_{sc} T_{sb}^{-1}$ to obtain $[\mathcal{S}]$ and θ as follows:

$$[\mathcal{S}] = \begin{bmatrix} 0 & -1 & 3 \\ 1 & 0 & -3 \\ 0 & 0 & 0 \end{bmatrix}.$$

Alternatively, we can observe that the displacement is not a pure translation—T_{sb} and T_{sc} have rotation components that differ by an angle of 30°—and quickly determine that $\theta = 30°$ and $\omega_3 = 1$. We can also graphically determine the point $q = (q_x, q_y)$ on the x-y plane that the screw axis must pass through; for our example this point is given by $q = (3, 3)$. Since the screw motion has zero pitch ($h = 0$), using the relation $v = -\omega \times q + h\omega$ leads to

$$(v_x, v_y) = (q_y, -q_x) = (-3, 3).$$

4.3.3.3 Transformation Under Change of Reference Frames

We now examine how the twist vector for a screw motion transforms under a change of reference frames. For this purpose consider the general screw motion of pitch h (see Figure 4.12). Pick an arbitrary point q on this screw axis, and denote its coordinates in terms of reference frames {a} and {b} respectively by $q_a, q_b \in \mathbb{R}^3$. Let the twist for this screw motion as seen from frame {a} be given by $\mathcal{S}_a = (\omega_a, v_a)$, where $v_a = -\omega_a \times q_a + h\omega_a$. Similarly, let the twist for this same screw motion as seen from frame {b} be $\mathcal{S}_b = (\omega_b, v_b)$, where $v_b = -\omega_b \times q_b + h\omega_b$. Given the homogeneous transformation $T_{ba} = (R_{ba}, p_{ba}) \in SE(3)$, we now try to express (ω_b, v_b) in terms of (ω_a, v_a) and (R_{ba}, p_{ba}).

From our previous results we know that $\omega_b = R_{ba}\omega_a$ and $q_b = R_{ba}q_a + p_{ba}$. It follows that

$$\begin{aligned} v_b &= -R_{ba}\omega_a \times (R_{ba}q_a + p_{ba}) + hR_{ba}\omega_a \\ &= -[R_{ba}\omega_a]R_{ba}q_a - [R_{ba}\omega_a]p_{ba} + hR_{ba}\omega_a \\ &= -R_{ba}[\omega_a]R_{ba}^T R_{ba}q_a + [p_{ba}]R_{ba}\omega_a + hR_{ba}\omega_a \\ &= -R_{ba}[\omega_a]q_a + R_{ba}h\omega_a + [p_{ba}]R_{ba}\omega_a \\ &= R_{ba}(-[\omega_a]q_a + h\omega_a) + [p_{ba}]R_{ba}\omega_a \\ &= R_{ba}v_a + [p_{ba}]R_{ba}\omega_a, \end{aligned} \tag{4.119}$$

where we have made use of the properties $u \times v = [u]v$ and $R[u]R^T = [Ru]$ for any $u, v \in \mathbb{R}^3$ and $R \in SO(3)$. These equations for ω_b and v_b can be written in the equivalent matrix form

$$\begin{bmatrix} [\omega_b] & v_b \\ 0 & 0 \end{bmatrix} = \begin{bmatrix} R_{ba} & p_{ba} \\ 0 & 1 \end{bmatrix} \begin{bmatrix} [\omega_a] & v_a \\ 0 & 0 \end{bmatrix} \begin{bmatrix} R_{ba}^T & -R_{ba}^T p_{ba} \\ 0 & 1 \end{bmatrix}. \tag{4.120}$$

The above can be written as $[\mathcal{S}_b] = T_{ba}[\mathcal{S}_a]T_{ba}^{-1}$, which can be also expressed in vector form as

$$\begin{bmatrix} \omega_b \\ v_b \end{bmatrix} = \begin{bmatrix} R_{ba} & 0 \\ [p_{ba}]\,R_{ba} & R_{ba} \end{bmatrix} \begin{bmatrix} \omega_a \\ v_a \end{bmatrix}. \tag{4.121}$$

We introduce the following transformation to express the above relation:

Definition 4.8. Given $\mathcal{S} = (\omega, v) \in \mathbb{R}^6$, $\mathcal{S}' = (\omega', v') \in \mathbb{R}^6$, $T = (R, p) \in SE(3)$, the **Adjoint map** $\mathcal{S}' = \mathrm{Ad}_T(\mathcal{S})$ is defined as follows:

$$\mathcal{S}' = \begin{bmatrix} \omega' \\ v' \end{bmatrix} = \begin{bmatrix} R & 0 \\ [p]\,R & R \end{bmatrix} \begin{bmatrix} \omega \\ v \end{bmatrix} = \mathrm{Ad}_T(\mathcal{S}). \tag{4.122}$$

The notation $[\mathrm{Ad}_T]$ is used to denote the 6×6 matrix representation of the linear transformation Ad_T:

$$[\mathrm{Ad}_T] = \begin{bmatrix} R & 0 \\ [p]\,R & R \end{bmatrix}. \tag{4.123}$$

Using this notation Equation (4.122) can also be expressed as follows:

$$\mathcal{S}' = [\mathrm{Ad}_T]\mathcal{S}. \tag{4.124}$$

The adjoint map can also be equivalently expressed in the following matrix form:

$$\begin{aligned} [\mathcal{S}'] &= T[\mathcal{S}]T^{-1} \\ \begin{bmatrix} [\omega'] & v' \\ 0 & 1 \end{bmatrix} &= \begin{bmatrix} R[\omega]R^T & [p]R\omega + Rv \\ 0 & 0 \end{bmatrix}. \end{aligned} \tag{4.125}$$

The adjoint map satisfies the following properties, all verifiable by direct calculation:

Proposition 4.19. *Let $T_1, T_2 \in SE(3)$, and $\mathcal{S} = (\omega, v)$. Then*

$$Ad_{T_1}\left(Ad_{T_2}(\mathcal{S})\right) = Ad_{T_1T_2}(\mathcal{S}). \tag{4.126}$$

Also, for any $T \in SE(3)$ the following holds:

$$Ad_T^{-1} = Ad_{T^{-1}}, \tag{4.127}$$

The second property follows from the first by choosing $T_1 = T^{-1}$ and $T_2 = T$, so that

$$\mathrm{Ad}_{T^{-1}}\left(\mathrm{Ad}_T(\mathcal{S})\right) = \mathrm{Ad}_{T^{-1}T}(\mathcal{S}) = \mathrm{Ad}_I(\mathcal{S}) = \mathcal{S}. \tag{4.128}$$

The following proposition states the previously derived transformation rule for the twist of a screw motion under a change of reference frames:

Proposition 4.20. *Suppose a screw motion is described in terms of reference frame $\{a\}$ by the twist $\mathcal{S}_a = (\omega_a, v_a)$, and in terms of reference frame $\{b\}$ by the twist $\mathcal{S}_b = (\omega_b, v_b)$. $\mathcal{S}_a$ and $\mathcal{S}_b$ are then related by*

$$\mathcal{S}_b = Ad_{T_{ba}}(\mathcal{S}_a) \tag{4.129}$$

$$\mathcal{S}_a = Ad_{T_{ab}}(\mathcal{S}_b). \tag{4.130}$$

We close this section by comparing the prescriptive and descriptive interpretations of a screw motion. Referring once again to Figure 4.11, the relationship between T_{01} and T_{02} can be expressed as follows:

$$T_{02} = e^{[\mathcal{S}]\theta}T_{01} \tag{4.131}$$

$$T_{01}T_{12}T_{01}^{-1} = e^{[\mathcal{S}]\theta}. \tag{4.132}$$

Here $e^{[\mathcal{S}]\theta}$ can be thought as a transformation that displaces frame T_{01} to T_{02}; this is the prescriptive interpretation of the screw motion $e^{[\mathcal{S}]\theta}$. T_{12} can also be

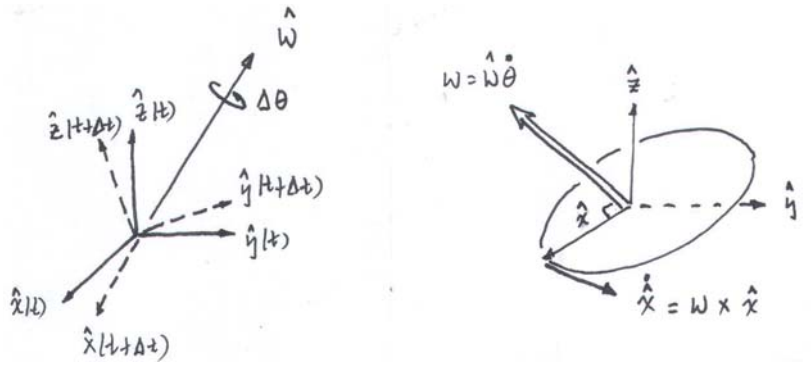

Figure 4.13: (a) The instantaneous angular velocity vector. (b) Calculating $\dot{\hat{\mathbf{x}}}$.

expressed as the matrix exponential $T_{12} = e^{[\mathcal{S}']\theta}$ for some $\mathcal{S}' = (\omega', v')$; here the screw motion $e^{[\mathcal{S}']\theta}$ is a descriptive representation for frame $\{2\}$ as seen from frame $\{1\}$. Applying the general matrix identity $Pe^{A}P^{-1} = e^{PAP^{-1}}$, we get

$$e^{[\mathcal{S}]\theta} = T_{01}e^{[\mathcal{S}']\theta}T_{01}^{-1} \tag{4.133}$$

$$= e^{\left(T_{01}[\mathcal{S}']T_{01}^{-1}\right)\theta}. \tag{4.134}$$

In terms of the adjoint notation, the relation between the twists $\mathcal{S}$ and $\mathcal{S}'$ can now be expressed as

$$\mathcal{S} = \mathrm{Ad}_{T_{01}}(\mathcal{S}'). \tag{4.135}$$

Here $\mathcal{S}$ is the twist representation of the screw motion expressed in frame $\{0\}$ coordinates, while $\mathcal{S}'$ is the twist representation of the same screw motion in frame $\{1\}$ coordinates, which agrees with the previous proposition.

4.4 Velocities and Forces

4.4.1 Angular Velocities

We first examine the angular velocity of a rigid body. Referring to Figure 4.13(a), suppose a body frame with unit axes $\{\hat{\mathrm{x}}, \hat{\mathrm{y}}, \hat{z}\}$ is attached to the rotating body. Let us determine the time derivatives of these unit axes. Beginning with $\dot{\hat{\mathrm{x}}}$, first note that $\hat{\mathrm{x}}$ is of unit length; only the direction of $\hat{\mathrm{x}}$ can vary with time (the same goes for $\hat{\mathrm{y}}$ and $\hat{z}$). If we examine the body frame at times t and $t + \Delta t$—since what's relevant for us is the orientation of the body frame, for better visualization we draw the frame at the two instants with coinciding origins—the change in frame orientation from t to $t + \Delta t$ can be described as a rotation of angle $\Delta\theta$ about some unit axis $\hat{\mathrm{w}}$ passing through the origin.

In the limit as Δt approaches zero, the ratio $\frac{\Delta\theta}{\Delta t}$ becomes the rate of rotation $\dot{\theta}$, and $\hat{\mathrm{w}}$ can similarly be regarded as the instantaneous axis of rotation. In fact,

$\hat{\mathrm{w}}$ and $\dot{\theta}$ can be put together to define the **angular velocity vector** w as follows:

$$\mathrm{w} = \hat{\mathrm{w}}\dot{\theta}. \tag{4.136}$$

It is important to note here that both the rate of rotation $\dot{\theta}$ and the rotation axis direction $\hat{\mathrm{w}}$ can vary with time. Referring to Figure 4.13(b), it should be evident that

$$\dot{\hat{\mathrm{x}}} = \mathrm{w} \times \hat{\mathrm{x}} \tag{4.137}$$

$$\dot{\hat{\mathrm{y}}} = \mathrm{w} \times \hat{\mathrm{y}} \tag{4.138}$$

$$\dot{\hat{\mathrm{z}}} = \mathrm{w} \times \hat{\mathrm{z}}. \tag{4.139}$$

Let us now express these relations explicitly in terms of fixed frame coordinates. Let $R(t)$ be the rotation matrix describing the orientation of the body frame with respect to the fixed frame. Then the first column of $R(t)$, denoted $r_1(t)$, describes $\hat{\mathrm{x}}$ in fixed frame coordinates; similarly, $r_2(t)$ and $r_3(t)$ respectively describe $\hat{\mathrm{y}}$ and $\hat{\mathrm{z}}$ in fixed frame coordinates. Let $\omega_s \in \mathbb{R}^3$ be the angular velocity w expressed in fixed frame coordinates. The previous three velocity relations expressed in fixed frame coordinates become

$$\dot{r}_i = \omega_s \times r_i = [\omega_s] r_i, \quad i = 1, 2, 3.$$

The above three equations can be rearranged into the following single matrix equation:

$$\dot{R} = [\omega_s] R. \tag{4.140}$$

Since $R^{-1} = R^T$, the above can also be written

$$\dot{R} R^T = [\omega_s]. \tag{4.141}$$

This result shows that not only is $\dot{R}R^T$ always skew-symmetric, but also admits the physical interpretation as the angular velocity in fixed-frame coordinates.

Now let ω_b be w expressed in body frame coordinates. To see how to obtain ω_b from ω_s and vice versa, let us momentarily return to our earlier notational practice of writing R as R_{sb} (recall that R_{sb} means the orientation of the body frame $\{b\}$ as seem from the fixed frame $\{s\}$). Then ω_s and ω_b are two different vector representations of the same angular velocity vector w, with $\omega_s = R_{sb}\omega_b$ and $\omega_b = R_{sb}^{-1}\omega_s$. Since $R_{sb}^{-1} = R^T$, we have

$$\omega_b = R^T \omega_s. \tag{4.142}$$

Let us now express the above relation in skew-symmetric matrix form. Recall that for any $\omega \in \mathbb{R}^3$ and $R \in SO(3)$, $R[\omega]R^T = [R\omega]$ always holds. With this result, we now express both sides of Equation (4.142) in skew-symmetric matrix form:

$$\begin{aligned} [\omega_b] &= [R^T \omega_s] \\ &= R^T [\omega_s] R \\ &= R^T (\dot{R} R^T) R \\ &= R^T \dot{R} \end{aligned} \tag{4.143}$$

In summary, we have the following two equations that relate the rotation matrix R to the angular velocity w:

Proposition 4.21. *Let $R(t)$ denote the orientation of the rotating frame as seen from the fixed frame. Denote by w the angular velocity of the rotating frame. Then*

$$\dot{R}R^{-1} = [\omega_s] \tag{4.144}$$
$$R^{-1}\dot{R} = [\omega_b], \tag{4.145}$$

where $\omega_s \in \mathbb{R}^3$ is the fixed frame vector representation of w, and $\omega_b \in \mathbb{R}^3$ is the moving frame vector representation of w.

4.4.2 Spatial Velocities

We now consider both the linear and angular velocity of the moving frame. As before, denote by {s} and {b} the fixed (space) and moving (body) frames, respectively, and let

$$T_{sb}(t) = T(t) = \begin{bmatrix} R(t) & p(t) \\ 0 & 1 \end{bmatrix} \tag{4.146}$$

denote the homogeneous transformation of {b} as seen from {s} (to keep the notation uncluttered, for the time being we shall write T instead of the usual T_{sb}).

In the previous section we discovered that pre- or post-multiplying $\dot{R}$ by R^{-1} results in (a skew-symmetric representation of) the angular velocity vector, either in fixed or moving frame coordinates. One might reasonably ask if a similar property carries over to $\dot{T}$, i.e., whether $T^{-1}\dot{T}$ and $\dot{T}T^{-1}$ carry similar physical interpretations.

Let us first see what happens when we pre-multiply $\dot{T}$ by T^{-1}:

$$\begin{aligned} T^{-1}\dot{T} &= \begin{bmatrix} R^T & -R^T p \\ 0 & 1 \end{bmatrix} \begin{bmatrix} \dot{R} & \dot{p} \\ 0 & 0 \end{bmatrix} \\ &= \begin{bmatrix} R^T\dot{R} & R^T\dot{p} \\ 0 & 0 \end{bmatrix} \\ &= \begin{bmatrix} [\omega_b] & v_b \\ 0 & 0 \end{bmatrix}. \end{aligned} \tag{4.147}$$

Recall that $R^T\dot{R} = [\omega_b]$ is just the (skew-symmetric matrix representation of) the angular velocity expressed in moving frame coordinates. Also, $\dot{p}$ is the linear velocity of the moving frame origin expressed in fixed frame coordinates, and $R^T\dot{p} = v_b$ is this linear velocity expressed in moving frame coordinates. Putting these two observations together, we can conclude that $T^{-1}\dot{T}$ represents the linear and angular velocity of the moving frame in terms of the moving frame coordinates.

The previous calculation of $T^{-1}\dot{T}$ suggests that it is reasonable to merge ω_b and v_b into a single six-dimensional velocity vector. This is exactly what we shall do. Define

$$\mathcal{V}_b = \begin{bmatrix} \omega_b \\ v_b \end{bmatrix}, \quad [\mathcal{V}_b] = \begin{bmatrix} [\omega_b] & v_b \\ 0 & 0 \end{bmatrix} = T^{-1}\dot{T}. \tag{4.148}$$

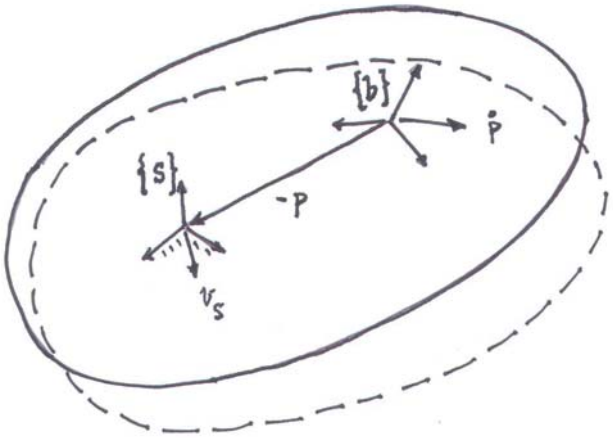

Figure 4.14: Physical interpretation of v_s. The initial (solid line) and displaced (dotted line) configurations of a rigid body.

We shall also use the more compact notation $\mathcal{V}_b = (\omega_b, v_b)$, so that $[\mathcal{V}_b]$ is the 4×4 matrix representation of $\mathcal{V}_b$. We shall call $\mathcal{V}_b$ the **spatial velocity** in the **moving** (or **body**) **frame**.

Now that we have a physical interpretation for $T^{-1}\dot{T}$, let us evaluate $\dot{T}T^{-1}$:

$$\begin{aligned} \dot{T}T^{-1} &= \begin{bmatrix} \dot{R} & \dot{p} \\ 0 & 0 \end{bmatrix} \begin{bmatrix} R^T & -R^T p \\ 0 & 1 \end{bmatrix} \\ &= \begin{bmatrix} \dot{R}R^T & \dot{p} - \dot{R}R^T p \\ 0 & 0 \end{bmatrix} \\ &= \begin{bmatrix} [\omega_s] & v_s \\ 0 & 0 \end{bmatrix}. \end{aligned} \tag{4.149}$$

Observe that the skew-symmetric matrix $[\omega_s] = \dot{R}R^T$ is the angular velocity expressed in fixed frame coordinates, but that $v_s = \dot{p} - \dot{R}R^T p$ is **not** the linear velocity of the moving frame origin expressed in the fixed frame (that quantity would simply be $\dot{p}$). On the other hand, if we write v_s as

$$v_s = \dot{p} - \omega_s \times p = \dot{p} + \omega_s \times (-p), \tag{4.150}$$

the physical meaning of v_s can now be inferred: imagining the moving frame is attached to an infinitely large rigid body, v_s is the instantaneous velocity of the point on this body corresponding to the fixed frame origin (see Figure 4.14).

As we did for ω_b and v_b, we also merge ω_s and v_s into a six-dimensional velocity:

$$\mathcal{V}_s = \begin{bmatrix} \omega_s \\ v_s \end{bmatrix}, \quad [\mathcal{V}_s] = \begin{bmatrix} [\omega_s] & v_s \\ 0 & 0 \end{bmatrix} = \dot{T}T^{-1}. \tag{4.151}$$

We shall also use the more compact notation $\mathcal{V}_s = (\omega_s, v_s)$, so that $[\mathcal{V}_s]$ is the 4×4 matrix representation of $\mathcal{V}_s$. We call $\mathcal{V}_s$ the **spatial velocity** in the **fixed** (or **space**) **frame**.

If we regard the fixed and moving bodies as being infinitely large, there is in fact an appealing and natural symmetry between $\mathcal{V}_s = (\omega_s, v_s)$ and $\mathcal{V}_b = (\omega_b, v_b)$:

(i) ω_b is the angular velocity in **moving frame** coordinates;

(ii) ω_s is the angular velocity in **fixed frame** coordinates;

(iii) v_b is the linear velocity of the **moving frame origin**, in **moving frame** coordinates;

(iv) v_s is the linear velocity of the **fixed frame origin** (regarded as a point on the moving rigid body), in **fixed frame coordinates**.

$\mathcal{V}_b$ can be obtained from $\mathcal{V}_s$ as follows:

$$\begin{aligned} [\mathcal{V}_b] &= T^{-1}\dot{T} \\ &= T^{-1}(\dot{T}T^{-1})T \\ &= T^{-1}\,[\mathcal{V}_s]\,T. \end{aligned} \tag{4.152}$$

Going the other way,

$$[\mathcal{V}_s] = T\,[\mathcal{V}_b]\,T^{-1}. \tag{4.153}$$

The reader may recognize that the relation between $\mathcal{V}_s$ and $\mathcal{V}_b$ is given precisely by the transformation rule for a twist vector of a screw motion under a change of reference frames. In fact, using the adjoint mapping Ad_T the above can be expressed as $\mathcal{V}_s = \mathrm{Ad}_T(\mathcal{V}_b)$, $\mathcal{V}_b = \mathrm{Ad}_{T^{-1}}(\mathcal{V}_s)$. This transformation rule can be more easily remembered if we write $T = T_{sb}$, in which case

$$\mathcal{V}_s = \mathrm{Ad}_{T_{sb}}(\mathcal{V}_b) \tag{4.154}$$

$$\mathcal{V}_b = \mathrm{Ad}_{T_{bs}}(\mathcal{V}_s). \tag{4.155}$$

In expanded form, the above becomes

$$\begin{bmatrix} \omega_s \\ v_s \end{bmatrix} = \begin{bmatrix} R & 0 \\ [p]\,R & R \end{bmatrix} \begin{bmatrix} \omega_b \\ v_b \end{bmatrix} \tag{4.156}$$

$$\begin{bmatrix} \omega_b \\ v_b \end{bmatrix} = \begin{bmatrix} R^T & 0 \\ -R^T\,[p] & R^T \end{bmatrix} \begin{bmatrix} \omega_s \\ v_s \end{bmatrix}. \tag{4.157}$$

The main results on spatial velocities derived thus far are summarized in the following proposition:

Proposition 4.22. *Given a fixed (space) frame $\{s\}$ and moving (body) frame $\{b\}$, let $T_{sb}(t) \in SE(3)$ be differentiable, where*

$$T_{sb}(t) = \begin{bmatrix} R(t) & p(t) \\ 0 & 1 \end{bmatrix}. \tag{4.158}$$

Then

$$T_{sb}^{-1}\dot{T}_{sb} = [\mathcal{V}_b] = \begin{bmatrix} [\omega_b] & v_b \\ 0 & 0 \end{bmatrix} \tag{4.159}$$

is the **spatial velocity in body coordinates**, *and*

$$\dot{T}_{sb}T_{sb}^{-1} = [\mathcal{V}_s] = \begin{bmatrix} [\omega_s] & v_s \\ 0 & 0 \end{bmatrix} \tag{4.160}$$

is the **spatial velocity in space coordinates**. $\mathcal{V}_s$ *and* $\mathcal{V}_b$ *are related by*

$$\mathcal{V}_s = \begin{bmatrix} \omega_s \\ v_s \end{bmatrix} = \begin{bmatrix} R & 0 \\ [p]\,R & R \end{bmatrix} \begin{bmatrix} \omega_b \\ v_b \end{bmatrix} = Ad_{T_{sb}}(\mathcal{V}_b) \tag{4.161}$$

$$\mathcal{V}_b = \begin{bmatrix} \omega_b \\ v_b \end{bmatrix} = \begin{bmatrix} R^T & 0 \\ -R^T[p] & R^T \end{bmatrix} \begin{bmatrix} \omega_s \\ v_s \end{bmatrix} = Ad_{T_{bs}}(\mathcal{V}_s). \tag{4.162}$$

4.4.3 Spatial Forces

Just as we found it advantageous to merge angular and linear velocities into a single six-dimensional spatial velocity vector, for the same reasons it will be useful to analogously merge forces and moments into a single six-dimensional **spatial force**. Toward this end, suppose a force f is being applied to a point p on a rigid body. Given some reference frame {a}, let $f_a \in \mathbb{R}^3$ denote the vector representation of f in frame {a} coordinates. This force then generates a moment with respect to the {a} frame origin; in {a} frame coordinates, this moment is

$$m_a = r_a \times f_a, \tag{4.163}$$

where $r_a \in \mathbb{R}^3$ is the vector from the {a} frame origin to p, expressed in {a} frame coordinates. We pair the force f_a and moment m_a into a single six-dimensional spatial force $\mathcal{F}_a = (m_a, f_a)$, and refer to it as the **spatial force** in frame {a} coordinates. Adopting the terminology from classical screw theory, a spatial force will also be referred to as a **wrench**.

Suppose we now wish to express the force and moment in terms of another reference frame {b}. Let $f_b \in \mathbb{R}^3$ denote the vector representation of f in {b} frame coordinates. The moment generated by this force with respect to the {b} frame origin is, again expressed in {b} frame coordinates,

$$m_b = r_b \times f_b, \tag{4.164}$$

where $r_b \in \mathbb{R}^3$ is the {b} frame representation of the vector from the {b} frame origin to p. As we did for $\mathcal{F}_a$, let us also bundle m_b and f_b into the six-dimensional spatial force $\mathcal{F}_b = (m_b, f_b)$, and refer to it as the **spatial force** in {b} frame coordinates.

We now determine the relation between $\mathcal{F}_a = (m_a, f_a)$ and $\mathcal{F}_b = (m_b, f_b)$. Referring to Figure 4.15, denote the transformation T_{ab} by

$$T_{ab} = \begin{bmatrix} R_{ab} & p_{ab} \\ 0 & 1 \end{bmatrix}.$$

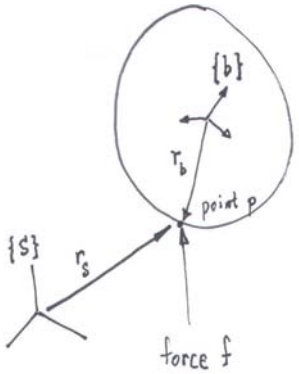

Figure 4.15: Relation between $\mathcal{F}_a$ and $\mathcal{F}_b$.

Pretty clearly $f_b = R_{ba} f_a$, which with the benefit of hindsight we shall write

$$f_b = R_{ab}^T f_a. \tag{4.165}$$

The moment m_b is given by $r_b \times f_b$, where $r_b = R_{ba}(r_a - p_{ab})$; this follows from the fact that the $r_a - p_{ab}$ is expressed in {a} frame coordinates, and must be transformed to {b} frame coordinates via multiplication by R_{ba}. Again with hindsight, we shall write

$$r_b = R_{ab}^T(r_a - p_{ab}).$$

The moment $m_b = r_b \times f_b$ can now be written in terms of f_a and m_a as

$$\begin{aligned} m_b &= R_{ab}^T(r_a - p_{ab}) \times R_{ab}^T f_a \\ &= [R_{ab}^T r_a] R_{ab}^T f_a - [R_{ab}^T p_{ab}] R_{ab}^T f_a \\ &= R_{ab}^T [r_a] f_a - R_{ab}^T [p_{ab}] f_a \\ &= R_{ab}^T m_a + R_{ab}^T [p_{ab}]^T f_a, \end{aligned} \tag{4.166}$$

where in the last line we make use of the fact that $[p_{ab}]^T = -[p_{ab}]$. Writing both m_b and f_b in terms of m_a and f_a we have, from Equations (4.165) and (4.166),

$$\begin{bmatrix} m_b \\ f_b \end{bmatrix} = \begin{bmatrix} R_{ab} & 0 \\ [p_{ab}]\, R_{ab} & R_{ab} \end{bmatrix}^T \begin{bmatrix} m_a \\ f_a \end{bmatrix}, \tag{4.167}$$

or in terms of spatial forces and the adjoint map,

$$\mathcal{F}_b = \mathrm{Ad}_{T_{ab}}^T(\mathcal{F}_a) = [\mathrm{Ad}_{T_{ab}}]^T \mathcal{F}_a. \tag{4.168}$$

The above shows that under a change of reference frames, spatial velocities transform via the adjoint map, whereas spatial forces transform via the adjoint transpose map. The following proposition formally states this result.

Chapter 5

Forward Kinematics

The **forward kinematics** of a robot refers to the calculation of the position and orientation of its end-effector frame from its joint values. Figure 5.1 illustrates the forward kinematics problem for the 3R planar open chain. Starting from the base link, the link lengths are L_1, L_2, and L_3. Choose a fixed frame $\{0\}$ with origin located at the base joint as shown, and assume an end-effector frame $\{4\}$ has been attached to the tip of the third link. The Cartesian position (x, y) and orientation ϕ of the end-effector frame as a function of the joint angles $(\theta_1, \theta_2, \theta_3)$ are then given by

$$x = L_1 \cos\theta_1 + L_2 \cos(\theta_1 + \theta_2) + L_3 \cos(\theta_1 + \theta_2 + \theta_3) \quad (5.1)$$

$$y = L_1 \sin\theta_1 + L_2 \sin(\theta_1 + \theta_2) + L_3 \sin(\theta_1 + \theta_2 + \theta_3) \quad (5.2)$$

$$\phi = \theta_1 + \theta_2 + \theta_3. \quad (5.3)$$

If one is only interested in the (x, y) position of the end-effector, the robot's task space is then taken to be the x-y plane, and the forward kinematics would then consist of Equations (5.1)-(5.2) only. If the end-effector's position and orientation both matter, the forward kinematics would then consist of the three equations (5.1)-(5.3).

While the above analysis can be done using only basic trigonometry, it is not difficult to imagine that for more general spatial chains, the analysis can become considerably more complicated. A more systematic method of deriving the forward kinematics would be to first attach reference frames to each of the links; in Figure 5.1 the three link reference frames are respectively labelled $\{1\}$, $\{2\}$, and $\{3\}$. The forward kinematics can then be written as a product of four $SE(2)$ matrices:

$$T_{04} = T_{01} T_{12} T_{23} T_{34},$$

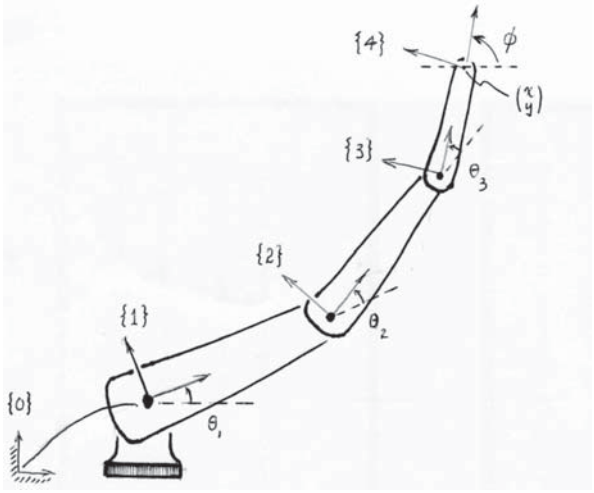

Figure 5.1: Forward kinematics of a 3R planar open chain.

where

$$T_{01} = \begin{bmatrix} \cos\theta_1 & -\sin\theta_1 & 0 \\ \sin\theta_1 & \cos\theta_1 & 0 \\ 0 & 0 & 1 \end{bmatrix}, \quad T_{12} = \begin{bmatrix} \cos\theta_2 & -\sin\theta_2 & L_1 \\ \sin\theta_2 & \cos\theta_2 & 0 \\ 0 & 0 & 1 \end{bmatrix}$$

$$T_{23} = \begin{bmatrix} \cos\theta_3 & -\sin\theta_3 & L_2 \\ \sin\theta_3 & \cos\theta_3 & 0 \\ 0 & 0 & 1 \end{bmatrix}, \qquad T_{34} = \begin{bmatrix} 1 & 0 & L_3 \\ 0 & 1 & 0 \\ 0 & 0 & 1 \end{bmatrix}. \tag{5.4}$$

Observe that T_{34} is constant, and that each remaining $T_{i-1,i}$ depends only on the joint variable θ_i.

Alternatively, if we regard each joint axis as being the axis of a zero-pitch screw motion, then observe that joint axis three can be thought of as applying a screw motion to link three. Assuming joints θ_1 and θ_2 are both held constant at zero, from the matrix exponential representation for screw motions covered in the previous chapter, we can write

$$T_{04} = e^{[\mathcal{S}_3]\theta_3} M, \tag{5.5}$$

where

$$M = \begin{bmatrix} 1 & 0 & L_1 + L_2 + L_3 \\ 0 & 1 & 0 \\ 0 & 0 & 1 \end{bmatrix}, \tag{5.6}$$

describes the position and orientation of frame $\{4\}$ when all joints are set to zero, and

$$[\mathcal{S}_3] = \begin{bmatrix} 0 & -1 & 0 \\ 1 & 0 & -(L_1 + L_2) \\ 0 & 0 & 0 \end{bmatrix}. \tag{5.7}$$

Similarly, joint axis two can be viewed as applying a screw motion to the link two-link three pair; assuming joint θ_1 is held constant at zero, we can write

$$T_{04} = e^{[\mathcal{S}_2]\theta_2} e^{[\mathcal{S}_3]\theta_3} M, \tag{5.8}$$

where $[\mathcal{S}_3]$ and M are as defined previously, and

$$[\mathcal{S}_2] = \begin{bmatrix} 0 & -1 & 0 \\ 1 & 0 & -L_1 \\ 0 & 0 & 0 \end{bmatrix}. \tag{5.9}$$

Finally, joint axis one can be viewed as applying a screw motion to the entire three-link assembly; for arbitrary values of $(\theta_1, \theta_2, \theta_3)$ we can therefore write

$$T_{04} = e^{[\mathcal{S}_1]\theta_1} e^{[\mathcal{S}_2]\theta_2} e^{[\mathcal{S}_3]\theta_3} M, \tag{5.10}$$

where $[\mathcal{S}_2]$, $[\mathcal{S}_3]$, and M are as defined previously, and

$$[\mathcal{S}_1] = \begin{bmatrix} 0 & -1 & 0 \\ 1 & 0 & 0 \\ 0 & 0 & 0 \end{bmatrix}. \tag{5.11}$$

The forward kinematics can thus be expressed as a product of matrix exponentials, each corresponding to a screw motion. Note that this latter derivation of the forward kinematics does not make use of any link reference frames.

In this chapter we shall consider the forward kinematics of general open chains, taking the task space to be the position and orientation of the end-effector frame in the most general case. Two widely used forward kinematic representations for open chains will be considered: the homogeneous transformation representation based on the **Denavit-Hartenberg** (D-H) parameters, which corresponds to Equation (5.4), and the screw-theoretic formulation based on the **Product of Exponentials** (PoE) formula, which corresponds to Equation (5.11). The advantage of the D-H representation is that it is a minimal representation, in the sense of requiring the smallest number of parameters to describe the robot's kinematic structure. The PoE representation is not minimal, but as we show later, has so many other advantages over the D-H representation (e.g., no link frames are necessary) that with few exceptions it will be our preferred choice of forward kinematics representation. We include the D-H representation mostly for completeness.

5.1 Denavit-Hartenberg Representation

The basic idea underlying the Denavit-Hartenberg approach to forward kinematics is to attach reference frames to each link of the open chain, and to derive the forward kinematics based on knowledge of the relative displacements between adjacent link frames. Assume that a fixed reference frame has been established, and that a reference frame (the end-effector frame) has been attached to some

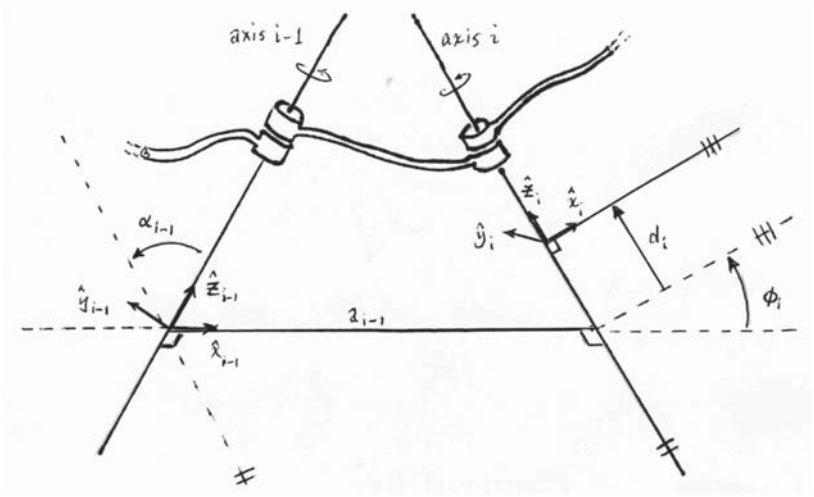

Figure 5.2: Illustration of Denavit-Hartenberg parameters.

point on the last link of the open chain. For a chain consisting of n one degree of freedom joints, the links are numbered sequentially from 0 to n, in which the ground link is labelled 0, and the end-effector frame is attached to some point on link n. Reference frames attached to the links are also correspondingly labelled from $\{0\}$ (the fixed frame) to $\{n\}$ (the end-effector frame). The joint variable corresponding to the i-th joint is denoted θ_i. The forward kinematics of the n-link open chain can then be expressed as

$$T_{0n}(\theta_1, \ldots, \theta_n) = T_{01}(\theta_1)T_{12}(\theta_2)\cdots T_{n-1,n}(\theta_n), \tag{5.12}$$

where $T_{i,i-1} \in SE(3)$ denotes the relative displacement between link frames $\{i-1\}$ and $\{i\}$. Depending on how the link reference frames have been chosen, for open chains each $T_{i-1,i}$ can be obtained in a straightforward fashion.

5.1.1 Assigning Link Frames

Rather than attaching reference frames to each link in some arbitrary fashion, in the Denavit-Hartenberg convention a set of rules for assigning link frames is observed. Figure 5.2 illustrates the frame assignment convention for two adjacent revolute joints $i-1$ and i that are connected by link $i-1$.

The first rule is that the $\hat{z}$-axis coincides with joint axis i, and $\hat{z}_{i-1}$ coincides with joint axis $i-1$. The direction of each link frame $\hat{z}$-axis is determined via the right-hand rule, i.e., such that positive rotations are counterclockwise about the $\hat{z}$-axis.

Once the $\hat{z}$-axis direction has been assigned, the next rule determines the origin of the link reference frame. First, find the line segment that orthogonally intersects both joint axes $\hat{z}_{i-1}$ and $\hat{z}_i$. For now let us assume that this line

segment is unique; the case where it is not unique (i.e., when the two joint axes are parallel), or fails to exist (i.e., when the two joint axes intersect), is addressed later. Connecting joint axes $i-1$ and i by a mutually perpendicular line, the origin of frame $\{i-1\}$ is then located at the point where this line intersects joint axis $i-1$.

Determining the remaining $\hat{\mathrm{x}}$- and $\hat{\mathrm{y}}$-axes of each link reference frame is now straightforward: the $\hat{\mathrm{x}}$ axis is chosen to be in the direction of the mutually perpendicular line pointing from the $i-1$ axis to the i axis. The $\hat{\mathrm{y}}$-axis is then uniquely determined from the cross-product $\hat{\mathrm{x}} \times \hat{\mathrm{y}} = \hat{\mathrm{z}}$. Figure 5.2 depicts the link frames i and $i-1$ chosen according to this convention.

Having assigned reference frames in this fashion for links i and $i-1$, we now define four parameters that exactly specify $T_{i-1,i}$:

- The length of the mutually perpendicular line, denoted by the scalar a_{i-1}, is called the **link length** of link $i-1$. Despite its name, this link length does not necessarily correspond to the actual length of the physical link.
- The **link twist** α_{i-1} is the angle from $\hat{\mathrm{z}}_{i-1}$ to $\hat{\mathrm{z}}_i$, measured about $\hat{\mathrm{x}}_{i-1}$.
- The **link offset** d_i is the distance from the intersection of $\hat{\mathrm{x}}_{i-1}$ and $\hat{\mathrm{z}}_i$ to the link i frame origin (the positive direction is defined to be along the $\hat{\mathrm{z}}_i$ axis).
- The **joint angle** ϕ_i is the angle from $\hat{\mathrm{x}}_{i-1}$ to $\hat{\mathrm{x}}_i$, measured about the $\hat{\mathrm{z}}_i$-axis in the right-hand sense.

These parameters constitute the Denavit-Hartenberg parameters. For an open chain with n one degree-of-freedom joints, the $4n$ Denavit-Hartenberg parameters are sufficient to completely describe the forward kinematics. In the case of an open chain with all joints revolute, the link lengths a_{i-1}, twists α_{i-1}, and offset parameters d_i are all constant, while the joint angle parameters ϕ_i act as the joint variables.

We now consider the case where the mutually perpendicular line is undefined or fails to be unique, as well as when some of the joints are prismatic, and finally, how to choose the ground and end-effector frames.

When Adjacent Revolute Joint Axes Intersect

If two adjacent revolute joint axes intersect each other, then the mutually perpendicular line between the joint axes fails to exist. In this case the link length is set to zero, and we choose $\hat{\mathrm{x}}_{i-1}$ to be perpendicular to the plane spanned by $\hat{\mathrm{z}}_{i-1}$ and $\hat{\mathrm{z}}_i$. There are two possibilities here, both of which are acceptable: one leads to a positive value of the twist angle α_{i-1}, while the other leads to a negative value.

When Adjacent Revolute Joint Axes are Parallel

The second special case occurs when two adjacent revolute joint axes are parallel. In this case there exist many possibilities for a mutually perpendicular

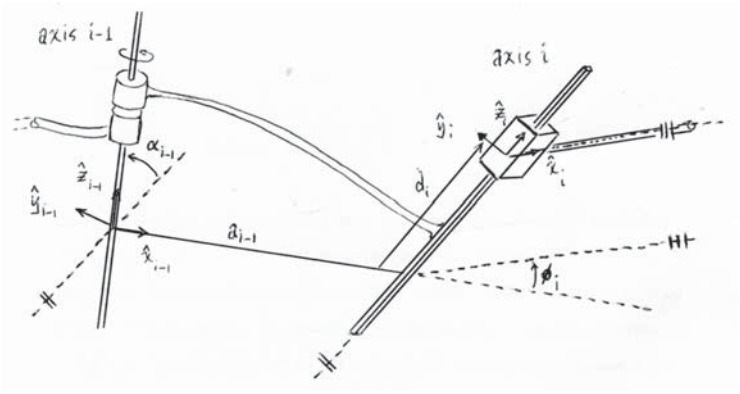

Figure 5.3: Link frame assignment convention for prismatic joints. Joint $i-1$ is a revolute joint, while joint i is a prismatic joint.

line, all of which are valid (more precisely, a one-parameter family of mutual perpendicular lines is said to exist). Again, it is important to detail precisely how the link frames are assigned. A useful guide is to try to choose the mutually perpendicular line that is the most physically intuitive, and simplifies as many Denavit-Hartenberg parameters as possible (e.g., such that their values become zero).

Prismatic Joints

For prismatic joints, the $\hat{z}$-direction of the link reference frame is chosen to be along the positive direction of translation. This convention is consistent with that for revolute joints, in which the $\hat{z}$-axis indicates the positive axis of rotation. With this choice the link offset parameter d_i now becomes the joint variable (see Figure 5.3). The procedure for choosing the link frame origin, as well as the remaining $\hat{x}$ and $\hat{y}$-axes, remains the same as for revolute joints.

Assigning the Ground and End-Effector Frames

Our frame assignment procedure described thus far does not specify how to choose the ground and final link frames. Here as before, a useful guideline is to choose initial and final frames that are the most physically intuitive, and simplify as many Denavit-Hartenberg parameters as possible. This usually implies that the ground frame is chosen to coincide with the link 1 frame in its zero (rest) position; in the event that the joint is revolute, this choice forces $a_0 = \alpha_0 = d_1 = 0$, while for a prismatic joint we have $a_0 = \alpha_0 = \phi_1 = 0$. The end-effector frame is typically attached to some reference point on the end-effector, usually at a location that makes the description of the task intuitive and natural, and also simplifies as many of the Denavit-Hartenberg parameters as possible (e.g., their values become zero).

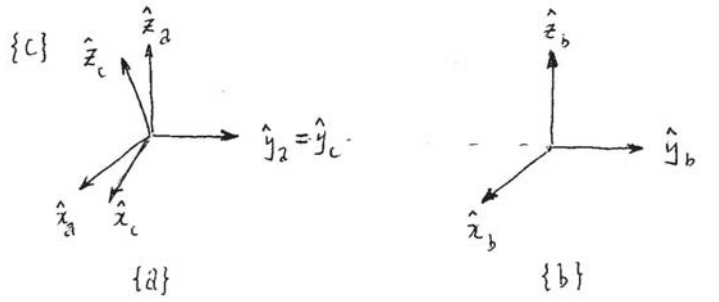

Figure 5.4: An example of three frames $\{a\}$, $\{b\}$, and $\{c\}$, in which the transformations T_{ab} and T_{ac} cannot be described by any set of Denavit-Hartenberg parameters.

It is important to realize that arbitrary choices of the ground and end-effector frames may not always be possible, since there may not exist a valid set of Denavit-Hartenberg parameters to describe the relative transformation; we elaborate on this point below.

5.1.2 Why Four Parameters are Sufficient

In our earlier study of spatial displacements, we argued that a minimum of six independent parameters were required to describe the relative displacement between two frames in space: three for the orientation, and three for the position. Based on this result, it would seem that for an n-link arm, a total of $6n$ parameters would be required to completely describe the forward kinematics (each $T_{i-1,i}$ in the above equation would require six parameters). Surprisingly, in the Denavit-Hartenberg parameter representation only four parameters are required for each transformation $T_{i-1,i}$. Although this result may at first appear to contradict our earlier results, this reduction in the number of parameters is accomplished by the carefully stipulated rules for assigning link reference frames. If the link reference frames had been assigned in arbitrary fashion, then more parameters would have been required.

Consider, for example, the link frames shown in Figure 5.4. The transformation from frame $\{a\}$ to frame $\{b\}$ is a pure translation along the $\hat{y}$-axis of frame $\{a\}$. If one were to try to express the transformation T_{ab} in terms of the Denavit-Hartenberg parameters (α, a, d, θ) as prescribed above, it should become apparent that no such set of parameter values exist. Similarly, the transformation T_{ac} also does not admit a description in terms of Denavit-Hartenberg parameters, as only rotations about the $\hat{x}$- and $\hat{z}$- axes are permissible. Under our Denavit-Hartenberg convention, only rotations and translations along the $\hat{x}$ and $\hat{z}$ axes are allowed, and no combination of such motions can achieve the transformations shown in Figure 5.4.

Given that the Denavit-Hartenberg convention uses exactly four parameters to describe the transformation between link frames, one might naturally wonder if the number of parameters can be reduced even further, by an even more clever set of link frame assignment rules. Denavit and Hartenberg show that this is not possible, and that four is the minimum number of parameters [7].

We end this section with a reminder that there are alternative conventions for assigning link frames. Whereas we chose the $\hat{z}$-axis to coincide with the joint axis, some authors choose the $\hat{x}$-axis, and reserve the $\hat{z}$-axis to be the direction of the mutually perpendicular line. To avoid ambiguities in the interpretation of the Denavit-Hartenberg parameters, it is essential to include a concise description of the link frames together with the parameter values.

5.1.3 Manipulator Forward Kinematics

Once all the transformations $T_{i-1,i}$ between adjacent link frames are known in terms of their Denavit-Hartenberg parameters, the forward kinematics is obtained by sequentially multiplying these link transformations. Each link frame transformation is of the form

$$\begin{aligned} T_{i-1,i} &= \mathrm{Rot}(\hat{x}, \alpha_{i-1}) \cdot \mathrm{Trans}(\hat{x}, a_{i-1}) \cdot \mathrm{Trans}(\hat{z}, d_i) \cdot \mathrm{Rot}(\hat{z}, \phi_i) \\ &= \begin{bmatrix} \cos\phi_i & -\sin\phi_i & 0 & a_{i-1} \\ \sin\phi_i \cos\alpha_{i-1} & \cos\phi_i \cos\alpha_{i-1} & -\sin\alpha_{i-1} & -d_i \sin\alpha_{i-1} \\ \sin\phi_i \sin\alpha_{i-1} & \cos\phi_i \sin\alpha_{i-1} & \cos\alpha_{i-1} & d_i \cos\alpha_{i-1} \\ 0 & 0 & 0 & 1 \end{bmatrix}, \end{aligned}$$

where

$$\mathrm{Rot}(\hat{x}, \alpha_{i-1}) = \begin{bmatrix} 1 & 0 & 0 & 0 \\ 0 & \cos\alpha_{i-1} & -\sin\alpha_{i-1} & 0 \\ 0 & -\sin\alpha_{i-1} & \cos\alpha_{i-1} & 0 \\ 0 & 0 & 0 & 1 \end{bmatrix} \tag{5.13}$$

$$\mathrm{Trans}(\hat{x}, a_{i-1}) = \begin{bmatrix} 1 & 0 & 0 & a_{i-1} \\ 0 & 1 & 0 & 0 \\ 0 & 0 & 1 & 0 \\ 0 & 0 & 0 & 1 \end{bmatrix} \tag{5.14}$$

$$\mathrm{Trans}(\hat{z}, d_i) = \begin{bmatrix} 1 & 0 & 0 & 0 \\ 0 & 1 & 0 & 0 \\ 0 & 0 & 1 & d_i \\ 0 & 0 & 0 & 1 \end{bmatrix} \tag{5.15}$$

$$\mathrm{Rot}(\hat{z}, \phi_i) = \begin{bmatrix} \cos\phi_{i-1} & -\sin\phi_{i-1} & 0 & 0 \\ -\sin\phi_{i-1} & \cos\phi_{i-1} & 0 & 0 \\ 0 & 0 & 1 & 0 \\ 0 & 0 & 0 & 1 \end{bmatrix}. \tag{5.16}$$

A useful way to visualize $T_{i,i-1}$ is to transport frame $\{i-1\}$ to frame $\{i\}$ via the following sequence of four transformations:

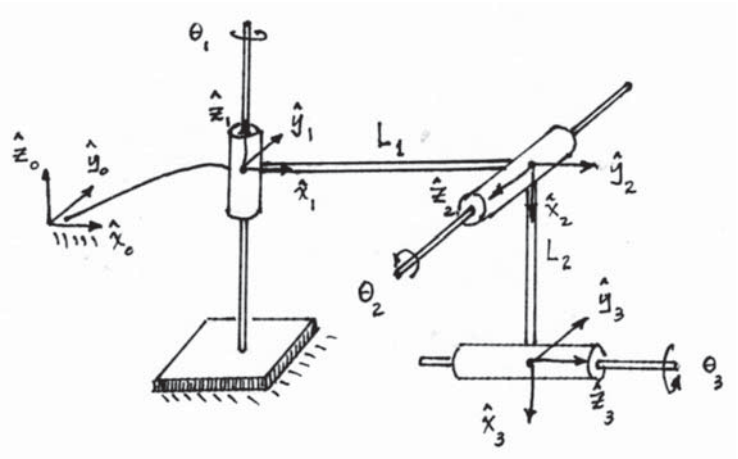

Figure 5.5: A 3R spatial open chain.

(i) Rotate frame $\{i-1\}$ about its $\hat{x}$ axis by an angle α_{i-1}.

(ii) Translate this new frame along its $\hat{x}$ axis by a distance a_{i-1}.

(iii) Translate this new frame along its $\hat{z}$ axis by a distance d_i.

(iv) Rotate this new frame about its $\hat{z}$ axis by an angle ϕ_i.

Note that switching the order of the first and second steps will not change the final form of $T_{i-1,i}$. Similarly, the order of the third and fourth steps can also be switched without affecting $T_{i-1,i}$.

5.1.4 Examples

We now derive the Denavit-Hartenberg parameters for some common spatial open chain structures.

Example: A 3R Spatial Open Chain

Consider the 3R spatial open chain of Figure 5.5, shown in its zero position (i.e., with all its joint variables set to zero). The assigned link reference frames are shown in the figure, and the corresponding Denavit-Hartenberg parameters listed in the following table:

i	α_{i-1}	a_{i-1}	d_i	ϕ_i
1	0	0	0	θ_1
2	90°	L_1	0	$\theta_2 - 90^\circ$
3	-90°	L_2	0	θ_3

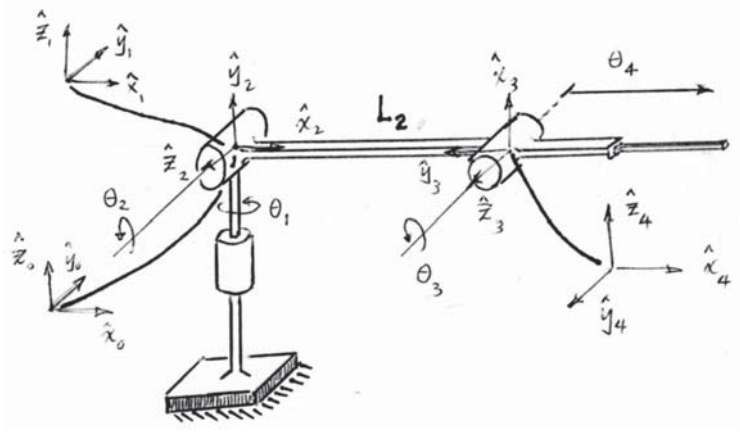

Figure 5.6: An RRRP spatial open chain.

Note that frames {1} and {2} are uniquely specified from our frame assignment convention, but that we have some latitude in choosing frames {0} and {3}. Here we choose the ground frame {0} to coincide with frame {1} (resulting in $\alpha_0 = a_0 = d_1 = 0$), and frame {3} such that $\hat{\mathrm{x}}_3 = \hat{\mathrm{x}}_2$ (resulting in no offset to the joint angle θ_3).

Example: A Spatial RRRP Open Chain

The next example we consider is the four degree-of-freedom RRRP spatial open chain of Figure 5.6, here shown in its zero position. The link frame assignments are as shown, and the corresponding Denavit-Hartenberg parameters are listed in the following table:

i	α_{i-1}	a_{i-1}	d_i	ϕ_i
1	0	0	0	θ_1
2	90°	0	0	θ_2
3	0	L_2	0	$\theta_3 + 90°$
4	90°	0	θ_4	0

The four joint variables are $(\theta_1, \theta_2, \theta_3, \theta_4)$, where θ_4 is the displacement of the prismatic joint. As in the previous example, the ground frame {0} and final link frame {4} have been chosen to make as many of the Denavit-Hartenberg parameters zero.

Example: A Spatial 6R Open Chain

The final example we consider is a widely used six 6R robot arm (Figure 5.7). This open chain has six rotational joints: the first three joints function as a Cartesian positioning device, while the last three joints act as a *ZYZ* type

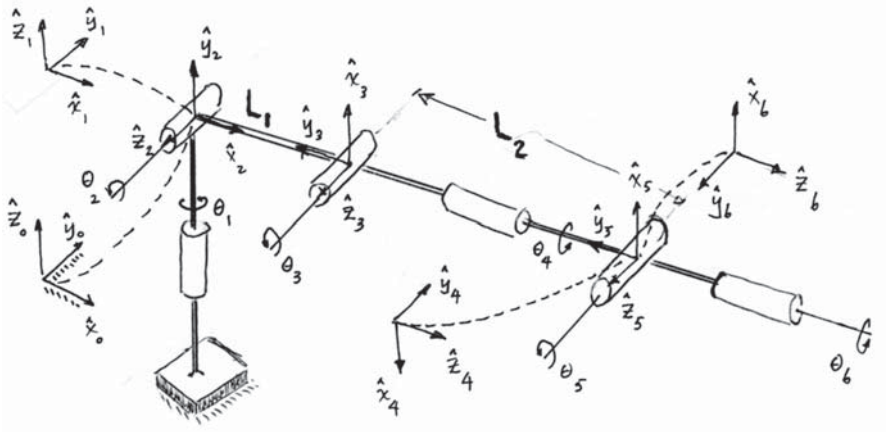

Figure 5.7: A 6R spatial open chain.

wrist. The link frames are shown in the figure, and the corresponding Denavit-Hartenberg parameters are listed in the following table:

i	α_{i-1}	a_{i-1}	d_i	ϕ_i
1	0	0	0	θ_1
2	90°	0	0	θ_2
3	0	L_1	0	$\theta_3 + 90°$
4	90°	0	L_2	$\theta_4 + 180°$
5	90°	0	0	$\theta_5 + 180°$
6	90°	0	0	θ_6

5.2 Product of Exponentials Formula

In this section we present an alternative representation of the forward kinematics, called the **product of exponentials** (PoE) formula, that is based on the matrix exponential representation for screw motions introduced in the previous chapter. We begin by recalling the Chasles-Mozzi theorem: Any displacement of a rigid body can be expressed as a finite rotation about some fixed line in space (the screw axis), followed by a finite translation parallel to the fixed line. Since both the rotation and translation are taken about the same fixed line, reversing their order still results in the same displacement.

To state things more precisely, assume a fixed frame has been chosen, and a body-fixed frame attached to the rigid body. If the body is displaced from some initial configuration $M \in SE(3)$ to another configuration $T \in SE(3)$, the displacement can then be expressed as

$$T = e^{[\mathcal{S}]\theta} M, \;\; [\mathcal{S}] = \begin{bmatrix} [\omega] & v \\ 0 & 0 \end{bmatrix}, \tag{5.17}$$

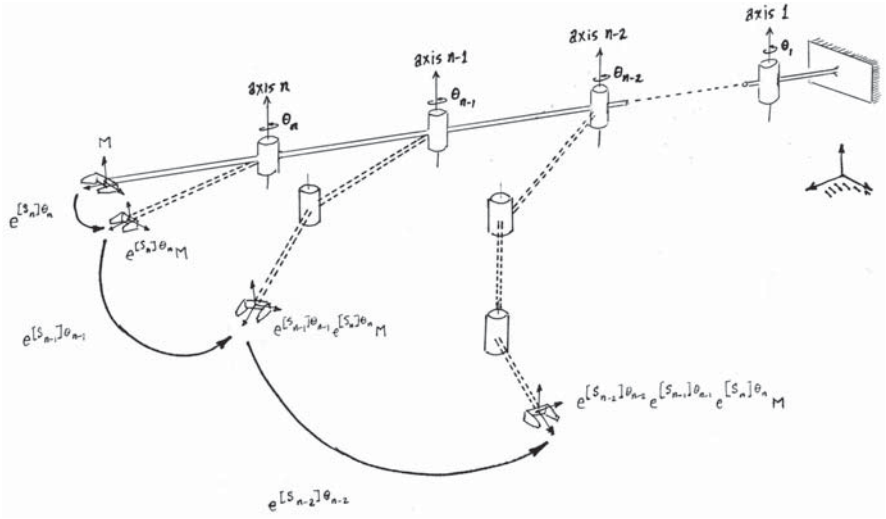

Figure 5.8: Illustration of the PoE formula for an n-link spatial open chain.

where $\mathcal{S} = (\omega, v)$ denotes the six-dimensional twist representation of the screw motion and $[\mathcal{S}]$ its 4×4 matrix representation, and $\theta \in \mathbb{R}$ is the joint displacement. Recall that for displacements that are not pure translations, $\omega \in \mathbb{R}^3$ is a unit vector in the direction of the screw axis and $[\omega] \in \mathbb{R}^{3\times 3}$ its skew-symmetric matrix representation, and $v = -\omega \times q + h\omega$, where $q \in \mathbb{R}^3$ is a point on the screw axis and $h \in \mathbb{R}$ is the screw pitch. If the displacement is a pure translation, ω is zero, and $v \in \mathbb{R}^3$ is a unit vector in the direction of positive translation.

The two limiting cases for a general screw motion are a pure rotation (corresponding to zero pitch $h = 0$) and a pure translation (corresponding to infinite pitch $h = \infty$). These two motions also happen to correspond to the two most prevalent joint types found in robots, the revolute joint and prismatic joint. The PoE formula takes advantage of this identification, by expressing the motions of revolute and prismatic joints as screw motions. We now derive the PoE formula for general spatial open chains.

5.2.1 First Formulation

The key concept behind the PoE formula is to regard each joint as applying a screw motion to all the outward links. To illustrate, consider a general spatial open chain like the one shown in Figure 5.8, consisting of n single dof joints that are connected serially. Choose a fixed frame, and also an end-effector frame attached to the last link—unlike the Denavit-Hartenberg convention, there are no restrictions placed on the choice of fixed and end-effector frames. Place the robot in its zero position by setting all joint values to zero, with the direction of positive displacement (rotation for revolute joints, translation for prismatic joints) for each joint specified.

Let $M \in SE(3)$ denote the configuration of the end-effector frame when the robot is in its zero position. Suppose only joint n is displaced to some joint value θ_n. The end-effector frame M then undergoes a screw motion of the form

$$T = e^{[\mathcal{S}_n]\theta_n} M, \tag{5.18}$$

where $T \in SE(3)$ is the newly displaced configuration of the end-effector frame, and $\mathcal{S}_n = (\omega_n, v_n)$ is the twist vector describing the motion for joint n. For example, if joint $_n$ is revolute (corresponding to a screw motion of zero pitch), then $\omega_n \in \mathbb{R}^3$ is a unit vector in the positive direction of joint axis n, and $v_n = -\omega_n \times q_n$, with q_n any arbitrary point on joint axis n. If joint n is prismatic, then $\omega_n = 0$, and $v \in \mathbb{R}^3$ is a unit vector in the direction of positive translation. We remind the reader that all vector quantities here are expressed in terms of the fixed frame.

If we assume joint $n-1$ is also allowed to vary, then this has the effect of applying a screw motion to link $n-1$ (and by extension to link n, since link n is connected to link $n-1$ via joint n). The end-effector frame thus undergoes a screw motion of the form

$$T = e^{[\mathcal{S}_{n-1}]\theta_{n-1}} \left(e^{[\mathcal{S}_n]\theta_n} M \right). \tag{5.19}$$

Continuing with this reasoning and now allowing all the joints $(\theta_1, \ldots, \theta_n)$ to vary, it follows that

$$T = e^{[\mathcal{S}_1]\theta_1} \cdots e^{[\mathcal{S}_{n-1}]\theta_{n-1}} e^{[\mathcal{S}_n]\theta_n} M. \tag{5.20}$$

This is the product of exponentials formula describing the forward kinematics of an n-dof open chain. Specifically, we will call Equation (5.20) the **space form** of the product of exponentials formula. We note the following features of the product of exponentials formula:

- No link reference frames need to be assigned. Only the fixed and end-effector frames need to be chosen (note that there are no restrictions on how these frames are chosen), together with a definition of the robot's zero position, and the direction of positive displacement for each joint (rotation in the case of a revolute joint, translation in the case of a prismatic joint).
- Placing the robot in its zero position, if joint i is revolute, then $\omega_i \in \mathbb{R}^3$ is a unit vector in the (positive) direction of the joint axis, and $v = -\omega_i \times q_i$, where $q_i \in \mathbb{R}^3$ is an arbitrary point on joint axis i. If joint i is prismatic, then $\omega_i = 0$ and $v_i \in \mathbb{R}^3$ is a unit vector in the direction of (positive) translation. Unlike the Denavit-Hartenberg parameters, where the joint variable involves either ϕ_i or d_i depending on whether the joint is revolute or prismatic, in the product of exponentials formula the joint variable is always labelled in a consistent fashion by θ_i.

Compared to the Denavit-Hartenberg parameters, the fact that no link reference frames are used, and that the fixed and end-effector frames can be assigned without any restrictions, considerably simplies the forward kinematic analysis. Further advantages will come to light when we examine the velocity kinematics in the next chapter.

5.2.2 Examples

We now derive the forward kinematics for some common spatial open structures using the product of exponentials formula.

Example: 3R Spatial Open Chain

We return to the previous 3R open chain example of Figure 5.5. Choose the fixed frame $\{0\}$ and end-effector frame $\{3\}$ as indicated in the figure, and express all vectors and homogeneous transformations in terms of the fixed frame. The forward kinematics will be of the form

$$T = e^{[\mathcal{S}_1]\theta_1} e^{[\mathcal{S}_2]\theta_2} e^{[\mathcal{S}_3]\theta_3} M,$$

where $M \in SE(3)$ is the end-effector frame configuration when the robot is in its zero position. By inspection M can be obtained as

$$M = \begin{bmatrix} 0 & 0 & 1 & L_1 \\ 0 & 1 & 0 & 0 \\ -1 & 0 & 0 & -L_2 \\ 0 & 0 & 0 & 1 \end{bmatrix}.$$

The twist $\mathcal{S}_1 = (\omega_1, v_1)$ for joint axis 1 is then given by $\omega_1 = (0, 0, 1)$ and $v_1 = (0, 0, 0)$ (the fixed frame origin (0,0,0) is a convenient choice for the point q_1 lying on joint axis 1). To determine the twist $\mathcal{S}_2$ for joint axis 2, observe that joint axis 2 points in the $-\hat{y}_0$ axis direction, so that $\omega_2 = (0, -1, 0)$. Choose $q_2 = (L_1, 0, 0)$, in which case $v_2 = -\omega_2 \times q_2 = (0, 0, -L_1)$. Finally, to determine the twist $\mathcal{S}_3$ for joint axis, note that $\omega_3 = (1, 0, 0)$. Choosing $q_3 = (0, 0, -L_2)$, it follows that $v_3 = -\omega_3 \times q_3 = (0, L_2, 0)$.

In summary, we have the following 4×4 matrix representations for the three joint twist vectors $\mathcal{S}_1$, $\mathcal{S}_2$, and $\mathcal{S}_3$:

$$[\mathcal{S}_1] = \begin{bmatrix} 0 & -1 & 0 & 0 \\ 1 & 0 & 0 & 0 \\ 0 & 0 & 0 & 0 \\ 0 & 0 & 0 & 1 \end{bmatrix}$$

$$[\mathcal{S}_2] = \begin{bmatrix} 0 & 0 & -1 & 0 \\ 0 & 0 & 0 & 0 \\ 1 & 0 & 0 & -L_1 \\ 0 & 0 & 0 & 1 \end{bmatrix}$$

$$[\mathcal{S}_3] = \begin{bmatrix} 0 & 0 & 0 & 0 \\ 0 & 0 & -1 & L_2 \\ 0 & 1 & 0 & 0 \\ 0 & 0 & 0 & 1 \end{bmatrix}.$$

It will be more convenient to list the twist vectors in the following tabular form:

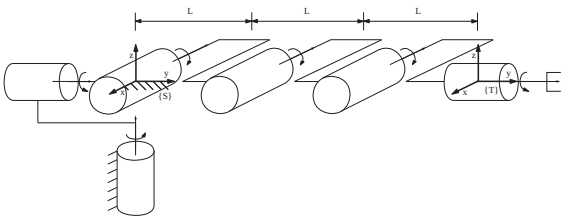

Figure 5.9: POE forward kinematics for the 6R open chain.

i	ω_i	v_i
1	(0, 0, 1)	(0, 0, 0)
2	(0, -1, 0)	(0, 0, $-L_1$)
3	(1, 0, 0)	(0, L_2, 0)

Example: 6R Spatial Open Chain

We now derive the forward kinematics of the 6R open chain of Figure 5.9. The zero position and the direction of positive rotation for each joint axis are as shown in the figure. A fixed frame $\{0\}$ and end-effector frame $\{6\}$ are also assigned as shown. The end-effector frame M in the zero position is then

$$M = \begin{bmatrix} 1 & 0 & 0 & 0 \\ 0 & 1 & 0 & 3L \\ 0 & 0 & 1 & 0 \\ 0 & 0 & 0 & 1 \end{bmatrix} \tag{5.21}$$

The screw axis for joint 1 is in the direction $\omega_1 = (0, 0, 1)$. The most convenient choice for point q_1 lying on joint axis 1 is the origin, so that $v_1 = (0, 0, 0)$. The screw axis for joint 2 is in the $\hat{y}$ direction of the fixed frame, so $\omega_2 = (0, 1, 0)$. Choosing $q_2 = (0, 0, 0)$, we have $v_2 = (0, 0, 0)$. The screw axis for joint 3 is in the direction $\omega_3 = (-1, 0, 0)$. Choosing $q_3 = (0, 0, 0)$ leads to $v_3(0, 0, 0)$. The screw axis for joint 4 is in the direction $\omega_4 = (-1, 0, 0)$. Choosing $q_4 = (0, L, 0)$ leads to $v_4 = (0, 0, -L)$. The screw axis for joint 5 is in the direction $\omega_5 = (-1, 0, 0)$; choosing $q_5 = (0, 2L, 0)$ leads to $v_5 = (0, 0, -2L)$. The screw axes for joint 6 is in the direction $\omega_6 = (0, 1, 0)$; choose $q_6 = (0, 0, 0)$ leads to $v_6 = (0, 0, 0)$. In summary, the twists $\mathcal{S}_i = (\omega_i, v_i)$, $i = 1, \ldots 6$ are as follows:

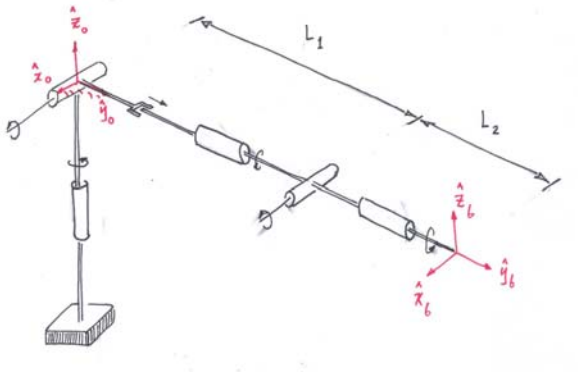

Figure 5.10: The RRPRRR spatial open chain.

i	ω_i	v_i
1	(0, 0, 1)	(0, 0, 0)
2	(0, 1, 0)	(0, 0, 0)
3	(-1, 0, 0)	(0, 0, 0)
4	(-1, 0, 0)	(0, 0, $-L$)
5	(-1, 0, 0)	(0, 0, $-2L$)
6	(0, 1, 0)	(0, 0, 0)

Example: A RRPRRR Spatial Open Chain

In this example we consider the six degree-of-freedom RRPRRR spatial open chain of Figure 5.10. The end-effector frame in the zero position is given by

$$M = \begin{bmatrix} 1 & 0 & 0 & 0 \\ 0 & 1 & 0 & L_1 + L_2 \\ 0 & 0 & 1 & 0 \\ 0 & 0 & 0 & 1 \end{bmatrix}.$$

The values of the screw twists $\mathcal{S}_i = (\omega_i, v_i)$ are listed in the following table:

i	ω_i	v_i
1	(0, 0, 1)	(0, 0, 0)
2	(1, 0, 0)	(0, 0, 0)
3	(0, 0, 0)	(0, 1, 0)
4	(0, 1, 0)	(0, 0, 0)
5	(1, 0, 0)	(0, 0, $-L_1$)
6	(0, 1, 0)	(0, 0, 0)

Note that the third joint is prismatic, so that $\omega_3 = 0$ and v_3 is a unit vector in the direction of positive translation.

5.2.3 Relation with the Denavit-Hartenberg Representation

The product of exponentials formula can also be derived directly from the Denavit-Hartenberg parameter-based representation of the forward kinematics. As before, denote the relative displacement between adjacent link frames by

$$T_{i-1,i} = \mathrm{Rot}(\hat{\mathrm{x}}, \alpha_{i-1}) \cdot \mathrm{Trans}(\hat{\mathrm{x}}, a_{i-1}) \cdot \mathrm{Trans}(\hat{z}, d_i) \cdot \mathrm{Rot}(\hat{z}, \phi_i).$$

If joint i is revolute, the first three matrices can be regarded as constant, and ϕ_i becomes the revolute joint variable. Define $\theta_i = \phi_i$, and

$$M_i = \mathrm{Rot}(\hat{\mathrm{x}}, \alpha_{i-1}) \cdot \mathrm{Trans}(\hat{\mathrm{x}}, a_{i-1}) \cdot \mathrm{Trans}(\hat{z}, d_i), \tag{5.22}$$

and write $\mathrm{Rot}(\hat{z}, \theta_i)$ as the following matrix exponential:

$$\mathrm{Rot}(\hat{\mathrm{z}}, \theta_i) = e^{[\mathcal{A}_i]\theta_i}, \quad [\mathcal{A}_i] = \begin{bmatrix} 0 & -1 & 0 & 0 \\ 1 & 0 & 0 & 0 \\ 0 & 0 & 0 & 0 \\ 0 & 0 & 0 & 0 \end{bmatrix}. \tag{5.23}$$

With the above definitions we can write $T_{i-1,i} = M_i e^{[\mathcal{A}_i]\theta_i}$.

If joint i is prismatic, then d_i becomes the joint variable, ϕ_i is a constant parameter, and the order of $\mathrm{Trans}(\hat{z}, d_i)$ and $\mathrm{Rot}(\hat{z}, \phi_i)$ in $T_{i-1,i}$ can be reversed (recall that reversing translations and rotations taken along the same axis still results in the same motion). In this case we can still write $T_{i-1,i} = M_i e^{[\mathcal{A}_i]\theta_i}$, where $\theta_i = d_i$ and

$$M_i = \mathrm{Rot}(\hat{\mathrm{x}}, \alpha_{i-1})\mathrm{Trans}(\hat{\mathrm{x}}, a_{i-1})\mathrm{Rot}(\hat{z}, \phi_i) \tag{5.24}$$

$$[\mathcal{A}_i] = \begin{bmatrix} 0 & 0 & 0 & 0 \\ 0 & 0 & 0 & 0 \\ 0 & 0 & 0 & 1 \\ 0 & 0 & 0 & 0 \end{bmatrix}. \tag{5.25}$$

Based on the above, for an n-link open chain containing both revolute and prismatic joints, the forward kinematics can be written

$$T_{0,n} = M_1 e^{[\mathcal{A}_1]\theta_1} M_2 e^{[\mathcal{A}_2]\theta_2} \cdots M_n e^{[\mathcal{A}_n]\theta_n} \tag{5.26}$$

where θ_i denotes joint variable i, and $[\mathcal{A}_i]$ is either of the form (5.23) or (5.25) depending on whether joint i is revolute or prismatic.

We now make use of the matrix identity $Me^P M^{-1} = e^{MPM^{-1}}$, which holds for any nonsingular $M \in \mathbb{R}^{n\times n}$ and arbitrary $P \in \mathbb{R}^{n\times n}$. The above can also be rearranged as $Me^P = e^{MPM^{-1}}M$. Beginning from the left of Equation (5.26), if we repeatedly apply this identity, after n iterations we obtain the product of exponentials formula as originally derived:

$$\begin{aligned} T_{0n} &= e^{M_1[\mathcal{A}_1]M_1^{-1}\theta_1}(M_1M_2)e^{[\mathcal{A}_2]\theta_2}\cdots e^{[\mathcal{A}_n]\theta_n} \\ &= e^{M_1[\mathcal{A}_1]M_1^{-1}\theta_1}e^{(M_1M_2)[\mathcal{A}_2](M_1M_2)^{-1}\theta_2}(M_1M_2M_3)e^{[\mathcal{A}_3]\theta_3}\cdots e^{[\mathcal{A}_n]\theta_n} \\ &= e^{[\mathcal{S}_1]\theta_1}\cdots e^{[\mathcal{S}_n]\theta_n}M, \end{aligned} \tag{5.27}$$

where

$$[\mathcal{S}_i] = (M_1 \cdots M_{i-1})[\mathcal{A}_i](M_1 \cdots M_{i-1})^{-1}, \quad i = 1, \ldots, n \tag{5.28}$$

$$M = M_1 M_2 \cdots M_n. \tag{5.29}$$

We now re-examine the physical meaning of the $\mathcal{S}_i$ by recalling how a screw twist transforms under a change of reference frames. If $\mathcal{S}_a$ represents the screw twist for a given screw motion with respect to frame $\{a\}$, and $\mathcal{S}_b$ represents the screw twist for the same physical screw motion but this time with respect to frame $\{b\}$, then recall that $\mathcal{S}_a$ and $\mathcal{S}_b$ are related by

$$[\mathcal{S}_b] = T_{ba}[\mathcal{S}_a]T_{ba}^{-1}, \tag{5.30}$$

or using the adjoint notation $\mathrm{Ad}_{T_{ba}}$,

$$\mathcal{S}_b = \mathrm{Ad}_{T_{ba}}(\mathcal{S}_a). \tag{5.31}$$

Seen from the perspective of this transformation rule, Equation (5.29) suggests that $\mathcal{A}_i$ is the screw twist for joint axis i as seen from link frame $\{i\}$, while $\mathcal{S}_i$ is the screw twist for joint axis i as seen from the fixed frame $\{0\}$.

5.2.4 Second Formulation

The matrix identity $e^{M^{-1}PM} = M^{-1}e^P M$ can also be expressed as $Me^{M^{-1}PM} = e^P M$. Beginning with the right-most term of the previously derived product of exponentials formula, if we repeatedly apply this identity, after n iterations we obtain

$$\begin{aligned} T &= e^{[\mathcal{S}_1]\theta_1} \cdots e^{[\mathcal{S}_n]\theta_n} M \\ &= e^{[\mathcal{S}_1]\theta_1} \cdots M e^{M^{-1}[\mathcal{S}_n]M\theta_n} \\ &= e^{[\mathcal{S}_1]\theta_1} \cdots M e^{M^{-1}[\mathcal{S}_{n-1}]M\theta_{n-1}} e^{M^{-1}[\mathcal{S}_n]M\theta_n} \\ &= M e^{[\mathcal{B}_1]\theta_1} e^{[\mathcal{B}_2]\theta_2} \cdots e^{[\mathcal{B}_n]\theta_n}, \end{aligned} \tag{5.32}$$

where each $[\mathcal{B}_i] = M^{-1}[\mathcal{S}_i]M$, $i = 1, \ldots, n$. This is an alternative form of the product of exponentials formula. Note that M^{-1} is the relative displacement of the fixed frame as seen from the end-effector frame; since each

$$\mathcal{B}_i = \mathrm{Ad}_{M^{-1}}(\mathcal{S}_i), \tag{5.33}$$

$\mathcal{B}_i$ is the screw twist for joint i expressed in terms of the end-effector frame at the zero position. We will call Equation (5.32) the **body form** of the product of exponentials formula.

Example: 6R Spatial Open Chain

We now express the forward kinematics for the same 6R open chain of Figure 5.9 in the second form

$$T = Me^{[\mathcal{B}_1]\theta_1} e^{[\mathcal{B}_2]\theta_2} \cdots e^{[\mathcal{B}_6]\theta_6}.$$

Assume the same fixed and end-effector frames and zero position as the previous example. M is still the same as Equation (5.21), obtained as the end-effector frame as seen from the fixed frame with the chain in its zero position. The screw twists for each joint axes, however, are now expressed with respect to the end-effector frame in its zero position:

i	ω_i	v_i
1	(0, 0, 1)	$(-3L,\ 0,\ 0)$
2	(0, 1, 0)	(0, 0, 0)
3	(-1, 0, 0)	$(0,\ 0,\ -3L)$
4	(-1, 0, 0)	$(0,\ 0,\ -2L)$
5	(-1, 0, 0)	$(0,\ 0,\ -L)$
6	(0, 1, 0)	(0, 0, 0)

5.3 Summary

- Given an open chain with a reference frame attached to some point on its last link—this frame is denoted the **end-effector frame**—the forward kinematics is the mapping from the joint values to the position and orientation of the end-effector frame.

- In the **Denavit-Hartenberg** representation, the forward kinematics of an open chain is described in terms of relative displacements between reference frames attached to each link. If the link frames are sequentially labelled $\{0\}, \ldots, \{n\}$, where $\{0\}$ is the fixed frame and $\{n\}$ is the end-effector frame, then the forward kinematics is expressed as

$$T_{0n} = T_{01}(\theta_1) \cdots T_{n-1,n}(\theta_n)$$

  where θ_i denotes the joint i variable.

- The Denavit-Hartenberg convention requires that reference frames assigned to each link obey a strict convention. Following this convention, the link frame transformation $T_{i-1,i}$ between link frames $\{i-1\}$ and $\{i\}$ can be parametrized using a minimum of four parameters (the **Denavit-Hartenberg parameters**): the link twist α_{i-1}, link length a_{i-1}, link offset d_i, and joint angle ϕ_i.

- The forward kinematics can also be expressed as the following **product of exponentials** (the **space form**):

$$T_{0n} = e^{[\mathcal{S}_1]\theta_1} \cdots e^{[\mathcal{S}_n]\theta_n} M,$$

  where $\mathcal{S}_i = (\omega_i, v_i)$ denotes the screw twist associated with joint i expressed in fixed frame coordinates, θ_i is the joint i variable, and $M \in SE(3)$ denotes the position and orientation of the end-effector frame when the robot is in its zero position. A choice of fixed frame and end-effector

frame, together with a specification of the robot's zero position and direction of positive rotation or translation of each of the robot's joints, then completely specifies the product of exponentials formula.

- The product of exponentials formula can also be written in the equivalent **body form**:

$$T_{0n} = M e^{[\mathcal{B}_1]\theta_1} \cdots e^{[\mathcal{B}_n]\theta_n},$$

where $[\mathcal{B}]_i = M^{-1}[\mathcal{S}_i]M$, $i = 1, \ldots, n$. $\mathcal{B}_i = (\omega_i, v_i)$ is the screw twist corresponding to joint axis i, expressed in terms of the end-effector frame with the robot in its zero position.

Notes and References

In the original paper by Denavit and Hartenberg [7], the four parameters are defined without appealing to any reference frames, e.g., the link length is defined to be length of the mutually perpendicular line between the joint axes, the twist angle is obtained by first projecting the two adjacent axes to the plane perpendicular to the common normal and measuring the angle between the axes, etc. The convention of choosing the $\hat{z}$-axis to be along the joint axis and the $\hat{x}$-axis to be along the common normal is not standard; other authors, for example, choose the joint axis to be in the $\hat{x}$-direction. The product of exponentials formula is first presented by Brockett in [4]. Computational aspects of the product of exponentials formula are also discussed in [27].

Chapter 6

Velocity Kinematics and Statics

A robot's **velocity kinematics** refers to the relationship between the robot's joint rates and the linear and angular velocity of its end-effector. Whereas the forward kinematics of typical robots is usually nonlinear and complicated, it turns out that the equations for velocity kinematics are linear: at any instant during a robot's motion, the end-effector's linear and angular velocity can be obtained simply by multiplying the joint rate vector by a (configuration-dependent) **Jacobian** matrix. This linear relationship is exploited to great effect in many applications, ranging from algorithms for inverse kinematics and trajectory generation to manipulation planning and control. The Jacobian matrix also turns out to play a central role in tasks involving static and dynamic contact between the end-effector and the environment.

In this chapter we derive the Jacobian matrix for open chains, and examine its role in velocity analysis, statics, and the identification of kinematic singularities. Later chapters on inverse kinematics, motion planning, and control will also draw upon these concepts in a fundamental way. The material in this chapter is based upon the treatment of rigid body velocities given in Chapter 3, and it may be useful to review this material first.

6.1 Manipulator Jacobian

6.1.1 Space Jacobian

In this section we derive the relationship between an open chain's joint rate vector $\dot{\theta}$ and the end-effector's spatial velocity $\mathcal{V}_s$. We first recall a few basic properties from linear algebra and linear differential equations: (i) if $A, B \in \mathbb{R}^{n\times n}$ are both invertible, then $(AB)^{-1} = B^{-1}A^{-1}$; (ii) if $A \in \mathbb{R}^{n\times n}$ is constant and $\theta(t)$ is a scalar function of t, then $\frac{d}{dt}e^{A\theta} = Ae^{A\dot{\theta}}\dot{\theta} = e^{A\theta}A\dot{\theta}$; (iii) $(e^{A\theta})^{-1} = e^{-A\theta}$.

Now consider an n-link open chain whose forward kinematics is expressed in the following product of exponentials form:

$$T(\theta_1, \ldots, \theta_n) = e^{[\mathcal{S}_1]\theta_1} e^{[\mathcal{S}_2]\theta_2} \cdots e^{[\mathcal{S}_n]\theta_n} M. \tag{6.1}$$

The spatial velocity of the end-effector frame with respect to the fixed frame, $\mathcal{V}_s$, is given by $[\mathcal{V}_s] = \dot{T}T^{-1}$, where

$$\begin{aligned} \dot{T} &= (\frac{d}{dt} e^{[\mathcal{S}_1]\theta_1}) \cdots e^{[\mathcal{S}_n]\theta_n} M + e^{[\mathcal{S}_1]\theta_1} (\frac{d}{dt} e^{[\mathcal{S}_2]\theta_2}) \cdots e^{[\mathcal{S}_n]\theta_n} M + \ldots \\ &= [\mathcal{S}_1]\dot{\theta}_1 e^{[\mathcal{S}_1]\theta_1} \cdots e^{[\mathcal{S}_n]\theta_n} M + e^{[\mathcal{S}_1]\theta_1} [\mathcal{S}_2]\dot{\theta}_2 e^{[\mathcal{S}_2]\theta_2} \cdots e^{[\mathcal{S}_n]\theta_n} M + \ldots \end{aligned}$$

Also,

$$T^{-1} = M^{-1} e^{-[\mathcal{S}_n]\theta_n} \cdots e^{-[\mathcal{S}_1]\theta_1}.$$

Multiplying $\dot{T}$ and T^{-1}, we have

$$[\mathcal{V}_s] = [\mathcal{S}_1]\dot{\theta}_1 + e^{[\mathcal{S}_1]\theta_1} [\mathcal{S}_2] e^{-[\mathcal{S}_1]\theta_1} \dot{\theta}_2 + e^{[\mathcal{S}_1]\theta_1} e^{[\mathcal{S}_2]\theta_2} [\mathcal{S}_3] e^{-[\mathcal{S}_2]\theta_2} e^{-[\mathcal{S}_1]\theta_1} \dot{\theta}_3 + \ldots.$$

The above can also be expressed in vector form by means of the adjoint mapping:

$$\mathcal{V}_s = \mathcal{S}_1\dot{\theta}_1 + \mathrm{Ad}_{e^{[\mathcal{S}_1]\theta_1}}(\mathcal{S}_2)\dot{\theta}_2 + \mathrm{Ad}_{e^{[\mathcal{S}_1]\theta_1} e^{[\mathcal{S}_2]\theta_2}}(\mathcal{S}_3)\dot{\theta}_3 + \ldots \tag{6.2}$$

Observe that $\mathcal{V}_s$ is a sum of n spatial velocities of the form

$$\mathcal{V}_s = \mathcal{V}_{s1}(\theta)\dot{\theta}_1 + \ldots + \mathcal{V}_{sn}(\theta)\dot{\theta}_n, \tag{6.3}$$

where each $\mathcal{V}_{si}(\theta) = (\omega_{si}(\theta), v_{si}(\theta))$ depends explictly on the joint values $\theta \in \mathbb{R}^n$. In matrix form,

$$\begin{aligned} \mathcal{V}_s &= \begin{bmatrix} \mathcal{V}_{s1}(\theta) & \mathcal{V}_{s2}(\theta) & \cdots & \mathcal{V}_{sn}(\theta) \end{bmatrix} \begin{bmatrix} \dot{\theta}_1 \\ \vdots \\ \dot{\theta}_n \end{bmatrix} \\ &= J_s(\theta)\dot{\theta}. \end{aligned} \tag{6.4}$$

The matrix $J_s(\theta)$ is said to be the **Jacobian** in fixed (**space**) frame coordinates, or more simply the **space Jacobian**.

Definition 6.1. Let the forward kinematics of an n-link open chain be expressed in the following product of exponentials form:

$$T = e^{[\mathcal{S}_1]\theta_1} \cdots e^{[\mathcal{S}_n]\theta_n} M. \tag{6.5}$$

The **space Jacobian** $J_s(\theta) \in \mathbb{R}^{6\times n}$ relates the joint rate vector $\dot{\theta} \in \mathbb{R}^n$ to the end-effector spatial velocity $\mathcal{V}_s$ via $\mathcal{V}_s = J_s(\theta)\dot{\theta}$. The i-th column of $J_s(\theta)$ is

$$\mathcal{V}_{si}(\theta) = Ad_{e^{[\mathcal{S}_1]\theta_1} \ldots e^{[\mathcal{S}_{i-1}]\theta_{i-1}}}(\mathcal{S}_i), \tag{6.6}$$

for $i = 2, \ldots, n$, with the first column $\mathcal{V}_{s1}(\theta) = \mathcal{S}_1$. □

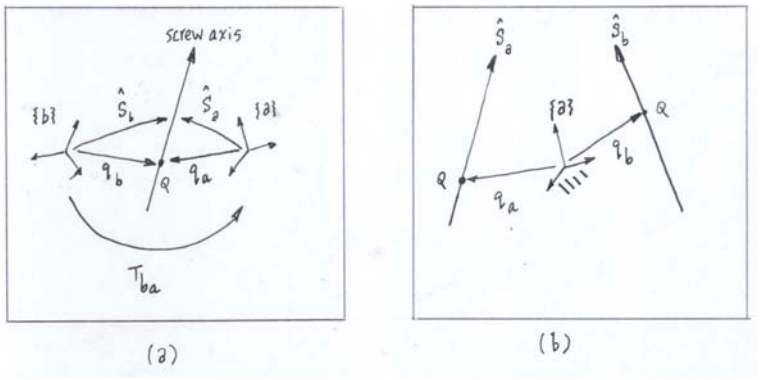

Figure 6.1: Physical interpretation of the screw adjoint transformation $Ad_{T_{ba}}$: (a) describing the same screw motion in terms of two different reference frames $\{a\}$ and $\{b\}$; (b) An initial screw axis displaced a transformation T_{ba}.

To understand the physical meaning behind the columns of $J_s(\theta)$, recall from Chapter 3 that if $\mathcal{S}_a = (\omega_a, v_a)$ is the vector describing a screw motion in frame $\{a\}$ coordinates, and $\mathcal{S}_b = (\omega_b, v_b)$ is a vector describing the same screw motion in frame $\{b\}$ coordinates, then $\mathcal{S}_b$ and $\mathcal{S}_a$ are related by $\mathcal{S}_b = \mathrm{Ad}_{T_{ba}}(\mathcal{S}_a)$ (see Figure 6.1-(a)). Another physical interpretation of this transformation is from the perspective of reference frame $\{a\}$ only. Referring to Figure 6.1-(b), suppose the vector $\mathcal{S}_a$ describes the initial screw axis with respect to frame $\{a\}$, and the vector $\mathcal{S}_b$ describes the screw axis after it has undergone a rigid body displacement T_{ba}. It follows that

$$\omega_b = R_{ba}\omega_a. \tag{6.7}$$

The point q on the screw axis is now displaced from its initial location q_a to

$$q_b = T_{ba}q_a = R_{ba}q_a + p_{ba}. \tag{6.8}$$

Then from the definition $v_b = -\omega_b \times q_b + h_b\omega_b$, where $h_b = h_a$ (the screw pitch is a scalar quantity, and hence independent of the choice of reference frames), we have

$$\begin{aligned} v_b &= -\omega_b \times q_b + h_b\omega_b \\ &= -R_{ba}\omega_a \times (R_{ba}q_a + p_{ba}) + h_b R_{ba}\hat{\omega}_a \\ &= R_{ba}\left(-[\omega_a]q_a + h_a\omega_a\right) - R_{ba}[\omega_a]R_{ba}^T p_{ba} \\ &= R_{ba}v_a + [p_{ba}]R_{ba}\omega_a, \end{aligned}$$

where in the last two lines we have again made use of the matrix identity $R[\omega]R^T = [R\omega]$ for $R \in SO(3)$ and $\omega \in \mathbb{R}^3$. Equations (6.7) and (6.9) can be combined in the form

$$\begin{bmatrix} \omega_b \\ v_b \end{bmatrix} = \begin{bmatrix} R_{ba} & 0 \\ [p_{ba}]\,R_{ba} & R_{ba} \end{bmatrix} \begin{bmatrix} \omega_a \\ v_a \end{bmatrix}, \tag{6.9}$$

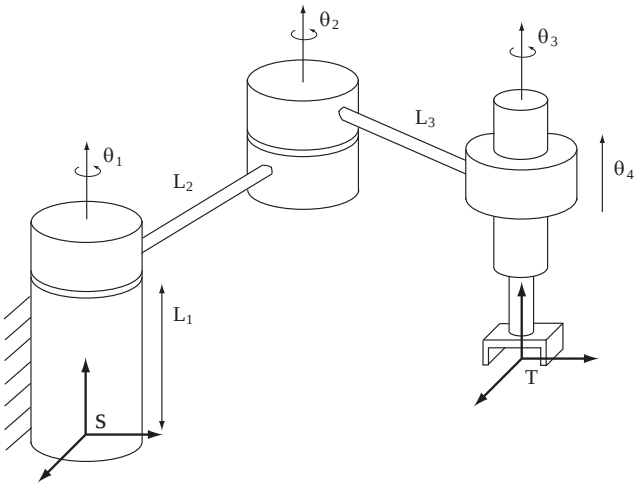

Figure 6.2: Space Jacobian for a spatial $RRRP$ chain.

which is precisely $\mathcal{S}_b = \mathrm{Ad}_{T_{ba}}(\mathcal{S}_a)$.

Returning now to the equation for the space Jacobian (6.2), observe that the i-th term of the right-hand side of (6.2) is of the form $\mathrm{Ad}_{T_{i-1}}(\mathcal{S}_i)$, where $T_{i-1} = e^{[\mathcal{S}_1]\theta_1} \cdots e^{[\mathcal{S}_{i-1}]\theta_{i-1}}$; recall here that $\mathcal{S}_i$ is the screw vector describing the i-th joint axis in terms of the fixed frame with the robot in its zero position. $\mathrm{Ad}_{T_{i-1}}(\mathcal{S}_i)$ can therefore be viewed as the screw vector describing the i-th joint axis after it undergoes the rigid body displacement T_{i-1}. But physically this is the same as moving the first $i-1$ joints from their zero position to the current values $\theta_1, \ldots, \theta_{i-1}$. Therefore, the i-th column $\mathcal{V}_{si}(\theta)$ of $J_s(\theta)$ is simply the screw vector describing joint axis i, expressed in fixed frame coordinates as a function of the joint variables $\theta_1, \ldots, \theta_{i-1}$.

In summary, the procedure for determining the columns of $J_s(\theta)$ is similar to that for deriving the $\mathcal{S}_i$ in the product of exponentials formula $e^{[\mathcal{S}_1]\theta_1} \cdots e^{[\mathcal{S}_n]\theta_n} M$: each column $\mathcal{V}_{si}(\theta)$ is the screw vector describing joint axis i, expressed in fixed frame coordinates, but for arbitrary θ rather than $\theta = 0$.

Example: Space Jacobian for a Spatial RRRP Chain

We now illustrate the procedure for finding the space Jacobian for the spatial $RRRP$ chain of Figure 6.2. Denote the i-th column of $J_s(\theta)$ by $\mathcal{V}_i = (\omega_i, v_i)$.

- Observe that ω_1 is constant and in the $\hat{z}$-direction: $\omega_1 = (0, 0, 1)$. Picking q_1 to be the origin, $v_1 = (0, 0, 0)$.
- ω_2 is also constant in the $\hat{z}$-direction, so $\omega_2 = (0, 0, 1)$. Pick $q_2 = (L_1 c_1, L_1 s_1, 0)$, where $c_1 = \cos\theta_1$, $s_1 = \sin\theta_1$. Then $v_2 = -\omega_2 \times q_2 = (L_1 s_1, -L_1 c_1, 0)$.
- The direction of ω_3 is always fixed in the $\hat{z}$-direction regardless of the values of θ_1 and θ_2, so $\omega_3 = (0, 0, 1)$. Picking $q_3 = (L_1 c_1 + L_2 c_{12}, L_1 s_1 +$

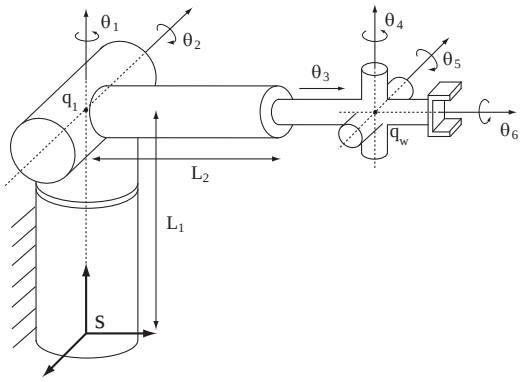

Figure 6.3: Space Jacobian for the spatial $RRPRRR$ chain.

$L_2 s_{12}, 0)$, where $c_{12} = \cos(\theta_1 + \theta_2)$, $s_{12} = \sin(\theta_1 + \theta_2)$, it follows that $v_3 = (L_1 s_1 + L_2 s_{12}, -L_1 c_1 - L_2 c_{12}, 0)$.

- Since the final joint is prismatic, $\omega_4 = (0, 0, 0)$, and the joint axis direction is given by $v_4 = (0, 0, -1)$.

The space Jacobian is therefore

$$J_s(\theta) = \begin{bmatrix} 0 & 0 & 0 & 0 \\ 0 & 0 & 0 & 0 \\ 1 & 1 & 1 & 0 \\ 0 & L_1 s_1 & L_1 s_1 + L_2 s_{12} & 0 \\ 0 & -L_1 c_1 & -L_1 c_1 - L_2 c_{12} & 0 \\ 0 & 0 & 0 & -1 \end{bmatrix}.$$

Example: Space Jacobian for Spatial RRPRRR Chain

We now derive the space Jacobian for the spatial $RRPRRR$ chain of Figure 6.3. The base frame is chosen as shown in the figure.

- The first joint axis is in the direction $\omega_1 = (0, 0, 1)$. Picking $q_1 = (0, 0, L_1)$, we get $v_1 = -\omega_1 \times q_1 = (0, 0, 0)$.
- The second joint axis is in the direction $\omega_2 = (-c_1, -s_1, 0)$. Picking $q_2 = (0, 0, L_1)$, we get $v_2 = -\omega_2 \times q_2 = (L_1 s_1, -L_1 c_1, 0)$.
- The third joint is prismatic, so $\omega_3 = (0, 0, 0)$. The direction of the prismatic joint axis is given by

$$v_3 = \mathrm{Rot}(\hat{z}, \theta_1)\mathrm{Rot}(\hat{x}, -\theta_2) \begin{bmatrix} 0 \\ 1 \\ 0 \end{bmatrix} = \begin{bmatrix} -s_1 c_2 \\ c_1 c_2 \\ -s_2 \end{bmatrix}.$$

- Now consider the wrist portion of the chain. The wrist center is located at the point

$$q_w = \begin{bmatrix} 0 \\ 0 \\ L_1 \end{bmatrix} + \mathrm{Rot}(\hat{z}, \theta_1)\mathrm{Rot}(\hat{x}, -\theta_2) \begin{bmatrix} 0 \\ L_1 + \theta_3 \\ 0 \end{bmatrix} = \begin{bmatrix} -(L_2 + \theta_3)s_1c_2 \\ (L_2 + \theta_3)c_1c_2 \\ L_1 - (L_2 + \theta_3)s_2 \end{bmatrix}.$$

  Observe that the directions of the wrist axes depend on θ_1, θ_2, and the preceding wrist axes. These are

$$\begin{aligned}
\omega_4 &= \mathrm{Rot}(\hat{z}, \theta_1)\mathrm{Rot}(\hat{x}, -\theta_2) \begin{bmatrix} 0 \\ 0 \\ 1 \end{bmatrix} = \begin{bmatrix} -s_1s_2 \\ c_1s_2 \\ c_2 \end{bmatrix} \\
\omega_5 &= \mathrm{Rot}(\hat{z}, \theta_1)\mathrm{Rot}(\hat{x}, -\theta_2)\mathrm{Rot}(\hat{z}, \theta_4) \begin{bmatrix} -1 \\ 0 \\ 0 \end{bmatrix} = \begin{bmatrix} -c_1c_4 + s_1c_2s_4 \\ -s_1c_4 - c_1c_2s_4 \\ s_2s_4 \end{bmatrix} \\
\omega_6 &= \mathrm{Rot}(\hat{z}, \theta_1)\mathrm{Rot}(\hat{x}, -\theta_2)\mathrm{Rot}(\hat{z}, \theta_4)\mathrm{Rot}(\hat{x}, -\theta_5) \begin{bmatrix} 0 \\ 1 \\ 0 \end{bmatrix} \\
&= \begin{bmatrix} -c_5(s_1c_2c_4 + c_1s_4) + s_1s_2s_5 \\ c_5(c_1c_2c_4 - s_1s_4) - c_1s_2s_5 \\ -s_2c_4c_5 - c_2s_5 \end{bmatrix}.
\end{aligned}$$

The space Jacobian can now be computed and written in matrix form as follows:

$$J_s(\theta) = \begin{bmatrix} \omega_1 & \omega_2 & 0 & \omega_4 & \omega_5 & \omega_6 \\ 0 & -\omega_2 \times q_2 & v_3 & -\omega_4 \times q_w & -\omega_5 \times q_w & -\omega_6 \times q_w \end{bmatrix}.$$

Although the resulting Jacobian is quite complicated, note that we were able to calculate the entire Jacobian without having to explicitly differentiate the forward kinematic map.

6.1.2 Body Jacobian

In the previous section we derived the relationship between the joint rates and $[\mathcal{V}_s] = \dot{T}T^{-1}$, the end-effector's spatial velocity expressed in fixed frame coordinates. Here we derive the relationship between the joint rates and $[\mathcal{V}_b] = T^{-1}\dot{T}$, the end-effector spatial velocity in end-effector frame coordinates. For this purpose it will be more convenient to express the forward kinematics in the alternate product of exponentials form:

$$T(q) = Me^{[\mathcal{B}_1]\theta_1}e^{[\mathcal{B}_2]\theta_2} \cdots e^{[\mathcal{B}_n]\theta_n}. \tag{6.10}$$

Computing $\dot{T}$,

$$\begin{aligned}
\dot{T} &= Me^{[\mathcal{B}_1]\theta_1} \cdots e^{[\mathcal{B}_{n-1}]\theta_{n-1}}(\frac{d}{dt}e^{[\mathcal{B}_n]\theta_n}) + Me^{[\mathcal{B}_1]\theta_1} \cdots (\frac{d}{dt}e^{[\mathcal{B}_{n-1}]\theta_{n-1}})e^{[\mathcal{B}_n]\theta_n} + \ldots \\
&= Me^{[\mathcal{B}_1]\theta_1} \cdots e^{[\mathcal{B}_n]\theta_n}[\mathcal{B}_n]\dot{\theta}_n + Me^{[\mathcal{B}_1]\theta_1} \cdots e^{[\mathcal{B}_{n-1}]\theta_{n-1}}[\mathcal{B}_{n-1}]e^{[\mathcal{B}_n]\theta_n}\dot{\theta}_{n-1} + \ldots \\
&\quad + Me^{[\mathcal{B}_1]\theta_1}[\mathcal{B}_1]e^{[\mathcal{B}_2]\theta_2} \cdots e^{[\mathcal{B}_n]\theta_n}\dot{\theta}_1.
\end{aligned}$$

Also,

$$T^{-1} = e^{-[\mathcal{B}_n]\theta_n} \cdots e^{-[\mathcal{B}_1]\theta_1} M^{-1}.$$

Multiplying T^{-1} and $\dot{T}$,

$$\begin{aligned}[\mathcal{V}_b] &= [\mathcal{B}_n]\dot{\theta}_n + e^{-[\mathcal{B}_n]\theta_n}[\mathcal{B}_{n-1}]e^{[\mathcal{B}_n]\theta_n}\dot{\theta}_{n-1} + \cdots \\ &\quad + e^{-[\mathcal{B}_n]\theta_n} \cdots e^{-[\mathcal{B}_2]\theta_2}[\mathcal{B}_1]e^{[\mathcal{B}_2]\theta_2} \cdots e^{[\mathcal{B}_n]\theta_n}\dot{\theta}_1,\end{aligned}$$

or in vector form,

$$\mathcal{V}_b = \mathcal{B}_n\dot{\theta}_n + \mathrm{Ad}_{e^{-[\mathcal{B}_n]\theta_n}}(\mathcal{B}_{n-1})\dot{\theta}_{n-1} + \ldots + \mathrm{Ad}_{e^{-[\mathcal{B}_n]\theta_n}\cdots e^{-[\mathcal{B}_2]\theta_2}}(\mathcal{B}_1)\dot{\theta}_1. \quad (6.11)$$

$\mathcal{V}_b$ can therefore be expressed as a sum of n spatial velocities, i.e.,

$$\mathcal{V}_b = \mathcal{V}_{b1}(\theta)\dot{\theta}_1 + \ldots + \mathcal{V}_{bn}(\theta)\dot{\theta}_n, \quad (6.12)$$

where each $\mathcal{V}_{bi}(\theta) = (\omega_{bi}(\theta), v_{bi}(\theta))$ depends explictly on the joint values θ. In matrix form,

$$\begin{aligned}\mathcal{V}_b &= \begin{bmatrix} \mathcal{V}_{b1}(\theta) & \mathcal{V}_{b2}(\theta) & \cdots & \mathcal{V}_{bn}(\theta) \end{bmatrix} \begin{bmatrix} \dot{\theta}_1 \\ \vdots \\ \dot{\theta}_n \end{bmatrix} \\ &= J_b(\theta)\dot{\theta}.\end{aligned} \quad (6.13)$$

The matrix $J_b(q)$ is the Jacobian in the end-effector (or **body**) frame coordinates, or more simply the **body Jacobian**.

Definition 6.2. Let the forward kinematics of an n-link open chain be expressed in the following product of exponentials form:

$$T = Me^{[\mathcal{B}_1]\theta_1} \cdots e^{[\mathcal{B}_n]\theta_n}. \quad (6.14)$$

The **body Jacobian** $J_b(\theta) \in \mathbb{R}^{6\times n}$ relates the joint rate vector $\dot{\theta} \in \mathbb{R}^n$ to the end-effector spatial velocity $\mathcal{V}_b = (\omega_b, v_b)$ via

$$\mathcal{V}_b = J_b(\theta)\dot{\theta}. \quad (6.15)$$

The i-th column of $J_b(\theta)$ is given by

$$\mathcal{V}_{b,i}(\theta) = \mathrm{Ad}_{e^{-[\mathcal{B}_n]\theta_n}\cdots e^{-[\mathcal{B}_{i+1}]\theta_{i+1}}}(\mathcal{B}_i), \quad (6.16)$$

for $i = n, n-1, \ldots, 2$, with $\mathcal{V}_{bn}(\theta) = \mathcal{B}_n$. □

Analogous to the columns of the space Jacobian, a similar physical interpretation can also be given to the columns of $J_b(\theta)$: each column $\mathcal{V}_{bi}(\theta) = (\omega_{bi}(\theta), v_{bi}(\theta))$ of $J_b(\theta)$ is the screw vector for joint axis i, expressed in coordinates of the end-effector frame rather than the fixed frame. The procedure for determining the columns of $J_b(\theta)$ is similar to the procedure for deriving the forward kinematics in the product of exponentials form $Me^{[\mathcal{B}_1]\theta_1} \cdots e^{[\mathcal{B}_n]\theta_n}$, the only difference being that each of the joint screws are derived for arbitrary θ rather than $\theta = 0$.

6.1.3 Relationship between the Space and Body Jacobian

If we denote the fixed frame by $\{s\}$, and the robot arm's end-effector frame by $\{b\}$, then the forward kinematics can be written $T_{sb}(\theta)$. The spatial velocity of the tip frame can be written in terms of the fixed and end-effector frame coordinates as

$$[\mathcal{V}_s] = \dot{T}_{sb}T_{sb}^{-1} \tag{6.17}$$
$$[\mathcal{V}_b] = T_{sb}^{-1}\dot{T}_{sb}, \tag{6.18}$$

with $\mathcal{V}_s$ and $\mathcal{V}_b$ related by $\mathcal{V}_s = \mathrm{Ad}_{T_{sb}}(\mathcal{V}_b)$. $\mathcal{V}_s$ and $\mathcal{V}_b$ are also related to their respective Jacobians via

$$\mathcal{V}_s = J_s(\theta)\dot{\theta} \tag{6.19}$$
$$\mathcal{V}_b = J_b(\theta)\dot{\theta}. \tag{6.20}$$

Equation (6.19) can therefore be written

$$\mathrm{Ad}_{T_{sb}}(\mathcal{V}_b) = J_s(\theta)\dot{\theta}. \tag{6.21}$$

Applying $\mathrm{Ad}_{T_{bs}}$ to both sides of (6.21), and using the general property $\mathrm{Ad}_M \cdot \mathrm{Ad}_N = \mathrm{Ad}_{MN}$ of the adjoint map, we obtain

$$\begin{aligned} \mathrm{Ad}_{T_{bs}}(\mathrm{Ad}_{T_{sb}}(\mathcal{V}_b)) &= \mathrm{Ad}_{T_{bs}T_{sb}}(\mathcal{V}_b) \\ &= \mathcal{V}_b \\ &= \mathrm{Ad}_{T_{bs}}\left(J_s(q)\dot{\theta}\right). \end{aligned}$$

Since we also have $\mathcal{V}_b = J_b(\theta)\dot{\theta}$ for all $\dot{\theta}$, it follows that $J_s(\theta)$ and $J_b(\theta)$ are related by

$$J_s(\theta) = \mathrm{Ad}_{T_{sb}}\left(J_b(\theta)\right). \tag{6.22}$$

Writing $\mathrm{Ad}_{T_{sb}}$ in 6×6 matrix form $[\mathrm{Ad}_{T_{sb}}]$, the above can also be expressed as

$$J_s(\theta) = [\mathrm{Ad}_{T_{sb}}]J_b(\theta). \tag{6.23}$$

The body Jacobian can in turn be obtained from the space Jacobian via

$$J_b(\theta) = Ad_{T_{bs}}\left(J_s(\theta)\right) = [\mathrm{Ad}_{T_{bs}}]J_s(\theta). \tag{6.24}$$

6.2 Statics of Open Chains

A rigid body is said to be in **static equilibrium** if it is motionless, and the resultant forces and moments applied to the body are all zero. Let us briefly review the notion of moments, by considering a force $\mathbf{f}$ acting on a rigid body. If the rigid body's center of mass does not lie on the line of action of the force, then the force will cause the rigid body to rotate; this rotation is caused by a moment. More precisely, the moment

*mbox***m** generated by **f** about some reference point **P** in physical space is defined to be the cross product

$$\vec{m} = \mathbf{r} \times \mathbf{f}, \tag{6.25}$$

where **r** is the vector from **P** to the point on the rigid body at which the force is applied. For a rigid body subject to a collection of forces and moments, if both the sum of the forces and sum of the moments are zero, then the body will be stationary, and is said to be in static equilibrium. When summing moments it is important that each of the moments be expressed with respect to the same reference point **P**.

A robot arm is said to be in static equilibrium if all of its links are in static equilibrium. In this section we shall examine, for robot arms that are in static equilibrium, the relationship between any external forces and moments applied at the end-effector, and the forces and torques experienced at each of the joints. Such a situation arises, for example, when a six degree-of-freedom arm is pushing against an immobile wall.

We first review spatial forces (also referred to as wrenches in the classical screw theory literature), which are obtained by merging forces and moments into a single six-dimensional quantity, much like spatial velocities are obtained by merging linear and angular velocities into a single six-dimensional vector. As we did for spatial velocities, we shall also examine how spatial forces transform under a change of reference frames.

We then review the principle of virtual work, but expressed in terms of spatial velocities and spatial forces. Applying the virtual work principle to a robot arm assumed to be in static equilibrium leads to our main result, which states that any external spatial forces applied at the end-effector frame are linearly related to the torques experienced at the joints.

6.2.1 Spatial Forces

Just as we found it advantageous to merge a moving frame's angular velocity $\omega \in \mathbb{R}^3$ with its linear velocity $v \in \mathbb{R}^3$ into a single six-dimensional spatial velocity $\mathcal{V} = (\omega, v)$, for the same reasons it will be useful to analogously define a six-dimensional **spatial force**, by merging a three-dimensional force vector $f \in \mathbb{R}^3$ with a three-dimensional moment vector $m \in \mathbb{R}^3$ as follows:

$$\mathcal{F} = \begin{bmatrix} m \\ f \end{bmatrix}, \tag{6.26}$$

which for notational convenience we will also write $\mathcal{F} = (m, f)$.

Let us find explicit expressions for the spatial force in terms of specific reference frames. For this purpose consider a rigid body with a moving (body) frame $\{b\}$ attached. Expressing everything in terms of the $\{b\}$ frame, let $f_b \in \mathbb{R}^3$ denote a force vector that is applied to a point p on the body. This force then generates a moment with respect to the $\{b\}$ frame origin; in $\{b\}$ frame coordinates, this moment is

$$m_b = r_b \times f_b, \tag{6.27}$$

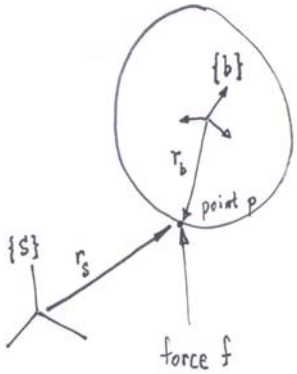

Figure 6.4: Relation between $\mathcal{F}_b$ and $\mathcal{F}_s$.

where $r_b \in \mathbb{R}^3$ is the vector from the $\{b\}$ frame origin to p. We shall pair the force f_b and moment m_b into a single six-dimensional spatial force $\mathcal{F}_b = (m_b, f_b)$, and refer to it as the **spatial force in body frame coordinates**.

Suppose we now wish to express the force and moment in terms of the fixed (space) frame $\{s\}$. Let $f_s \in \mathbb{R}^3$ denote the force vector being applied to point p of the rigid body, this time expressed in $\{s\}$ frame coordinates. The moment generated by this force with respect to the $\{s\}$ frame origin is, again in $\{s\}$ frame coordinates,

$$m_s = r_s \times f_s, \tag{6.28}$$

where $r_s \in \mathbb{R}^3$ is the vector from the $\{s\}$ frame origin to p. As we did for $\mathcal{F}_b$, let us also bundle f_s and m_s into the six-dimensional spatial force $\mathcal{F}_s = (m_s, f_s)$, and refer to it as the **spatial force in space frame coordinates**.

We now determine the relation between $\mathcal{F}_b = (m_b, f_b)$ and $\mathcal{F}_s = (m_s, f_s)$. Referring to Figure 6.4, denote the transformation T_{sb} by

$$T_{sb} = \begin{bmatrix} R_{sb} & p_{sb} \\ 0 & 1 \end{bmatrix}.$$

Pretty clearly $f_b = R_{bs} f_s$, which with the benefit of hindsight we shall write in the somewhat unconventional form

$$f_b = R_{sb}^T f_s. \tag{6.29}$$

The moment m_b is given by $r_b \times f_b$, where $r_b = R_{bs}(r_s - p_{sb})$; this follows from the fact that the $r_s - p_{sb}$ is expressed in $\{s\}$ frame coordinates, and must be transformed to $\{b\}$ frame coordinates via multiplication by R_{bs}. Again with hindsight, we shall write

$$r_b = R_{sb}^T (r_s - p_{sb}).$$

The moment $m_b = r_b \times f_b$ can now be written in terms of f_s and m_s as

$$\begin{array}{rcl} m_b & = & R_{sb}^T(r_s - p_{sb}) \times R_{sb}^T f_s \\ & = & [R_{sb}^T r_s] R_{sb}^T f_s - [R_{sb}^T p_{sb}] R_{sb}^T f_s \\ & = & R_{sb}^T [r_s] f_s - R_{sb}^T [p_{sb}] f_s \\ & = & R_{sb}^T m_s + R_{sb}^T [p_{sb}]^T f_s, \end{array} \tag{6.30}$$

where in the last line we make use of the fact that $[p_{sb}]^T = -[p_{sb}]$. Writing both m_b and f_b in terms of m_s and f_s, we have, from Equations (6.29) and (6.30),

$$\begin{bmatrix} m_b \\ f_b \end{bmatrix} = \begin{bmatrix} R_{sb} & 0 \\ [p_{sb}]\, R_{sb} & R_{sb} \end{bmatrix}^T \begin{bmatrix} m_s \\ f_s \end{bmatrix}, \tag{6.31}$$

or in terms of spatial forces and the adjoint map,

$$\mathcal{F}_b = \mathrm{Ad}_{T_{sb}}^T(\mathcal{F}_s) = [\mathrm{Ad}_{T_{sb}}]^T \mathcal{F}_s. \tag{6.32}$$

We see that under a change of reference frames, spatial velocities transform under the adjoint map, whereas spatial forces transform under the adjoint transpose map. In fact, the introduction of the rigid body is superfluous; the above relation holds for all spatial forces described in terms of two different reference frames. The following proposition formally states this result.

Proposition 6.1. *Given a force* $\mathbf{f}$*, let* $\mathbf{m}$ *be the moment generated by* $\mathbf{f}$ *with respect to some point* $\mathbf{P}$ *in physical space. Given a reference frame* $\{a\}$*, let* $f_a \in \mathbb{R}^3$ *and* $m_a = r_a \times f_a \in \mathbb{R}^3$ *be representations of* $\mathbf{f}$ *and* $\mathbf{m}$ *in frame* $\{a\}$ *coordinates, where* $r_a \in \mathbb{R}^3$ *is the vector from the* $\{a\}$ *frame origin to p, also expressed in* $\{a\}$ *frame coordinates. Similarly, given another reference frame* $\{b\}$*, let* $f_b \in \mathbb{R}^3$ *and* $m_b = r_b \times f_b \in \mathbb{R}^3$ *be representations of* $\mathbf{f}$ *and* $\mathbf{m}$ *frame* $\{b\}$ *coordinates, where* $r_b \in \mathbb{R}^3$ *is the vector from the* $\{b\}$ *frame origin to p, also expressed in* $\{b\}$ *frame coordinates. Defining the spatial forces* $\mathcal{F}_a = (r_a \times f_a, f_a)$ *and* $\mathcal{F}_b = (r_b \times f_b, f_b)$*,* $\mathcal{F}_a$ *and* $\mathcal{F}_b$ *are related by*

$$\mathcal{F}_b = Ad_{T_{ab}}^T(\mathcal{F}_a) = [Ad_{T_{ab}}]^T \mathcal{F}_a \tag{6.33}$$

$$\mathcal{F}_a = Ad_{T_{ba}}^T(\mathcal{F}_b) = [Ad_{T_{ba}}]^T \mathcal{F}_b. \tag{6.34}$$

6.2.2 Static Analysis and the Virtual Work Principle

When a robot arm is in static equilibrium, it turns out that the Jacobian of the forward kinematics also relates any external forces and torques applied at the end-effector to the torques experienced at each of the joints. This can be shown by appealing to the **Principle of Virtual Work**, which we now describe. Fix a reference frame, and consider a rigid body moving with velocity v and angular velocity ω, and subject to a resultant force f and resultant moment m. The work done by the rigid body over some time interval $[t_0, t_1]$ is given by the integral

$$\text{Work} = \int_{t_0}^{t_1} f^T v + m^T \omega \, dt \tag{6.35}$$

In terms of spatial forces and velocities, (6.35) can also be expressed as

$$\text{Work} = \int_{t_0}^{t_1} \mathcal{F}^T \mathcal{V}\, dt, \tag{6.36}$$

where $\mathcal{F} = (m, f)$ and $\mathcal{V} = (\omega, v)$. The work of a system of rigid bodies is simply the sum of the work done by each of the rigid bodies.

For a single rigid body, suppose that the resultant force and moment are applied to the body over an infinitesimal time interval δt, resulting in an infinitesimally small displacement of the body. If the body is in static equilibrium, the body is stationary and thus will produce no work. This infinitesimal displacement over δt can still be thought of as a virtual displacement. The virtual work principle states that under static equilibrium, the work of any external forces and moments acting on a rigid body is always zero for any admissible virtual displacement of the body. This principle also extends to robot arms, and more generally to any system of connected rigid bodies: for any admissible virtual displacement of the system (i.e., one that does not violate any kinematic constraints), the total virtual work of the external forces and moments acting on the system is zero.

Now consider an n-link robot arm assumed to be in static equilibrium, and suppose a force and moment are applied to the tip. For now all quantities are defined in terms of the end-effector (body) frame: let $\mathcal{F}_b = (m_b, f_b)$ be an external spatial force applied over some infinitesimal time interval $[t_0, t_0 + \delta t]$, and $\mathcal{V}_b = (\omega_b, v_b)$ be the (instantaneous) spatial velocity of the end-effector. The net virtual work done by the robot is given by Equation (6.35). Assuming the robot is lossless, from the virtual work principle this infinitesimal work should be the same as that produced by any torques applied at the joints:

$$\text{Virtual Work} = \int_{t_0}^{t_0+\delta t} \mathcal{F}_b^T \mathcal{V}_b\, dt = \int_{t_0}^{t_0+\delta t} \tau^T \dot{\theta}\, dt,$$

where $\dot{\theta} \in \mathbb{R}^n$ is the vector of joint velocities, and $\tau \in \mathbb{R}^n$ is the vector of joint torques. Since $\mathcal{V}_b = J_b(\theta)\dot{\theta}$, we have

$$\int_{t_0}^{t_0+\delta t} F_b^T J_b(\theta)\dot{\theta}\, dt = \int_{t_0}^{t_0+\delta t} \tau^T \dot{\theta}\, dt.$$

Since this equality must hold over all intervals $[t_0, t_0 + \delta t]$, the integrands must be equal:

$$\mathcal{F}_b^T J_b(\theta)\dot{\theta} = \tau^T \dot{\theta}.$$

Moreover, since the above equality must hold for all admissible virtual displacements $\dot{\theta}\, \delta t$—in this case $\dot{\theta}$ can be arbitrary—it follows that

$$\tau = J_b^T(\theta)\mathcal{F}_b. \tag{6.37}$$

Let us replicate the derivation of $\tau = J_b^T(\theta)\mathcal{F}_b$, but this time expressing all quantities in terms of the fixed (space) frame. Let $\mathcal{V}_s = (\omega_s, v_s)$ denote the

spatial velocity of the end-effector, and $\mathcal{F}_s = (m_s, f_s)$ the spatial force applied at the end-effector frame origin, all expressed in fixed frame coordinates. Here f_s is the external applied force expressed in fixed frame coordinates, while m_s is the external applied moment about the fixed frame origin. Recalling from the earlier section on spatial forces that $\mathcal{F}_b$ and $\mathcal{F}_s$ are related by $\mathcal{F}_b = [\mathrm{Ad}_{T_sb}]^T \mathcal{F}_s$, and that $J_b(\theta)$ and $J_s(\theta)$ are further related by $J_b(\theta) = [\mathrm{Ad}_{T_{bs}}] J_s(\theta)$, Equation (6.37) can be rewritten

$$\begin{aligned} \tau &= J_b^T(\theta)\mathcal{F}_b = \left([\mathrm{Ad}_{T_{bs}}] J_s(\theta)\right)^T [\mathrm{Ad}_{T_sb}]^T \mathcal{F}_s \\ &= J_s^T(\theta) \left([\mathrm{Ad}_{T_sb}][Ad_{T_{bs}}]\right)^T \mathcal{F}_s \\ &= J_s^T(\theta)\mathcal{F}_s. \end{aligned} \tag{6.38}$$

We can therefore write the statics relation in the general form

$$\tau = J^T(\theta)\mathcal{F}, \tag{6.39}$$

with the understanding that $J(\theta)$ and $\mathcal{F}$ are expressed in terms of the same frame. Often in robotics one is interested in determining what joint torques are necessary, under static equilibrium assumptions, to produce a given desired $\mathcal{F}$; the static relation provides an explicit answer to this question.

One could also ask the opposite question, namely, what is the spatial force at the tip generated by a given joint torque? If J^T is a square invertible matrix, then clearly $\mathcal{F} = J^{-T}(\theta)\tau$. However, if the dimension of the joint vector n is greater than the dimension of $\mathcal{F}$ (six), then the inverse of J^T does not exist. What this implies physically is that the robot arm has extra degrees of freedom. Because of the extra degrees of freedom, some of the robot's links can move even when the end-effector is fixed (for example, the planar four-bar linkage can be regarded as a $3R$ planar open chain with its tip fixed to the base joint). Internal motions are generated as a result of the applied joint torques, and the static equilibrium condition is no longer satisfied. Robots whose joint degrees of freedom exceed the dimension of its task space are called **kinematically redundant**; in the next chapter we shall examine the inverse kinematics of kinematically redundant robot arms.

6.3 Singularities

The forward kinematics Jacobian also allows us to identify postures at which the robot's end-effector loses the ability to move instantaneously in a certain direction, or rotate instantaneously about certain axes; such a posture is called a **kinematic singularity**, or simply a **singularity**. Mathematically a singular posture of a robot arm is one in which the Jacobian loses rank. To understand why, consider the body Jacobian $J_b(\theta)$, whose columns are denoted $\mathcal{V}_{bi}$, $i =$

$1, \ldots, n$. Then

$$\begin{aligned} \mathcal{V}_b &= \left[\begin{array}{cccc} \mathcal{V}_{b1}(\theta) & \mathcal{V}_{b2}(\theta) & \cdots & \mathcal{V}_{bn}(\theta) \end{array} \right] \left[\begin{array}{c} \dot{\theta}_1 \\ \vdots \\ \dot{\theta}_n \end{array} \right] \\ &= \mathcal{V}_{b1}(\theta)\dot{\theta}_1 + \ldots + \mathcal{V}_{bn}(\theta)\dot{\theta}_n. \end{aligned}$$

Thus, the set of all possible instantaneous spatial velocities of the tip frame is given by a linear combination of the $\mathcal{V}_{bi}$. As long as $n \geq 6$, the maximum rank that $J_b(\theta)$ can attain is six. Singular postures correspond to those values of θ at which the rank of $J_b(\theta)$ drops below six; at such postures the tip frame loses to the ability to generate instantaneous spatial velocities in in one or more dimensions.

The mathematical definition of a kinematic singularity is independent of the choice of body or space Jacobian. To see why, recall the relationship between $J_s(\theta)$ and $J_b(\theta)$: $J_s(q) = [Ad_{T_{sb}}(J_b(\theta)) = [\mathrm{Ad}_{T_{sb}}]J_b(\theta)$, or more explicitly,

$$J_s(\theta) = \left[\begin{array}{cc} R_{sb} & 0 \\ [p_{sb}]\, R_{sb} & R_{sb} \end{array} \right] J_b(\theta).$$

Then the rank of $J_s(\theta)$ is equal to the rank of $[\mathrm{Ad}_{T_{sb}}]J_b(\theta)$. We now claim that the matrix $[\mathrm{Ad}_{T_{sb}}]$ is always invertible. This can be established by examining the linear equation

$$\left[\begin{array}{cc} R_{sb} & 0 \\ [p_{sb}]\, R_{sb} & R_{sb} \end{array} \right] \left[\begin{array}{c} x \\ y \end{array} \right] = 0.$$

Its unique solution is $x = y = 0$, implying that the matrix $[\mathrm{Ad}_{T_{sb}}]$ is invertible. Since multiplying any matrix by an invertible matrix does not change its rank, it follows that

$$\text{rank } J_s(\theta) = \text{rank } J_b(\theta),$$

as claimed; singularities of the space and body Jacobian are the one and the same.

Kinematic singularities are also independent of the choice of fixed frame. In some sense this is rather obvious—choosing a different fixed frame is equivalent to simply relocating the robot arm, which should have absolutely no effect on whether a particular posture is singular or not. This obvious fact can be verified by referring to Figure 6.5-(a). The forward kinematics with respect to the original fixed frame is denoted $T(\theta)$, while the forward kinematics with respect to the relocated fixed frame is denoted $T'(\theta) = PT(\theta)$, where $P \in SE(3)$ is constant. Then the body Jacobian of $T'(\theta)$, denoted $J'_b(\theta)$, is obtained from $T'^{-1}\dot{T}'$. A simple calculation reveals that

$$T'^{-1}\dot{T}' = (T^{-1}P^{-1})(P\dot{T}) = T^{-1}\dot{T},$$

i.e., $J'_b(\theta) = J_b(\theta)$, so that the singularities of the original and relocated robot arms are the same.

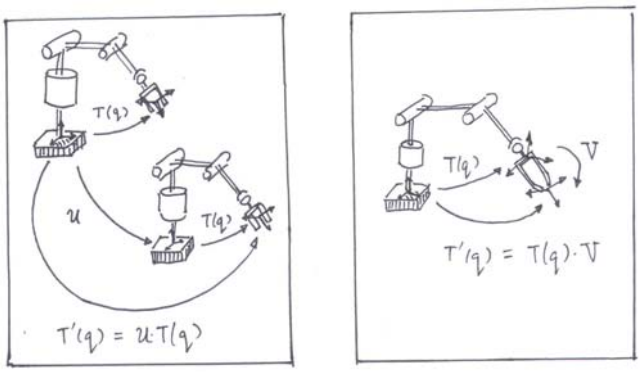

Figure 6.5: Kinematic singularities are invariant with respect to choice of fixed and end-effector frames. (a) Choosing a different fixed frame, which is equivalent to relocating the base of the robot arm; (b) Choosing a different end-effector frame.

Somewhat less obvious is the fact that kinematic singularities are also independent of the choice of end-effector frame. Referring to Figure 6.5-(b), suppose the forward kinematics for the original end-effector frame is given by $T(\theta)$, while the forward kinematics for the relocated end-effector frame is $T'(\theta) = T(\theta)Q$, where $Q \in SE(3)$ is constant. This time looking at the space Jacobian—recall that singularities of $J_b(\theta)$ coincide with those of $J_s(\theta)$—let $J'_s(\theta)$ denote the space Jacobian of $T'(\theta)$. A simple calculation reveals that

$$\dot{T}'T'^{-1} = (\dot{T}Q)(Q^{-1}T^{-1}) = \dot{T}T^{-1},$$

i.e., $J'_s(\theta) = J_s(\theta)$, so that kinematic singularities are invariant with respect to choice of end-effector frame.

In the remainder of this section we shall consider some common kinematic singularities that occur in six degree of freedom open chains with revolute and prismatic joints. We now know that either the space or body Jacobian can be used for our analysis; we shall use the space Jacobian in the examples below.

Case I: Two Collinear Revolute Joint Axes

The first case we consider is one in which two revolute joint axes are collinear (see Figure 6.6). Without loss of generality these joint axes can be labelled 1 and 2. The corresponding columns of the Jacobian are

$$\mathcal{V}_{s1}(\theta) = \begin{bmatrix} \omega_1 \\ -\omega_1 \times q_1 \end{bmatrix}, \quad \mathcal{V}_{s2}(\theta) = \begin{bmatrix} \omega_2 \\ -\omega_2 \times q_2 \end{bmatrix}$$

Since the two joint axes are collinear, we must have $\omega_1 = \pm\omega_2$; let us assume the positive sign. Also, $\omega_i \times (q_1 - q_2) = 0$ for $i = 1, 2$. Then $\mathcal{V}_{s1} - \mathcal{V}_{s2} = 0$, which implies that $\mathcal{V}_{s1}$ and $\mathcal{V}_{s2}$ lie on the same line in six-dimensional space.

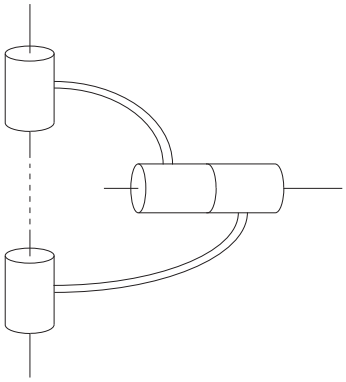

Figure 6.6: A kinematic singularity in which two joint axes are collinear.

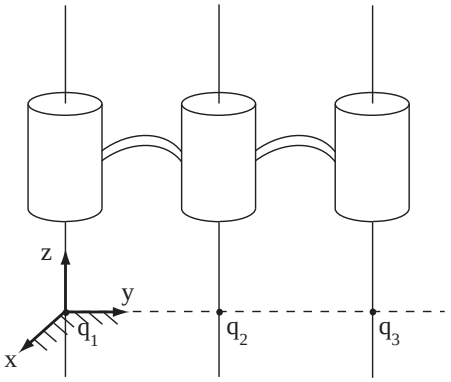

Figure 6.7: A kinematic singularity in which three revolute joint axes are parallel and coplanar.

Therefore, the set $\{\mathcal{V}_{s1}, \mathcal{V}_{s2}, \ldots, \mathcal{V}_{s6}\}$ cannot be linearly independent, and the rank of $J_s(\theta)$ must be less than six.

Case II: Three Coplanar and Parallel Revolute Joint Axes

The second case we consider is one in which three revolute joint axes are parallel, and also lie on the same plane (three coplanar axes—see Figure 6.7). Without loss of generality we label these as joint axes 1, 2, and 3. In this case we choose the fixed frame as shown in the figure; then

$$J_s(\theta) = \begin{bmatrix} \omega_1 & \omega_1 & \omega_1 & \cdots \\ 0 & -\omega_1 \times q_2 & -\omega_1 \times q_3 & \cdots \end{bmatrix}$$

and since q_2 and q_3 are points on the same unit axis, it is not difficult to verify that the above three vectors cannot be linearly independent.

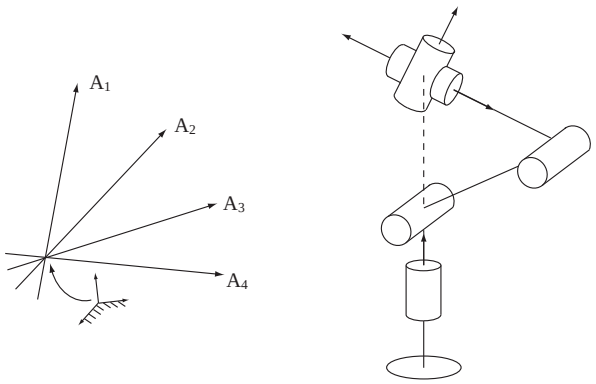

Figure 6.8: A kinematic singularity in which four revolute joint axes intersect at a common point.

Case III: Four Revolute Joint Axes Intersecting at a Common Point

Here we consider the case where four revolute joint axes intersect at a common point (Figure 6.8). Again, without loss of generality label these axes from 1 to 4. In this case we choose the fixed frame origin to be the common point of intersection, so that $q_1 = \ldots = q_4 = 0$. In this case

$$J_s(\theta) = \begin{bmatrix} \omega_1 & \omega_2 & \omega_3 & \omega_4 & \cdots \\ 0 & 0 & 0 & 0 & \cdots \end{bmatrix}.$$

The first four columns clearly cannot be linearly independent; one can be written as a linear combination of the other three. Such a singularity occurs, for example, when the wrist center of an elbow-type robot arm is directly above the shoulder.

Case IV: Four Coplanar Revolute Joints

Here we consider the case in which four revolute joint axes are coplanar. Again, without loss of generality label these axes from 1 to 4. Choose a fixed frame such that the joint axes all lie on the x-y plane; in this case the unit vector $\omega_i \in \mathbb{R}^3$ in the direction of joint axis i is of the form

$$\omega_i = \begin{bmatrix} \omega_{ix} \\ \omega_{iy} \\ 0 \end{bmatrix}.$$

Similarly, any reference point $q_i \in \mathbb{R}^3$ lying on joint axis i is of the form

$$q_i = \begin{bmatrix} q_{ix} \\ q_{iy} \\ 0 \end{bmatrix},$$

and subsequently

$$v_i = -\omega_i \times q_i = \begin{bmatrix} 0 \\ 0 \\ \omega_{iy} q_{ix} - \omega_{ix} q_{iy} \end{bmatrix}.$$

The first four columns of the space Jacobian $J_s(\theta)$ are

$$\begin{bmatrix} \omega_{1x} & \omega_{2x} & \omega_{3x} & \omega_{4x} \\ \omega_{1y} & \omega_{2y} & \omega_{3y} & \omega_{4y} \\ 0 & 0 & 0 & 0 \\ 0 & 0 & 0 & 0 \\ 0 & 0 & 0 & 0 \\ \omega_{1y} q_{1x} - \omega_{1x} q_{1y} & \omega_{2y} q_{2x} - \omega_{2x} q_{2y} & \omega_{3y} q_{3x} - \omega_{3x} q_{3y} & \omega_{4y} q_{4x} - \omega_{4x} q_{4y} \end{bmatrix}.$$

which clearly cannot be linearly independent.

Case V: Six Revolute Joints Intersecting a Common Line

The final case we consider is six revolute joint axes intersecting a common line. Choose a fixed frame such that the common line lies along the $\hat{z}$-axis, and select the intersection between this common line and joint axis i as the reference point $q_i \in \mathbb{R}^3$ for axis i; each q_i is thus of the form $q_i = (0, 0, q_{iz})$, and

$$v_i = -\omega_i \times q_i = (\omega_{iy} q_{iz}, -\omega_{ix} q_{iz}, 0)$$

$i = 1, \ldots, 6$. The space Jacobian $J_s(\theta)$ thus becomes

$$J_s(\theta) = \begin{bmatrix} \omega_{1x} & \omega_{2x} & \omega_{3x} & \omega_{4x} & \omega_{5x} & \omega_{6x} \\ \omega_{1y} & \omega_{2y} & \omega_{3y} & \omega_{4y} & \omega_{5y} & \omega_{6y} \\ \omega_{1z} & \omega_{2z} & \omega_{3z} & \omega_{4z} & \omega_{5z} & \omega_{6z} \\ \omega_{1y} q_{1z} & \omega_{2y} q_{2z} & \omega_{3y} q_{3z} & \omega_{4y} q_{4z} & \omega_{5y} q_{5z} & \omega_{6y} q_{6z} \\ -\omega_{1x} q_{1z} & -\omega_{2x} q_{2z} & -\omega_{3x} q_{3z} & -\omega_{4x} q_{4z} & -\omega_{5x} q_{5z} & -\omega_{6x} q_{6z} \\ 0 & 0 & 0 & 0 & 0 & 0 \end{bmatrix},$$

which is clearly singular.

6.4 Manipulability

In the previous section we saw that at a kinematic singularity, a robot's end-effector loses the ability to move or rotate in one or more directions. A kinematic singularity is a binary proposition—a particular configuration is either kinematically singular, or it isn't—and it is reasonable to ask whether it is possible to quantify the proximity of a particular configuration to a singularity. The answer is yes; in fact, one can even do better and quantify not only the proximity to a singularity, but also determine the directions in which the end-effector's ability to move is diminished, and to what extent. The **manipulabiity ellipsoid** allows one to geometrically visualize the directions in which the end-effector can

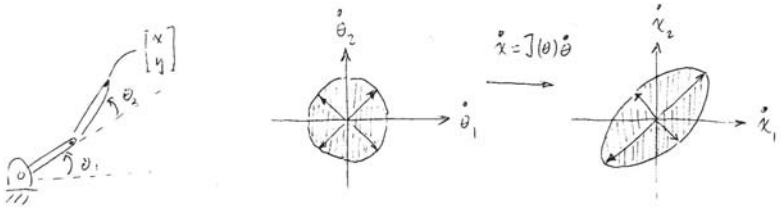

Figure 6.9: The manipulability ellipsoid for a planar $2R$ open chain.

move with the least "effort" (in a sense to be made precise below); directions that are orthogonal to these directions in contrast require the greatest effort.

We illustrate the notion of manipulability ellipsoids through the planar $2R$ open chain example of Figure 6.9. Considering only the Cartesian position of the tip, the velocity forward kinematics is of the form $\dot{x} = J(\theta), \dot{\theta}$:

$$\begin{bmatrix} \dot{x}_1 \\ \dot{x}_2 \end{bmatrix} = \begin{bmatrix} L_1 \cos\theta_1 & L_1 \cos\theta_1 + L_2 \cos(\theta_1 + \theta_2) \\ L_1 \sin\theta_1 & L_1 \sin\theta_1 + L_2 \sin(\theta_1 + \theta_2) \end{bmatrix} \begin{bmatrix} \dot{\theta}_1 \\ \dot{\theta}_2 \end{bmatrix}. \tag{6.40}$$

Suppose the configuration θ is nonsingular, so that $J(\theta)$ is invertible. Since $J(\theta)$ is a linear transformation that maps joint velocities to tip velocities, one can conjecture that a unit circle in the space of joint velocities maps to an ellipsoid in the space of tip velocities. To see why, the unit circle is parametrized by the constraint $\|\dot{\theta}\|^2 = 1$; the same constraint expressed in terms of tip velocities is $\|J^{-1}(\theta)\dot{x}\|^2 = 1$. Denoting the elements of $J^{-1}(\theta)$ by

$$J^{-1}(\theta) = \begin{bmatrix} a & b \\ c & d \end{bmatrix},$$

the constraint on tip velocities becomes

$$\alpha\dot{x}_1^2 + \beta\dot{x}_1\dot{x}_2 + \gamma\dot{x}_2^2 = 1,$$

where $\alpha = a^2 + b^2$, $\beta = 2(ab + cd)$, $\gamma = b^2 + d^2$. As is well known this is the equation for an ellipse centered at the origin (provided $\beta^2 - 4\alpha\gamma < 0$, which it is).

The major axes of the ellipse indicate the directions in which the tip can move (or more technically, generate velocities) with the least amount of effort (effort here corresponding to input velocities). By the same reasoning, the minor axes indicate the directions of motion for which the greatest amount of effort is required. As the arm configuration approaches a kinematic singularity, the ellipsoid eventually collapses to a line directed along the direction of allowable motion. The proximity of a particular configuration to a singularity can be measured in several ways, e.g., by the ratio of the lengths between the major and minor axes, with a minimum value of 1 indicating that the tip can move uniformly easily in all directions—such configurations are also sometimes referred

to as **isotropic** configurations. In the absence of any preferred directions of the end-effector, such an isotropic configuration would be a reasonable choice for a robot performing generic tasks.

The above formulation can be generalized to spatial open chains more or less straightforwardly; without working out the details of the derivation (which require some further results from linear algebra and finite dimensional optimization—some of these details are examined in the exercises), we now formulate the manipulability ellipsoid for an n degree of freedom open chain ($n \geq 6$). Let $J_b(\theta) \in \mathbb{R}^{6\times n}$ be the body Jacobian (the choice of body Jacobian is arbitrary—the space Jacobian could just as easily have been chosen), which can be partitioned into its angular and linear velocity components $J_\omega(\theta) \in \mathbb{R}^{3\times n}$ and $J_v(\theta) \in \mathbb{R}^{3\times n}$ as follows:

$$\omega_b = J_\omega(\theta)\dot{\theta} \tag{6.41}$$

$$v_b = J_v(\theta)\dot{\theta}. \tag{6.42}$$

At this point one may ask why we choose to partition the Jacobian in this way. The reason is that the notion of a manipulability ellipsoid in the six-dimensioal space of spatial velocities (ω, v) makes little if any sense—the physical units for angular velocities are different from those for linear velocities. Any ellipsoid that merges these physically different quantities will depend, ultimately, on the choice of length scale for physical space, which as is well known is arbitrary. On the other hand, ellipsoids restricted to the space of Cartesian velocities $v_b \in \mathbb{R}^3$ are quite meaningful (as are its counterpart ellipsoids restricted to the space of angular velocities $\omega \in \mathbb{R}^3$).

We now formulate the Cartesian velocity manipulability ellipsoid associated with $J_v(\theta)$; the angular velocity manipulability ellipsoid can be formulated in an identical fashion. Assuming $J_v(\theta)$ is nonsingular at the configuration θ, $J_v(\theta)$ then maps a unit sphere in $\mathbb{R}^n$, parametrized as $\|\dot{\theta}\|^2 = 1$, to a three-dimensional ellipsoid in $\mathbb{R}^3$. The principal axes of this ellipsoid can be obtained as the eigenvectors of $J_v J_v^T \in \mathbb{R}^{3\times 3}$, with the length of each principal axis given by the corresponding eigenvalue.

A three-dimensional ellipsoid can also be drawn in the space of joint velocities as follows. First, observe that $J_v^T J_v$ is $n \times n$, but with rank 3 (as a result of our assumption that $J_v(\theta)$ is of maximal rank 3). Consequently only three of its eigenvalues are nonzero; they are, in fact, the three eigenvalues of $J_v J_v^T$. The three eigenvectors corresponding to these nonzero eigenvalues are then precisely the joint velocity vectors that map to the three principal axes of the ellipsoid in the space of Cartesian velocities.

In the absence of any preferred directions of the end-effector, one can argue that an ellipsoid that most closely resembles a sphere is the most desirable. Configurations in which the ellipsoid is spherical are called isotropic configurations, and are marked by the eigenvalues—which are proportional to the lengths of the ellipsoid's principal axes—having identical value.

6.5 Summary

- Let the forward kinematics of an n-link open chain be expressed in the following product of exponentials form:

$$T = e^{[\mathcal{S}_1]\theta_1} \cdots e^{[\mathcal{S}_n]\theta_n} M.$$

The **space Jacobian** $J_s(\theta) \in \mathbb{R}^{6\times n}$ relates the joint rate vector $\dot{\theta} \in \mathbb{R}^n$ to the end-effector spatial velocity $\mathcal{V}_s$ via $\mathcal{V}_s = J_s(\theta)\dot{\theta}$. The i-th column of $J_s(\theta)$ is

$$\mathcal{V}_{si}(\theta) = Ad_{e^{[\mathcal{S}_1]\theta_1 \cdots e^{[\mathcal{S}_{i-1}]\theta_{i-1}}}}(\mathcal{S}_i), \tag{6.43}$$

for $i = 2, \ldots, n$, with the first column $\mathcal{V}_{s1}(\theta) = \mathcal{S}_1$. $\mathcal{V}_{si}$ is the screw vector for joint i expressed in space frame coordinates, with the joint values θ assumed to be arbitrary rather than zero.

- Let the forward kinematics of an n-link open chain be expressed in the following product of exponentials form:

$$T = Me^{[\mathcal{B}_1]\theta_1} \cdots e^{[\mathcal{B}_n]\theta_n}. \tag{6.44}$$

The **body Jacobian** $J_b(\theta) \in \mathbb{R}^{6\times n}$ relates the joint rate vector $\dot{\theta} \in \mathbb{R}^n$ to the end-effector spatial velocity $\mathcal{V}_b = (\omega_b, v_b)$ via

$$\mathcal{V}_b = J_b(\theta)\dot{\theta}. \tag{6.45}$$

The i-th column of $J_b(\theta)$ is given by

$$\mathcal{V}_{b,i}(\theta) = \mathrm{Ad}_{e^{-[\mathcal{B}_n]\theta_n \cdots e^{-[\mathcal{B}_{i+1}]\theta_{i+1}}}}(\mathcal{B}_i), \tag{6.46}$$

for $i = n, n-1, \ldots, 2$, with $\mathcal{V}_{bn}(\theta) = \mathcal{B}_n$. $\mathcal{V}_{bi}$ is the screw vector for joint i expressed in body frame coordinates, with the joint values θ assumed to be arbitrary rather than zero. The body Jacobian is related to the space Jacobian via the relation

$$\begin{aligned} J_s(\theta) &= [\mathrm{Ad}_T sb] J_b(\theta) \\ J_b(\theta) &= [\mathrm{Ad}_T bs] J_s(\theta) \end{aligned}$$

where $T_{sb} = T$.

- Consider a force $\mathbf{f}$ applied to some point p on a rigid body. The moment $\mathbf{m}$ generated by $\mathbf{f}$ with respect to the $\{s\}$ frame origin is $\mathbf{m} = \mathbf{r} \times \mathbf{f}$, where $\mathbf{r}$ is the vector from p to the $\{s\}$ frame origin. Let $m_s \in \mathbb{R}^3$ and $f_s \in \mathbb{R}^3$ be vector representations of $\mathbf{m}$ and $\mathbf{f}$ in $\{s\}$ frame coordinates. The **spatial force in space coordinates** $\mathcal{F}_s \in \mathbb{R}^6$ is defined to be $\mathcal{F}_s = (m_s, f_s)$.

- Consider a rigid body with a body frame $\{b\}$ attached, and a force $\mathbf{f}$ applied to some point p on the rigid body. The moment $\mathbf{m}$ generated by $\mathbf{f}$ with respect to the $\{b\}$ frame origin is then $\mathbf{m} = \mathbf{r} \times \mathbf{f}$, where $\mathbf{r}$ is now

the vector from p to the $\{b\}$ frame origin. Let $m_b \in \mathbb{R}^3$ and $f_b \in \mathbb{R}^3$ be vector representations of $\mathbf{m}$ and $\mathbf{f}$ in $\{b\}$ frame coordinates. The **spatial force in body coordinates** $\mathcal{F}_b \in \mathbb{R}^6$ is defined to be $\mathcal{F}_b = (m_b, f_b)$. $\mathcal{F}_b$ and $\mathcal{F}_s$ are related by

$$\begin{aligned} \mathcal{F}_b &= \mathrm{Ad}^T_{T_{sb}}(\mathcal{F}_s) = [\mathrm{Ad}_{T_{sb}}]^T \mathcal{F}_s \\ \mathcal{F}_s &= \mathrm{Ad}^T_{T_{bs}}(\mathcal{F}_b) = [\mathrm{Ad}_{T_{bs}}]^T \mathcal{F}_b. \end{aligned}$$

- Consider a spatial open chain with n one degree of freedom joints that is also assumed to be in static equilibrium. Let $\tau \in \mathbb{R}^n$ denote the vector of joint torques and forces, and $\mathcal{F} \in \mathbb{R}^6$ be the spatial force applied at the end-effector, in either space or body frame coordinates. Then τ and $\mathcal{F}$ are related by
$$\tau = J_b^T(\theta)\mathcal{F}_b = J_s^T(\theta)\mathcal{F}_s.$$

- A kinematically singular configuration for an open chain, or more simply a **kinematic singularity**, is any configuration $\theta \in \mathbb{R}^n$ at which the rank of the Jacobian (either $J_s(\theta)$ or $J_b(\theta)$) is not maximal. For spatial open chains of mobility six consisting of revolute and prismatic joints, some common singularities include (i) two collinear revolute joint axes; (ii) three coplanar and parallel revolute joint axes; (iii) four revolute joint axes intersecting at a common point; (iv) four coplanar revolute joints, and (v) six revolute joints intersecting a common line.

6.6 Notes and References

The terms spatial velocity and spatial force were first coined by Roy Featherstone [**?**], and are also referred to in the literature as twists and wrenches, respectively. There is a well developed calculus of twists and wrenches that is covered in treatments of classical screw theory, e.g., [**?**], [**?**]. Singularities of closed chains are discussed in the later chapter on closed chain kinematics. Manipulability ellipsoids and their dual, force ellipsoids, are discussed in greater detail in [**?**].

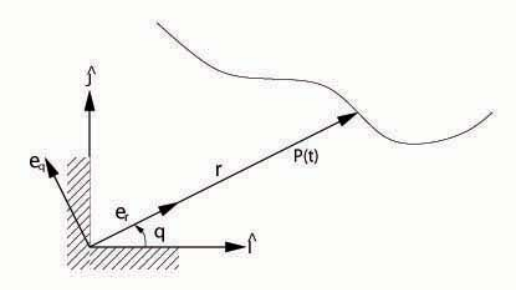

Figure 6.10: Polar coordinates.

6.7 Exercises

1. Given a particle moving in the plane, define a moving reference frame $\{\hat{e}_r, \hat{e}_\theta\}$ such that its origin is fixed to the origin of the fixed frame, and its $\hat{e}_r$ axis always points toward the particle (Figure 6.10). Let (r, θ) be the polar coordinates for the particle position, i.e., r is the distance of the particle from the origin, and θ is the angle from the horizontal line to the $\hat{e}_r$ axis. The particle position $\vec{p}$ can then be written

$$\vec{p} = r\hat{e}_r,$$

and its velocity $\vec{v}$ is given by

$$\vec{v} = \dot{r}\hat{e}_r + r\dot{\hat{e}}_r.$$

The acceleration $\vec{v}$ is the time derivative of $\vec{v}$.
(a) Express $\dot{\hat{e}}_r$ in terms of $\hat{e}_r$ and $\hat{e}_\theta$.
(b) Show that $\vec{v}$ and $\vec{a}$ are given by

$$\begin{aligned} \vec{v} &= \dot{r}\hat{e}_r + r\dot{\theta}\hat{e}_\theta \\ \vec{a} &= (\ddot{r} - r\dot{\theta}^2)\hat{e}_r + (r\ddot{\theta} + 2\dot{r}\dot{\theta})\hat{e}_\theta. \end{aligned}$$

2. Let $\{\hat{I}, \hat{J}\}$ denote the unit axes of the fixed frame, and let

$$\vec{p} = X(t)\hat{I} + Y(t)\hat{J}$$

denote the position of a particle moving in the plane (see Figure 6.11). Suppose the path traced by the particle has nonzero curvature everywhere, so that for every point on the path there exists some circle tangent to the path; the center of this circle is called the **center of curvature**, while its radius is the **radius of curvature**. Clearly both the center and radius of curvature vary along the path, and are well-defined only at points of nonzero curvature (or, at points where the curvature is zero, the center of curvature can be regarded to lie at infinity).

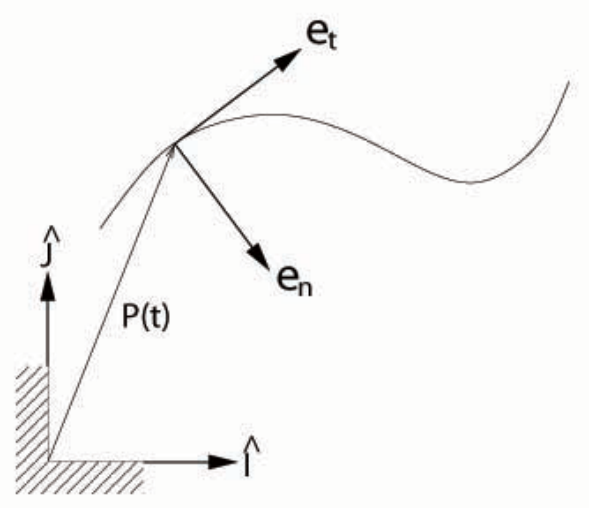

Figure 6.11: Tangential-normal coordinates.

Now attach a moving reference frame $\{\hat{e}_t, \hat{e}_n\}$ to the particle, in such a way that that $\hat{e}_t$ always points in the same direction as the velocity vector; $\hat{e}_n$ then points toward the center of curvature. Since the speed of the particle is given by

$$v = \sqrt{\dot{X}^2 + \dot{Y}^2}.$$

and $\hat{e}_t$ always points in the direction of the velocity vector, it follows that the velocity vector $\vec{v}$ of the particle can be written

$$\vec{v} = v\hat{e}_t,$$

while its acceleration is given by

$$\vec{a} = \dot{v}\hat{e}_t + v\dot{\hat{e}}_t.$$

(a) Show that $\dot{\hat{e}}_t = \|\dot{\hat{e}}_t\|\hat{e}_n$, or

$$\hat{e}_n = \frac{\dot{\hat{e}}_t}{\|\dot{\hat{e}}_t\|},$$

and that consequently the acceleration $\vec{a}$ is

$$\vec{a} = \dot{v}\hat{e}_t + v\|\dot{\hat{e}}_t\|\hat{e}_n.$$

(b) The radius of curvature ρ can be found from the following formula:

$$\begin{aligned} \rho &= \frac{v^3}{\ddot{X}\dot{Y} - \ddot{Y}\dot{X}} \\ &= \frac{(\dot{X}^2 + \dot{Y}^2)^{3/2}}{\dot{X}\ddot{Y} - \dot{Y}\ddot{X}}. \end{aligned}$$

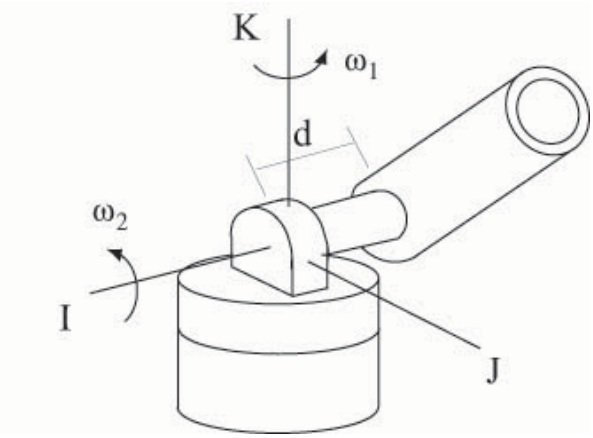

Figure 6.12: A cannon mounted on a $2R$ rotating platform.

Using the formula, show that the acceleration $\vec{a}$ can be written

$$\vec{a} = \dot{v}\hat{e}_t + \frac{v^2}{\rho}\hat{e}_n.$$

3. In standard treatments of particle kinematics using moving frames, two moving particles, A and B, are assumed, with a moving frame $\{\hat{x}, \hat{y}, \hat{z}\}$ attached to particle A. Writing the position of particle B as

$$\vec{p}_B = \vec{p}_A + \vec{p}_{B|A},$$

where $\vec{p}_{B|A}$ denotes the vector from A to B, the following formulas for the velocity and acceleration of B are usually provided:

$$\begin{aligned}
\vec{v}_B &= \vec{v}_A + \left(\dot{\vec{p}}_{B|A}\right)_{xyz} + \vec{\omega} \times \vec{p}_{B|A} \\
\vec{a}_B &= \vec{a}_A + \left(\ddot{\vec{p}}_{B|A}\right)_{xyz} + 2\vec{\omega} \times \left(\dot{\vec{p}}_{B|A}\right)_{xyz} + \vec{\alpha} \times \vec{p}_{B|A} + \vec{\omega} \times (\vec{\omega} \times \vec{p}_{B|A}),
\end{aligned}$$

where $\vec{\omega}$ and $\vec{\alpha}$ respectively denote the angular velocity and angular acceleration vector of the moving frame, and $\left(\dot{\vec{p}}_{B|A}\right)_{xyz}$ $\left(\ddot{\vec{p}}_{B|A}\right)_{xyz}$ are certain time derivatives of $\vec{p}_{B|A}$. Writing $\vec{p}_A$ and $\vec{p}_{B|A}$ in terms of fixed and moving frame coordinates, i.e.,

$$\begin{aligned}
\vec{p}_A &= X\hat{X} + Y\hat{Y} + Z\hat{Z} \\
\vec{p}_{B|A} &= x\hat{x} + y\hat{y} + z\hat{z},
\end{aligned}$$

derive the above formulas for $\vec{v}_B$ and $\vec{a}_B$. Be sure to explicitly identify all terms, in particular $\left(\dot{\vec{p}}_{B|A}\right)_{xyz}$ and $\left(\ddot{\vec{p}}_{B|A}\right)_{xyz}$.

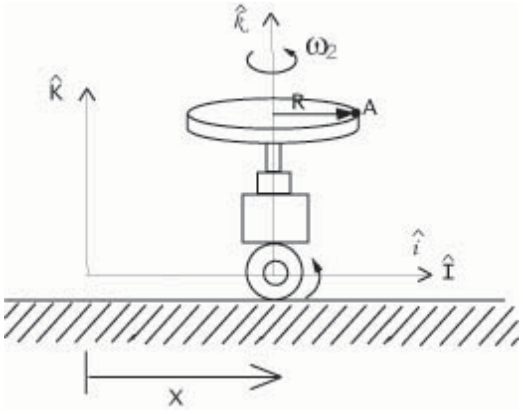

Figure 6.13: A circular plate of radius R.

4. Figure 6.12 depicts a cannon mounted on a $2R$ rotating platform at time $t = 0$. The platform rotates at constant angular velocities ω_1 and ω_2 radians/sec as shown. The axis of the cannon barrel is displaced at a distance d from the origin of the fixed frame. Assume that a cannonball is fired at $t = 0$ from the same height as the $\hat{I}$ axis, at a constant speed v_0 along the axis of the barrel.
(a) Choose a moving frame and describe how the frame moves.
(b) Determine the velocity of the cannonball at $t = 0$ in terms of the moving frame chosen in part (a).

5. As shown in Figure 6.13, a revolving circular plate of radius R, rotating at a constant angular velocity of ω_2 radians/sec, is mounted on a wheeled mobile base that moves periodically back and forth along the $\hat{I}$ axis according to

$$x(t) = a \sin \omega_1 t.$$

(a) Assuming $t = 0$ at the instant shown in the figure, determine the velocity of point A as a function of t in fixed frame coordinates.
(b) Determine the acceleration of point A as a function of t in fixed frame coordinates.

6. The circular pipe of Figure 6.14 is rotating about the $\hat{X}$ axis at a constant rate ω_1 radians/sec, while a marble D is circling the pipe at a constant speed u.
(a) Find the angle θ at which the magnitude of the velocity of D is maximal. What is the maximal velocity magnitude at this angle?
(b) Find the angle θ at which the magnitude of the acceleration of D is maximal. What is the maximal acceleration magnitude at this angle?

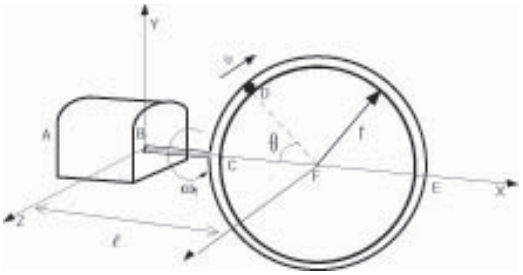

Figure 6.14: A marble traversing a rotating circular pipe.

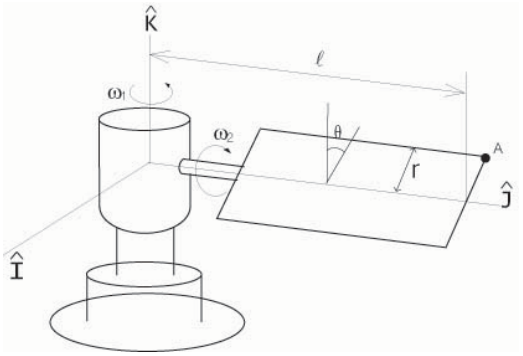

Figure 6.15: A satellite with a rotating panel.

7. The satellite of Figure 6.15 is rotating about its own vertical $\hat{K}$ axis at a constant rate ω_1 radians/sec, while at the same time its solar panel rotates at a constant rate ω_2 radians/sec as shown.
(a) Determine the velocity of point A when $\omega_1 = 0.5$, $\omega_2 = 0.25$, $l = 2m$, $r = 0.5m$, and $\theta = 30°$.
(b) Determine the acceleration of point A under the same conditions as part (a).

8. The two revolute joints in the spherical $2R$ open chain of Figure 6.16 rotating at constant angular velocities ω_1 radians/sec and ω_2 radians/sec as shown. Denote by r the length of link AB, while θ is the angle between link AB and the x-y plane.
(a) Choose a moving frame and explain how the frame moves.
(b) Determine the angular velocity and angular of link AB in terms of your moving frame coordinates chosen in part (a).
(c) Determine the velocity of point B in terms of the chosen moving frame coordinates.

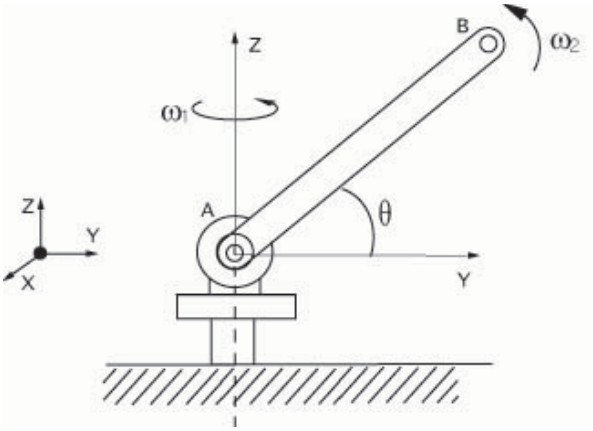

Figure 6.16: A spherical $2R$ open chain.

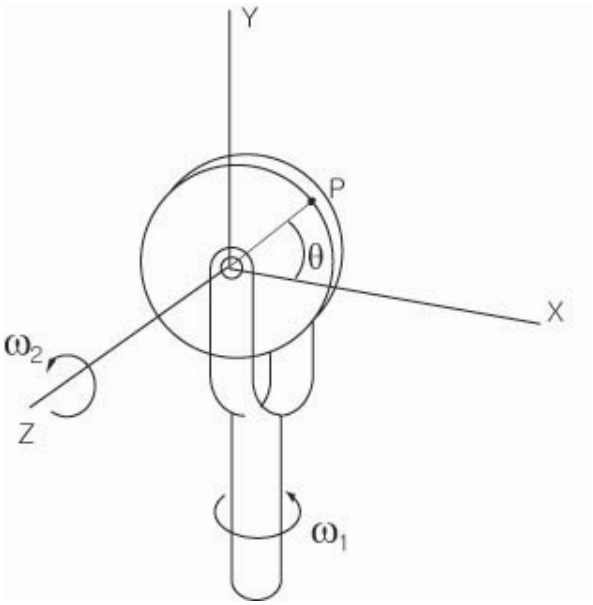

Figure 6.17: A rotating disk.

(d) Determine the acceleration of point B in terms of the chosen moving frame coordinates.
(e) Setting $\omega_1 = 0.1$, $\omega_2 = 0.2$, and $r = 100mm$, determine the velocity and acceleration of point B in terms of the fixed frame coordinates when $\theta = \pi/6$.

9. As shown in Figure 6.17, a disk of radius r spins at a constant angular

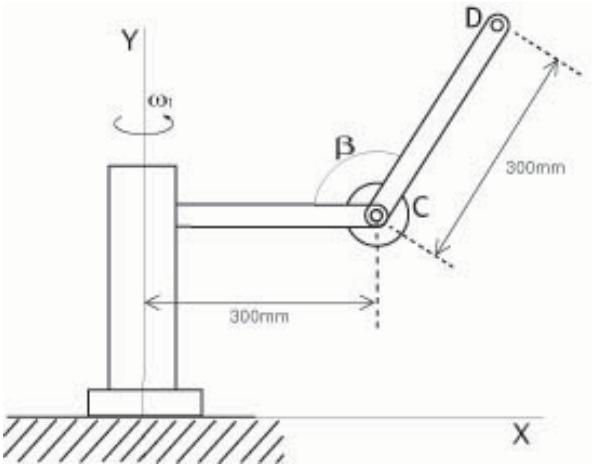

Figure 6.18: A toroidal $2R$ open chain.

velocity of ω_2 radians/sec about its horizontal axis, while at the same time the disk assembly rotates about the vertical axis at a constant angular velocity of ω_1 radians/sec.
(a) Determine the angular velocity and the angular acceleration of the disk in terms of fixed frame coordinates.
(b) Determine the velocity and the acceleration of point P as a function of the angle θ.

10. As shown in Figure 6.18, the two revolute joints of the toroidal $2R$ open chain are rotating at a constant angular velocity $\omega_1 = 0.6$ radians/sec about the $\hat{Y}$ axis, and $\omega_2 = 0.45$ radians/sec about the horizontal axis through C. When $\beta = 120°$, determine the following in terms of fixed frame coordinates:
(a) the angular acceleration of link CD.
(b) the velocity of point D.
(c) the acceleration of point D.

11. Figure 6.19 shows an RRP open chain at $t = 0$. The revolute joints rotate at constant angular velocities ω_1 and ω_2 radians/sec. Suppose the vertical position of point B is given by $x(t) = \sin t$. Determine the following quantities in terms of fixed frame coordinates.
(a) The velocity of point B at $t = 0$.
(b) The acceleration of point B at $t = 0$.

12. The square plate of Figure 6.20 rotates about axis $\hat{I}$ with angular velocity $\omega_2 = 0.5$ radians/sec and angular acceleration $\alpha_2 = 0.01$ radians/sec^2, while the circular disk attached to the square plate rotates about the axis normal

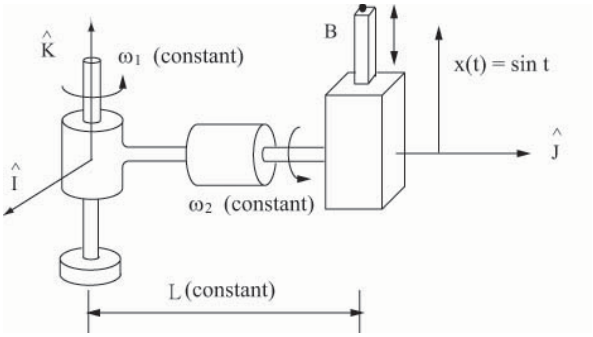

Figure 6.19: An *RRP* open chain.

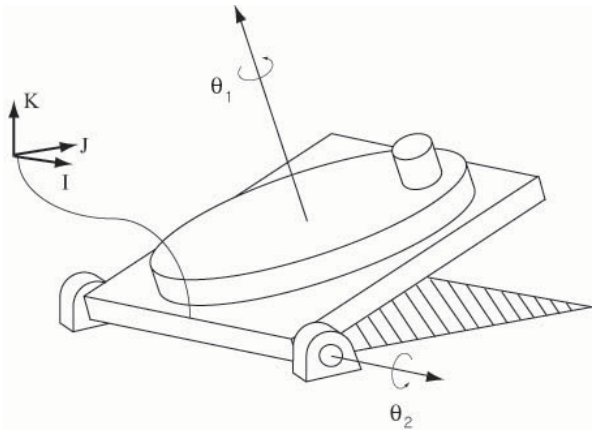

Figure 6.20: A rotating square plate.

to the plate with angular velocity $\omega_1 = 1$ radians/sec and angular acceleration $\alpha_1 = 0.5$ radians/sec^2. The radius of the circular disk is $R = 5m$, while the length of each side of the square plate is $2R = 10m$. The distance from the center of the circular disk to the small circular knob is $d = 3m$. Assume that both the disk and the square plate have zero thickness. Setting $\theta_1 = 0^\circ$ and $\theta_2 = 45^\circ$, find the following in terms of fixed frame coordinates:
(a) The velocity of the circular knob.
(b) The acceleration of the circular knob.

13. A person is riding the $2R$ gyro swing of Figure 6.21. Joint θ oscillates periodically according to $\theta(t) = \cos t$, and the circular plate connected to the axis of the gyro swing rotates with constant angular velocity ω_2 radians/sec. At $t = 0$, the person on the circular plate is at the maximal height as shown in the figure. Setting $l = 1$, $r = 1$, and $\omega_2 = 1$ radian/sec, determine the velocity of the person in terms of the given fixed frame coordinates when $t = \frac{\pi}{2}$.

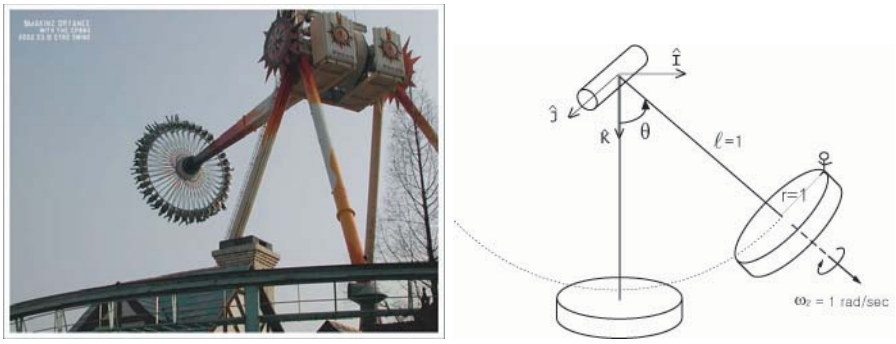

Figure 6.21: A $2R$ gyro swing.

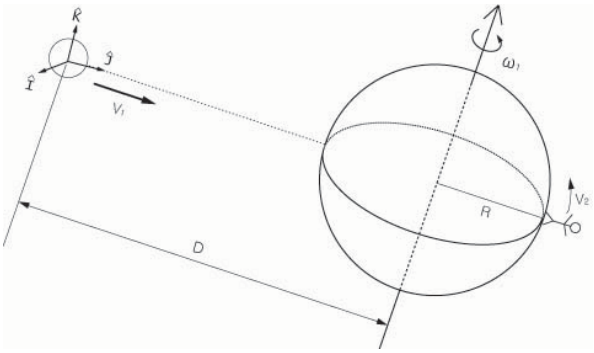

Figure 6.22: A meteorite approaching the earth.

14. As shown in Figure 6.22, a meteorite is approaching a rotating asteroid along the meteorite's $\hat{J}$ axis with velocity $v_1 = 100$ m/sec. Suppose the radius of the asteroid is $R = 1000m$, and the distance of the meteorite from the asteroid is initially $D = 10^7 m$. The asteroid takes 6 hours to complete a full revolution. An astronaut stands at the point antipodal to the expected point of collision, and unwittingly starts walking north along a longitudinal arc at a velocity of $v_2 = 1$ m/sec. After three hours, determine the velocity of the astronaut in terms of the moving frame coordinates attached to the meteorite. of the moving frame at the meteorite.

15. As shown in Figure 6.23, a clock of radius r is mounted on a gimbal assembly as shown. The angles θ_1, θ_2, and θ_3 are adjustable to arbitrary values; in the figure the angles are all assumed to be set to zero. A moving frame $\{T\}$ is attached to the tip of the clock's second hand, with its $\hat{x}$-axis aligned along the tip of the hand as shown. Setting $r = 1m$, $a = 3m$, $b = 7m$, answer the

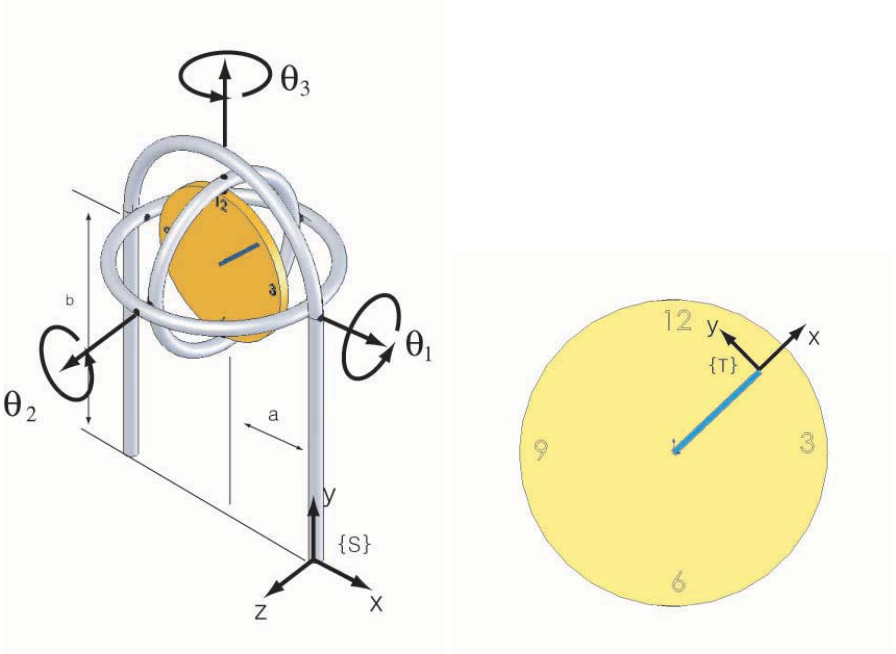

Figure 6.23: A clock mounted on a gimbal assembly.

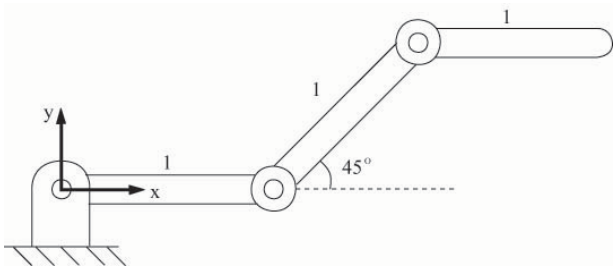

Figure 6.24: A $3R$ planar open chain.

following:
(a) Assuming the second hand starts at 12 at $t = 0$, when the second hand reaches 10, find $T_{ST} \in SE(3)$ as a function of the angles $(\theta_1, \theta_2, \theta_3)$.
(b) Setting $\theta_1 = 90°$, $\theta_2 = 0$, $\theta_3 = 90°$, find the the velocity of the tip of the second hand at the moment it passes 10.

16. The $3R$ planar open chain of Figure 6.24 is shown in its zero position.
(a) Suppose the tip must apply a force of $5N$ in the $\hat{x}$-direction. What torques should be applied at each of the joints?

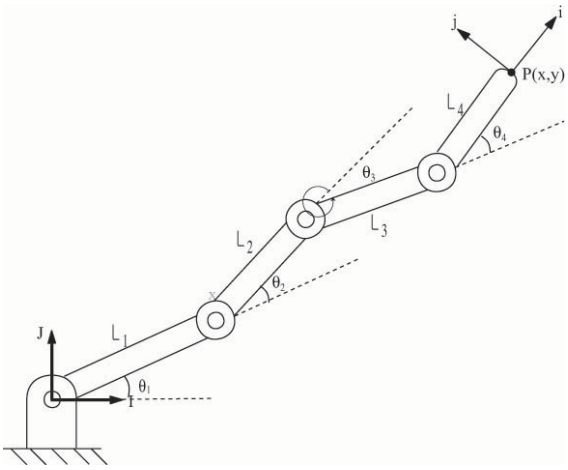

Figure 6.25: A planar $4R$ open chain.

(b) Suppose the tip must now apply a force of $5N$ in the $\hat{y}$-direction. What torques should be applied at each of the joints?

17. Answer the following questions for the $4R$ planar open chain of Figure 6.25.
(a) Derive the forward kinematics in the form

$$T(\theta) = e^{[\mathcal{S}_1]\theta_1} e^{[\mathcal{S}_2]\theta_2} e^{[\mathcal{S}_3]\theta_3} e^{[\mathcal{S}_4]\theta_4} M.$$

where each $\mathcal{S}_i \in \mathbb{R}^3$ and $M \in SE(2)$.
(b) Derive the body Jacobian.
(c) Suppose the chain is in static equilibrium at the configuration $\theta_1 = \theta_2 = 0, \theta_3 = \frac{\pi}{2}, \theta_4 = -\frac{\pi}{2}$, and a force $f = (10, 10, 0)$ and moment $m = (0, 0, 10)$ are applied to the tip (both f and m are expressed with respect to the fixed frame). What are the torques experienced at each of the joints?
(d) Under the same conditions as (c), suppose that a force $f = (-10, 10, 0)$ and moment $m = (0, 0, -10)$ are applied to the tip. What are the torques experienced at each of the joints?
(e) Find all kinematic singularities for this chain.

18. Referring to Figure 6.26, the rigid body rotates about the point (L, L) with angular velocity $\dot{\theta} = 1$.
(a) Find the position of point P on the moving body with respect to the fixed reference frame in terms of θ.
(b) Find the velocity of point P in terms of the fixed frame.
(c) What is T_{fb}, the displacement of frame $\{b\}$ as seen from the fixed frame $\{f\}$?
(d) Find the spatial velocity of T_{fb} in body coordinates.

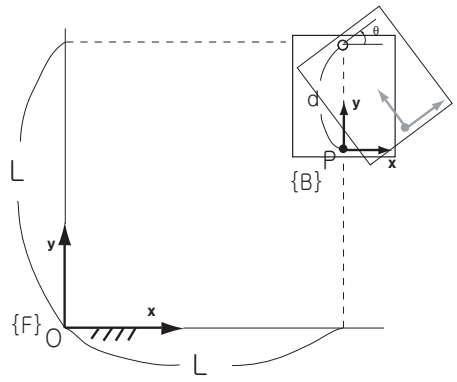

Figure 6.26: A rigid body rotating in the plane.

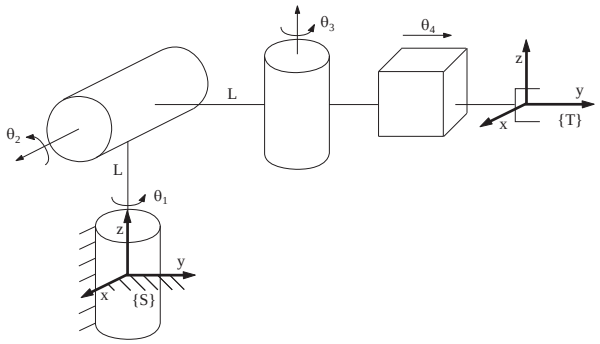

Figure 6.27: An *RRRP* spatial open chain.

(e) Find the spatial velocity of T_{fb} in space coordinates.
(f) What is the relation between the spatial velocities obtained in (d) and (e)?
(g) What is the relation between the spatial velocity obtained in (d) and $\dot{P}$ obtained in (b)?
(h) What is the relation between the spatial velocity obtained in (e) and $\dot{P}$ obtained in (b)?

19. The *RRRP* chain of Figure 6.27 is shown in its zero position.
(a) Determine the body Jacobian $J_b(\theta)$ when $\theta_1 = \theta_2 = 0, \theta_3 = \pi/2, \theta_4 = L$.
(b) Determine the linear velocity of the end-effector frame, in fixed frame coordinates, when $\theta_1 = \theta_2 = 0, \theta_3 = \pi/2, \theta_4 = L$ and $\dot{\theta_1} = \dot{\theta_2} = \dot{\theta_3} = \dot{\theta_4} = 1$.

20. The spatial $3R$ open chain of Figure 6.28 is shown in its zero position.
(a) In its zero position, suppose we wish to make the end-effector move with linear velocity $v_{tip} = (10, 0, 0)$, where v_{tip} is expressed with respect to the space frame $\{s\}$. What are the necessary input joint velocities $\dot{\theta_1}, \dot{\theta_2}, \dot{\theta_3}$?

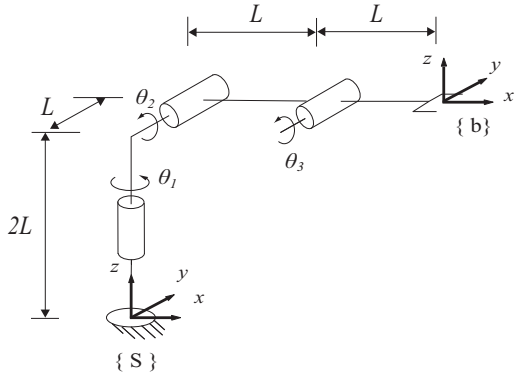

Figure 6.28: A spatial $3R$ open chain.

(b) Suppose the robot is in the configuration $\theta_1 = 0, \theta_2 = 45°, \theta_3 = -45°$. Assuming static equilibrium, suppose we wish to generate an end-effector force $f_b = (10, 0, 0)$, where f_b is expressed with respect to the end-effector frame $\{b\}$. What are the necessary input joint torques τ_1, τ_2, τ_3?
(c) Under the same conditions as in (b), suppose we now seek to generate an end-effector moment $m_b = (10, 0, 0)$, where m_b is expressed with respect to the end-effector frame {b}. What are the necessary input joint torques τ_1, τ_2, τ_3?
(d) Suppose the maximum allowable torques for each joint motor are

$$\|\tau_1\| \leq 10, \|\tau_2\| \leq 20, \|\tau_3\| \leq 5.$$

In the home position, what is the maximum force that can be applied by the tip in the end-effector frame x-direction?

21. The spatial $PRRRRP$ open chain of Figure 6.29 is shown in its zero position.
(a) At the zero position, find the first three columns of the space Jacobian.
(b) Find all configurations at which the first three columns of the space Jacobian become linearly dependent.
(c) Suppose the chain is in the configuration $\theta_1 = \theta_2 = \theta_3 = \theta_5 = \theta_6 = 0, \theta_4 = 90^o$. Assuming static equilibrium, suppose a pure force $f_b = (10, 0, 10)$ is applied to the origin of the end-effector frame, where f_b is expressed in terms of the end-effector frame. Find the joint torques τ_1, τ_2, τ_3 experienced at the first three joints.

22. Consider the $PRRRRR$ spatial open chain of Figure 6.30 shown in its zero position. The distance from the origin of the fixed frame to the origin of the end-effector frame at the home position is L.
(a) Determine the first three columns of the space Jacobian J_s.
(b) Determine the last two columns of the body Jacobian J_b.

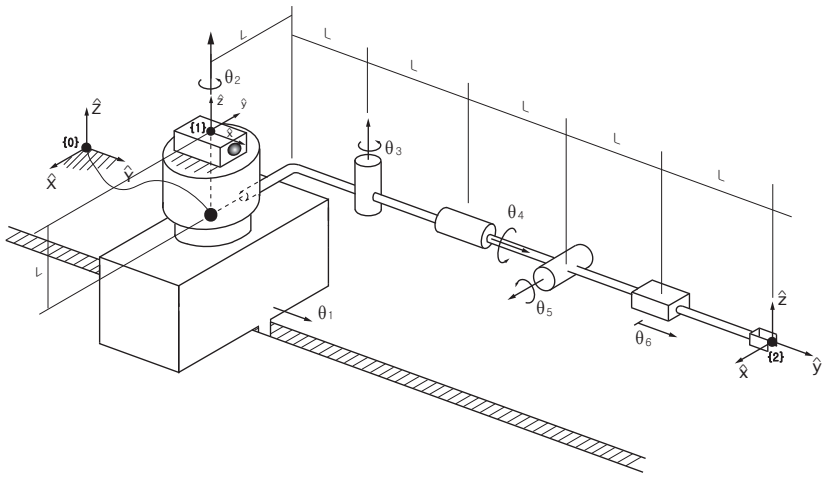

Figure 6.29: A spatial $PRRRRP$ open chain.

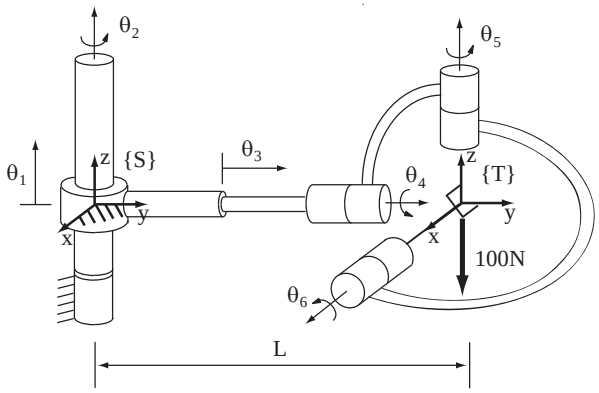

Figure 6.30: A $PRRRRR$ spatial open chain.

(c) For what value of L is the home position a singularity?
(d) In the zero position, what joint torques must be applied in order to generate a pure end-effector force of $100N$ in the -$\hat{z}$ direction?

23. Find all kinematic singularities of the $3R$ wrist with the following forward kinematics:

$$R = e^{[\omega_1]\theta_1} e^{[\omega_2]\theta_2} e^{[\omega_3]\theta_3}$$

where $\omega_1 = (0, 0, 1)$, $\omega_2 = (1/\sqrt{2}, 0, 1/\sqrt{2})$, and $\omega_3 = (1, 0, 0)$.

24. Show that a six degree of freedom spatial open chain is in a kinematic singularity when any two of its revolute joint axes are parallel, and any prismatic

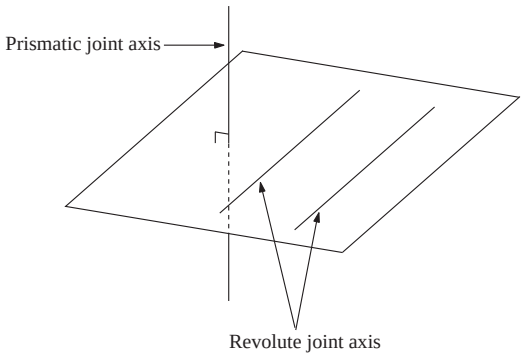

Figure 6.31: A kinematic singularity involving prismatic and revolute joints.

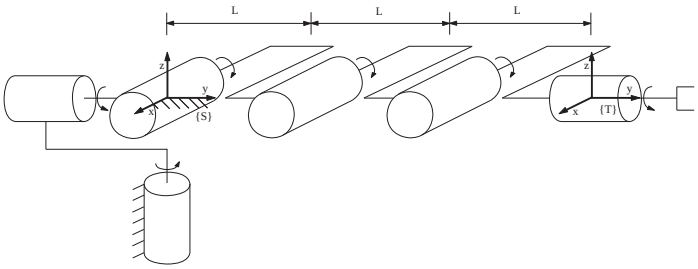

Figure 6.32: Singularities of an elbow-type $6R$ open chain.

joint axis is normal to the plane spanned by the two parallel revolute joint axes (see Figure 6.31).

25. (a) Determine the space Jacobian $J_s(\theta)$ of the $6R$ spatial open chain of Figure 6.32.
(b) Find the kinematic singularities of the given chain. Explain each singularity in terms of the alignment of the joint screws, and the directions in which the end-effector loses one or more degrees of freedom of motion.

26. The spatial $PRRRRP$ open chain of Figure 6.33 is shown in its zero position.
(a) Determine the first 4 columns of the space Jacobian $J_s(\theta)$.
(b) Determine whether the zero position is a kinematic singularity.
(c) Calculate the joint torques required for the tip to apply the following end-effector spatial forces:

(i) $F_s = (0, 1, -1, 1, 0, 0)^T$

(ii) $F_s = (1, -1, 0, 1, 0, -1)^T$.

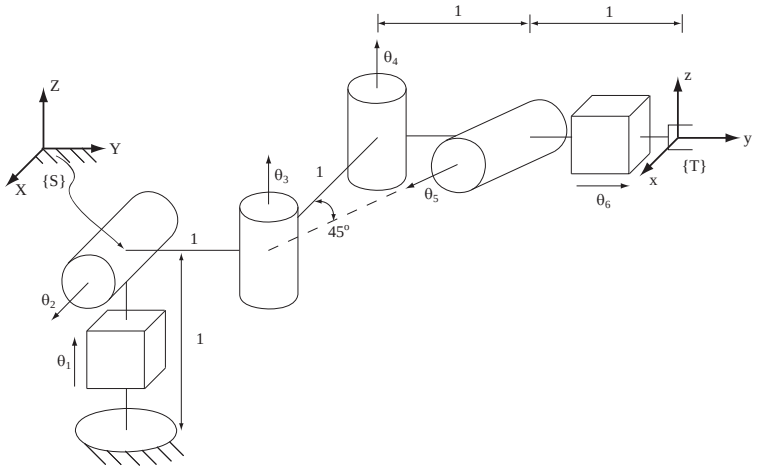

Figure 6.33: A spatial $PRRRRP$ open chain with a skewed joint axis.

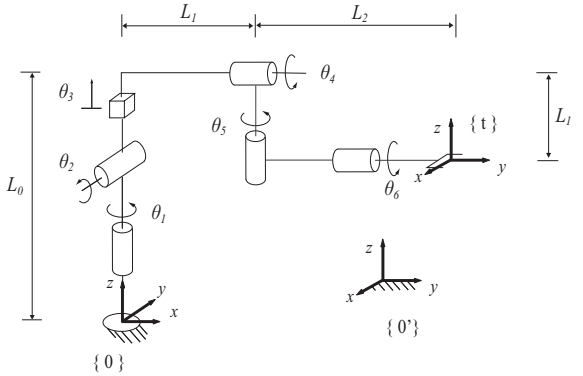

Figure 6.34: A spatial $RRPRRR$ open chain.

27. The spatial $RRPRRR$ open chain of Figure 6.34 is shown in its zero position.
(a) For the fixed frame $\{0\}$ and tool frame $\{\mathrm{t}\}$ as shown, express the forward kinematics in the following product of exponentials form:

$$T(\theta) = e^{[\mathcal{S}_1]\theta_1} e^{[\mathcal{S}_2]\theta_2} e^{[\mathcal{S}_3]\theta_3} e^{[\mathcal{S}_4]\theta_4} e^{[\mathcal{S}_5]\theta_5} e^{[\mathcal{S}_6]\theta_6} M.$$

(b) Find the first three columns of the space Jacobian $J_s(\theta)$.
(c) Suppose that the fixed frame $\{0\}$ is moved to another location $\{0'\}$ as shown in the figure. Find the first three columns of the space Jacobian $J_s(\theta)$ with respect to this new fixed frame.

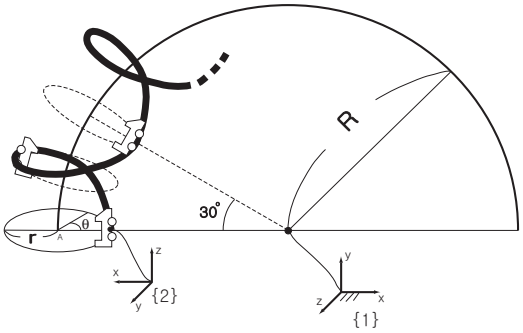

Figure 6.35: A rollercoaster undergoing a screw motion.

(d) Determine if the zero position is a kinematic singularity, and if so, provide a geometric description in terms of the joint screw axes.

28. The rollercoaster of Figure 6.35 undergoes a screw motion as shown: point A traces a circle of radius R, and the rollercoaster moves in screw-like fashion at a distance r from this larger circle. The roller coaster completes one revolution about this larger circle when point A traverses 30° along the larger circle.
(a) Find T_{12}, the relative displacement of the rollercoaster frame $\{2\}$ as seen from the fixed frame $\{1\}$, in terms of the angle θ as indicated in the figure.
(b) Derive the space Jacobian for $T_{12}(\theta)$.

29. Two frames $\{a\}$ and $\{b\}$ are attached to a moving rigid body. Show that the spatial velocity of $\{a\}$ in space frame coordinates is the same as the spatial velocity of $\{b\}$ in space frame coordinates.

30. Consider an n-link open chain, with reference frames attached to each link. Let

$$T_{0k} = e^{[\mathcal{S}_1]\theta_1} \cdots e^{[\mathcal{S}_k]\theta_k} M_k, \quad k = 1, \ldots, n$$

be the forward kinematics up to link frame $\{k\}$. Let $J_s(\theta)$ be the space Jacobian for T_{0n}. The columns of $J_s(\theta)$are denoted

$$J_s(\theta) = \left[\begin{array}{ccc} \mathcal{V}_{s1}(\theta) & \cdots & \mathcal{V}_{sn}(\theta) \end{array} \right].$$

Let $[\mathcal{V}_k] = \dot{T_{0k}} T_{0k}^{-1}$ be the spatial velocity of link frame $\{k\}$ in frame $\{k\}$ coordinates.
(a) Derive explicit expressions for $\mathcal{V}_2$ and $\mathcal{V}_3$.
(b) Based on your results from (a), derive a recursive formula for $\mathcal{V}_{k+1}$ in terms of $\mathcal{V}_k$, $\mathcal{V}_{s1}, \ldots, \mathcal{V}_{s,k+1}$, and $\dot{\theta}$.

Chapter 7

Inverse Kinematics of Open Chains

For a general n degree of freedom open chain with forward kinematics $T(\theta)$, $\theta \in \mathbb{R}^n$, the inverse kinematics problem can be stated as follows: given a homogeneous transform $X \in SE(3)$, find solutions θ that satisfy $T(\theta) = X$. To highlight the main features of the inverse kinematics problem, let us consider the two-link planar open chain of Figure 6.1-(a) as a motivational example. Considering only the position of the end-effector and ignoring its orientation, the forward kinematics can be expressed as

$$\begin{bmatrix} x \\ y \end{bmatrix} = \begin{bmatrix} L_1 \cos\theta_1 + L_2 \cos(\theta_1 + \theta_2) \\ L_1 \sin\theta_1 + L_2 \sin(\theta_1 + \theta_2) \end{bmatrix}. \tag{6.1}$$

Assuming $L_1 > L_2$, the set of reachable points, or the workspace, is an annulus of innner radius $L_1 - L_2$ and outer radius $L_1 + L_2$. Given some end-effector position (x, y), it is not hard to see that there will be either zero, one, or two solutions depending on whether (x, y) lies in the exterior, boundary, or interior of this annulus (the case of two solutions is given by the familiar elbow-up and elbow-down configurations as illustrated in Figure **??**).

Finding an explicit solution (θ_1, θ_2) for a given (x, y) is also not difficult. Referring this time to Figure 6.1-(b), assume that (x, y) lies in the first quadrant, i.e., both x and y are positive (solutions for the other quadrants follow straightforwardly). Angle β, restricted to lie in the interval $[0, \pi]$, can be determined from the law of cosines:

$$L_1^2 + L_2^2 - 2L_1L_2 \cos\beta = x^2 + y^2,$$

from which it follows that

$$\begin{aligned} \beta &= \cos^{-1}\left(\frac{L_1^2 + L_2^2 - x^2 - y^2}{2L_1L_2}\right) \\ \theta_2 &= \pi - \beta. \end{aligned}$$

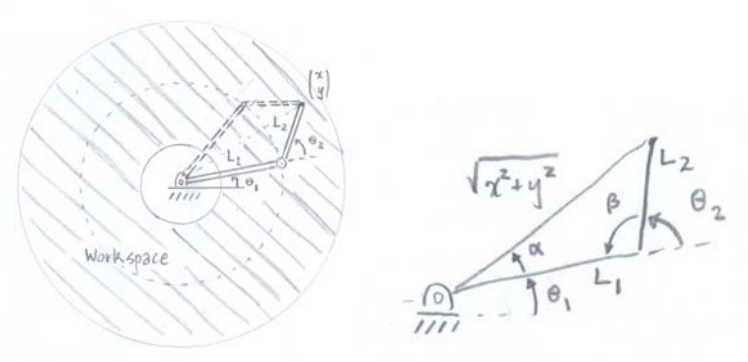

(a) Workspace and elbow-up and elbow-down configurations.

(b) Geometric solution.

Figure 6.1: $2R$ planar open chain inverse kinematics.

Also from the law of cosines,

$$\alpha = \cos^{-1}\left(\frac{x^2+y^2+L_1^2-L_2^2}{2L_1\sqrt{x^2+y^2}}\right).$$

and since $\tan(\theta_1+\alpha) = y/x$, it follows that

$$\theta_1 = \tan^{-1}\frac{y}{x} - \alpha.$$

The above values for θ_1 and θ_2 correspond to the elbow-down solution. The elbow-up solution is given by

$$\theta_1 = \tan^{-1}\frac{y}{x} + \alpha, \quad \theta_2 = \pi + \beta.$$

If x^2+y^2 lies outside the range $[L_1-L_2, L_1+L_2]$, then no solution exists. Again, the case when (x, y) lies in other quadrants follows straightforwardly from the above solution for the first quadrant.

This simple motivational example illustrates that for open chains, the inverse kinematics problem may have multiple solutions; this is in contrast to the forward kinematics, where a unique end-effector displacement T exists for a given joint value θ. In fact, three-link planar open chains have an infinite number of solutions for points (x, y) lying in the interior of the workspace; in this case the chain possesses an extra degree of freedom, and is said to be kinematically redundant.

This chapter begins by considering the inverse kinematics of spatial open chains with six degrees of freedom. A finite number of solutions exists in this case, and we first make some simplifying assumptions about the kinematic structure that lead to analytic solutions. As we shall see, these assumptions are not restrictive, as they accommodate the most commonly used six degree of freedom

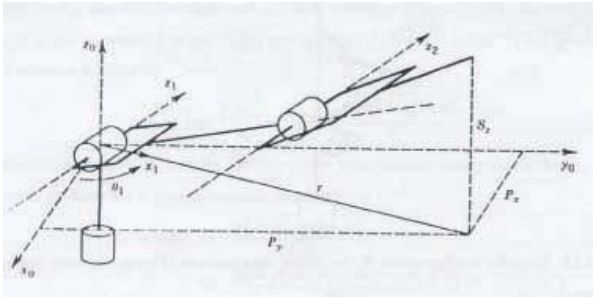

Figure 6.2: Inverse position kinematics of a 6R PUMA-type arm.

open chains. We then specialize the Newton-Raphson method for nonlinear root finding to the inverse kinematics problem. The result is an iterative numerical algorithm that, provided the initial guess is sufficiently close to the true solution, eventually converges to the solution. The chapter concludes with a discussion of pseudo-inverse based inverse kinematics solutions for redundant open chains.

6.1 Analytic Inverse Kinematics

We begin by writing the forward kinematics of a spatial six degree of freedom open chain in the following product of exponentials form:

$$T(\theta) = e^{[S_1]\theta_1} e^{[S_2]\theta_2} e^{[S_3]\theta_3} e^{[S_4]\theta_4} e^{[S_5]\theta_5} e^{[S_6]\theta_6} M.$$

Given some $X \in SE(3)$, the inverse kinematics problem is concerned with finding all solutions $\theta \in \mathbb{R}^6$ that satisfy $T(\theta) = Y$. In the following subsections we shall make some simplifying assumptions about the kinematic structure of the open chain that will lead to analytic solutions for the inverse kinematics.

6.1.1 6R PUMA-Type Arm

We first consider a $6R$ arm of the PUMA type (see Figure 6.2). Such arms are characterized by (i) the last three joint axes intersecting orthogonally at a common point (the wrist center) to form an orthogonal wrist; (ii) the first two axes intersecting orthogonally to form a shoulder joint; and (iii) the elbow joint axis being parallel with the horizontal shoulder joint axis. Such arms may also have an offset at the shoulder (see Figure 6.3). The inverse kinematics problem for PUMA-type arms can be decoupled into an inverse position and inverse orientation subproblem, which we now discuss.

We first consider the simple case of a zero-offset PUMA-type arm. Referring to Figure 6.2 and expressing all vectors in terms of fixed frame coordinates, denote components of the wrist center $p \in \mathbb{R}^3$ by $p = (p_x, p_y, p_z)$. Projecting p onto the x-y plane, it can be seen that

$$\theta_1 = \tan^{-1} \frac{p_y}{p_x},$$

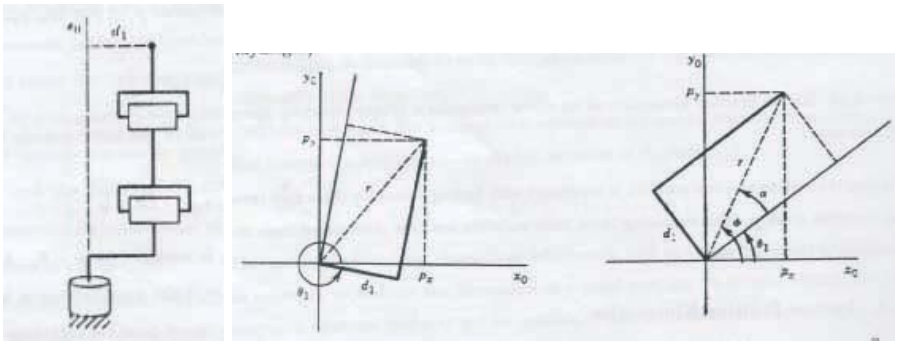

(a) Elbow arm with offset.

(b) Kinematic diagram.

Figure 6.3: A 6R PUMA-type arm with a shoulder offset.

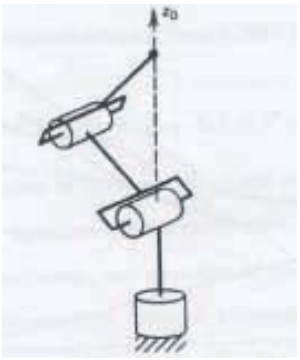

Figure 6.4: Singular configuration of the zero-offset $6R$ PUMA-type arm.

where the atan2() function can be used instead of $\tan^{-1}$. Note that a second valid solution for θ_1 is given by

$$\theta_1 = \tan^{-1} \frac{p_y}{p_x} + \pi,$$

provided that the original solution for θ_2 is replaced by $\pi - \theta_2$. As long as $p_x, p_y \neq 0$, both these solutions are valid. When $p_x = p_y = 0$ the arm is in a singular configuration (see Figure 6.4), and there are infinitely many possible solutions for θ_1.

If there is an offset $d_1 \neq 0$ as shown in Figure 6.3, then in general there will be two solutions for θ_1, denoted the **right** and **left arm** solutions (Figure 6.3). As seen from the figure, $\theta_1 = \phi - \alpha$, where $\phi = \tan^{-1}(\frac{p_y}{p_x})$ and $\alpha = \tan^{-1}(\frac{\sqrt{r^2 - d_1^2}}{d_1}) =$

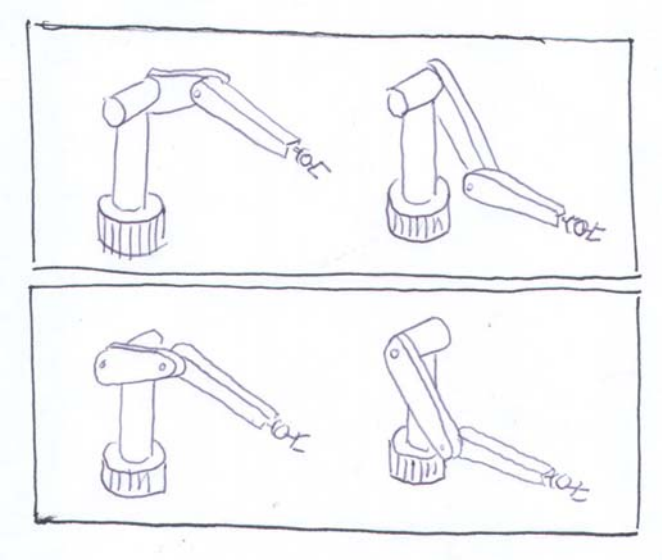

Figure 6.5: Four possible inverse kinematics solutions for the 6R PUMA type arm with shoulder offset.

$\tan^{-1}(\frac{\sqrt{p_x^2+p_y^2-d_1^2}}{d_1})$. The second solution is given by

$$\theta_1 = \tan^{-1}(\frac{p_y}{p_x}) - \tan^{-1}(\frac{-\sqrt{p_x^2+p_y^2-d_1^2}}{d_1})$$

Determining angles θ_2 and θ_3 for the PUMA-type arm now reduces to the inverse kinematics problem for a planar two-link chain:

$$\begin{aligned}\cos\theta_3 &= \frac{r^2+s^2-a_2^2-a_3^2}{2a_2a_3} \\ &= \frac{p_x^2+p_y^2+(p_z^2-d_1)^2-a_2^2-a_3^2}{2a_2a_3}\end{aligned}$$

If we let $\cos\theta_3 = D$, then θ_3 is given by

$$\theta_3 = \tan^{-1}(\pm\frac{\sqrt{1-D^2}}{D})$$

θ_2 can be obtained in a similar fashion as

$$\begin{aligned}\theta_2 &= \tan^{-1}(\frac{s}{r}) - \tan^{-1}(\frac{a_3s_3}{a_2+a_3c_3}) \\ &= \tan^{-1}(\frac{p_z-d_1}{\sqrt{p_x^2+p_y^2}}) - \tan^{-1}(\frac{a_3s_3}{a_2+a_3c_3})\end{aligned}$$

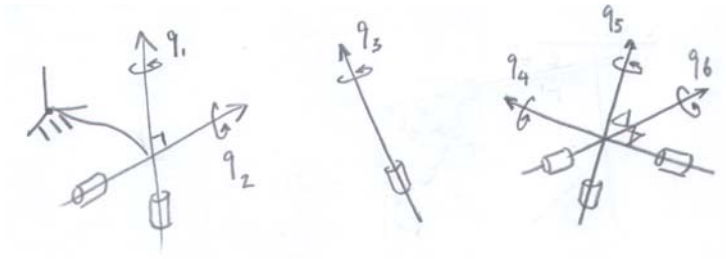

Figure 6.6: A $6R$ spatial open chain of the generalized PUMA type.

The two solutions for θ_3 correspond to the well-known elbow up and elbow down configurations for the two-link planar arm. In general, a PUMA-type arm with an offset will have four solutions to the inverse position problem, as shown in Figure 6.5; the upper postures are called left-arm solutions (elbow-up and elbow-down), while the lower postures are called right-arm solutions (elbow-up and elbow-down).

We now solve the inverse orientation problem, i.e., finding values for $(\theta_4, \theta_5, \theta_6)$ given the end-effector frame orientation. This is completely straightforward: since the final three joints form a 3R wrist with orthogonal axes, the joint values can be determined via an appropriate set of Euler angles as discussed in Chapter 3 (e.g., ZYX, ZYZ, depending on how the final three joint axes are aligned when in the zero position).

6.1.2 Generalized 6R PUMA-Type Arms

We now relax some of the assumptions made for the 6R PUMA-type arm: a **generalized 6R PUMA-type arm** is characterized by (i) the first two joint axes intersecting orthogonally, and (ii) the last three joint axes intersecting orthogonally at a common point. Referring to Figure 6.6, place the fixed frame origin at the intersection of joint axes 1 and 2, and let $r_w \in \mathbb{R}^3$ be the fixed frame representation of the point of intersection of the final three axes. The assumptions about the joint axes then lead to the following relations among the joint screws $S_i = (\omega_i, -\omega_i \times r_i)$, $i = 1, \ldots, 6$, where r_i denotes a reference point on axis i:

- $\omega_1^T \omega_2 = 0$;
- $\omega_4^T \omega_5 = 0$ and $\omega_5^T \omega_6 = 0$.

The inverse kinematics problem can now be stated as finding solutions θ to

$$e^{[S_1]\theta_1} e^{[S_2]\theta_2} e^{[S_3]\theta_3} e^{[S_4]\theta_4} e^{[S_5]\theta_5} e^{[S_6]\theta_6} = XM^{-1}, \tag{6.2}$$

where

$$\begin{aligned} S_1 &= (\omega_1, 0) \\ S_2 &= (\omega_2, 0) \\ S_3 &= (\omega_3, -\omega_3 \times r_3) \\ S_4 &= (\omega_4, -\omega_4 \times r_w) \\ S_5 &= (\omega_5, -\omega_5 \times r_w) \\ S_6 &= (\omega_6, -\omega_6 \times r_w), \end{aligned}$$

and the right-hand side XM^{-1} is given; denote this known quantity by $X_1 = XM^{-1}$. Solving the inverse kinematics then proceeds in three steps:

Step 1: Solve for θ_3

We first multiply both sides of Equation (6.2) by r_w (here multiplication of a vector by a homogeneous transformation is understood in the usual sense, i.e.,

$$Tr_w = Rr_w + p, \;\; T = \begin{bmatrix} R & p \\ 0 & 1 \end{bmatrix}.$$

The net effect is to consecutively apply the screw motions defined by $e^{[S_6]\theta_6}$, $e^{[S_5]\theta_5}$, and $e^{[S_4]\theta_4}$ to r_w. However, since all three of these screw motions are zero pitch (all joints are revolute), and r_w is a point lying on all three screw axes, it follows that

$$e^{[S_4]\theta_4} e^{[S_5]\theta_5} e^{[S_6]\theta_6} r_w = r_w.$$

We are thus left with

$$e^{[S_1]\theta_1} e^{[S_2]\theta_2} e^{[S_3]\theta_3} r_w = X_1 r_w = p_1, \tag{6.3}$$

where the vector $p_1 = X_1 r_w$ is known.

Now take the norm of both sides of (6.3). Since both $e^{[S_1]\theta_1}$ and $e^{[S_2]\theta_2}$ are pure rotations, and the general identity $\|Rv\| = \|v\|$ holds for any rotation R and vector v, Equation (6.3) becomes

$$\|e^{[S_3]\theta_3} r_w\| = \|p_1\|.$$

This is a problem of the general form

$$\|e^{[S]\theta} p\| = c,$$

where $S = (\omega, -\omega \times r)$, $p \in \mathbb{R}^3$, and the scalar $c > 0$ are known, and the objective is to find all values of $\theta \in [0, 2\pi]$ satisfying this equality. solve this problem. Referring to Figure 6.7, define the vectors $w, u, v \in \mathbb{R}^3$ according to

$$\begin{aligned} z &= e^{[S]\theta} p \\ u &= p - r \\ v &= w - r, \end{aligned}$$

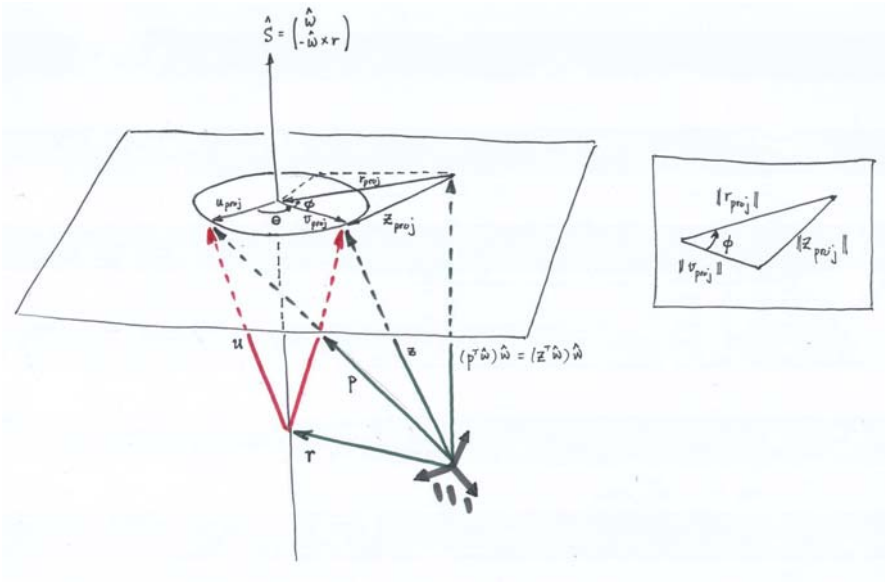

Figure 6.7: Solving $\|e^{[S]\theta}p\| = c$ for θ.

with $\|z\| = c$ given. We shall now project the vectors p, u, v, r, and z onto the plane normal to the screw axis and containing p: define these respectively to be

$$\begin{aligned} p_{proj} &= p - (p^T\omega)\omega \\ u_{proj} &= u - (u^T\omega)\omega \\ v_{proj} &= v - (v^T\omega)\omega \\ r_{proj} &= r - (r^T\omega)\omega \\ z_{proj} &= z - (z^T\omega)\omega. \end{aligned}$$

Note that u_{proj} and q_{proj} are known *a priori*. From the figure it can be seen that

$$\|(z^T\omega)\omega\| = \|(p^T\omega)\omega\| = |p^T\omega|.$$

Since $z_{proj} = z - (z^T\omega)\omega$ and $\|z\|^2 = c^2$, it follows that

$$\|z_{proj}\|^2 = c^2 - (p^T\omega)^2,$$

which is also known *a priori*. Let us first find the angle $\psi = \theta + \phi$, where ϕ is defined as indicated in the figure. Since

$$u_{proj}^T(-q_{proj}) = \|u_{proj}\| \cdot \|q_{proj})\| \cos(\theta + \phi) \tag{6.4}$$

$$u_{proj} \times (-q_{proj}) = \hat{\omega}\ (\|u_{proj}\| \cdot \|q_{proj}\| \sin(\theta + \phi))\,, \tag{6.5}$$

from the latter equality it follows that

$$\omega^T\,(u_{proj} \times (-q_{proj})) = \|u_{proj}\|\|q_{proj}\| \sin(\theta + \phi). \tag{6.6}$$

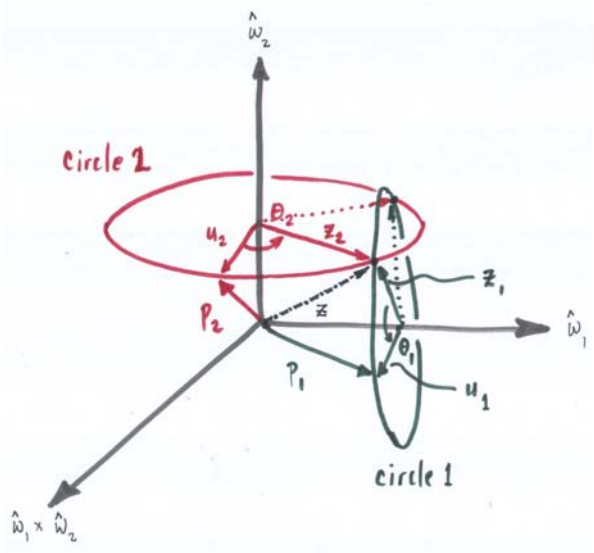

Figure 6.8: Solving $e^{[\omega_1]\theta_1} e^{[\omega_2]\theta_2} p_2 = p_1$ for θ_1 and θ_2.

From Equations (6.4) and (6.6) we have

$$\psi = \tan^{-1}\left(\frac{\omega^T(u_{proj} \times q_{proj})}{u_{proj}^T q_{proj}}\right). \tag{6.7}$$

We now determine ϕ from the law of cosines: referring to the inset of Figure 6.7,

$$\|r_{proj}\|^2 + \|v_{proj}\|^2 - 2\|r_{proj}\| \cdot \|v_{proj}\| \cos\phi = \|z_{proj}\|^2.$$

Since $\|z_{proj}\|^2 = c^2 - (p^T\omega)^2$ is known, and $\|v_{proj}\| = \|u_{proj}\|$ is also known, ϕ can be determined as follows:

$$\phi = \cos^{-1}\left(\frac{\|r_{proj}\|^2 + \|v_{proj}\|^2 - \|z_{proj}\|^2}{2\|r_{proj}\| \cdot \|v_{proj}\|}\right). \tag{6.8}$$

From the figure it should be apparent that there can be up to two solutions for θ:

$$\theta = \psi \pm \phi.$$

If $\phi = 0$, the two solutions collapse to a single solution, while a solution does not exist in the event that ϕ does not exist.

Step 2: Solve for θ_1 and θ_2

Having solved for θ_3, Equation (6.3) can be written

$$e^{[S_1]\theta_1} e^{[S_2]\theta_2} p_2 = p_1, \tag{6.9}$$

where $p_2 = e^{[S_3]\theta_3} r_w$ and p_1 are both known. Observe that $S_1 = (\omega_1, 0)$ and $S_2 = (\omega_2, 0)$ are both pure rotations, and ω_1 and ω_2 are orthogonal to each other. Thus, only the rotation component of (6.9) needs to be considered:

$$e^{[\omega_1]\theta_1} e^{[\omega_2]\theta_2} p_2 = p_1. \tag{6.10}$$

Referring to Figure **??**, clearly a necessary condition for a solution (θ_1, θ_2) to exist is that $\|p_1\| = \|p_2\|$. Assuming this is the case, the solutions are then marked by the intersection of the two circles indicated in Figure 6.8. In the general case there can be up to two solutions, with one or no solution also a possibility.

Assuming a solution exists, let $z \in \mathbb{R}^3$ be the vector p_2 rotated about $\hat{\omega}_2$ by angle θ_2. z can also be obtained by rotating p_1 about ω_1 by an angle $-\theta_1$. Mathematically,

$$z = e^{[\omega_2]\theta_2} p_2 = e^{-[\omega_1]\theta_1} p_1.$$

Clearly $\{\omega_1, \omega_2, \omega_1 \times \omega_2\}$ forms an orthonormal basis for $\mathbb{R}^3$. Further observe that the ω_1 component of z is the same as the ω_1 component of p_1, and the ω_2 component of z is the same as the ω_2 component of p_2). z can therefore be expressed in terms of this orthonormal basis as

$$z = (p_1^T \omega_1)\omega_1 + (p_2^T \omega_2)\omega_2 \pm c(\omega_1 \times \omega_2)$$

for some scalar constant $c \geq 0$. The length $\|z\|$ is then, straightforwardly,

$$\|z\| = (p_1^T \omega_1)^2 + (p_2^T \omega_2)^2 + c^2.$$

Since z is also a rotated version of p_2 (and also of p_1), it follows that $\|z\| = \|p_2\| = \|p_1\|$. Solving the above for c^2, z can now be written

$$z = (p_1^T \omega_1)\omega_1 + (p_2^T \omega_2)\omega_2 \pm \sqrt{\|p_2\|^2 - (p_1^T \omega_1)^2 - (p_2^T \omega_2)}(\omega_1 \times \omega_2).$$

If $c = 0$ then there exists a unique solution (θ_1, θ_2), while if c does not exist, then no solution (θ_1, θ_2) exists.

Having found up to two possible solutions for z, what remains is to find θ_1 and θ_2 for each z. This is relatively straightforward: letting u_1 and z_1 respectively be the projections of p_1 and z onto circle 1, and u_2 and z_2 respectively be the projections of p_2 and z onto circle 2, it follows that

$$\begin{aligned} \theta_1 &= \cos^{-1}(u_1^T z_1) \\ \theta_2 &= \cos^{-1}(u_2^T z_2). \end{aligned}$$

Step 3: Solve for θ_4, θ_5, and θ_6

Having found θ_1, θ_2, and θ_3, it remains to solve for θ_4, θ_5, and θ_6. We have

$$\begin{aligned} e^{[S_4]\theta_4} e^{[S_5]\theta_5} e^{[S_6]\theta_6} &= e^{-[S_3]\theta_3} e^{-[S_2]\theta_2} e^{-[S_1]\theta_1} X M^{-1} \\ &= X_2, \end{aligned} \tag{6.11}$$

where the right-side X_2 is now known. Recall that $\omega_4^T\omega_5 = 0$ and $\omega_5^T\omega_6 = 0$; this implies that ω_4 and ω_6 are either orthogonal or parallel. Assume for the time being that ω_6 is orthogonal to ω_4, or more precisely, $\omega_6 = \omega_4 \times \omega_5$ (the parallel case will be considered later). Define the transformation

$$T_w = \begin{bmatrix} R_w & r_w \\ 0 & 1 \end{bmatrix}, \quad R_w = \begin{bmatrix} \omega_6 & -\omega_5 & \omega_4 \end{bmatrix} \in SO(3).$$

Multiplying both sides of (6.11) by T_w^{-1} leads to

$$\begin{aligned} T_w^{-1} e^{[S_4]\theta_4} e^{[S_5]\theta_5} e^{[S_6]\theta_6} &= T_w^{-1} X_2 \\ e^{T_w^{-1}[S_4]T_w\theta_4} e^{T_w^{-1}[S_5]T_w\theta_5} e^{T_w^{-1}[S_6]T_w\theta_6} &= T_w^{-1} X_2 T_w. \end{aligned}$$

Noting that $T_w^{-1}[S_i]T_w$ is the 4×4 matrix representation of the adjoint mapping $Ad_{T_w^{-1}}(S_i)$, it can be verified by calculation that

$$\begin{aligned} Ad_{T_w^{-1}}(S_6) &= \begin{bmatrix} 0 & 0 & 0 & 0 \\ 0 & 0 & -1 & 0 \\ 0 & 1 & 0 & 0 \\ 0 & 0 & 0 & 0 \end{bmatrix} \\ Ad_{T_w^{-1}}(S_5) &= \begin{bmatrix} 0 & 0 & 1 & 0 \\ 0 & 0 & 0 & 0 \\ -1 & 0 & 0 & 0 \\ 0 & 0 & 0 & 0 \end{bmatrix} \\ Ad_{T_w^{-1}}(S_4) &= \begin{bmatrix} 0 & -1 & 0 & 0 \\ 1 & 0 & 0 & 0 \\ 0 & 0 & 0 & 0 \\ 0 & 0 & 0 & 0 \end{bmatrix}. \end{aligned}$$

As long as the translational component of $T_w^{-1}X_1T_w$ is zero, the solution $(\theta_4, \theta_5, \theta_6)$ can now be obtained from the following:

$$\mathrm{Rot}(\hat{z}, \theta_1) \cdot \mathrm{Rot}(\hat{y}, \theta_2) \cdot \mathrm{Rot}(\hat{x}, \theta_3) = \bar{R},$$

where $\bar{R}$ is the rotational component of $T_w^{-1}X_1T_w$. The solution $(\theta_4, \theta_5, \theta_6)$ therefore corresponds to the ZYX Euler angles that parametrize $\bar{R}$:

$$\begin{aligned} \theta_5 &= \mathrm{atan2}(-\bar{r}_{31}, \pm\sqrt{\bar{r}_1 1^2 + \bar{r}_{21}^2}) \\ \theta_4 &= \mathrm{atan2}(\bar{r}_{21}, \bar{r}_{11}) \\ \theta_6 &= \mathrm{atan2}(\bar{r}_{32}, \bar{r}_{33}), \end{aligned}$$

where $\bar{r}_{ij}$ denotes the ij-th entry of $\bar{R}$. Recall that there are two solutions determined by the choice of sign for θ_5.

The above derivation can be repeated for the case when ω_6 and ω_4 are parallel, in which case the solutions $(\theta_4, \theta_5, \theta_6)$ will now correspond to the ZYZ Euler angles.

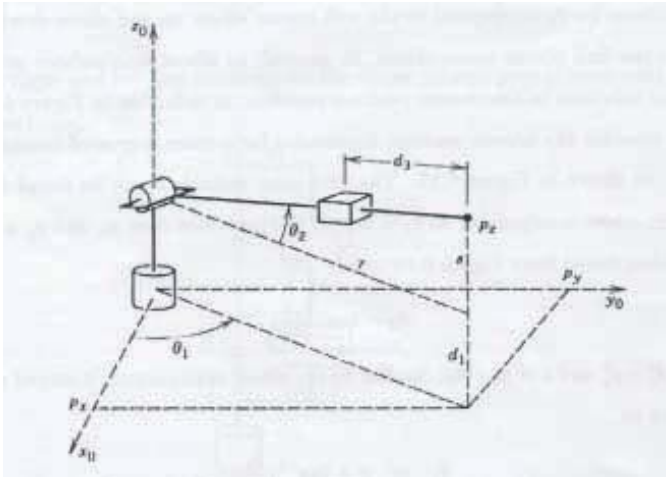

Figure 6.9: The first three joints of a Stanford-type arm.

Like the earlier 6R PUMA-type arm, since there are up to two possible solutions for θ_3, and also for (θ_1, θ_2) and $(\theta_4, \theta_5, \theta_6)$, for the generalized PUMA-type robot arm one can expect up to $2 \times 2 \times 2 = 8$ possible inverse kinematic solutions.

6.1.3 Stanford-Type Arms

If the elbow joint in a 6R PUMA-type arm is replaced by a prismatic joint as shown in Figure 6.9, we then have a Stanford-type arm. Here we consider the inverse position kinematics for the arm of Figure 6.9; the inverse orientation kinematics is identical to that for the PUMA-type arm and is not repeated here.

The first joint variable θ_1 an be found in a similar fashion to the PUMA-type arm: $\theta_1 = \tan^{-1}(\frac{p_y}{p_x})$ (provided that p_x and p_y are not both zero). θ_2 is then found from Figure 6.9 to be

$$\theta_2 = \tan^{-1}(\frac{s}{r})$$

where $r^2 = p_x^2 + p_y^2$ and $s = p_z - d_1$. Similar to the PUMA-type arm, a second solution for θ_1, θ_2 is given by

$$\begin{aligned} \theta_1 &= \pi + \tan^{-1}(\frac{p_y}{p_x}) \\ \theta_2 &= \pi - \tan^{-1}(\frac{p_y}{p_x}) \end{aligned}$$

The translation distance d_3 is found from the relation

$$(d_3 + a_2)^2 = r^2 + s^2$$

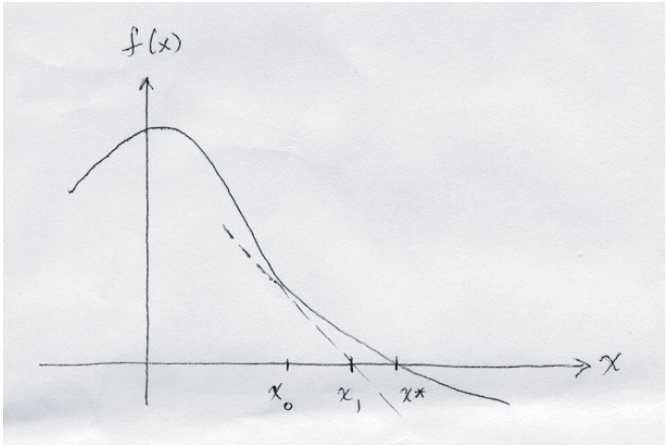

Figure 6.10: The Newton-Raphson method for nonlinear root-finding.

as

$$\begin{aligned} d_3 &= \sqrt{r^2 + s^2} \\ &= \sqrt{p_x^2 + p_y^2 + (p_z - d_1)^2} - a_2 \end{aligned}$$

Ignoring the negative square root solution for d_3, we obtain two solutions to the inverse position kinematics as long as the wrist center p does not intersect the z-axis of the fixed frame. If there is an offset, then as in the case of the PUMA-type arm there will be a left and right arm solution.

If the elbow joint in the **generalized** 6R PUMA-type arm is replaced by a prismatic joint, the resulting arm is then referred to as a **generalized Stanford-type arm**. The inverse kinematics proceeds in the same way as for the generalized PUMA-type arm; the only difference occurs in the first step (obtaining θ_3). The screw vector for the third joint now becomes $\mathcal{S}_3 = (0, v_3)$, with $\|v_3\| = 1$, and θ_3 is found by solving the equation

$$\|e^{[\mathcal{S}_3]\theta_3} p\| = c,$$

for some given $p \in \mathbb{R}^3$ and nonnegative positive scalar c. The above equation reduces to solving the following quadratic in θ_3:

$$\theta_3^2 + 2(p^T v_3)\theta_3 + (\|p\|^2 - c^2) = 0.$$

Imaginary, as well as negative solutions, naturally should be excluded.

6.2 Numerical Inverse Kinematics

In cases where the inverse kinematics equations do not admit analytic solutions, one must resort to numerical methods. Even in cases where an analytic solution

exists, numerical methods are often used to improve the accuracy of these solutions. For example, in a generalized PUMA-type arm, the last three axes may not exactly intersect at a common point, and the shoulder joint axes may not be exactly orthogonal. In such cases, rather than throw away any analytic inverse kinematic solutions that are available, such solutions can be used as the initial point in an iterative procedure for numerically solving the inverse kinematics.

There exist a variety of iterative methods for finding the roots of a nonlinear equation, and our aim is not to discuss these in detail—any text on numerical analysis will cover these methods in depth—but rather to develop ways in which to transform the inverse kinematics equations such that they are amenable to existing numerical methods.

However, it is useful to review at least one fundamental approach, the Newton-Raphson method. Suppose we wish to find the roots of the nonlinear equation $f(x) = 0$, where $f : \mathbb{R}^n \to \mathbb{R}^n$ is assumed twice differentiable. To first-order, $f(x)$ can be approximated about a point $x_0 \in \mathbb{R}^n$ by

$$f(x) \approx f(x_0) + \frac{\partial f}{\partial x}(x_0)(x - x_0) \tag{6.12}$$

where

$$\frac{\partial f}{\partial x}(x_0) = \begin{bmatrix} \frac{\partial f_1}{\partial x_1}(x_0) & \cdots & \frac{\partial f_1}{\partial x_n}(x_0) \\ \vdots & \ddots & \vdots \\ \frac{\partial f_n}{\partial x_1}(x_0) & \cdots & \frac{\partial f_n}{\partial x_n}(x_0) \end{bmatrix} \in \mathbb{R}^{n \times n}. \tag{6.13}$$

Setting $f(x) = 0$ and assuming $\frac{\partial f}{\partial x}(x_0)$ is invertible, we have

$$x = x_0 - \left(\frac{\partial f}{\partial x}(x_0) \right)^{-1} f(x_0). \tag{6.14}$$

If $f(x)$ is approximated in a neighborhood of x_0 by a linear function, then the root is given by the expression for x above.

The basic idea behind the Newton-Raphson method is make successive linear approximations of $f(x)$ as indicated (see Figure 6.10). Given an initial guess x_0, we approximate $f(x)$ in a neighborhood of x_0 by a linear function, and find the root; call this root x_1. $f(x)$ is then linearly approximated in a neighborhood of x_1 as before, and the root determined; call this root x_2. This iteration is successively repeated until some convergence criterion is satisfied, *e.g.*, the difference $\|x_{k+1} - x_k\| < \epsilon$ for some threshold $\epsilon \in \mathbb{R}$, or the function value itself is below some threshold $\|f(x_{k+1})\| < \epsilon$.

There exist many refinements to the above basic Newton-Raphson method, which we do not discuss here. Our focus will be to transform the inverse kinematics equations in a form that is amenable to numerical solution. For a six degree-of-freedom open chain, we will first have to reformulate the kinematic equations in the form $f : \mathbb{R}^6 \to \mathbb{R}^6$. There are several ways to do this.

Given $T(\theta) = X$, where $\theta \in \mathbb{R}^6$, $T(\cdot)$ represents the forward kinematics, and $X \in SE(3)$ is the given end-effector frame location, we first transform this equation to either $T(\theta)X^{-1} = I$ or $X^{-1}T(\theta) = I$. One way to reduce this to a

set of six independent equations is to take the matrix logarithm of both sides, i.e.,

$$\log X^{-1}T(\theta) = G(\theta) = 0. \tag{6.15}$$

It quickly becomes apparent that the $G(\theta)$ obtained via the logarithm will be quite complicated. In fact, the situation does not improve measurably if other parametrizations, e.g., using Euler angles for the rotation component, are used. Also, any numerical method will at some point need to differentiate $G(\theta)$, if not analytically, then via a finite difference approximation scheme.

One way to avoid these difficulties is to attempt to directly formulate a Newton-Raphson algorithm for open chain kinematics that explicitly uses the Jacobian. We now do so for the body Jacobian. Recall that the body Jacobian is obtained from

$$[\mathcal{V}_b] = T^{-1}\dot{T} = [J_b(\theta)\dot{\theta}],$$

where $J_b(\theta) \in \mathbb{R}^{6\times 6}$. Let us write these two equations in the following differential form:

$$[\mathcal{V}_b]\,\triangle t = T^{-1}\triangle T = [J_b(\theta)\,\triangle\theta]. \tag{6.16}$$

Suppose we have some initial guess $\theta_0 \in \mathbb{R}^6$. Since our objective is to find, for a given $X \in SE(3)$, θ that satisfies $X = T(\theta)$, we set T^{-1} in the previous equation to X^{-1}, and $\triangle T$ to $X - T(\theta_0)$. Making these substitutions, $[\mathcal{V}_b]\,\triangle t = T^{-1}\triangle T$ can be written

$$[\mathcal{V}_b]\,\triangle t = X^{-1}(X - T(\theta_0)) = I - X^{-1}T(\theta_0). \tag{6.17}$$

Let us further make a first-order approximation to $X^{-1}T(\theta_0)$ in terms of the exponential map. That is, suppose

$$\begin{aligned} X^{-1}T(\theta_0) &= e^{[\mathcal{S}]} \\ &= I + [\mathcal{S}] + \frac{1}{2!}[\mathcal{S}]^2 + \ldots, \end{aligned}$$

where $[\mathcal{S}] = \log \mathcal{X}^{-\infty}\mathcal{T}(\theta_\prime)$. Ignoring second and higher order terms,

$$X^{-1}T(\theta_0) \approx I + [\mathcal{S}],$$

With these substitutions, Equation (6.16) becomes

$$J_b(\theta)\,\triangle\theta = \mathcal{S}, \;\; [S] = \log X^{-1}T(\theta_0).$$

The above suggests the following algorithm for solving $T(\theta) = X$:

(i) **Initialization**: Given $X \in SE(3)$ and initial guess $\theta \in \mathbb{R}^6$.

(ii) While $\|X - T(\theta)\| > \epsilon$ do:

- Set $[\mathcal{S}] = \log X^{-1}T(\theta)$;
- Solve $J_b(\theta)\,\triangle\theta = \mathcal{S}$ for $\triangle\theta$;

- Set $\theta \leftarrow \theta + \triangle\theta$.

The above algorithm could also have been formulated in terms of the spatial Jacobian $J_s(\theta)$; the corresponding numerical inverse kinematics algorithm is as follows:

(i) **Initialization**: Given $X \in SE(3)$ and initial guess $\theta \in \mathbb{R}^6$.

(ii) While $\|X - T(\theta)\| > \epsilon$ do:

- Set $[\mathcal{S}] = \log T(\theta)X^{-1}$;
- Solve $J_s(\theta)\,\triangle\theta = \mathcal{S}$ for $\triangle\theta$;
- Set $\theta \leftarrow \theta + \triangle\theta$.

6.3 Inverse Kinematics of Redundant Open Chains

We close this chapter with a brief look at the inverse kinematics problem for redundant open chains. A spatial open chain is said to be kinematically redundant if it has mobility greater than six; in this case the inverse kinematics problem $X = T(\theta)$, where $\dim(\theta) > 6$, has in general an infinite number of solutions for any given X. An analytical characterization of all possible solutions is difficult, even with simplifying assumptions on the kinematic structure. Our focus in this section will therefore be on solving the differential version of the inverse kinematics problem: given a desired end-effector spatial velocity $\mathcal{V}$, the goal is to find a suitable joint velocity $\dot{\theta}$ that satisfies $\mathcal{V} = J(\theta)\dot{\theta}$ (this equation can be expressed in either space or body frame coordinates). Because $J(\theta) \in \mathbb{R}^{6\times n}$ with $n > 6$, there exists an $(n-6)$-parameter family of solutions for $\dot{\theta}$.

One solution for $\dot{\theta}$ that is both convenient and physically meaningful is the minimum norm solution, which we now describe. Among the many solutions to $\mathcal{V} = J(\theta)\dot{\theta}$, suppose we seek the $\dot{\theta}$ with the smallest norm $\|\dot{\theta}\|$ that satisfies $V\ J(\theta)\dot{\theta}$, where the norm $\|\cdot\|$ is defined in the more general form

$$\|\dot{\theta}\| = \sqrt{\dot{\theta}^T Q \dot{\theta}}$$

for some symmetric and positive definite matrix $Q \in \mathbb{R}^{n\times n}$. For example, if all of the joint actuators are identical, a reasonable choice for Q is the identity matrix. If the actuators have different sizes (in the sense of maximum attainable velocities, for example), then Q can be chosen to be a diagonal matrix, with each diagonal entry proportional to the size of its corresponding actuator.

The minimum-norm solution is well-known (consult any linear algebra textbook):

$$\dot{\theta} = QJ^T(JQJ^T)^{-1}\mathcal{V}.$$

That this $\dot{\theta}$ satisfies $J(\theta)\dot{\theta} = \mathcal{V}$ can be verified by direct substitution. Note that $JQJ^T \in \mathbb{R}^{6\times 6}$, so that as long as $J(\theta)$ is of maximal rank six (which is equivalent to the robot arm not being in a kinematically singular configuration),

JQJ^T will always be nonsingular. If joint values $\theta(t)$ are required, the following iteration can be used:

$$\theta(t + \triangle t) = \theta(t) + \triangle t \left(QJ(\theta(t))^T (J(\theta(t))QJ(\theta(t))^T)^{-1} \right) \mathcal{V}(t),$$

where $\mathcal{V}(t)$ is the desired spatial velocity profile for the end-effector frame. This inverse kinematics solution is useful when desired trajectories for the end-effector frame, $X(t) \in SE(3)$, are given over some time interval $[t_0, t_1]$, and we wish to determine the corresponding joint trajectory $\theta(t)$.

6.4 Summary

- Given a spatial open chain with forward kinematics $T(\theta)$, $\theta \in \mathbb{R}^n$, in the inverse kinematics problem one seeks to find, for some given $X \in SE(3)$, solutions θ that satisfy $X = T(\theta)$. Unlike the forward kinematics, the inverse kinematics problem can possess multiple solutions, or no solutions in the event that X lies outside the task space. For a spatial open chain, $n \leq 6$ typically leads to a finite number of inverse kinematic solutions, while $n > 6$ leads to an infinite number of solutions.

- The inverse kinematics can be solved analytically for a large class of open chains that possess some degree of structure. One important class is the generalized $6R$ PUMA-type arm; such an arm consists of a $3R$ orthogonal axis wrist connected to a $2R$ orthogonal axis shoulder by an elbow joint. Geometric algorithms have been developed for this class of arms that exploits the product of exponentials forward kinematics representation. Further assumptions on the joint axes, e.g., joint axes 2 and 3 are always parallel, lead to simpler analytic forms for the inverse kinematics.

- Another class of open chains that admit analytic inverse kinematic solutions are Stanford-type arms; these arms are obtained by replacing the elbow joint in the generalized $6R$ PUMA-type arm by a prismatic joint. Geometric inverse kinematic algorithms similar to those for PUMA-type arms have also been developed.

- Iterative numerical methods are used in cases where analytic inverse kinematics solutions are not available. These typically involve solving the inverse kinematics equations through an iterative procedure like the Newton-Raphson method, and require an initial point to be supplied. The performance of the iterative procedure depends to a large extent on the quality of the initial point, and only one inverse kinematic solution is produced per iteration. An iterative procedure based on the Jacobian of the forward kinematics has been developed for general six degree-of-freedom spatial open chains.

- In cases where $n > 6$, typically there exists an infinite number of solutions to the inverse kinematics. For such kinematically redundant open

chains, it is useful to consider the differential inverse kinematics problem: given some desired end-effector velocity profile $\mathcal{V}(t)$ and a current posture $\theta \in \mathbb{R}^n$, find the joint velocity vector $\dot{\theta}$ that satisfies $\mathcal{V} = J(\theta)\dot{\theta}$. While an infinite number of solutions $\dot{\theta}$ also exists in this case, the **minimum norm** solution is one particularly useful and convenient solution: it is the smallest joint velocity $\dot{\theta}$, in the sense of minimizing $\dot{\theta}^T Q \dot{\theta}$ for some given symmetric positive-definite $Q \in \mathbb{R}^{n \times n}$, that satisfies $\mathcal{V} = J(\theta)\dot{\theta}$. The explicit form of the solution $\dot{\theta}$ is given by

$$\dot{\theta} = QJ^T(JQJ^T)^{-1}\mathcal{V}.$$

Based on the above solution to the differential inverse kinematics, an iterative procedure for solving the inverse kinematics at discrete times can be obtained as follows:

$$\theta(t + \triangle t) = \theta(t) + \triangle t \left(QJ(\theta(t))^T (J(\theta(t))QJ(\theta(t))^T)^{-1}\right) \mathcal{V}(t).$$

One issue to be aware of in inverse kinematics schemes like the above is repeatability: when the end-effector frame is a periodic closed path, in principle one would also want the robot arm posture to follow a periodically repeating trajectory. Any iterative inverse kinematics scheme for redundant arms must satisfy a further set of conditions to be repeatabe.

6.5 Notes and References

The inverse kinematics of the most general $6R$ open chain is known to have up to 16 solutions; this result was first proved by Lee and Liang [15], and also by Raghavan and Roth [33]. Iterative numerical procedures for finding all sixteen solutions of a general $6R$ open chain are reported in [18]. A summary of inverse kinematics methods for kinematically redundant robot arms are discussed in [37]. The repeatability conditions for kinematically redundant inverse kinematics schemes are examined in [36].

Chapter 7

Kinematics of Closed Chains

Any kinematic chain that contains one or more loops is called a **closed chain**. Several examples of closed chains were encountered in Chapter 2, from the planar four-bar linkage to spatial mechanisms like the Stewart-Gough platform. In this chapter we shall analyze the kinematics of closed chains, paying special attention to a class of closed chains that we shall refer to as **parallel mechanisms**; these are closed chains consisting of a fixed and moving platform connected by a set of "legs"; these legs are mostly open chains, but sometimes can themselves be closed chains.

Figures 7.1-7.3 depict some well-known parallel mechanisms. The Stewart-Gough Platform is a six degree of freedom mechanism, used widely as both a motion simulator and six-axis force-torque sensor. It is typically realized as either a $6 \times UPS$ or $6 \times SPS$ platform; note that the additional torsional rotations of each of the six legs in the $6 \times SPS$ platform have no effect on the moving platform. When used as a force-torque sensor, the six prismatic joints experience internal linear forces whenever any external force is applied to the moving platform; by measuring these internal linear forces one can estimate the applied external force. The Delta robot is a three degree of freedom mechanism that has the unusual feature of the moving platform always remaining parallel to the fixed platform. Because the three actuators are all attached to the three revolute joints of the fixed upper platform, the moving parts are relatively light; this allows the Delta to achieve very fast motions. The Eclipse mechanism is another six degree of freedom parallel mechanism whose moving platform is capable of $\pm 90^\circ$ orientations with respect to ground, and also of rotating 360° about the vertical axis.

Closed chains admit a much greater variety of designs than open chains, and not surprisingly their kinematic analysis is considerably more complicated. This can be traced to two defining features of closed chains: (i) the configuration space is curved (e.g., a multidimensional surface embedded in a higher-

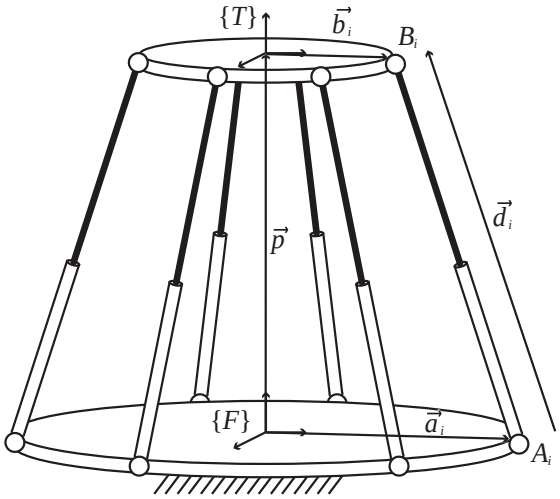

Figure 7.1: The Stewart-Gough platform.

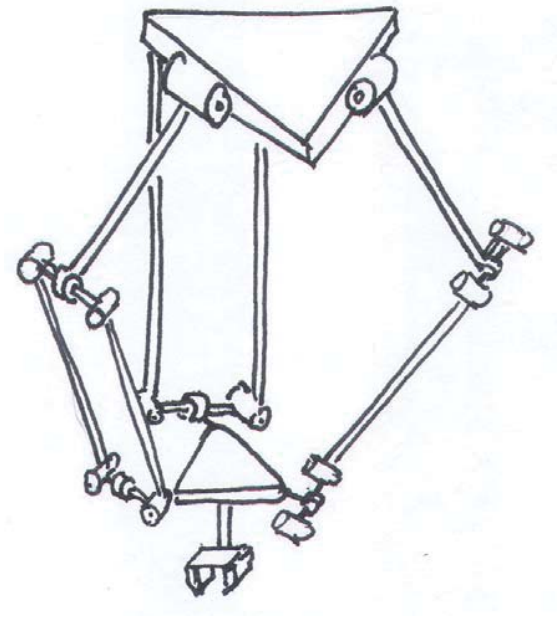

Figure 7.2: The Delta robot.

dimensional vector space), and (ii) not all of the joints are actuated. The presence of such non-actuated, or passive joints, together with the fact that the number of actuated joints may deliberately exceed the mechanism's kinematic

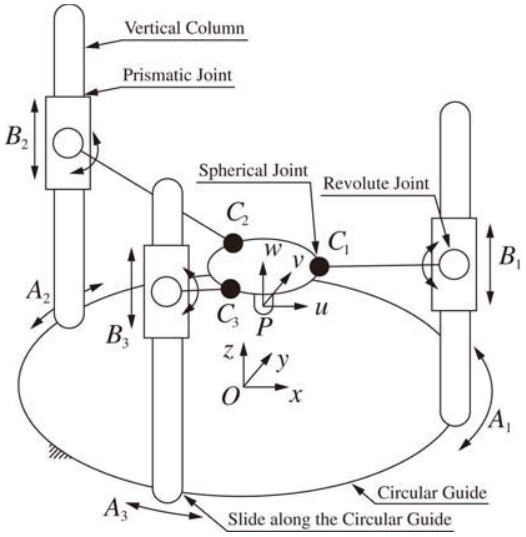

Figure 7.3: The Eclipse mechanism.

degrees of freedom—such mechanisms are said to be **redundantly actuated**—makes not only the position and differential kinematics analysis more challenging, but also introduces new types of singularities not witnessed in open chains.

Recall also that for open chains, the kinematic analysis proceeds in a more or less straightforward fashion with the formulation of the forward kinematics (*e.g.*, via the product of exponentials formalism) followed by that of the inverse kinematics. For general closed chains it is usually difficult to obtain an explicit set of equations for the forward kinematics in the form $X = T(\theta)$, where $X \in SE(3)$ is the end-effector frame and $\theta \in \mathbb{R}^n$ are the joint coordinates. The most effective approaches for closed chain kinematic analysis are based on a collection of tools and methodologies that exploit as much as possible any kinematic symmetries and other special features of the mechanism.

For this reason we shall proceed in this chapter with a series of case studies involving some well-known parallel mechanisms, and eventually build up a repetoire of kinematic analysis tools and methodologies that can be synthesized to handle more general closed chains. We shall consider only parallel mechanisms that are exactly actuated, i.e., the number of actuated degrees of freedom is equal to the mechanism's kinematic mobility. Methods for the forward and inverse position kinematics of parallel mechanisms are discussed, followed by the characterization and derivation of the constraint Jacobian, and the Jacobians of both the inverse and forward kinematics. The chapter concludes with an examination of the various kinematic singularities that can arise in closed chains.

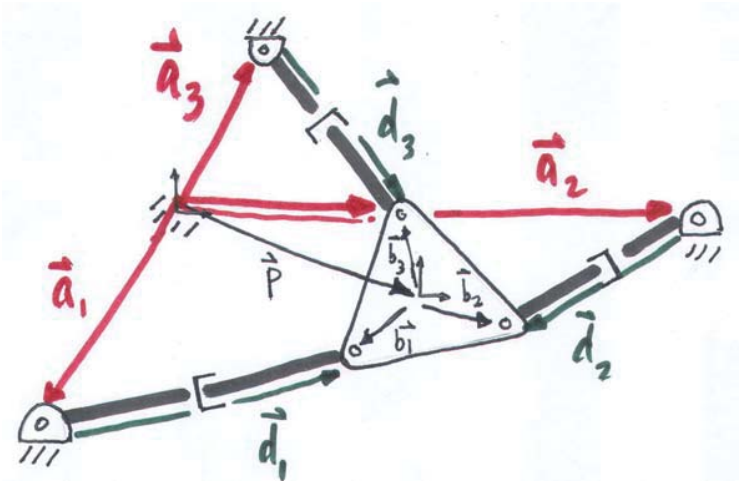

Figure 7.4: A three degree-of-freedom $3 \times RPR$ planar parallel mechanism.

7.1 Inverse and Forward Kinematics

This section examines methods for the inverse and forward kinematics of closed chains. Rather than attempt to develop a general methodology applicable to all types of closed chains, we consider two case studies, the $3 \times RPR$ planar parallel mechanism, and its spatial counterpart, the $3 \times SPS$ Stewart-Gough platform. The analysis of these two mechanisms draws upon some reduction techniques that result in a reduced form of the governing kinematic equations. We briefly describe how these methods can be generalized to the analysis of more general parallel mechanisms.

7.1.1 $3\times$RPR Planar Parallel Mechanism

The first example we consider is the planar $3 \times RPR$ parallel mechanism shown in Figure 7.4. It is easily verified from the planar version of Gruebler's formula that this mechanism has mobility three. Assign a fixed frame $\{s\}$ and end-effector frame $\{b\}$ as shown. Typically the three prismatic joints are actuated; denote the lengths of each of the three legs by s_i, $i = 1, 2, 3$. The forward kinematics problem is to determine, from given values of $s = (s_1, s_2, s_3)$, the end-effector frame's position and orientation.

Let $\vec{p}$ be the vector from the origin of the $\{s\}$ frame to the origin of the $\{b\}$ frame. Let ϕ denote the angle measured from the $\hat{x}$ axis of the $\{s\}$ frame to the $\{x\}$ axis of the $\{b\}$ frame. Further define the vectors $\vec{a}_i$, $\vec{b}_i$, $\vec{d}_i$, $i = 1, 2, 3$ as shown in the figure. From these definitions, clearly

$$\vec{d}_i = \vec{p} + \vec{b}_i - \vec{a}_i, \tag{7.1}$$

for $i = 1, 2, 3$. Let

$$\begin{aligned}
\begin{bmatrix} p_x \\ p_y \end{bmatrix} &= \vec{p} \text{ in } \{s\} \text{ frame coordinates} \\
\begin{bmatrix} a_{ix} \\ a_{iy} \end{bmatrix} &= \vec{a}_i \text{ in } \{s\} \text{ frame coordinates} \\
\begin{bmatrix} d_{ix} \\ d_{iy} \end{bmatrix} &= \vec{d}_i \text{ in } \{s\} \text{ frame coordinates} \\
\begin{bmatrix} b_{ix} \\ b_{iy} \end{bmatrix} &= \vec{b}_i \text{ in } \{b\} \text{ frame coordinates.}
\end{aligned}$$

Note that the vectors (a_{ix}, a_{iy}), (b_{ix}, b_{iy}), $i = 1, 2, 3$ are constant, and that with the exception of (b_{ix}, b_{iy}), all other vectors are expressed in $\{s\}$ frame coordinates. To express Equation (7.1) in terms of $\{s\}$ frame coordinates, it is first necessary to find the $\{s\}$ frame representation of the vector $\vec{b}_i$. This is straightforward: defining

$$R_{sb} = \begin{bmatrix} \cos\phi & -\sin\phi \\ \sin\phi & \cos\phi \end{bmatrix},$$

it now follows that

$$\begin{bmatrix} d_{ix} \\ d_{iy} \end{bmatrix} = \begin{bmatrix} p_x \\ p_y \end{bmatrix} + \begin{bmatrix} \cos\phi & -\sin\phi \\ \sin\phi & \cos\phi \end{bmatrix} \begin{bmatrix} b_{ix} \\ b_{iy} \end{bmatrix} - \begin{bmatrix} a_{ix} \\ a_{iy} \end{bmatrix},$$

for $i = 1, 2, 3$. Also, since $s_i^2 = d_{ix}^2 + d_{iy}^2$, we have

$$\begin{aligned}
s_i^2 &= (p_x + b_{ix}\cos\phi - b_{iy}\sin\phi - a_{ix})^2 \\
&\quad +(p_y + b_{ix}\sin\phi + b_{iy}\cos\phi - a_{iy})^2,
\end{aligned}$$

for $i = 1, 2, 3$.

Formulated as above, the inverse kinematics is trivial to compute: given values for (p_x, p_y, ϕ), the leg lengths (s_1, s_2, s_3) can be directly calculated from the above equations (negative values of s_i in most cases will not be physically realizable, and can be ignored). The forward kinematics problem, in contrast, is not trivial: here the objective is to determine, for given values of (s_1, s_2, s_3), the end-effector frame's position and orientation (p_x, p_y, ϕ). The following tangent half-angle substitution, widely used in kinematic analysis, transforms the above three equations into a system of polynomials in the newly defined scalar variable t:

$$\begin{aligned}
t &= \tan\frac{\phi}{2} \\
\sin\phi &= \frac{2t}{1+t^2} \\
\cos\phi &= \frac{1-t^2}{1+t^2}.
\end{aligned}$$

After considerable algebraic manipulation, this system of polynomials can eventually be reduced to a single sixth-order polynomial in t, which effectively shows that the $3 \times RPR$ mechanism may have up to six forward kinematics solutions (showing that six real solutions are possible requires further verification, which we do not pursue here).

7.1.2 Stewart-Gough Platform

We now examine the inverse and forward kinematics of the $6 \times SPS$ Stewart-Gough platform of Figure 7.1. In this design, the fixed and moving platforms are connected by six serial SPS structures, with the spherical joints passive, and the prismatic joints actuated. The derivation of the kinematic equations closely parallels that of our earlier planar $3 \times RPR$ mechanism. Let $\{s\}$ and $\{b\}$ denote the fixed and end-effector frames, respectively, and let $\vec{d_i}$ be the vector directed from joint A_i to joint B_i. Referring to Figure 7.1, we make the following definitions:

- $p \in \mathbb{R}^3 = \vec{p}$ in $\{s\}$ frame coordinates;
- $a_i \in \mathbb{R}^3 = \vec{a}_i$ in $\{s\}$ frame coordinates;
- $b_i \in \mathbb{R}^3 = \vec{b}_i$ in $\{b\}$ frame coordinates;
- $d_i \in \mathbb{R}^3 = \vec{d_i}$ in $\{s\}$ frame coordinates.
- $R \in SO(3)$ = orientation of $\{b\}$ as seen from $\{s\}$.

In order to derive the kinematic constraint equations, note that vectorially,

$$\vec{d_i} = \vec{p} + \vec{b}_i - \vec{a}_i, \quad i = 1, \ldots, 6.$$

Writing the above equations explicitly in $\{s\}$ frame coordinates,

$$d_i = p + Rb_i - a_i, \quad i = 1, \ldots, 6.$$

Denoting the length of leg i by s_i, we have

$$s_i^2 = d_i^T d_i = (p + Rb_i - a_i)^T (p + Rb_i - a_i),$$

for $i = 1, \ldots, 6$. Observe that a_i and b_i as defined above are all known constant vectors. Having written the constraint equations in this form, the inverse kinematics now becomes straightforward: given p and R, the six leg lengths s_i, $i = 1, \ldots, 6$ can be evaluated directly from the above equations (negative values of s_i in most cases will not be physically realizable, and can be ignored).

The forward kinematics is not as straightforward. Here we are given each of the leg lengths s_i, $i = 1, \ldots, 6$, and must solve for $p \in \mathbb{R}^3$ and $R \in SO(3)$. The six constraint equations, together with the rotation matrix constraint $R^T R = I$, constitute a set of twelve equations in twelve unknowns. Several methods exist for finding all solutions to such a set of polynomial equations, e.g., methods

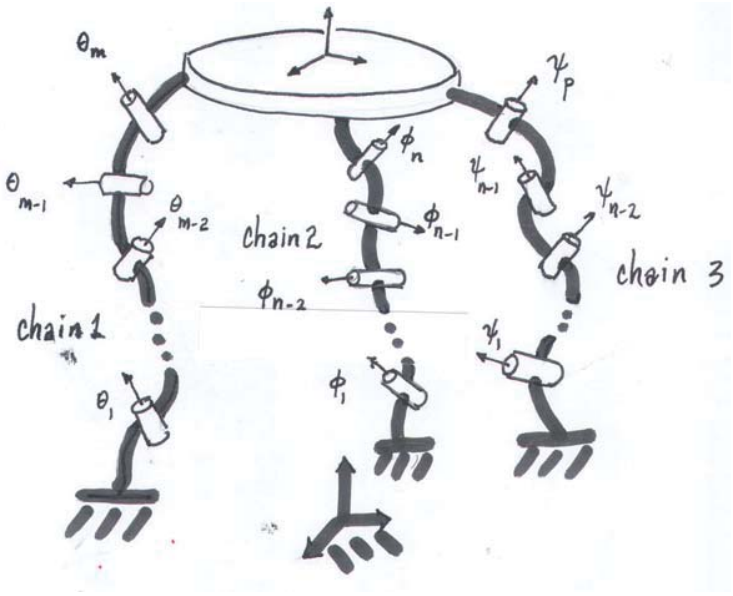

Figure 7.5: A general spatial parallel mechanism.

based on dialytic elimination, Grobner bases, etc. Of particular note is the work of Raghavan and Roth [**?**], who show that there can be at most forty solutions to the forward kinematics, and Husty [**?**], who develops a computational algorithm for finding all forty solutions analytically.

7.1.3 General Parallel Mechanisms

For both the $3 \times RPR$ mechanism and Stewart-Gough Platform, we were able to exploit certain features of the mechanism that resulted in a reduced set of equations; for example, in the case of the Stewart-Gough Platform, the fact that each of the "legs" can be modelled as straight lines considerably simplified the analysis. In this brief section we consider the more general case where the legs have the structure of an arbitrary open chain.

Consider such a parallel mechanism as shown in Figure 7.5; here the fixed and moving platforms are connected by three open chains. Denote the forward kinematics of the three chains by $T_1(\theta)$, $T_2(\phi)$, and $T_3(\psi)$, respectively, where $\theta \in \mathbb{R}^m$, $\phi \in \mathbb{R}^n$, and $\psi \in \mathbb{R}^p$. The loop closure conditions can be written

$$T_1(\theta) = T_2(\phi) \tag{7.2}$$
$$T_2(\phi) = T_3(\psi). \tag{7.3}$$

Equation 7.2 and 7.3 each consists of 12 equations (9 for the rotation component and 3 for the position component), 6 of which are independent (recall that the nine equations for the rotation component can be reduced to a set of three

independent equations from the rotation matrix constraint, i.e., $R^T R = I$); there are thus 24 equations, 12 of which are independent, with $n + m + p$ unknown variables, and the mobility of the mechanism is $d = 12 - (n + m + p)$.

In the forward kinematics problem, given values for d of the joint variables (θ, ϕ, ψ), Equations 7.2 and 7.2 can be solved for the remaining joint variables; note that multiple solutions will be likely. Once the joint values for any one of the open chain legs are known, the forward kinematics of that leg can then be evaluated to determine the forward kinematics of the closed chain.

In the inverse kinematics problem, we are given the end-effector frame displacement $T \in SE(3)$. Setting $T = T_1 = T_2 = T_3$, the objective is to solve Equations 7.2 and 7.2 for all the joint variables (θ, ϕ, ψ). As hinted by the case studies, for most parallel mechanisms there are often features of the mechanism that can be exploited to eliminate some of these equations, and to simplify them into a reduced form.

7.2 Differential Kinematics

We now consider the differential kinematics of parallel mechanisms. Unlike differential kinematics for open chains, in which the objective was to relate the input joint velocities to the spatial velocity of the end-effector frame, the analysis for closed chains is complicated by the fact that not all of the joints are actuated. Only the actuated joints can be prescribed input velocities; the velocities of the remaining passive joints must then be determined from the kinematic constraint equations. These passive joint velocities are usually required to eventually determine the spatial velocity of the closed chain's end-effector frame.

For open chains, the Jacobian of the forward kinematics played a defining role in both velocity and static analysis. For closed chains, in addition to the forward kinematics Jacobian, the Jacobian defined by the kinematic constraint equations—for this reason we refer to this latter Jacobian as the **constraint Jacobian**—also plays a central role in velocity and static analysis. Much like the case for the inverse and forward kinematic analysis of parallel mechanisms, often there are features of the mechanism that can be exploited to simplify and reduce the procedure for obtaining the Jacobians. We therefore begin with a case study of the Stewart-Gough platform, and show that the Jacobian of the inverse kinematics can be obtained straightforwardly via static analysis. Velocity analysis for more general parallel mechanisms is then detailed.

7.2.1 Stewart-Gough Platform

Earlier we saw that the inverse kinematics for the Stewart-Gough platform can be solved analytically; that is, given the end-effector frame orientation $R \in SO(3)$ and position $p \in \mathbb{R}^3$, the leg lengths $s \in \mathbb{R}^6$ can be obtained analytically in the functional form $s = g(R, p)$. In principle this equation can be differentiated and manipulated to eventually produce a differential version, e.g.,

$$\dot{s} = G(R, p)V_s, \tag{7.4}$$

where $\dot{s} \in \mathbb{R}^6$ denotes the leg velocities, $V_s \in \mathbb{R}^6$ is the end-effector's spatial velocity in fixed frame coordinates, and $G(R,p) \in \mathbb{R}^{6\times 6}$ is the Jacobian of the inverse kinematics. This derivation, however, will likely involve considerable algebraic manipulation.

Here we take a different approach based on static analysis. Based on the same virtual work considerations that were used to determine the static relationship for open chains, the static relationship for closed chains (expressed in the fixed frame) is also given by $\tau = J_s^T F_s$, where τ is the vector of input joint torques, F_s is (the fixed frame representation of) the external spatial force applied at the end-effector frame, and J_s denotes the space Jacobian of the forward kinematics.

For the Stewart-Gough platform, note that the only forces being applied to the moving platform occur at the spherical joints. Let

$$f_i = \omega_i \tau_i$$

be the three-dimensional linear force applied by leg i, where $\omega_i \in \mathbb{R}^3$ is a unit vector indicating the direction of the applied force, and $\tau_i \in \mathbb{R}$ is the magnitude of the linear force; we emphasize that f_i is expressed in terms of the fixed frame coordinates. The moment generated by f_i, denoted m_i, is then given by

$$m_i = r_i \times f_i,$$

where $r_i \in \mathbb{R}^3$ denotes the vector from the fixed frame origin to the point of application of the force (spherical joint i in this case); again, both r_i and m_i are expressed in fixed frame coordinates. It is not too difficult to see that this same moment can also be expressed as

$$m_i = q_i \times f_i,$$

where $q_i \in \mathbb{R}^3$ denotes the vector from the fixed frame origin to the base of leg i, i.e., the joint connecting leg i to the fixed base. Expressing the moment as $q_i \times f_i$ is preferred, since q_i as defined is constant.

Combining f_i and m_i into a six-dimensional spatial force $F_i = (m_i, f_i)$, the resultant spatial force F_s on the moving platform is then given by

$$\begin{aligned} F_s &= \sum_{i=1}^{6} F_i = \sum_{i=1}^{6} \begin{bmatrix} r_i \times f_i \\ \omega_i \end{bmatrix} \tau_i \\ &= \begin{bmatrix} -\omega_1 \times q_1 & \cdots & -\omega_6 \times q_6 \\ \omega_1 & \cdots & \omega_6 \end{bmatrix} \begin{bmatrix} \tau_1 \\ \vdots \\ \tau_6 \end{bmatrix}. \end{aligned}$$

Since earlier we asserted that the static relationship for the Stewart-Gough platform is also of the form $\tau = J_s^T F_s$, based on the previous derivation we can conclude that the inverse Jacobian J_s^{-1} (or equivalently, the Jacobian of the inverse kinematics) is given by

$$J_s^{-1} = \begin{bmatrix} -\omega_1 \times q_1 & \cdots & -\omega_6 \times q_6 \\ \omega_1 & \cdots & \omega_6 \end{bmatrix}^T.$$

7.2.2 General Parallel Mechanisms

Because of its kinematic structure, the Stewart-Gough platform lends itself particularly well to a static analysis, as each of the six joint forces are directed along their respective legs. The Jacobian (or more precisely, the inverse Jacobian) can therefore be derived in terms of the screws associated with each line. In this section we consider more general parallel mechanisms where a static analysis is not as straightforward. Using the previous three-legged, three degree-of-freedom spatial parallel mechanism of Figure 7.5 as an example, we illustrate a general procedure for determining the forward kinematics Jacobian; generalizing this method to arbitrary parallel mechanisms should be completely straightforward.

The mechanism of Figure 7.5 consists of two platforms connected by three legs, with each leg a five degree of freedom open chain. For the given fixed and end-effector frames as indicated in the figure, we first write the forward kinematics for the three chains as follows:

$$\begin{aligned} T_1(\theta_1, \theta_2, \ldots, \theta_5) &= e^{[S_1]\theta_1} e^{[S_2]\theta_2} \cdots e^{[S_5]\theta_5} M_1 \\ T_2(\phi_1, \phi_2, \ldots, \phi_5) &= e^{[P_1]\phi_1} e^{[P_2]\phi_2} \cdots e^{[P_5]\phi_5} M_2 \\ T_3(\psi_1, \psi_2, \ldots, \psi_5) &= e^{[Q_1]\psi_1} e^{[Q_2]\psi_2} \cdots e^{[Q_5]\psi_5} M_3. \end{aligned}$$

The kinematic loop constraints can be expressed as

$$T_1(\theta) = T_2(\phi) \tag{7.5}$$
$$T_2(\phi) = T_3(\psi). \tag{7.6}$$

Taking right differentials of both sides of the above two equations, we have

$$\dot{T}_1 T_1^{-1} = \dot{T}_2 T_2^{-1} \tag{7.7}$$
$$\dot{T}_2 T_2^{-1} = \dot{T}_3 T_3^{-1}. \tag{7.8}$$

Since $\dot{T}_i T_i^{-1} = [V_i]$, where V_i is the spatial velocity of chain i's end-effector frame, the above identities can also be expressed in terms of the forward kinematics Jacobian for each chain:

$$J_1(\theta)\dot{\theta} = J_2(\phi)\dot{\phi} \tag{7.9}$$
$$J_2(\phi)\dot{\phi} = J_3(\psi)\dot{\psi}, \tag{7.10}$$

which can also be rearranged as

$$\begin{bmatrix} J_1(\theta) & -J_2(\phi) & 0 \\ 0 & -J_2(\phi) & J_3(\psi) \end{bmatrix} \begin{bmatrix} \dot{\theta} \\ \dot{\phi} \\ \dot{\psi} \end{bmatrix} = 0. \tag{7.11}$$

At this point we now rearrange the fifteen joints into those that are actuated, and those that are passive. Let us assume without loss of generality that the three actuated joints are $(\theta_1, \phi_1, \psi_1)$. Define the vector of actuated joints $q_a \in \mathbb{R}^3$

and passive joints $q_p \in \mathbb{R}^{12}$ as

$$q_a = \begin{bmatrix} \theta_1 \\ \phi_1 \\ \psi_1 \end{bmatrix}, \quad q_p = \begin{bmatrix} \theta_2 \\ \vdots \\ \phi_5 \end{bmatrix},$$

and $q = (q_a, q_p) \in \mathbb{R}^{15}$. Equation (7.11) can now be rearranged into the form

$$\begin{bmatrix} H_a(q) & H_p(q) \end{bmatrix} \begin{bmatrix} \dot{q}_a \\ \dot{q}_p \end{bmatrix} = 0, \tag{7.12}$$

or equivalently

$$H_a \dot{q}_a + H_p \dot{q}_p = 0, \tag{7.13}$$

where $H_a \in \mathbb{R}^{12\times 3}$ and $H_p \in \mathbb{R}^{12\times 12}$. If H_p is invertible, we have

$$\dot{q}_p = -H_p^{-1} H_a \dot{q}_a. \tag{7.14}$$

Assuming H_p is invertible, once the velocities of the actuated joints are given, the velocities of the remaining passive joints can be obtained uniquely via Equation 7.14.

It still remains to derive the forward kinematics Jacobian with respect to the actuated joints, *i.e.*, to find $J_a(q) \in \mathbb{R}^{6\times 3}$ satisfying $V_s = J_a(q)\dot{q}_a$, where V_s is the spatial velocity of the end-effector frame. For this purpose we can use the forward kinematics for any of the three open chains; for example, in terms of chain 1, $J_1(\theta)\dot{\theta} = V_s$, and from Equation (7.14) we can write

$$\dot{\theta}_2 = g_2^T \dot{q}_a \tag{7.15}$$
$$\dot{\theta}_3 = g_3^T \dot{q}_a \tag{7.16}$$
$$\dot{\theta}_4 = g_4^T \dot{q}_a \tag{7.17}$$
$$\dot{\theta}_5 = g_5^T \dot{q}_a \tag{7.18}$$

where each $g_i(q) \in \mathbb{R}^3$, $i = 2, \ldots, 5$, can be obtained from Equation (7.14). Defining the row vector $e_1^T = (1, 0, 0)$, the differential forward kinematics for chain 1 can now be written

$$V_s = J_1(\theta) \begin{bmatrix} e_1^T \\ g_2^T \\ g_3^T \\ g_4^T \\ g_5^T \end{bmatrix} \begin{bmatrix} \dot{\theta}_1 \\ \dot{\phi}_1 \\ \dot{\psi}_1 \end{bmatrix}. \tag{7.19}$$

Since we are seeking $J_a(q)$ in $V_s = J_a(q)\dot{q}_a$, and $\dot{q}_a^T = (\dot{\theta}_1, \dot{\phi}_1, \dot{\psi}_1)$, from the above it now follows that

$$J_a(q) = J_1(q_1, \ldots, q_5) \begin{bmatrix} e_1^T \\ g_2(q)^T \\ g_3(q)^T \\ g_4(q)^T \\ g_5(q)^T \end{bmatrix}. \tag{7.20}$$

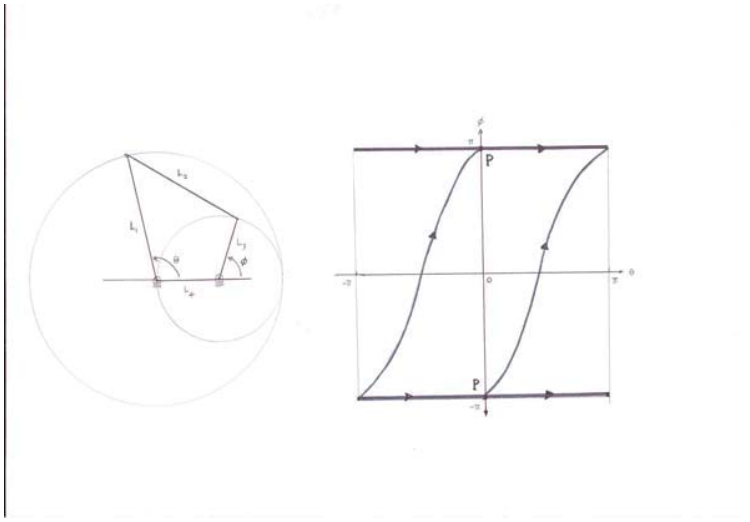

Figure 7.6: A planar four-bar linkage and its joint configuration space.

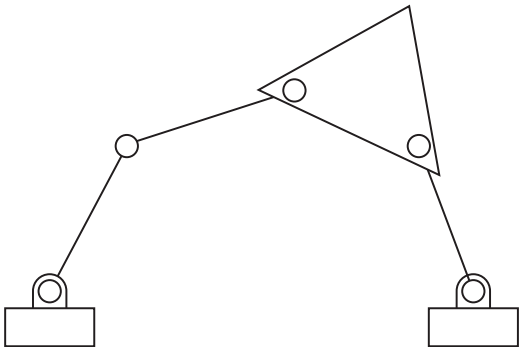

Figure 7.7: A planar five-bar linkage.

The above could also have been derived using either chain 2 or chain 3.

Given values for the actuated joints q_a, it still remains to solve for the passive joints q_p from the loop constraint equations. Eliminating as many elements of q_p *a priori* will obviously simplify the task. The second point to note is that $H_p(q)$ may become singular, in which case $\dot{q}_p$ cannot be obtained from $\dot{q}_a$. Configurations in which $H_p(q)$ becomes singular correspond to **actuator singularities**, which are discussed in the next section.

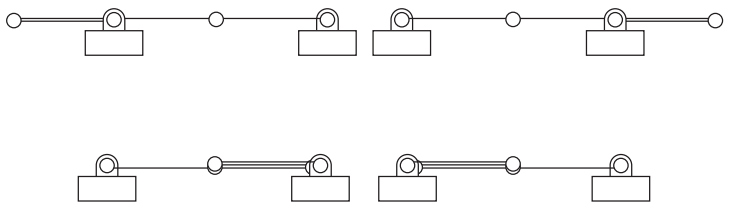

Figure 7.8: Configuration space singularities of the planar five-bar linkage.

7.3 Singularities

In this final section we shall examine the fundamental properties of closed chain singularities. Characterizing the singularities of closed chains involves many more subtleties than for open chains. Rather than attempt any such comprehensive classification for general closed chains, we instead choose to highlight the essential features of closed chain singularities via two planar examples: a four-bar linkage (see Figure 7.6), and a five-bar linkage (see Figure 7.7). The examples should also make clear how our approach to singularity analysis can be generalized to more complex closed chains.

We begin with the four-bar linkage. Recall that its configuration space is a curve embedded in a four-dimensional ambient space; even without appealing to equations, one can see that the allowable joint values for (θ, ϕ) of the four-bar form a curve of the type shown in Figure 7.6. In terms of the input and output angles θ and ϕ, the kinematic loop constraint equations can be expressed as

$$\phi = \tan^{-1}\frac{\beta}{\alpha} \pm \cos^{-1}\left(\frac{\gamma}{\sqrt{\alpha^2+\beta^2}}\right), \tag{7.21}$$

where

$$\alpha = 2L_3L_4 - 2L_1L_3\cos\theta \tag{7.22}$$

$$\beta = -2L_1L_3\sin\theta \tag{7.23}$$

$$\gamma = L_2^2 - L_4^2 - L_3^2 - L_1^2 + 2L_1L_4\cos\theta. \tag{7.24}$$

Obviously the existence and uniqueness of solutions depends on the link lengths $L_1, \ldots, L_4$; in particular, a solution fails to exist if $\gamma^2 \leq \alpha^2 + \beta^2$. The figure depicts the input-output graph for the choice of link lengths $L_1 = 4$, $L_2 = 4$, $L_3 = 3$, $L_4 = 2$; in this case both θ and ϕ can range from 0 to 2π.

One of the striking features of this graph is the **bifurcation point** P as indicated in the figure. Here two branches of the curve meet, resulting in a self-intersection of the curve with itself. If the four-bar is in the configuration indicated by P, it has the choice of following either branch. At no other point in the four-bar's joint configuration space does such a phenomenon occur.

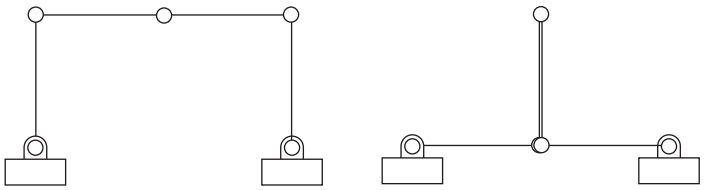

Figure 7.9: Actuator singularities of the planar five-bar linkage: the left is nondegenerate, while the right is degenerate.

.

We now turn to the five-bar linkage. The kinematic loop constraint equations can be written

$$L_1 \cos\theta_1 + \ldots + L_4 \cos(\theta_1 + \theta_2 + \theta_3 + \theta_4) = L_5 \tag{7.25}$$

$$L_1 \sin\theta_1 + \ldots + L_4 \sin(\theta_1 + \theta_2 + \theta_3 + \theta_4) = 0 \tag{7.26}$$

where we have eliminated joint variable θ_5 *a priori* from the loop closure conditions. Writing these two equations in the form $f(\theta_1, \ldots, \theta_4) = 0$, where $f : \mathbb{R}^4 \to \mathbb{R}^2$, the configuration space can be regarded as a two-dimensional surface in $\mathbb{R}^4$. Like the bifurcation point in the four-bar linkage, self-intersections of the surface can also occur. At such points the constraint Jacobian loses rank; for the five-bar, any point θ at which

$$\operatorname{rank}\left(\frac{\partial f}{\partial \theta}(\theta)\right) < 2 \tag{7.27}$$

corresponds to what we call a **configuration space singularity**. Figure 7.8 illustrates the possible configuration space singularities of the five-bar. Notice that thus far we have made no mention of which joints of the five-bar are actuated, or where the end-effector frame is placed; it is worth emphasizing that the notion of configuration space singularity is completely independent of the choice of actuated joints, or the end-effector frame.

We now consider the case when two joints of the five-bar are actuated. Referring to Figure 7.9, the actuated joints are indicated by filled circles. Under normal operating conditions, the motions of the actuated joints can be independently controlled. Alternatively, locking the actuated joints should immobilize the five-bar and turn it into a rigid structure.

For the **nondegenerate actuator singularity** shown on the left, rotating the two actuated joints in opposite directions will clearly have catastrophic consequences of the mechanism. For the **degenerate actuator singularity**

shown on the right, we have the opposite case: even when the actuated joints are locked in place, the inner two links are free to rotate.

The reason for classifying these singularities as **actuator singularities** is that, by relocating the actuators to a different set of joints, such singularities can be eliminated. For both the degenerate and nondegenerate actuator singularities of the five-bar, relocating one of the actuators to one of the three passive joints eliminates the singularity.

Intuitively visualizing the actuator singularities of the planar five-bar is straightforward enough, but for more complex spaatial closed chains this may be difficult. Actuator singularities can be characterized mathematically by the rank of the constraint Jacobian. As before, write the kinematic loop constraints in differential form:

$$\begin{bmatrix} H_a(q) & H_p(q) \end{bmatrix} \begin{bmatrix} \dot{q}_a \\ \dot{q}_p \end{bmatrix} = 0, \tag{7.28}$$

where $q_a \in \mathbb{R}^a$ is the vector of actuated joints, and $q_p \in \mathbb{R}^p$ is the vector of passive joints. It follows that the matrix

$$H(q) = \begin{bmatrix} H_a(q) & H_p(q) \end{bmatrix} \in \mathbb{R}^{p \times (a+p)}, \tag{7.29}$$

and that $H_p(q)$ is a $p \times p$ matrix.

With the above definitions, we have the following:

- If rank $H_p(q) < p$, then q is an **actuator singularity**. Distinguishing between **degenerate** and **nondegenerate** singularities involves additional mathematical subtleties, and relies on second-order derivative information that we shall not pursue further here.
- If rank $H(q) < p$, then q is a **configuration space singularity**. Note that under this condition $H_p(q)$ is also singular (the converse is not true, however). The configuration space singularities can thus be regarded as the intersection of all possible actuator singularities obtained over all possible combinations of actuated joints.

The final class of singularities involves the choice of an end-effector frame. For the five-bar, we ignore the orientation of the end-effector frame, and focus exclusively on its x-y location. Figure 7.10 shows the five-bar in an **end-effector singularity** for the given choice of end-effector location. Note that velocities along the indicated line are not possible in this configuration, similar to the case for singularities for open chains. Note that end-effector singularities are entirely independent of the choice of actuated joints (note that it was not necessary to specify which, or even how many, of the joints are actuated).

End-effector singularities can be mathematically characterized as follows. Choose any valid set of actuated joints q_a such that the mechanism is not at an actuator singularity. Write the forward kinematics in the form

$$f(q_a) = T \tag{7.30}$$

where T denotes the end-effector frame. One can then check for rank deficiencies in the Jacobian of f, as was done for open chains, to determine the presence of an end-effector singularity.

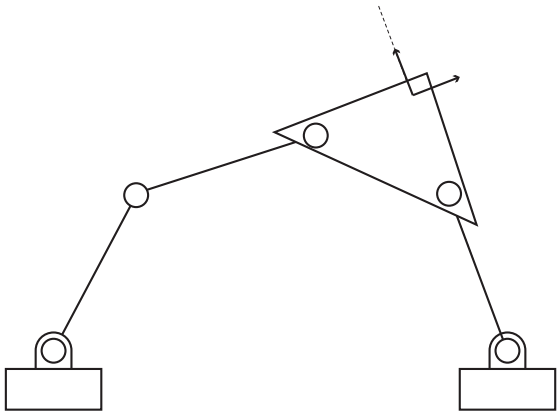

Figure 7.10: End-effector singularities of the planar five-bar linkage.

.

7.4 Summary

- Any kinematic chain that contains one or more loops is called a **closed chain**. **Parallel mechanisms** are a class of closed chain that are characterized by two platforms—one moving and one stationary—connected by several legs; the legs are typically open chains, but can themselves be closed chains. Compared to open chains, the kinematic analysis of closed chains is complicated by the fact that the configuration space is often curved, and only a subset of the joints are actuated.

- For a parallel mechanism whose actuated degrees of freedom equals its mobility, the inverse kinematics problem involves finding, from the given position and orientation of the moving platform, the values of all the actuated joints. For well-known parallel mechanisms like the planar $3 \times RPR$ and spatial Stewart-Gough platform, the inverse kinematics admits unique solutions.

- For a parallel mechanism whose actuated degrees of freedom equals its mobility, the forward kinematics problem involves finding, given values for all the actuated joints, the position and orientation of the moving platform. For well-known parallel mechanisms like the $3 \times RPR$ and the spatial Stewart-Gough platform, the forward kinematics usually admits multiple solutions. In the case of the most general Stewart-Gough platform, a maximum of 40 solutions are possible.

- The differential kinematics of a closed chain relates velocities of the actuated joints to the linear and angular velocities of the moving platform. For a closed chain consisting of n one degree of freedom joints, whose actuated degrees of freedom also equals its mobility m, let $\theta_a \in \mathbb{R}^m$ denote the vector of actuated joints, and $\theta_p \in \mathbb{R}^{n-m}$ denote the vector of passive joints.

The kinematic loop closure constraints are described by an equation of the form $h(\theta_a, \theta_p) = 0$, where $g : \mathbb{R}^n \to \mathbb{R}^{n-m}$. The forward kinematics can be expressed in the form $f(\theta_a) = T$, where $f : \mathbb{R}^m \to SE(3)$. The differential kinematics then involves derivatives of both f and g with respect to θ_a and θ_p. For platforms like the Stewart-Gough platorm, the differential kinematics can also be obtained from a static analysis, by exploiting the fact that just as for closed chains, the external forces $\mathcal{F}$ at the end-effector are related to the joint torques τ by $\tau = J^T\mathcal{F}$.

- Singularities for closed chains can be classifed into three types: (i) configuration space singularities occur at, e.g., self-intersections of the configuration space surface (or bifurcation points in the event that the configuration space is a curve); (ii) nondegenerate actuator singularities when the actuated joints cannot be independently actuated, while degenerate actuator singularities are characterized by the mechanism failing to become a rigid structure even when all the actuated joints are locked in place; (iii) end-effector singularities occur when the end-effector loses one or more degrees of freedom of mobility. Configuration space singularities are independent of choice of actuated joints, while actuator singularities depend on which joints are actuated. End-effector singularities depend on where the end-effector frame is placed, but do not depend on the choice of actuated joints.